Alma Mater Studiorum – Università di Bologna

DOTTORATO DI RICERCA

Scienze Farmaceutiche

Ciclo XXI

Settore scientifico disciplinare di afferenza: CHIM/08

New Synthetic Polyamines as Multi-Target-Directed Ligands for the Treatment of Alzheimer's Disease and Cancer: Design, Synthesis and Biological Evaluation

Presentata da: **Milelli Andrea**

Coordinatore Dottorato

Prof. Maurizio Recanatini

Relatore

Prof. Vincenzo Tumiatti

Correlatore

Prof. Carlo Melchiorre

Esame finale anno 2009

Contents

Preface

This PhD thesis has been carried out at the Department of Pharmaceutical Sciences, *Alma Mater Studiorum*-University of Bologna (Italy), under the supervision of Prof. Vincenzo Tumiatti.

The whole PhD thesis is devoted to the study of new Multi-Target-Directed Ligands (MTDLs) for the treatment of complex pathology such as Alzheimer's disease and Cancer.

This thesis is organized in two main sections: the first section is focused on the developed of new MTDLs for the treatment of Alzheimer's disease, while the second one concerns the development of new MTDLs for the cancer treatment.

Every section is organized in different chapters: the first chapter is a briefly introduction about the physiopathological aspects and the current approaches for the treatment of the disease. The second chapter concerns the aim of the thesis focused on the drug design. Chapter three contains the synthetic methods and the biological evaluation assays of the new synthesized compounds. Results and discussions are described in the chapters four and conclusions are presented in chapter five. Finally, in chapter six the experimental procedures are described.

In addition, I would like to thanks other research groups involved in the present investigation.

For the first part focused on the developement of MTDLs against AD:

- Prof. Vincenza Andrisano, Dr. Manuela Bartolini and Dr Francesca Mancini, Department of Pharmaceutical Sciences, University of Bologna;
- Prof. Maurizio Recanatini, Dr. Andrea Cavalli and Dr. Francesco Colizzi, Department of Pharmaceutical Sciences, University of Bologna.

For the second part about the development of new potential anticancer agents:

- Prof. Anna Gasperi Campani and her group, Department of Experimental Pathology, University of Bologna;
- Prof Claudio Stefanelli and his group, Department of Biochemistry, University of Bologna;
- Prof. Giovanni Capranico and his group, Department of Biochemistry, University of Bologna;
- Prof. Giannino Del Sal and his group, LNCIB, Area Science Park, University of Trieste;

In addition, I whish to thank MIUR (Rome), University of Bologna and Polo Scientifico-Didattico di Rimini for theie financial support.

Abstract

Alzheimer's disease (AD) and cancer represent two of the main causes of death worldwide. They are complex multifactorial diseases and several biochemical targets have been recognized to play a fundamental role in their development. Basing on their complex nature, a promising therapeutical approach could be represented by the so-called "Multi-Target-Directed Ligand" approach. This new strategy is based on the assumption that a single molecule could hit several targets responsible for the onset and/or progression of the pathology.

In particular in AD, most currently prescribed drugs aim to increase the level of acetylcholine in the brain by inhibiting the enzyme acetylcholinesterase (AChE). However, clinical experience shows that AChE inhibition is a palliative treatment, and the simple modulation of a single target does not address AD aetiology. Research into newer and more potent anti-AD agents is thus focused on compounds whose properties go beyond AChE inhibition (such as inhibition of the enzyme β-secretase and inhibition of the aggregation of β-amyloid). Therefore, the MTDL strategy seems a more appropriate approach for addressing the complexity of AD and may provide new drugs for tackling its multifactorial nature.

In this thesis, it is described the design of new MTDLs able to tackle the multifactorial nature of AD. Such new MTDLs designed are less flexible analogues of Caproctamine, one of the first MTDL owing biological properties useful for the AD treatment. These new compounds are able to inhibit the enzymes AChE, β-secretase and to inhibit both AChE-induced and self-induced β-amyloid aggregation. In particular, the most potent compound of the series is able to inhibit AChE in subnanomolar range, to inhibit β-secretase in micromolar concentration and to inhibit both AChE-induced and self-induced β-amyloid aggregation in micromolar concentration.

Cancer, as AD, is a very complex pathology and many different therapeutical approaches are currently use for the treatment of such pathology. However, due to its multifactorial nature the MTDL approach could be, in principle, apply also to this pathology. Aim of this thesis has been the development of new molecules owing different structural motifs able to simultaneously interact with some of the multitude of targets responsible for the pathology. The designed compounds displayed cytotoxic activity in different cancer cell lines. In particular, the most potent compounds of the series have been further evaluated and they were able to bind DNA resulting 100-fold more potent than the reference compound Mitonafide. Furthermore, these compounds were able to trigger apoptosis through caspases activation and to inhibit PIN1 (preliminary result). This last protein is a very promising target because it is overexpressed in many human cancers, it functions as critical catalyst for multiple oncogenic pathways and in several cancer cell lines depletion of PIN1 determines arrest of mitosis followed by apoptosis induction.

In conclusion, this study may represent a promising starting pint for the development of new MTDLs hopefully useful for cancer and AD treatment.

Section 1

1.1 Introduction

Alzheimer's disease (AD) is the most common cause of dementia, accounting for 50-60% of all cases. According to the World Health Organization, more than 37 million people worldwide have dementia and AD affects 18 million of them[1].

AD has been first described on November 4th, 1906, when Alois Alzheimer gave a lecture at a congress in Tubingen, Germany, showing the results of his post-mortem studies on a 51-years old woman from Frankfurt, called Auguste D. She showed progressive cognition and memory impairment, reduced comprehension, aphasia, disorientation and unpredictable behaviour[2]. What has been reported in that clinical description exemplified cardinal features of the disorder still observed nowdays. For many years, AD was considered a rare dementia occurred in presenile period and only in late 60's it was recognized as a typical senile dementia.

AD is a late-life dementia and, therefore, increasing age is one of the greatest risk factor. Due to the increasing life expectancy and the strong increase of age people, the number of people affected by AD is going to rise dramatically. In the next years, the number of people in Europe and in USA aged 80-90 years is expected to double and about one-third of the population will be older than 65 years and, thus, at risk of dementia diseases. It is estimated that currently in EU and USA the number of demented patients is 7-8 million and 4-5 million, respectively; these numbers will increase up to 14 million in EU and 16 million in USA by 2050[3].

With the expected increased in number of AD-affected people it will be observed an increasing in financial a social cost; according to Alzheimer's Association, costs for beneficiaries with AD are expected to increase of about 75% from 91 million USA Dollars in 2005 to 160 million USA Dollars in 2010. Thus, AD is becoming an enormous public, social and economical problem.

For these reasons, a growing number of scientists all over the world are focusing their investigations in finding new therapies to combat this devastating disease. Since the first AD description, little progress in defining the pathogenesis of AD occurred. In the early 70s, two characteristic lesions of this disease have been described and they are considered as typical hallmarks of the disease: the presence of neuritic plaques and neurofibrillary tangles. At the same time, it became clear that neurons involved in the biosynthesis of acetylcholine (ACh) went to a severe degeneration, especially in limbic and cerebral cortices. Based on these two findings, the oldest theory about the AD's pathogenesis has been developed: the cholinergic hypothesis, which asserts that a serious loss of cholinergic function in the Central Nervous System (CNS) contributed significally to the cognitive symptoms associated with AD[4]. Until now, the only drugs approved by FDA for the treatment of AD are based on the cholinergic hypothesis: they are drugs which increase the ACh levels in the CNS.

Within the last decades, a lot of studies have been devoted to identify the composition and the origin of the amyloid plaques and neurofibrillary tangles; based on these studies another new theory appeared and

becomes dominant in the AD research, the amyloid hypothesis[5]. The amyloid plaques were found mostly in the neocortex and contained a polypeptide known as β-amyloid protein. Because dense-core amyloid plaques are a specific lesion of AD, whereas neurofibrillary tangles are seen in a variety of neurodegenerative conditions, it has been argues that the accumulation of Aβ in the brain is the key step in the pathogenesis of AD. But, it is not completely clear how amyloid neurotoxicity induces neuronal death and how these mechanisms are linked with oxidative stress and redox-metal imbalance, phenomenon that have assumed a pivotal role in AD.

However, the basic pathophysiology of AD is still not well understood. Different pharmaceutical approaches, targeting the several hypotheses, are currently under investigation; nevertheless, the current registered drugs for AD are very limited and they are not able to alter or to prevent disease progression and they were approved only for the symptoms management[6].

Considering the complexity of AD and the involvement of multiple and interconnected pathological pathways, a combination of therapeutic agents may result in a more effective strategy of cure than the monotherapy. Besides the combination of known drugs, acting on different imbalanced mechanisms, new therapeutic approaches are based on the development of multipotent molecules able to interfere with more than one pathological event. In principle, this research guideline would lead to the discovery of an effective strategy of cure of AD and other neurodegenerative diseases[7].

1.1.1 Alzheimer Disease

AD is clinically characterized by a global decline of cognitive functions, together with behavioural disturbances and decreasing ability to perform basic activities of daily living. The cognitive symptoms include memory loss, disorientation, confusion, problems with reasoning and thinking, while behavioural symptoms include agitation, delusion, depression, hallucinations, insomnia and wandering.

Although the pathogenesis of AD is not yet fully understood, a lot of evidences show that it is a multifactorial disease caused by environmental and endogenous factors and with a significant genetic background.

Two forms of AD exist: a familial one (multiple family members are affected) and a sporadic one, in which one or few members of a family develop the disease. However, epidemiological studies suggest that more than 80% of AD cases are familiar[1]. At least 10 genes are associated with AD, and more than 50 genes are potentially involved in dementia.

Familial AD is an autosomal dominant disorder; the first mutation causing this form of AD has been identified in the Amyloid Precursor Protein (APP) gene on chromosome 21 even if this kind of mutation only explains very few familial cases. For the most cases of familial disease, mutations are observed in the highly homologous presenilin 1 (PS1) and presenilin 2 (PS2)[3]. Concerning the sporadic form of AD, the apolipoprotein E (ApoE) plays an important role; despite its mechanism of action is not well clear, ApoE seems to be essential for Aβ deposition, promoting Aβ fibrillisation and plaques formation[8]. However, these

mutations account only for 10% of AD cases and it seems clear that other genetic factors may be involved in AD.

Since Alois Alzheimer's seminal report, pathologists have considered the defining characteristic hallmarks of the disease to be Aβ deposits in senile plaques and neurofibrillary tangles (NFT), derived from filaments of abnormally phosphorylated τ protein. These two lesions are implicated in the neuronal functions disruption observed in the post mortem brain of AD patients. Despite the growing number of studies concerning the AD pathogenesis, the mechanism how these two events lead to dementia is not fully understood yet.

Different neurotransmitter systems go towards degeneration in AD progress; in particular, cholinergic neurons and synapses in the nucleus basalis, hippocampus and entorhinal cortex. Many evidences demonstrated that ACh is deeply involved in memory functions. Almost all the drugs currently in market for the treatment of AD have the cholinergic system as target of their pharmacological activity[9,10]. Moreover, other neurotransmitter systems are involved in the AD pathology development such as serotoninergic, dopaminergic and glutammatergic[11]. The last system represents also an important target for AD treatment; over-activation *N*-methyl-D-aspartate-sensitive glutamate (NMDA) receptors leads to excessive intracellular Ca^{2+} influx and the subsequent production of damaging free radicals contributing to cell injury and death. Moreover, both oxidative stress and increased intracellular Ca^{2+}, generated in response to Aβ, have been reported to enhance glutamate-mediated neurotoxicity *in vitro*. Furthermore, it has been suggested that Aβ can also increase NMDA responses and therefore excitotoxicity. There is increasing evidence that glutamate excitotoxicity is associated with oxidative stress and Aβ formation[12]. For these reasons, Memantine, a non competitive NMDA receptor antagonist, is commercially available in US and Europe for the treatment of moderate to severe AD. This drug acts by reducing the calcium-mediate neurodegeneration in several brain areas[13].

Accumulating evidences suggest that oxidative stress is an early event in AD[14]. Extensive literature points to oxidative stress as pivotal in the pathogenesis of AD, suggesting that it occurs prior to the onset of symptoms in AD, and that oxidative damage occurs before plaques formation[15].

Cholinergic hypothesis

The "cholinergic hypothesis" have been developed in 80's when the importance of the cholinergic system in the process of memory have been clearly understood. Based on these evidences, different studies showed how reduction of the cholinergic transmission is one of the causes of AD.

This theory have been proposed after the observation that low doses of natural cholinergic agents, such as atropine and scopolamine, could induce the same pattern of cognitive disorder seen in elderly volunteers. Different other studies using non human primates showed how scopolamine induces the same memory loss observed in aged monkeys[16]. These studies first showed that age memory loss could be reduced using drugs able to increase the cholinergic activity[17].

The “cholinergic hypothesis” has been further validated by the observation that AD pathology is associates with a significant loss of presynaptic cholinergic markers, such as Choline AcetilTransferase (ChAT), a key enzyme in the biosynthesis of ACh[18]. Furthermore, other studies have demonstrated a reduction in the number of nicotinic and muscarinic M_2 receptors subtype and acetylcholinesterase (AChE) in patients affected by Alzheimer Disease[19,20]. Moreover, disruption of the coupling between M_1 receptor and its second messenger G protein has been observed[21].

These studies clearly demonstrated that cognitive and behavioural disorders associated with AD derived from the reduction of ACh and cholinergic transmission and, therefore, the “cholinergic hypothesis” represents the principal therapeutic approach to AD[22].

Acetylcholine is the neurotransmitter that interacts with cholinergic receptors and modulates different physiological function in the CNS e in the Peripheral Nervous System. It is produced in the cytoplasm of cholinergic neurons by the enzyme ChAT from choline and coenzyme A and it is stored in synaptic vesicles. After it is releasing in the synaptic cleft, it can have excitatory or inhibitory effect depending on the type of tissue and the nature of the receptor activated; it is metabolized into choline and acetic acid by enzyme Acetylcholinesterase (AChE). Cholinergic receptors can be divided in two types based on the pharmacological response to various agonist and antagonist:

1) nicotinic receptors (nAChR), which have nicotine as natural ligand;
2) muscarinic receptors (mAChR), which bind muscarine.

These two receptor systems have different structures, localization, functions and are associated with different biochemical pathways.

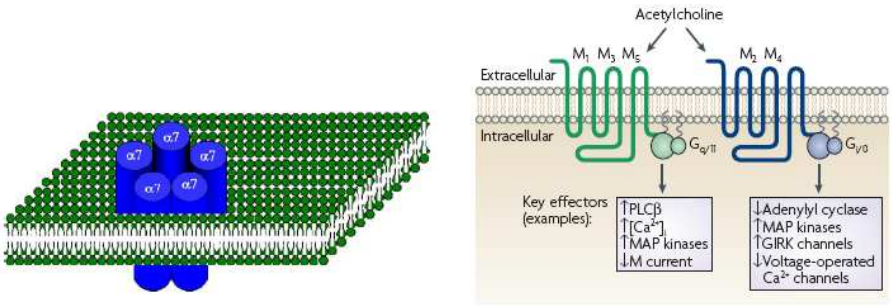

Figure 1. Schematic representation of one subtype of nAChR (alfa7) and mAChR[23,24].

Both these two receptor systems are implicated in AD.

Several experimental evidences have reported a reduction in central nicotinic receptors[25] and M_2 muscarinic subtype receptors both located in presynaptic cholinergic terminals in AD patients. However, a relative preservation of postsynaptic M_1 and M_3 receptors has been observed. In addition, some evidences showed a disruption of the link between M_1 receptor and its coupled G-protein[18].

Therefore, such receptors system could be considered a valuable target for the treatment of AD (see section 1.2 for more detailed discussion).

Acetylcholinesterase

Cholinesterases are a ubiquitous class of serine hydrolyses that hydrolyze choline esters. Two forms of cholinesterases, encoded by two distinct genes, occur in mammalian:

- Acetylcholinesterase (AChE) which selectively hydrolyzes ACh and its main role is the termination of impulse transmission at cholinergic synapses, by rapid hydrolysis of ACh in both central and peripheral nervous system;
- Butyrylcholinesterase (BChE) which hydrolyzes other choline ester (BChE is less selective than AChE) but its role is not completely understood; from recent experimental evidences, BChE seems to be able to reduce β-amyloid precipitation[26,27].

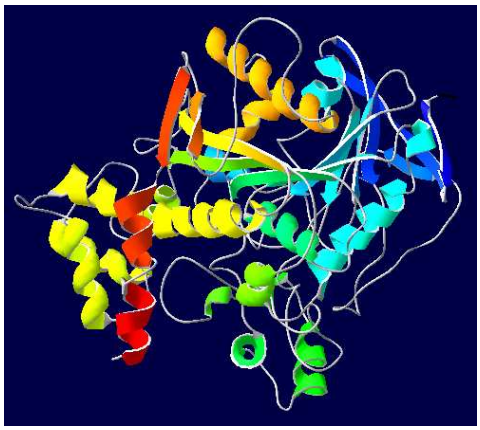

Figure 2. Representation of the secondary structure of AChE[28].

AChE is present in nervous tissue, muscle, plasma and blood cells and it displays also non-cholinergic function, such as hydrolysing of encephalines and substance P. Since the discovery of "cholinergic hypothesis", AChE has been widely investigated and it has become one of the most well known enzymatic systems.

On the other hand, the functions of BChE are not completely clear; in brain, BChE has been found in association with dopaminergic system while in periphery it is abundant in liver as well as in the cardiac muscle. BChE has been suggested to act as a protective enzymatic system to guard AChE against inhibition by false substrates, preserving the critical function of AChE in its regulation of cardiovascular, neuromuscular and central cholinergic activities.

In 1991 Sussman and co-workers solved the three dimensional structure of *Torpedo Californica* AChE (*Tc*AChE) that is structurally homologue to the muscle and nerve AChE of vertebrate. The enzyme monomer is a α/β fold protein, MW 65612, which contains 537 amino acids. It consists of a 12-strained central mixed β sheets surrounded by 14 α-helices and bears a striking resemblance to several hydrolases[29].

AChE is characterized by the presence of two main binding sites:

1) catalytic active site, where the hydrolyse of the substrate ACh takes place;
2) peripheral anionic site (PAS), which presents non-catalytic functions.

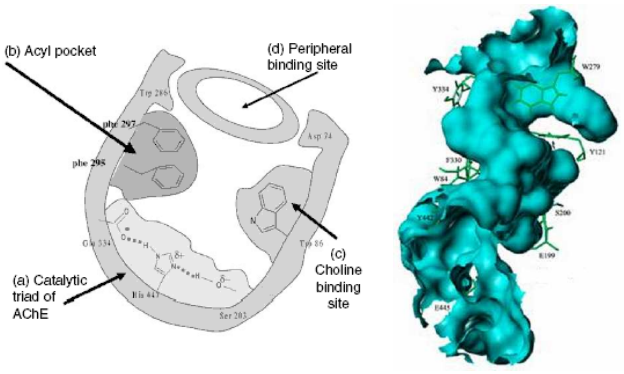

Figure 3. Structure of AChE[29].

*Tc*AChE active site was found to be at the bottom of a deep and narrow gorge, lined by aromatic residues. AChE has been always classified as a serine hydrolase and it presents at the end of the gorge the so-called catalytic triad formed by Asp-His-Ser. Ser200 is the residue responsible of the nucleophilic attack of carbonyl moiety of ACh and the following esterase activity. The nucleophilic properties of Ser200 are enhanced by His residue in the active site, identified as His440 by mutagenesis studies. The third residue has been indentified as Glu327 rather Asp by site-directed mutagenesis studies. In human AChE (*h*AChE) the catalytic triad includes Ser198, His483 and Glu327. Near the bottom of the cavity there is Trp84 which represents the anchoring site of the cationic portion of AChE, through a cation-π interaction[30] .

The Peripheral Anionic Site (PAS) is located at the rim of the gorge and it is formed by several amino acids such as Tyr72, Tyr123, Tyr341, Glu285, Asp74 and Trp286[31].

AChE presents many non-catalytic functions and it has been suggested that PAS could mediate heterologous protein association processes in synaptogenesis, neuronal differentiation and neurodegeneration. Several studies demonstrated that AChE could play a key role during the formation of senile plaques because it is able to accelerate the A*β* deposition. This process is affected by PAS inhibitors and not by active site inhibitors suggesting the crucial role of PAS in the senile plaques formation process[32]. In 2003, Bartolini *et al.* examinated different well known AChE inhibitors and no correlation between AChE inhibitory activity and the ability to prevent A*β* aggregation have been found[33]. Moreover, BChE, which lacks the PAS, was not able to affect the amyloid formation[32]. AChE-A*β* interaction has been characterized

in vitro: they form a complex that presents a fibrillogenic activity and determines also an increase in toxicity of the fibrils[34,35].

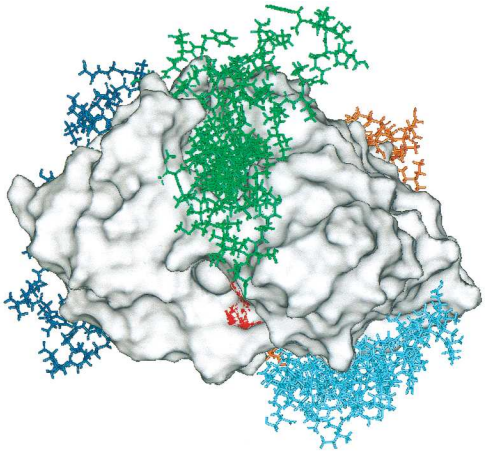

Figure 4. Docking simulation of Aβ on AChE[35].

Hence, AChE inhibitors able to interact with both catalytic and peripheral sites could offer an effective therapeutic approach for AD treatment.

Indeed, with the exception of Memantine, all the anti-Alzheimer drugs currently in therapy are AChEI (see section 1.2 for further details).

Amyloid hypothesis

Amyloid β peptide was isolated for the first time 20 years ago from the brain of patients affected by AD and Down's Syndrome and some years later this peptide has been recognized as the primary component of senile plaques of AD brain tissue[36,37]. Amyloid β peptide derived from an Amyloid Precursor Protein (APP), and the gene encoding for this protein is located on chromosome 21.

The amyloid hypothesis states that Aβ plays a central role in the pathogenesis of AD; it is hypothesized that Aβ accumulation in plaques or as partial soluble filaments initiates a pathological cascade leading to neuronal dysfunction, tangles formation, inflammation, and oxidative damage, with neurodegeneration and dementia as the final outcome. The amyloid cascade hypothesis is based on a complex of subsequential events, starting with Aβ overproduction and/or a decreased clearance, which results in oligomerization and deposition as diffuse plaques. Several lines of evidence have recently demonstrated that soluble oligomers of Aβ, but not monomers or insoluble amyloid fibrils, might be responsible for synaptic dysfunction (Figure 5)[38,39,40].

In any case, Aβ aggregates might directly injure the synapses and neurites of brain neurons, activate microglia and astrocytes, modify kinase/phosphatase activity and ionic homeostasis, and promote a heterogeneous state of oxidative stress.

Senile plaques are extracellular deposits of amyloid fibrils formed by different fragments of peptide *β*: the major component of the amyloid core is the 42 amino acids residue Aβ_{42}[41].

A*β* after being released from its precursor APP can coalesce into deposit called "diffuse plaques"; these plaques induce further deposition of other Amyloid plaques. Then, such plaques could reorganise into *β*-pleated sheets and fibrilise into neuritic plaques leading to different events which culminate in neuronal loss and synaptic dysfunction[42]

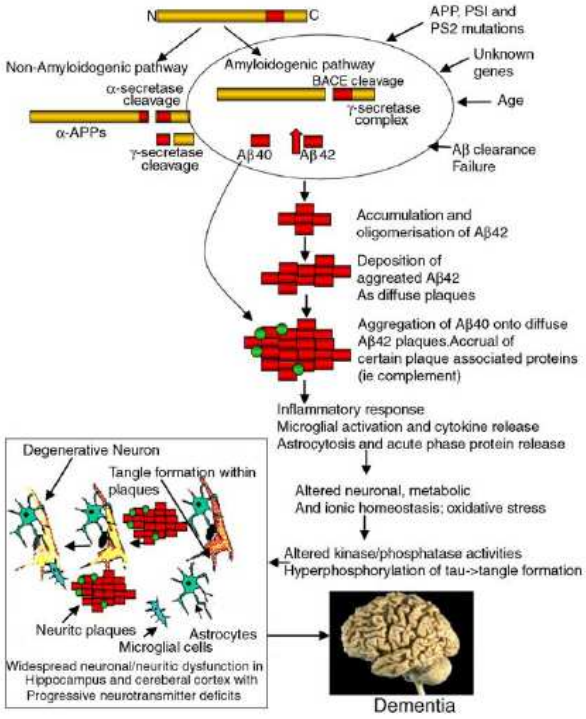

Figure 5. The amyloid cascade hypothesis[42]

Amyloid plaques are deposit of *β*-amyloid insoluble peptides derived from the precursor APP[43] which is widely expressed in cells throughout the body and its amounts are influenced by the physiological state of the cells. Several isoforms of APP exist but the most abundant form in brain is constituted APP695[44].

APP could be processed following two different pathways: the amyloidogenic and the non-amyloidogenic pathway[45]. The non-amyloidogenic pathway involved the enzyme α-secretase while the amyloidogenic involved two other secretases, β- and γ-secretase. The APP cleavage by α-secretase releases a large soluble fragment (α-APP) and the retention of an 83 amino acid fragment. In the amyloidogenic pathway, β-secretase (BACE) cleaves APP generating an extracellular soluble fragment called β-APP and an intracellular COOH-terminal fragment called C99. Such fragment is further processed by γ-secretase to produce peptides of different length such as Aβ_{40} and the pathogenic Aβ_{42}[46,47].

Very interesting, the APP intracellular domain derived from the cleavage of C99 by γ-secretase could translocate into the nucleus and modulate the expression of different genes, such as apoptotic genes (Figure 6)[48].

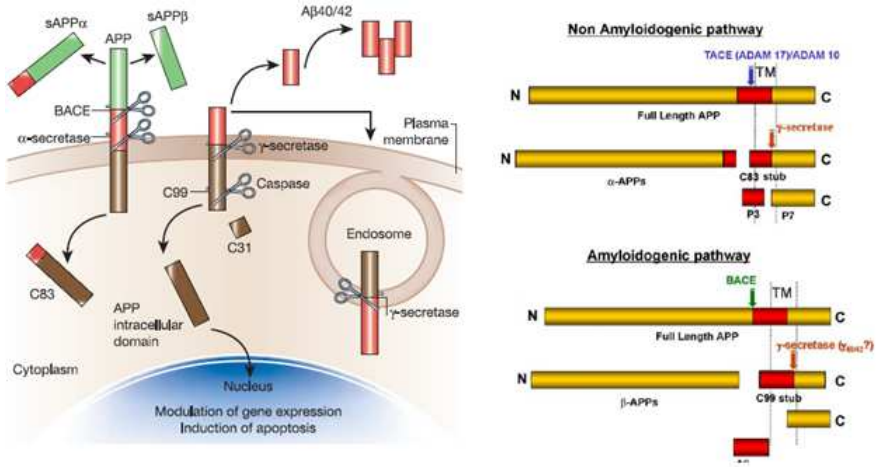

Figure 6. Pathways of APP processing[42,44].

However, other factors could contribute to A*β* formation such as high level of cholesterol in the cells[49].

Regarding the enzymes involved in the *β*-amyloid formation, BACE and γ-secretase have received many attentions as possible therapeutical targets.

BACE1 is an aspartyl protease that requires two aspartates, Asp93 and Asp 289, for its activity. BACE-RNAm is highly expressed in the brain and in other human tissues and it is mainly expressed in the Golgi and in endosomes[50,51].

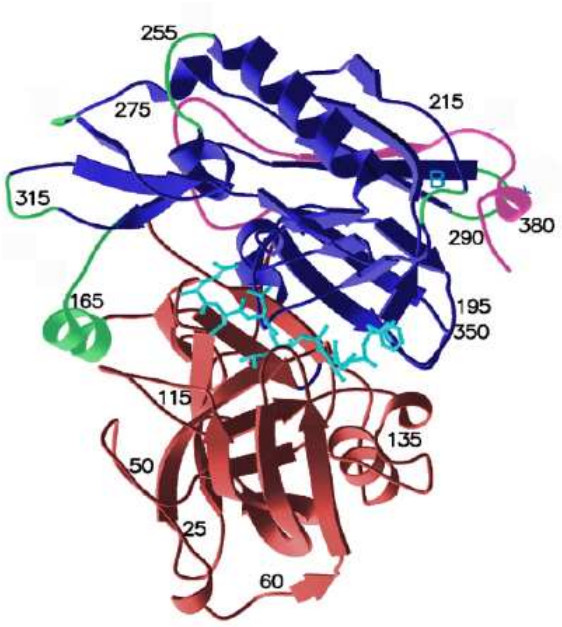

Figure 7. Ribbon model of the crystal structure of β-secretase catalytic domain[52,53].

γ-secretase has a central role in AD pathogenesis but for a long time it has been a mystery for all the scientists. Now, it is known that γ-secretase is a multiprotein complex of Presenilins (PS1 or PS2), Nicastrin, Aph1 and Pen2. Both PS1/2 regulate the activity of γ-secretase. However, studies carried out in animal lacking PS1 but not PS2 showed a decreased levels of *β*-amyloid suggesting that PS1 has a major role in APP processing than PS2[54,55]. Indeed, also PS1 is an aspartyl protease.

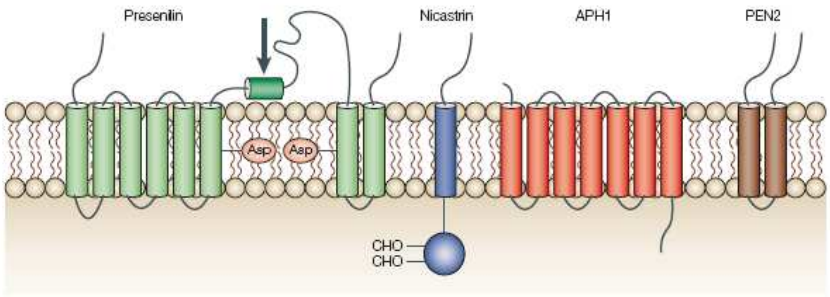

Figure 8. γ-secretase complex[56].

Fundamental for γ-secretase activity is Nicastrin and the N-terminal part of its transmembrane domain is involved in interaction with PS1. Nicastrin works as γ-secretase receptor since it binds the N-terminal side of APP and recruits it within the γ-secretase complex for further cleavage[57]. Pen2 and Aph1 seem to be necessary to stabilize the mature PS1-Nicastrin complex[58]

γ-secretase complex has several different substrates other than APP, including NOTCH 1-4, and ErbB-4 receptor[59]. The finding that knockout of the γ-secretase component PES-1 caused a lethal phenotype similar

to a NOTCH 1 knockout, indicate that γ-secretase cleavage of NOTCH 1 is essential during embryonic development. However, NOTCH signalling is also important in adult tissue and its inhibition might affect haematopoiesis and thymocyte differentiation. Recently, chronic *in vivo* administration of a potent γ-secretase inhibitor at doses that inhibited Aβ production was shown to block thymocyte differentiation, inhibit splenic B-cell maturation, and cause severe changes in the gastrointestinal tract[60].

Recently it has been found that caspases could also cleave APP leading to a second apoptosis-promoter peptide called CT31 (Figure 9)[61].

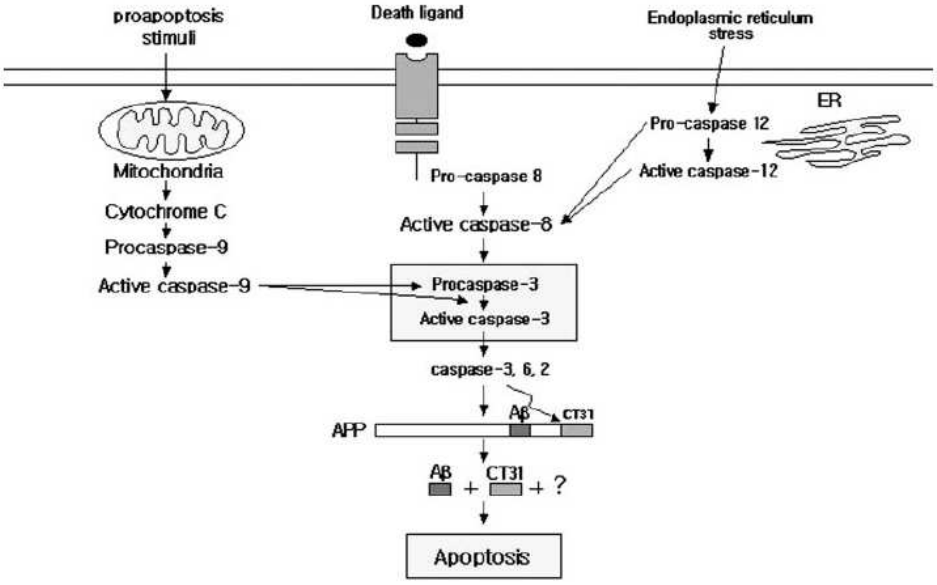

Figure 9. Probable processing of APP by caspases[62].

β-amyloid is able to induce neurotoxicity through several mechanisms[62]. It has been demonstrated that Aβ induces formation of Reactive Oxygen Species (ROS) that cause lipid peroxidation and protein oxidation[63]. Moreover, Aβ causes accumulation of hydrogen peroxide in cultured hyppocampal neurons.

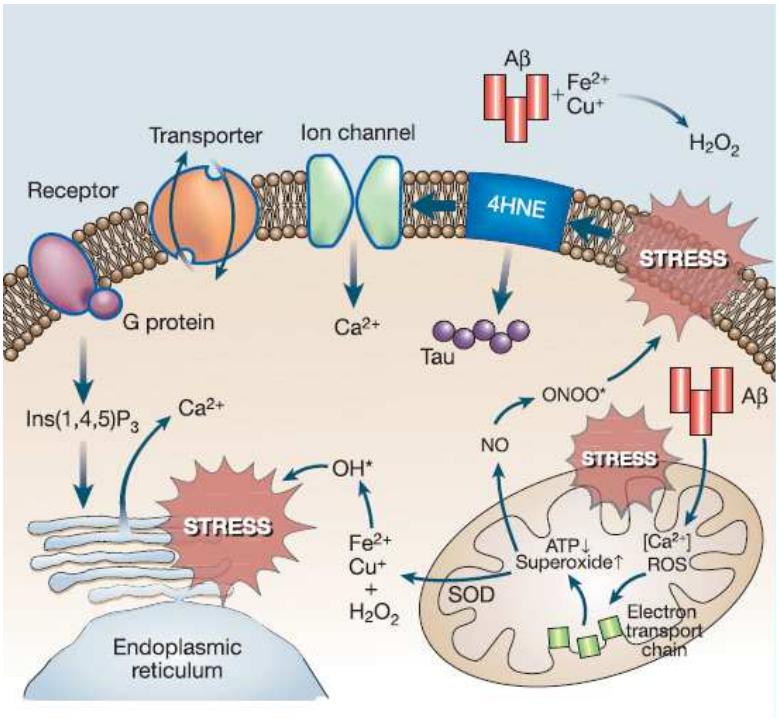

Figure 10. Neurotoxic action of Aβ involving ROS generation[44].

Furthermore, Aβ has effect on calcium homeostasis. Calcium is one of the most important messengers in the brain and it is essential for neuronal development and signal transmission. Aβ increases calcium influx through voltage-gated calcium channel, forms a cation-selective ion channel after Aβ peptide incorporation into the cell membrane and reduces magnesium blockade of NMDA receptors to allow increase of intracellular calcium[62].

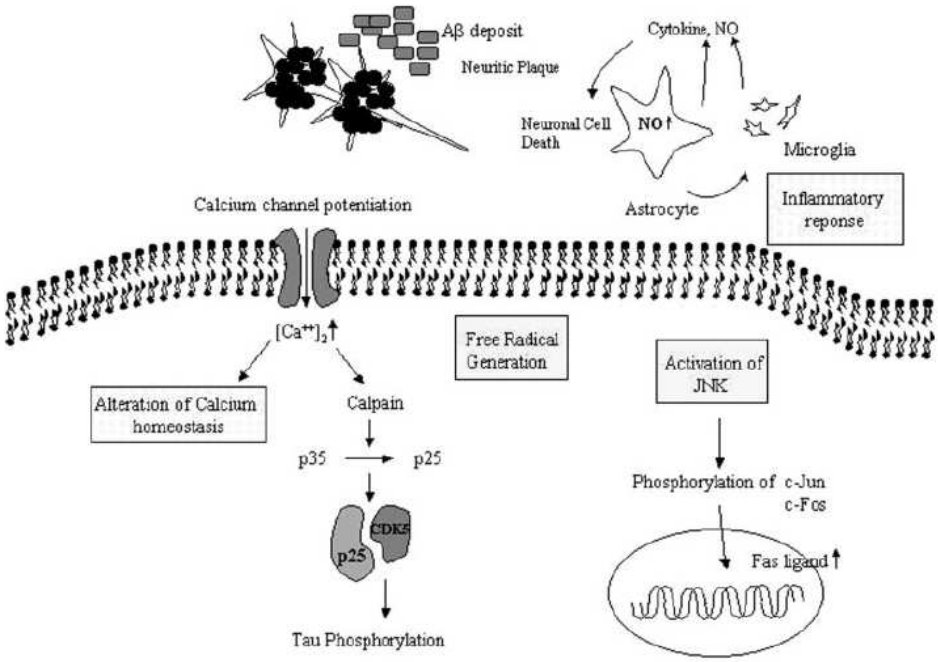

Figure 11. Neurotoxic mechanisms of Aβ[62].

Neurofibrillary tangles

In addition to amyloid deposits, neurofibrillary tangles (NFTs) are typical AD markers and the discovery that Aβ in the vicinity of neurons enhanced τ phosphorylation in cellular cultures and in brain, suggested a link between the two lesions.

NFTs, which are insoluble filamentous accumulation found in degenerating neurons[42], are composed of highly phosphorylated aggregates of a microtubule-associate protein τ, self associated into paired helical filaments (PHF-τ).

In AD, τ becomes hyperphosphorylated and self-aggregated and such resulting tangles accumulate within neurons leading to neuronal death. However, the mechanism of such aggregation is still not well understood even if it is clear that phosphorylation of τ is a key factor.

τ, when is "normally phosphorylated", plays many physiological roles in regulating neurite growth, axonal transport and microtubule stability[64]. τ is a neuronal protein that could exist in 6 different isoforms in adult brain. It possesses many sites that can be phosphorylated: for example, the longest adult brain form has almost eighty Ser and Thr and five Tyr residues[65]. Phosphorylation is essential for τ proper functions, however, its hyperphosphorylation has been observed in many neurodegenerative diseases[66].

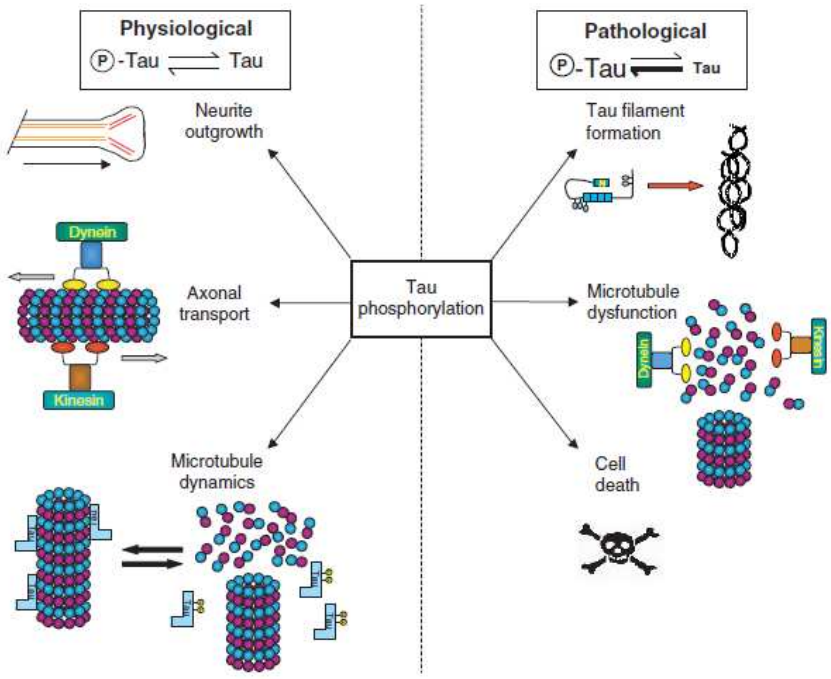

Figure 12. Physiological and pathological roles of τ phosphorylation[64].

PHF-τ induces neurotoxicity through several mechanisms, such as:

1. disassembly of microtubules[67];
2. comprising microtubule stability and functions[68];

3. disruption of intracellular compartments essential for normal metabolism[69].

Oxidative stress

Neurodegenerative diseases, such as AD, are characterized by an extensive evidence of oxidative stress, which might be responsible for the dysfunction or neuronal cells death contributing to the disease pathogenesis. Oxidative stress is the result of an imbalance in pro-oxidant/antioxidant homeostasis that leads to the generation of toxic ROS, such as hydrogen peroxide, nitric oxide, superoxide and the highly reactive hydroxyl radicals.

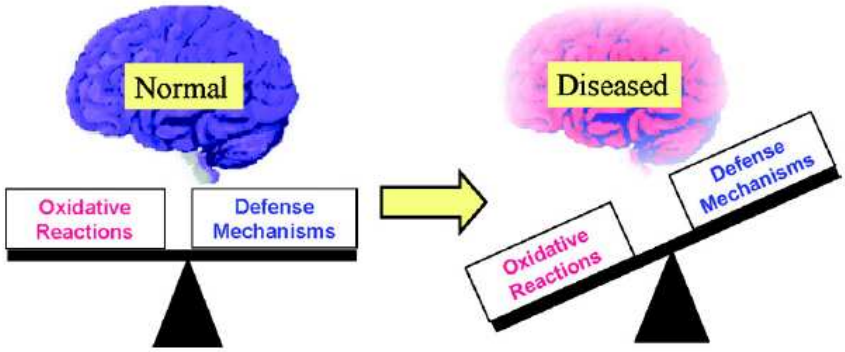

Figure 13. Imbalance in pro-oxidant/antioxidant in normal and pathological condition[70].

Although many questions about the mechanism of oxygen regulation remain unanswered, it has been widely confirmed that oxidative stress contributes to the neurodegeneration process, and plays a key role in Aβ neurotoxicity[70,71,72,73,74]. Zn^{2+}, Cu^{2+} and Fe^{3+} have been found in high concentration in different regions of brain and *in vitro* studies showed that Zn^{2+} could induce aggregation and precipitation of Aβ[75]. The same Aβ aggregation can be induced by Cu^{2+} and Fe^{3+} [76].

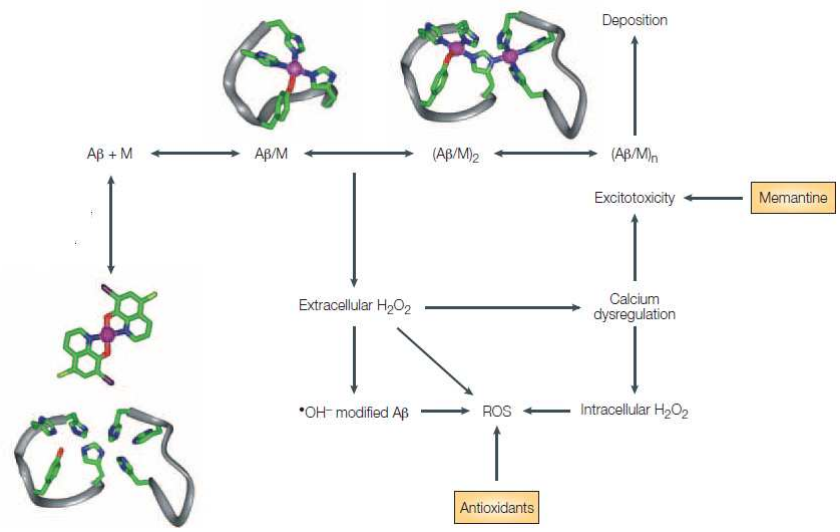

Figure 14. Oxidative stress in AD[72].

Aβ possesses histidine residues at 6, 13 and 14 position which are able to coordinate metal ions. Such interaction has been confirmed by spectroscopic studies[77]. Accordingly, it has been demonstrated that methylation of the histidine side chain abolishes the metal coordination.

When such metals coordinate to Aβ redox reaction takes place that reduces the oxidation state of the metals and produces hydrogen peroxide from atmospheric oxygen.

Oxygen is in a triplet-spin state and therefore interaction with most of the organic molecules is forbidden. However, different metallo-proteins could activate O_2 to ROS following different pathways, such as Fenton and Haber-Weiss reaction[78].

Aβ reduces Cu^{2+} and Fe^{3+} and leads to production of ROS. The chemical reactions occur are the following:

$$(A\beta)_2 + M^{(n+1)} \longrightarrow A\beta{:}A\beta^{+\cdot} + M^{n+}$$

Then, reduced metals Cu^{2+} and Fe^{3+} react with molecular oxygen to produce superoxide anion:

$$M^{n+} + O_2 \longrightarrow M^{(n+1)} + O_2^{-}$$

Superoxide anion can undergo to dismutation leading to hydrogen peroxide.

$$2\,O_2^{-} + 2\,H^{+} \longrightarrow H_2O_2 + O_2$$

Reduced metals then react with hydrogen peroxide following Fenton reaction to generate the highly reactive hydroxyl radical (OH·):

$$M^{(n+1)} + H_2O_2 \longrightarrow M^{(n+1)} + OH\bullet + OH^-$$

Furthermore, OH· could be formed by the Haber-Weiss reaction catalyzed by $M^{(n+1)}/M^{n+}$:

$$O_2^- + H_2O_2 \longrightarrow OH\bullet + OH^- + O_2$$

Once generated, ROS can react with a multitude of different molecules leading to impaired cellular functions, formation of toxic species, and neuronal cell death. Lipid peroxidation, resulting from attack by radicals on the double bond of unsaturated fatty acids, such as arachidonic and linoleic acids, is a sensible marker of oxidative stress. This reaction generates highly reactive lipid peroxy radicals that produce downstream products, such as 4-hydroxy-2,3-nonenal (HNE), acrolein, malondialdehyde, and F_2-isoprostanes which have been detected at high level in cerebrospinal fluid of AD patients[79].

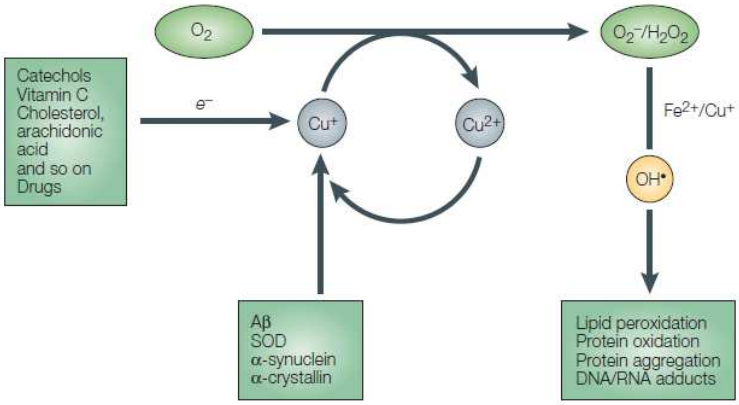

Figure 15. ROS generation by abnormal reaction of O_2 with protein-bound Fe or Cu[72].

Moreover, HNE and acrolein generate further toxicity by cross linking to cysteine, lysine, and histidine residues via Michael addition, leading to an altered reuptake of glutamate and by promoting excitotoxicity[80] and stimulating apoptotic cascade. The beneficial effects of memantine, a NMDA receptors antagonist, in rescue AD pathology are thought to be related to the reduction of these excitotoxic phenomenons.

Glutamate-induced toxicity

Excessive activation of glutamate NMDA receptors (NMDAR) plays a fundamental role in AD[81,82,83]. Glutamate is the most important excitatory neurotransmitter and exerts its physiological and pathological binding to specific glutamate-receptors. Two classes of such receptors exist:

1. metabotropic receptors, that belong to a G-protein coupled receptor family

2. ionotropic receptors, which are ion-channel receptors belonging to the ionotropic family[84].

The latter receptors system could be further divided basing on their sensitivity to synthetic agonist in: α-amino-3-hydroxy-5-methyl-4-isoxazole propionic acid (AMPA) receptors, *N*-methyl-D-aspartate (NMDA) receptors and kainate receptors. In particular, the NMDA receptor is a cornerstone in AD pathogenesis. Pathological overactivation of NMDAR causes an excessive influx of Ca^{2+} triggering several cell-damages biochemical pathways, which include (Figure 16):

- mitochondrial ROS formation leading to caspase activation and apoptosis;
- activation of nitric oxide synthase leading to an increase production of toxic peroxinitrite ($ONOO^-$);
- stimulation of p38 MAPK that induces transcription of proapoptotic factors[12].

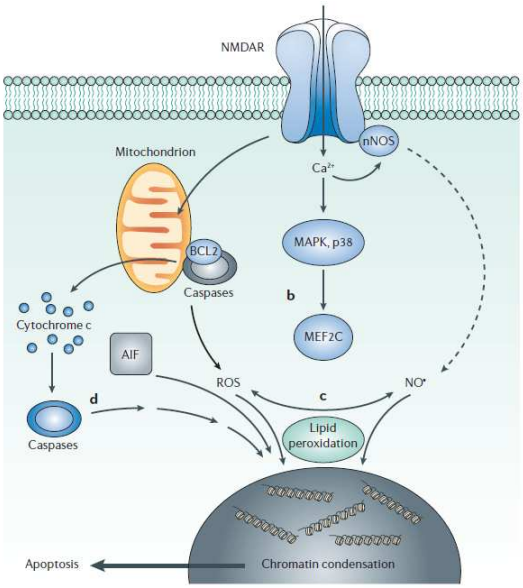

Figure 16. Death pathways triggered by excessive NMDAR activity[12].

Furthermore, several links exist between Aβ and NMDA-mediates events. In particular, Aβ seems to increase NMDA responses and, therefore, exicitoxicity[85]. Furthermore, Aβ could inhibit glutamate reuptake leading to an increase concentration of such neurotransmitter in the synaptic cleft[86]. In addition, NMDA hyperactivation seems to increase the hyperphosphorylation of τ-protein[87] However, NMDAR present several binding sites that could represent potential target for blocking excitotoxicity.

1.1.2 Therapeutical Approaches to AD

In the past years, important progresses have been made in understanding the pathomechanism leading to AD and new therapeutic targets have become available to design new molecular entities able to prevent the disease progression[81,88].

However, to date the therapeutic strategies for the treatment of AD have been mainly centred on the restoration of cholinergic functionality and until 2003, the only drugs licensed for AD treatment were acetylcholinesterase (AChE) inhibitors (AChEIs) such as Donepezil, Galantamine, Rivastigmine and Tacrine. This last AChEI, however, has been recently withdrawn from the market due to its serious side effects[89].

More recently, the role of an overactivation of glutamate receptors in neuronal death has been definitely cleared out, and the NMDA antagonist Memantine has been approved in the US in the late 2003 (Figure 17)[90].

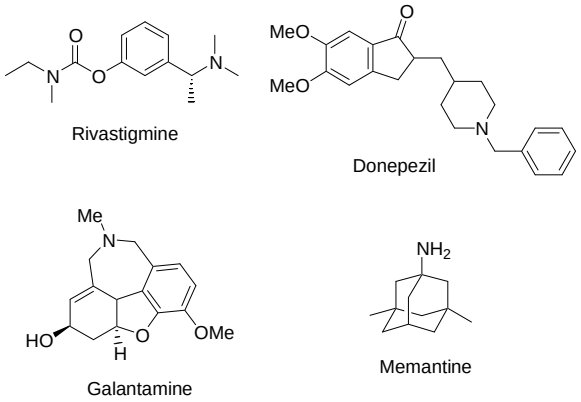

Figure 17. Anti-AD drugs currently approved.

Cholinomimetic Therapy

Based on the "cholinergic hypothesis", a drug able to potentiate central cholinergic function should be useful in the treatment of AD[18]. The treatment of the cholinergic deficit in AD could be addressed through several strategies.

One of the first attempts to treat AD was focused on increasing the synthesis of ACh by supplying its precursors as lecithin and choline; however, this approach failed probably because there are sufficient levels of ACh precursor in AD brain and other factors are responsible for the cholinergic deficit[91].

Another useful approach is directed toward the modulation of cholinergic receptors. In particular, several pharmacological studies showed that M_1 muscarinic receptor subtypes mediates many of the cognition-enhancing effects of ACh and M_1 activation could inhibit deposition of Aβ through different pathways[24,92].

Therefore, many selective M_1 agonists have been developed as cognition-enhancing drugs. Some of these drugs, such as Milameline, Sucomeline and SDZ 210-086, despite of exerting cognition-enhancing effects, showed several side effects[93].

Furthermore, M_2 muscarinic receptor subtypes are important in learning, memory and neuronal plasticity. Presynaptic autoreceptors M_2 mediate inhibition of hippocampal and cortical release of ACh[94]. Therefore, blockade of M_2 autoreceptors should lead to an increase in ACh level by negative feed-back effect[95]. Selective M_2 antagonists, such as BIBN-99 increase extracellular levels of ACh and cognitive function in both memory-impaired aged rats and normal rats[96]. A new class of M_2 antagonists has been developed in the Schering-Plough laboratories, and the lead compound SCH 57790, although showing a promising *in vivo* profile, was not further developed because of the presence of a metabolic labile moiety[97]. Several analogues of SCH 57790 have been synthesized with a better pharmacokinetic profiles and improved M_2 selectivity, and among others, SCH 76050 emerged as a potent and selective M_2 antagonist, but with a poor pharmacokinetic profile[98].

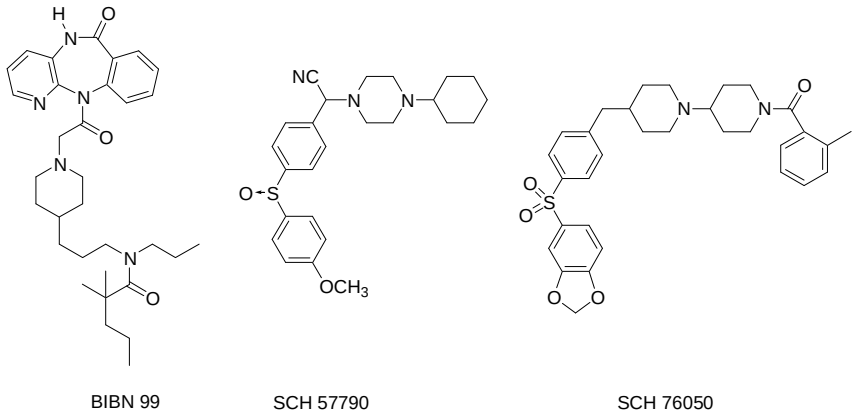

Figure 18. Chemical structure of M_2 mAChR antagonists.

Unfortunately, in the late stages of AD a severe M_2 receptors degeneration is observed limiting the potential use of M_2 antagonists in AD treatment.

AD patients are characterized by a significant decrease of a wide number of nicotinic receptors (nAChR) and several experimental evidences show a strictly connection between AD and nAChR.

Nevertheless, nowdays only few molecules interacting with the nAChR system are under investigation for the treatment of AD. ABT418 developed in the Abbot Laboratories is a α4β2 agonist actually in phase II clinical trials and many its analogues are currently under investigation[99]. In addition, analogues of alkaloid of Epibatin, such as SIB1553A, are currently study for AD treatment[100].

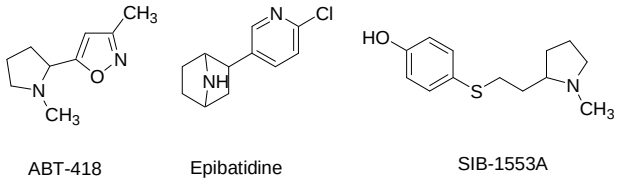

ABT-418 Epibatidine SIB-1553A

Figure 19. Structure of nAChR agonists.

However, several problems limit the development on nAChR ligands for AD therapy; perhaps, the main problem associate with the use of nAChR agonist is the fast desensitisation of these receptors to the effect of these agonists.

ACh, after its release in the synaptic cleft, is rapidly hydrolyzed by the action of AChE and BChE. Inhibition of such enzymes should lead to an increase in concentration of ACh leading to an enhancement of the cholinergic tone.

Nowdays, the most effective method to improve cholinergic deficit is to inhibit AChE even if clinical experience shows that cholinesterases inhibition is just a palliative treatment, which does not address AD's etiology[101,102].

The first inhibitor of AChE (AChEI) approved in 1993 by FDA to treat AD was Tacrine (Cognex®). Tacrine was synthesized more than 40 years ago; it is a reversible inhibitor of AChE with a strong affinity for the catalytic site but it is not able to interact with PAS. Furthermore, it is active towards monoamine oxidase. Tacrine appears to improve cognitive functions, and behavioural deficits but, unfortunately, serious adverse side effects have limited its use: it displays hepatotoxic effects and for this reason it has been withdrawn from the market[103].

Three other commercial drugs available for the treatment from mild to moderate AD in US and Europe are Donepezil, Rivastigmine and Galantamine.

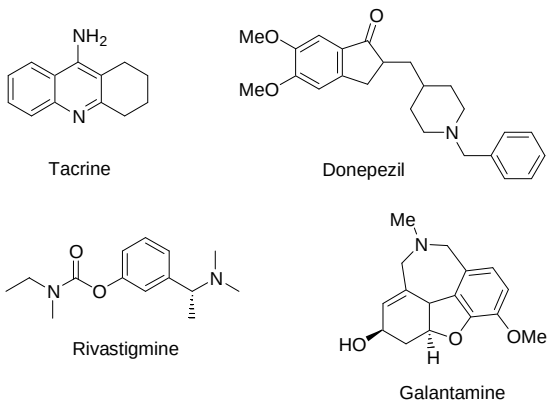

Tacrine Donepezil

Rivastigmine Galantamine

Figure 20

Donepezil (Aricept®) is a piperidine reversible inhibitor of AChE that displays increased activity and selectivity that means it has fewer adverse effects and can be tolerated in higher dose with limited side effects such as nausea and diarrhea[104]. Rivastigmine (Exelon®) is a long-acting pseudo-irreversible AChE inhibitor generally well tolerated; indeed, the side effects usually concern the gastrointestinal system.

Galantamine (Reminyl®) has a more complex biological profile, because besides AChE inhibitory activity it is able to activate nicotinic acetylcholine receptors. This dual mechanism of action could potentially increase its potency as cognitive enhancer drug[105].

Several other natural compounds potentially active in AD treatment are currently under investigation as cognitive enhancing agents. Among these, Huperzine A, an alkaloid isolated from the Chinese traditional herb *Huperzia Serrata*, is a potent, selective, and long-acting AChE inhibitor, and it is endowed with high efficacy in improving memory in different animal models and clinical trials. (see section 1.3 for further discussion about AChE inhibitors)

The palliative nature of AChE inhibitors based strategy is the most commonly objection against cholinergic hypothesis and, although reduction in ACh pathways has been shown in biopsies from AD patients within a year of onset of symptoms[106]. It is not completely clear if the cholinergic deficit occurs early in the course of the disease or it is a consequence of other pathological events. It seems clear that the AChEIs capability to relieve symptoms of AD may depend on the integrity of the neuronal cholinergic system and, in severe cases, it could result insufficient. Moreover, significant variability exists in the response to the AChE inhibitors treatment, with some subjects apparently resulting unresponsive at any tested dose. While the ultimate goal for AD treatment would obviously involve the pathogenesis and aetiology of the disease, clinical use of AChE inhibitors have shown a temporary stabilization of cognitive impairment. Despite the controversial debate upon the cholinergic hypothesis and the development of several new approaches for AD treatment not related to the modulation of cholinergic activity, this theory is far from being considerate merely an historical approach. Some investigators have recently reported an apparent retardation of the progression of the neurodegenerative process in patients treated with AChEIs. Furthermore, the finding that non classical modulation of AChE activity can interfere with the accumulation and precipitation of Aβ, hence, downstream, with the deposition of senile plaques, could afford a rational link between the two more important strategies of AD therapy[107]. Therefore, it seems that the cholinergic hypothesis will continue to drive drug discovery with the aim to design and synthesize new multipotent AChEIs combining the ability to increase the cholinergic response with inhibition of the Aβ-aggregation deposition.

Anti-amyloid Strategies

Within the years, the so called “Amyloid hypothesis” has assumed a central role in understanding the mechanisms leading to neuronal death in AD. Therefore, it is not surprising that many efforts have

concentrated in reducing/modulating Aβ-production[42,108.] Indeed, the decrease of Aβ in the brain should ameliorate the symptoms of Aβ and this could be achieved by interfering at different level of the Aβ cascade.

- *Lowering Aβ production: Secretase inhibition*

Two secretases are involved in the cleavage of APP leading to Aβ release and formation of β-amyloid plaques: β-secretase (BACE1 and 2) and γ-secretase.

In particular, BACE1 seems to be an attractive drug target since BACE1 knockout mice do not produce Aβ[109] and its crystal structure has been recently solved[53].

To date, many peptidomimetics and non-peptidomimetics BACE1-inhibitors have been developed[52,110]. In particular, several new peptidomimetics β-secretase inhibitors were developed starting from truncated polypeptides bearing non-cleavable transition state mimicking groups.

The prototype of BACE1 peptidomimetic inhibitors of the first generation is represented by OM99-2 designed as transition-state analogue and endowed with an IC_{50} of 0.002 μM. Furthermore, using X-Ray structure-based modification of OM99-2 new low molecular weight peptidomimetics BACE1 inhibitor have been developed (**I)** (Figure 21)[111].

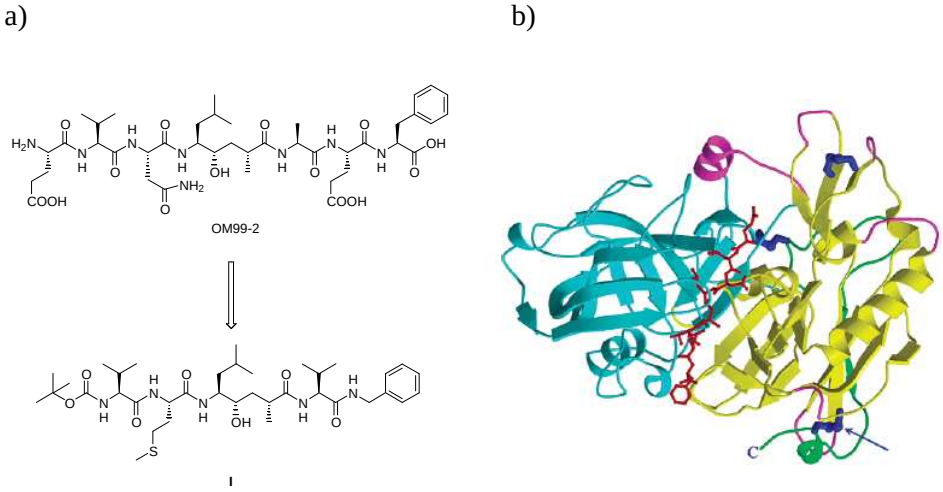

Figure 21. a) Chemical structure of peptidomimetic BACE1 inhibitors OM99-2 and **I**; b) crystal structure of OM99-2 with BACE1[110,111].

Later, cell-permeable BACE1 inhibitors able to induce reduction of Aβ in human embryonic kidney (HEK) cells have been developed by Elan/Pharmacia. Their lead compound **II** showed an IC_{50} of 0.03 μM[112]; truncation of the N-terminus and C-terminus of **II** led to the identification of the smaller peptides inhibitor **III**, with an IC_{50} of 0.3 μM[113]. Further structural modification of **III** allowed to discover **IV** as potent and cell-permeable BACE1 inhibitor, with an IC_{50} of 0.12 μM; the corresponding diacid **V** was more potent (IC_{50} = 0.02 μM) but, due the poor cell permeability, it showed no inhibition of Aβ in HEK cell (Figure 22)[114].

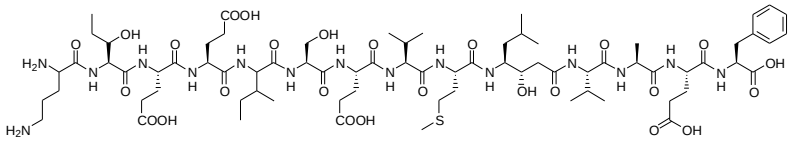

II

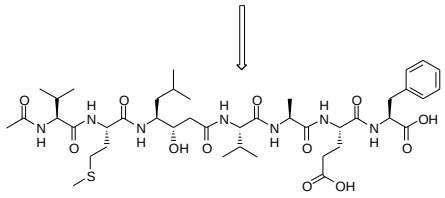

III

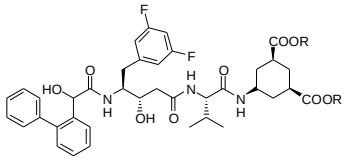

IV, R=CH_3
V, R=H

Figure 22

In 2006, a potent BACE1 inhibitor have been designed in which the tetrazole ring were introduced as bioister of the carboxylic acid to give **VI** and **VII**, which displaied an IC_{50} of 4.8 and 1.2 nM, respectively (Figure 23)[115].

Furthermore, in order to obtain better pharmacokinetic profile, compounds, characterized by an hydroxyethylamino residue, were developed on the assumption that basic nitrogen could lead to an increase in inhibitory potency. The most potend compounds of this series were **VIII** and **XI** which displaied an IC_{50} of 5 nM and 20 nM, respectively[116].

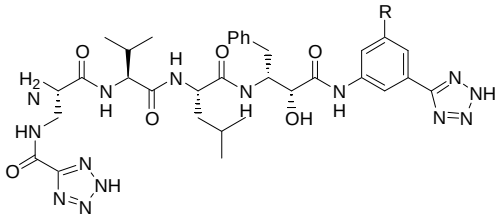

VI: R = H
VII: R = 2H-tetrazol-5yl

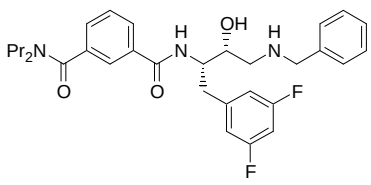

VIII, R= I
IX, R= OMe

Figure 23. Chemical structure of **VI-VII** and hydroxyehtylamino-based BACE1 inhibitors **VIII-IX**.

Inhibitors based on the peptidomimetic strategy suffer from well-known difficulties typical of polypeptides, such as poor blood–brain barrier crossing and poor oral bioavailability.

Despite many BACE1 inhibitors peptidomimetics have been designed, also many non-peptidomimetic BACE1 inhibitors have been developed[117].

In 2001, aminoethyl-substituted tetraline have been discovered and the most potent compound of the series was **X** with an IC_{50} of 0.35 μM[118]. Also Vertex disclosed several BACE1 inhibitors able to inhibit the enzyme in a micro molar range and the most potent was **XI**[119].

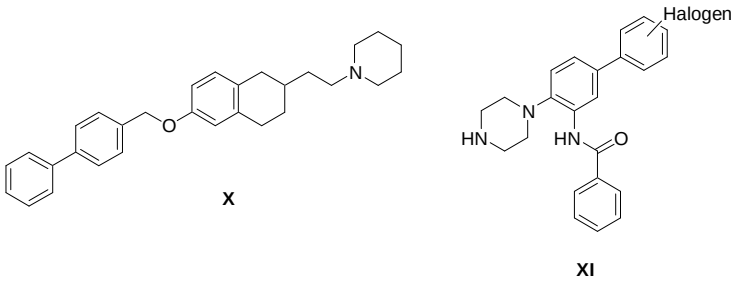

Figure 24. Most potent compound based on the aminoethyl-substituted tetraline scaffold **X**, and Vertex's inhibitor **XI**.

A series of derivatives endowed with an aminoquinazoline scaffold were discovered (**XII** and **XIII**) all characterized by high BACE1 inhibitor activity (K_i = 0.9 μM and K_i = 11 μM, respectively)[120].

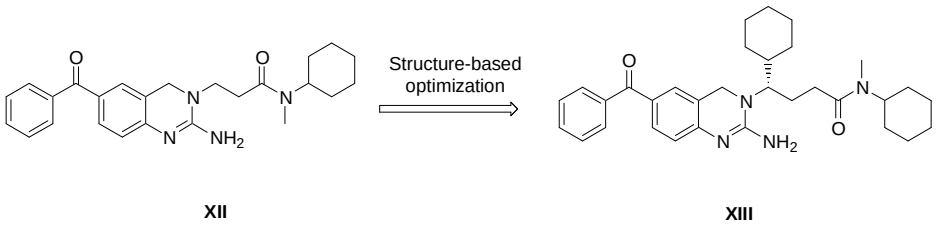

Figure 25. Aminoquinazoline-based BACE1 inhibitors.

As reported before, BACE1 represents a better pharmacological target than γ-secretase. Indeed, despite many efforts in designing γ-secretase inhibitors, interferences with Notch signalling lead to several side effects that precluded the clinical development of such inhibitors. However, compounds that inhibit γ-secretase with little effect on Notch could result useful in AD therapy[121].

One of the first γ-secretase inhibitor is the dipeptidic compound DAPT that inhibits Aβ production with an IC_{50} of 115 nM in human primary neuronal cultures[122].

A very interesting inhibitor developed by Bristol-Myers Squibb is BMS-299897 that displayed an IC_{50} of 7 nM and seemed to be selective for γ-secretase over Notch[123].

However, the most potent γ-secretase inhibitor was LY-411575 with an IC_{50} of 119 pM[124]. Unfortunately, this compound in mice interferes with maturation of B- and T-lymphocytes once again due the inhibition of Notch signalling[125].

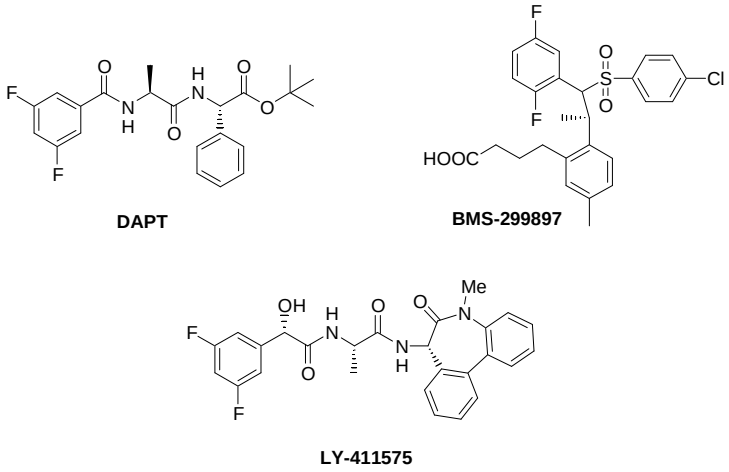

Figure 26. Some γ-secretase inhibitors.

Recently, an allotter binding site on the γ-secretase has been discovered[121].

Interestingly, some nonsteroidal anti-inflammatory drugs (NSAIDs), such as ibuprofen, indomethacin and sulindac sulfide, are able to reduce the release of $A\beta_{42}$ and to increase the release of less amyloidogenic $A\beta_{38}$[126]. The effect of NSAIDs on amyloidogenic-pathway is not mediated by interaction with COX but they interact directly with the γ-secretase complex. However, despite the mechanism of action of the NSAIDs on γ-secretase is not elucidated, seems that NSAIDs do not interfere with the Notch[127].

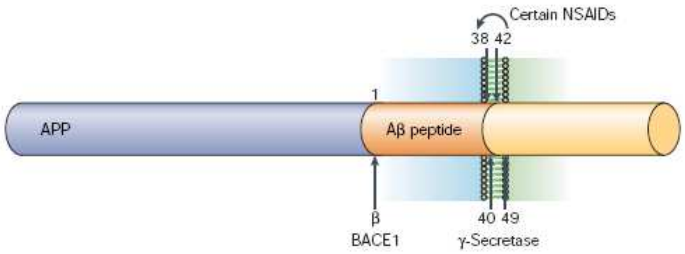

Figure 27. Modulation of γ-secretase cleavage by NSAIDs[46].

Thanks to these studies, the NSAID *R*-flurbiprofen (Tarenflurbil®) is now in Phase III clinical trials in the US for AD treatment. It modulates the A*β*-production without interacting with COX; however, it is important to point out, that the other enantiomer, *S*-flurbiprofen, is the active inhibitor of COX[128].

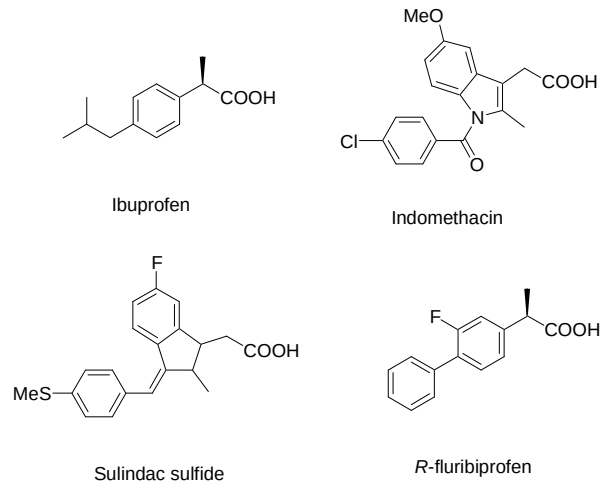

Figure 28. NSAIDs modulators of γ-secretase.

Recent studies led to the discovery of a nucleotide binding site on the γ-secretase complex; this site allows to allosteric modulation of γ-secretase without affecting the Notch pathways. ATP increase A*β* production and, therefore, compounds interacting with the ATP binding site could be potential useful in AD. Among these compounds, Imanib, an Abl kinase inhibitor, is able to inhibit the A*β* production and it does not interact with the Notch pathway[129].

- *β-sheet breakers*

Amyloid plaques are one of the characteristic hallmarks of AD leading to neuronal death. Therefore, compounds able to interfere with the refold and/or the formation of A*β*-aggregates should have neuroprotective effects[88,130].

Soto and coworkers proposed that short peptide able to bind A*β* may destabilize, in principle, the amyloidogenic A*β* conformer and preclude amyloid formation[131]. They developed a series of peptides based on the structure of the central hydrophobic regions within the N-terminal domain of A*β*-protein; in order to disrupt β-sheet formation they inserted a proline moiety. Among the different small polypeptides designed, the most active on different models was **XIV**.

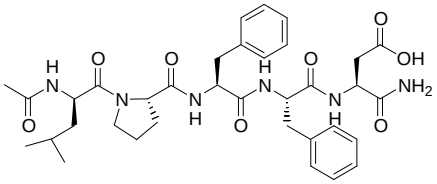

XIV

Figure 29. Structure of Soto's pentapeptide.

These peptides initially bind to Aβ and the formed complex is stabilized by hydrophobic interaction. Then, the peptides induce conformational changes in the β-sheet structure. This is probably due the presence of proline which can interconvert its *cis* and *trans* conformation.

However, it is well known that peptides have poor drug-like profile mainly due their pharmacokinetic characteristics.

Nevertheless, other compounds are able to induce disaggregation of Aβ-fibrils such as the antibiotic Rifampicin and Daunomicin[132] .

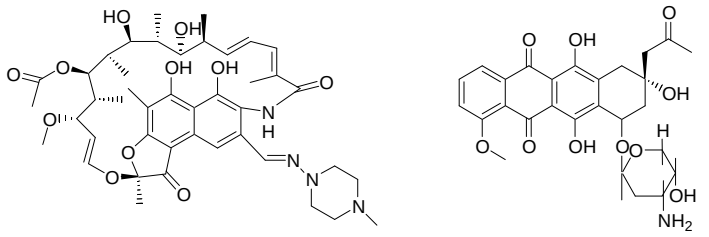

Figure 30. Chemical structures of Rifampicin and Daunomycin.

- *Cholesterol-reducing approach*

Several experimental evidences show that cholesterol modulated the Aβ production[46,108]. Although the mechanism of how cholesterol can influence this metabolic pathway is not well clear, it seems that high cholesterol levels favourites the BACE-mediate APP proteolysis (the amyloidogenic pathway) while low cholesterol levels increase the APP processing *via* α-secretase[133]. Indeed, agents able to reduce the cholesterol concentration, such statins, show a decrease level of Aβ in mice and guinea pigs[134,135].

A very promising approach could be the use of inhibitors of acyl-coenzyme A cholesterol acyltransferase; this enzyme catalyzes the formation of cholesteryl-esters from cholesterol and its inhibition lead to a reduction in Aβ formation[49].

- *Aβ immunotherapy*

This new approach directed towards Aβ_{42} derived from the first observation, by Shenk and coworkers, about the reduction of APP levels in transgenic mouse after vaccination with aggregated Aβ_{42}[136].

The mechanism of how this reduction takes place is not well known, however, three different mechanisms[81] have been proposed in order to explain such findings:

1. antibodies bound to Aβ in the brain and trigger microglia to Aβ phagocytose via Fc-receptors;
2. antibodies may behave as chaperone and destroy or prevent Aβ aggregation[137] ;
3. antibodies may sequester Aβ in the plasma inducing a rapid efflux of Aβ from the brain[138,139].

Noteworthy, the first A$\beta_{1\text{-}42}$ antigen in clinical trial displayed very promising results in ameliorate the Aβ-associated AD's signs; however, it had to be stopped in Phase II because it induces T-cell mediate autoimmune response[140,141].

- *Metal-chelating approach*

High concentrations of metal ions, such as Cu^{2+}, Fe^{2+}, and Zn^{2+}, have been found within Aβ deposits in AD brains. Metal ions have been shown to modify the Aβ peptide and to induce its aggregation. Therefore, metal-chelators can solubilise Aβ in AD brains[142].

Several metal chelators developed, such as diethylenetriaminepentaacetic acid (DTPA), triethylenetetraamine (TETA), and desferrioxamine (DFO), beside their ability to chelate metal ions, were able to reduce the production of hydrogen peroxide derived from the interaction of Cu^{2+} and Fe^{3+} with A$\beta_{1\text{-}42}$ [143].

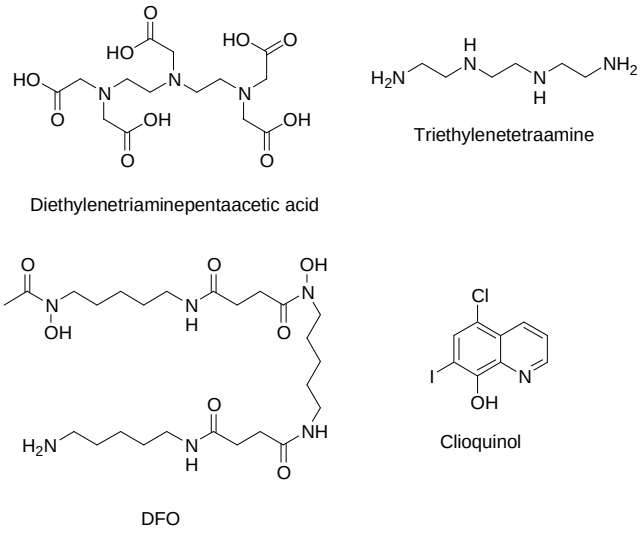

Figure 31. Chemical structure of different metal-chelators.

Another metal-chelator is clioquinol. Clioquinol, already known as antifungal and antiprotozoal drug, is able to chelate metal ions and to induce reduction of Aβ accumulation[144].

However, although a metal chelator could represent a promising agent to reduced metal-mediated brain injury, their protracted use could present serious side effects by interfering with the normal function of physiological metalloenzymes.

- *τ-hyperphosphorylation directed strategies*

Neurofibrillary tangles (NFTs) are typical AD markers and are aggregates composed of highly phosphorylated τ protein. Inhibition of the formation of such aggregates could represent a promising approach in AD's treatment. This goal could be achieved following different approaches.

The first one is the development of τ-kinases inhibitor; indeed; τ-protein posses many phosphorylation sites and many important kinase target τ, such as glycogen synthase kinase 3β (GSK-3), microtubule-affinity-

regulating kinase (MAPK) and protein kinase A. Unfortunately, not so many inhibitors of these kinases have been developed.

At the same time, activation of phosphatases could lead to a restoration of correct τ functionality. Nevertheless, also in this field the research did not provide significant progress yet; on the other hand, it was reported that Memantina inhibits τ hyperphosphorylation by restoration of protein Phosphatases PP2A activity[145].

Molecules that can inhibit τ-aggregation should be useful to protect neurons against neurofibrillary tangles. Therefore, many small molecules as τ-aggregation inhibitor have been developed[146].

An appealing class of τ-aggregation inhibitors is based on the rhodanine scaffold. In 2007 Waldmann and coworkers reported several derivatives of rhodanines (2-thioxothiazolidin-4-ones)[147].

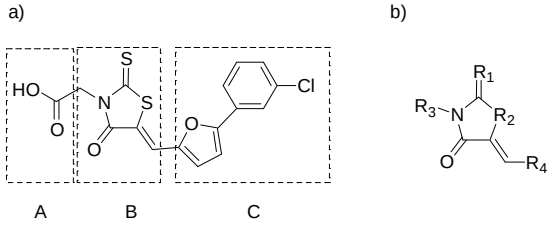

Figure 32. a) Structure of the hit compound rhodanine b) Variations of the core[147].

In general, the presence of a carboxylic acid function is important for the disassembly activity *in vitro* because its esterification or its replacement with an imidazole or benzimidazole group lead to a decreased activity. The modification of the heterocyclic side chain leads to reduction of the activity as well as modification of the aromatic side chain. These two elements seem to be important to establish hydrophobic or π-stacking interactions with τ-protein. Structure-Activity Relationships based on rhodanine-derivatives designed by Waldmann and coworkers are summarized in Figure 33:

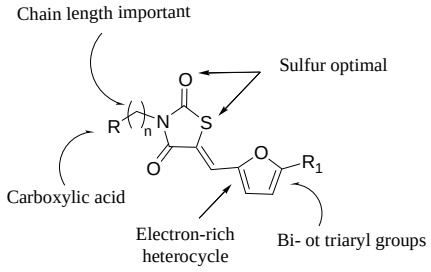

Figure 33. Structure-activity relationships of rhodamine derivatives[147].

Furthermore, N-phenylamines and Anthraquinones display inhibitory effects on *τ*-aggregation. In particular, in the anthraquinone series, it is important to point out that all derivatives, endowed with this particular biologica property, present a tricyclic structure with one or more β-hydroenone groups[148].

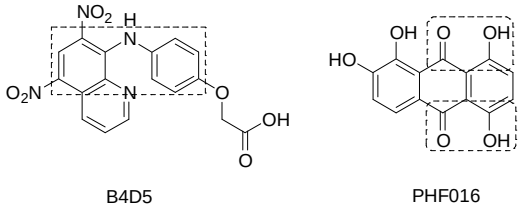

B4D5 PHF016

Figure 34. Selected examples of N-phenylamines (B4D5) and Anthraquinones (PHF016).

FMoreover, Benzothiazole-based compounds have been developed. Such compounds present a cationic charge that could interact by electrostatic bond with the target and the benzothiazole ring may establish additional hydrophobic interactions. Among these derivatives, N744 displays the higher activity with an IC_{50} of 300 nM[149].

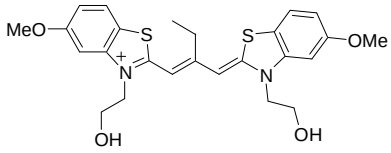

N744

Figure 35. Chemical structure of the Benzothiazole N774.

Phenothiazine derivatives also display inhibitory activity toward *τ*-aggregation; in particular, Thionin display an IC_{50} of 12 μM and its activity is probably due to the planarity of the central core (Figure 36)[148].

Porphyrin, such as Hemin, is the only organometallic example of *τ*-aggregation inhibitor. The metal ion is fundamental for the activity since its analogue, lacking the metal, is less active. The mechanism of action is not clear; however, it is also able to inhibit $A\beta_{42}$ aggregation by coordinating histidine residue and this could explain also the *τ*-aggregation inhibitory effect[148].

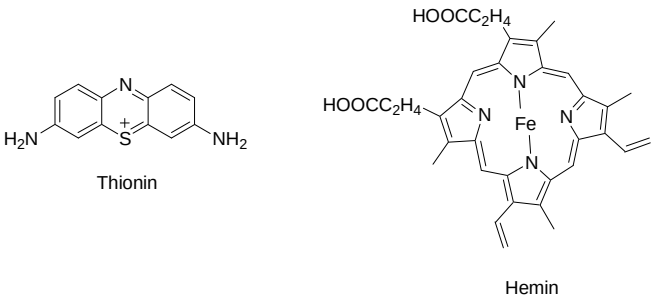

Figure 36. Structure of Thionin and Hemin.

- *Targeting NMDAR-mediated neurotoxicity:*

Among the several biochemical pathways leading to neuronal death in AD, NMDAR plays a key role[84]. Its excessive activation, leading to toxic levels of Ca^{2+} in the cells, has been observed and therefore the use of NMDAR antagonist may represent a useful therapeutical approach[81]. However, many NMDA receptor antagonists also produce highly undesirable side effects at doses within their putative therapeutic range. Nevertheless, the only drug approved for AD treatment that does not interfere with the cholinergic system is an antagonist of NMDAR, Memantine. It was approved in 2003 in US for the treatment of moderate to severe cases of AD[150]. It is a non-competitive NMDAR antagonist derived from amantadine, an anti-influenza agent. Memantine exerts its effect on NMDAR activity by binding at or near the Mg^{2+} site within the ion receptor channel.

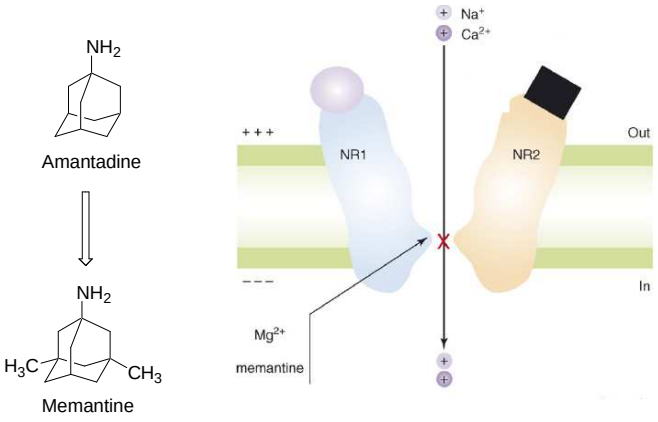

Figure 37. Chemical structure of Amantadine and Memantine and its binding site on NMDAR[84].

- *Antioxidant therapy*

ROS and other radical species are deeply involved in the cellular damage leading to neuronal death. Radical scavenger would protect cells from free radicals because they are able to accept a radical or a free

electron. Many free radical scavengers are known, such as vitamin E and C, melatonin, flavonoids and carotenoids, and none of them shows serious side effects[88].

Vitamin E (α-Tocoferol) and its analogue Raxofelast and MDL 74180DA, exerts antioxidant and anti-apoptotic properties in various experimental models of AD; they have been successfully tested in clinical trials[151].

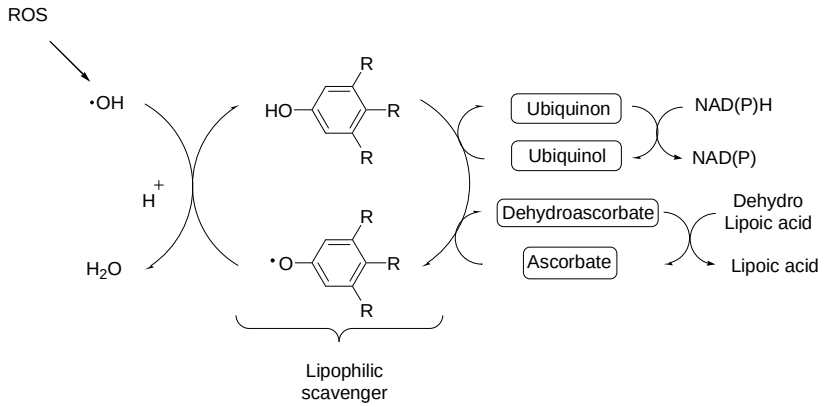

Figure 38. Radical scavenger action[151].

Furthermore, it has been reported that derivatives of estradiol, as 17β-estradiol and its isomer 17α-estradiol and their analogues, block the intracellular accumulation of ROS. Interestingly, 17β-estradiol reduces the formation of $A\beta_{40}$ and $A\beta_{42}$ from APP[152].

Perhaps, the most promising radical scavenger is Melatonin. It is a hormone able to react with hydroxyradical forming non-toxic derivatives that are easily metabolized[153]. In addition, it reacts with peroxynitrile and ROS and displaing other interesting activities, such as the inhibition of the amyloid fibril formation and anti-apoptotic effects[154].

N-acetylserotonin, a melatonin precursor, inhibits lipid peroxidation and shows higher anti-amyloid activity than melatonin[155].

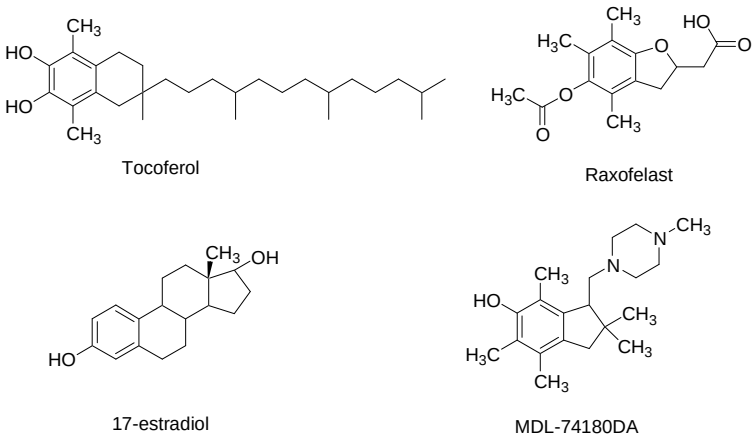

Figure 39. Selected examples of antioxidants.

1.1.3 The "Multi-Target-Directed Ligand" approach in AD

The "one-molecule-one-target" paradigm has led to the discovery of many successful drugs, and it will probably remain a milestone for years to come. However, it should be noted that a highly selective ligand for a given target does not always result in a clinically efficacious drug. This may occur because:

a. the ligand does not recognize the target *in vivo*,
b. the ligand does not reach the site of action,
c. the interaction with the respective targets does not have enough impact on the diseased system to restore it, effectively.

Reasons for the latter might lie in the multifactorial nature of many diseases. Drugs hitting a single target may be inadequate for the treatment of diseases like neurodegenerative syndromes, diabetes, cardiovascular diseases, and cancer, which involve multiple pathogenic factors. When a single medicine is not sufficient to effectively treat a disease, a multiple-medication therapy (MMT) (also referred to as a "cocktail" or "combination of drugs") may be used. Usually, an MMT is composed of two or three different drugs that combine different therapeutic mechanisms. But this approach might be disadvantageous for patients with compliance problems. A second approach might be the use of a multiple-compound medication (MCM) (also referred to as a "single-pill drug combination"), which implies the incorporation of different drugs into the same formulation in order to simplify dosing regimens and improve patient compliance. Finally, a third strategy is now emerging on the basis of the assumption that a single compound may be able to hit multiple targets.

In the Multi-Target-Directed Ligand (MTDL) approach to drug discovery, a drug could recognize (in principle, with comparable affinities) different targets involved in the cascade of pathological events leading to a given disease. Thus, such medication would be highly effective for treating multifactorial diseases[7,156].

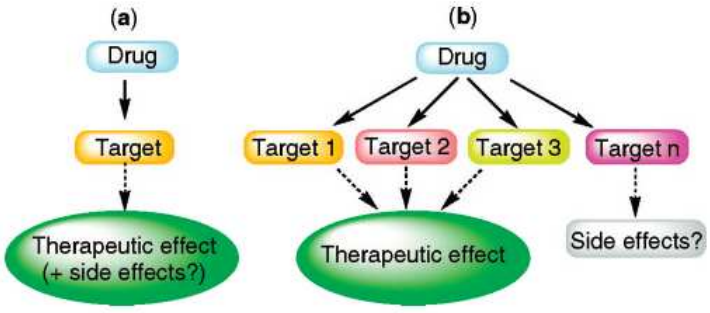

Figure 40. Pathways leading to the discovery of new medications: (a) Target-driven drug discovery approach; (b) MTDLs approach to drug discovery[7].

Although the pathogenesis of AD is not yet fully understood, it is a multifactorial disease caused by genetic, environmental, and endogenous factors. The central event in AD pathogenesis is an imbalance between Aβ production and clearance. The enhanced activity of β- and γ-secretases leads to increased release of amyloidogenic Aβ_{42}, which forms oligomers and then extracellular deposits (senile plaques). One way to confront AD pathogenesis may be to combat the oligomerization by means of small molecules. A role for metal ions and ROS in the Aβ oligomerization has also been advanced. Therefore, metal chelation and antioxidant activities are two general mechanisms to be considered in the search for disease-modifying anti-AD drug candidates. Also, β- and γ-secretase inhibitors may be promising lead compounds because they tackle an early event in AD pathogenesis. Mitochondrial dysfunction plays a fundamental role in the neuronal death associated with AD, as it is likely that intracellular Aβ could compromise the function of this organelle. τ hyperphosphorylation leading to tangle formation is regarded as a downstream event but could contribute to reinforcing neuronal dysfunction and cognitive impairment. Moreover, neuroinflammation of CNS cells has been recognized as an invariable feature of all neurodegenerative disorders. Therefore, MTDLs emerge as valuable tools for hitting the multiple targets implicated in AD aetiology.

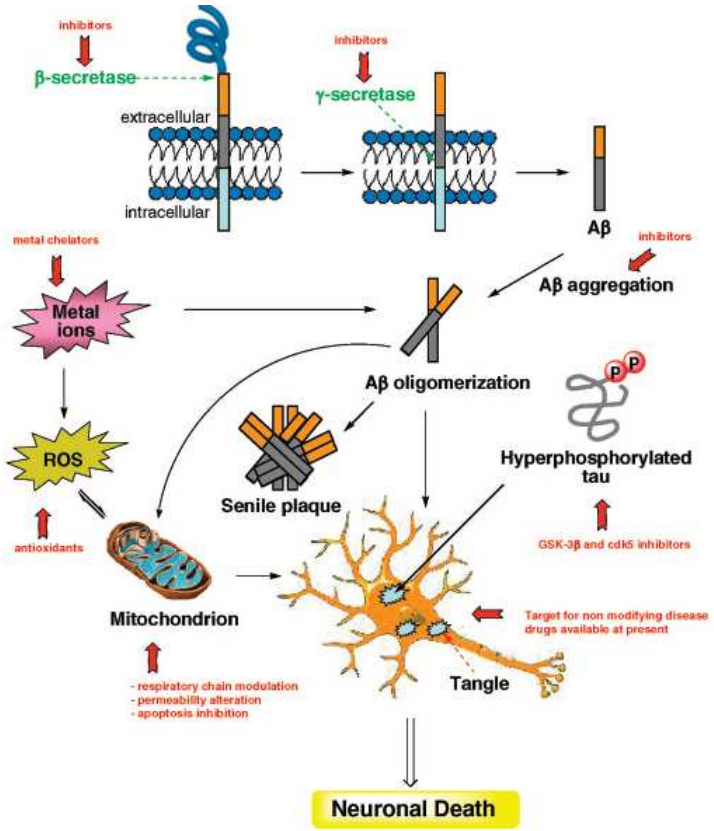

Figure 41. Possible molecular causes of neuronal death and protective mechanisms in AD.

To obtain novel MTDLs, a design strategy is usually applied in which distinct pharmacophores of different drugs are combined in the same structure to afford hybrid molecules. In principle, each pharmacophore of these new drugs should retain the ability to interact with its specific site(s) on the target

and, consequently, to produce specific pharmacological responses that, taken together, should slow or block the neurodegenerative process. One of the most widely adopted approaches in the field has been to modify the molecular structure of an AChEI in order to provide it with additional biological properties useful for treating AD. Some MTDLs developed for the treatment of AD are following reported.

Dual Binding AChEI

In the MTDL design strategy context, major research efforts have been devoted to the development of the so-called "dual binding site" AChEIs. By simultaneously interacting with AChE catalytic and peripheral sites, these AChEIs might address the disease mechanisms by reducing Aβ aggregation[157]. Indeed, Inestrosa and coworkers discovered that AChE exerts Aβ pro-aggregating action[158]. AChE promotes the formation of Aβ fibrils by PAS of the enzyme and therefore, AChE inhibitors able to bind at PAS can block pro-aggregating action of the enzyme[107,159].

Several molecules are able to bind PAS such as propidium, decametonium, ambenonium, and also donepezil.

The above mentioned involvement of AChE in non-cholinergic action drives medicinal chemists to design molecule able to bind simultaneously both sites of AChE[160].

Pang and coworkers developed dimers of tacrine with the aim to increase its affinity towards AChE. The most potent of the series was **XV**, which resulted 500-folds more potent than tacrine in inhibiting *h*AChE[161]. Furthermore, this compound acts NMDAR as antagonist[162], as inhibitor of the nitric oxide synthase and it is able to reduce *in vitro* Aβ formation by inhibition of BACE-1[163].

Several structure-activity relationships have been carried out on these compounds that are summarized in Figure 42.

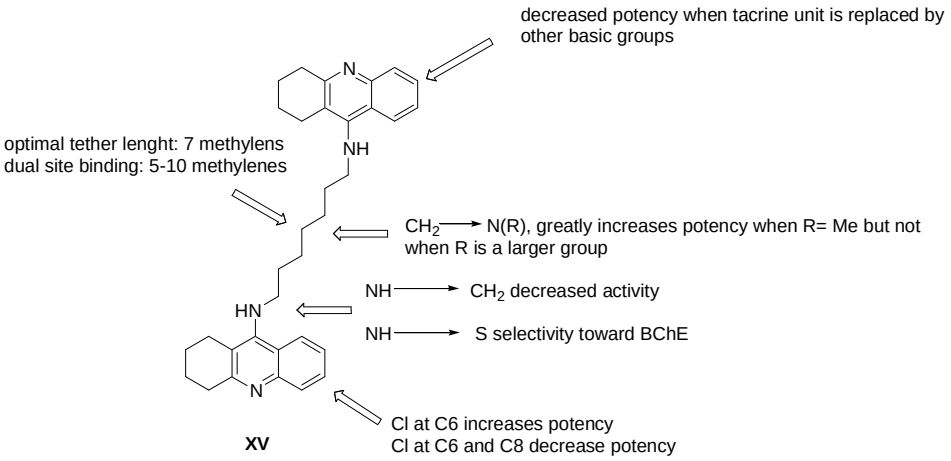

Figure 42. Structure-Activity relationships of Bis-tacrine derivatives[160].

In 2003, Sharpless and coworkers developed an elegant target-guided *in situ* click-chemistry approach to obtain new dual-binding AChE inhibitors[164]. In this approach, they chose tacrine as catalytic-site inhibitor

and phenylphenanthridium and other molecules as PAS-inhibitor and these compounds were decorated with alkyl-azide and alkyl-acetylene of varying chain length to allow to undergo to a Huisgen 1,3-dipolar cycloaddition leading to 1,2,3-triazole ring. The reaction was carried out in the presence of AChE to facilitate the formation of the desired product. Therefore, a series of 49 binary mixture of reagent were incubates in *Electrophorus electricus* AChE potentially give rise to 98 products but only one was formed (**XVI**) (Figure 43 and 44).

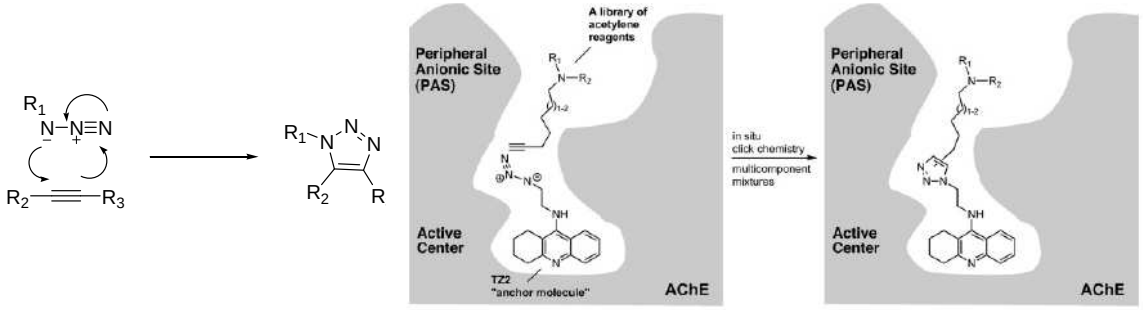

Figure 43. a) Huisgen 1,3-dipolar cycloaddition; b) *In situ* AChE-mediated click chemistry[164,165,166].

XVI is one of the most potent AChE inhibitor having K_d values between 77 fM (*Torpedo Californica* AChE) and 410 fM (*murine* AChE) while tacrine and propidium are 18 and 1100 nM on *murine* AChE respectively. It is important to point out that the **XVI** *anti* isomer was not obtained using this approach and it was chemically synthesized and resulted less active by two-order of magnitude in comparison with its *syn* isomer.

X-Ray structure of both *syn* and *anti* isomer of **XVI** complexes with murine AChE confirmed that **XVI** is a dual-binding inhibitor and the triazole ring is not just a passive linker but establish hydrogen-bonding and stacking interactions with amino acids in the AChE mid gorge[165,166].

a) b)

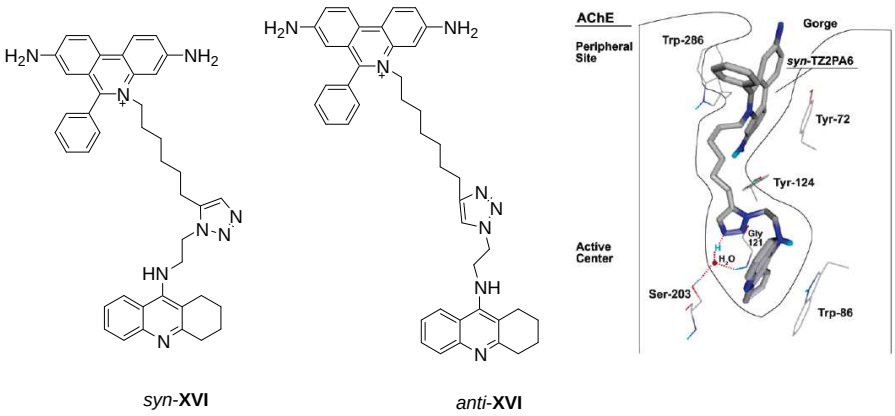

syn-**XVI** *anti*-**XVI**

Figure 44. a) Chemical structure of **XVI**; b) X-Ray of **XVI** in mouse AChE[164,165,166].

Caproctamine represents one of the first examples of a successfully designed dual-binding AChEI endowed with additional pharmacological effects beneficial in AD. Caproctamine, developed from Benextramine using the universal template approach (Figure 45), emerged as an effective pharmacological tool in AD because of a well-balanced affinity profile as AChEI and competitive muscarinic M_2 receptor antagonist[167]. Caproctamine is able to interact with both AChE sites, and antagonism of muscarinic M_2 autoreceptors would facilitate the release of ACh in the synapse.

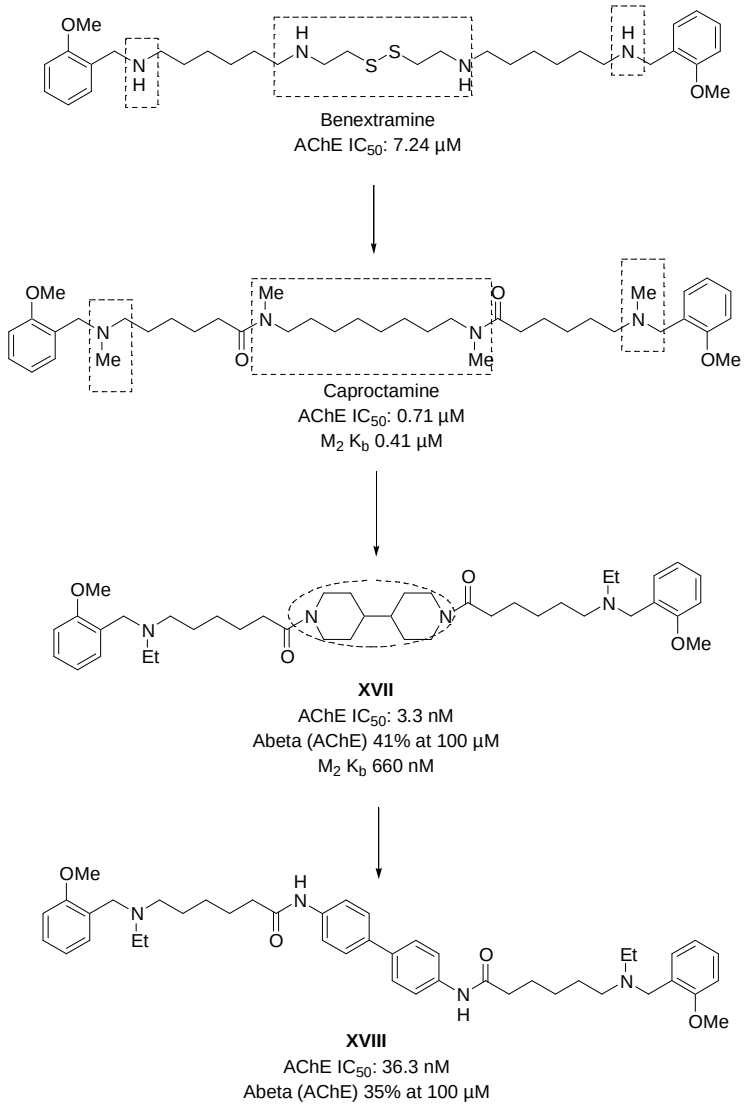

Figure 45. Design of Caproctamine and derivatives.

SAR studies carried out on Caproctamine structure were expanded the role of the octamethylene spacer separating its two amide functions. This was performed by its replacement with less flexible dipiperidine and dianiline moieties (Figure 45). Compound **XVII** and **XVIII** were the most potent AChEIs and they displayed significant muscarinic M_2 receptor antagonism. Although all the derivatives caused a mixed type of AChE inhibition (active site and PAS), only **XVII** and **XVIII**, which bear an inner constrained spacer, were able to inhibit AChE-induced Aβ aggregation to a greater extent than donepezil (see section 1.4 for further details about caproctamine and derivatives).

Another interesting compound is AP2238 that was designed by combining in the same molecule two different moieties for an optimal interaction with both AChE sites (Figure 46). It showed the ability to counteract Aβ aggregation with a higher potency than other tested AChEIs[168].

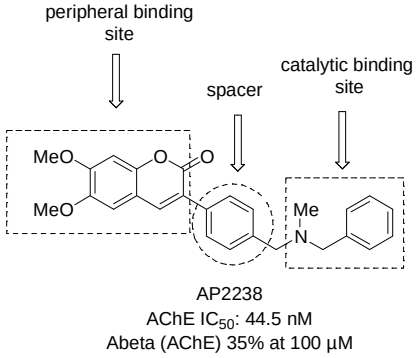

Figure 46. Design strategy leading to AP2238.

Dual binding site AChEIs were designed by linking pharmacophoric groups of both AChE sites ligand with a polyamine chain as spacer. The structural motif of propidium was linked to the tetrahydroaminoacridine system of tacrine affording novel heterobivalent polyamine ligands (Figure 47). Heterodimerization resulted in a remarkable increase in AChE potency. Indeed, compound **XIX** was nearly 20000-fold more potent than propidium and 300-fold more potent than tacrine in preventing the proaggregating effect of AChE toward Aβ[169].

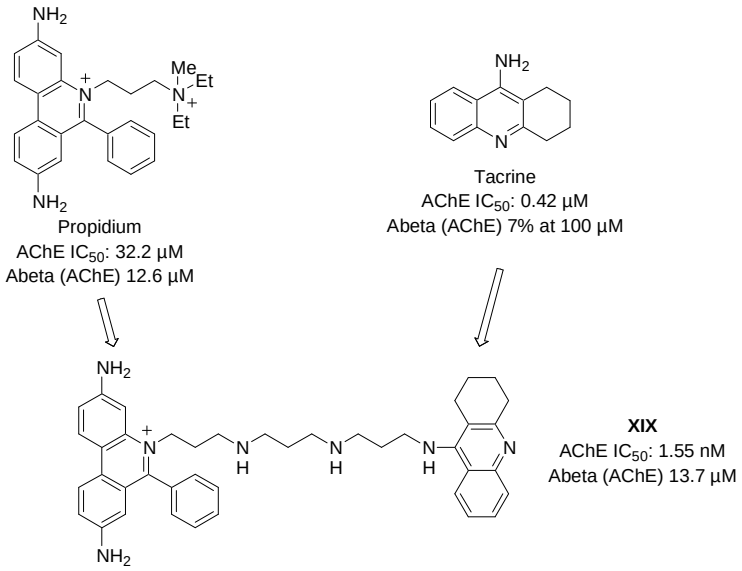

Figure 47. Design strategy leading to **XIX**.

An improved AChE-induced Aβ aggregation inhibitory profile was shown by a series of heterodimers in which a 1,2,3,4-tetrahydroacridine moiety of tacrine was linked through a proper spacer to an indole ring suitable for PAS interaction (Figure 48). In particular, compounds **XX** and **XI** emerged as the most potent AChEIs of the series, displaying IC_{50} values of 20 and 60 pM, respectively and they are the most potent derivatives so far reported to inhibit the AChE-mediated Aβ aggregation[170] .

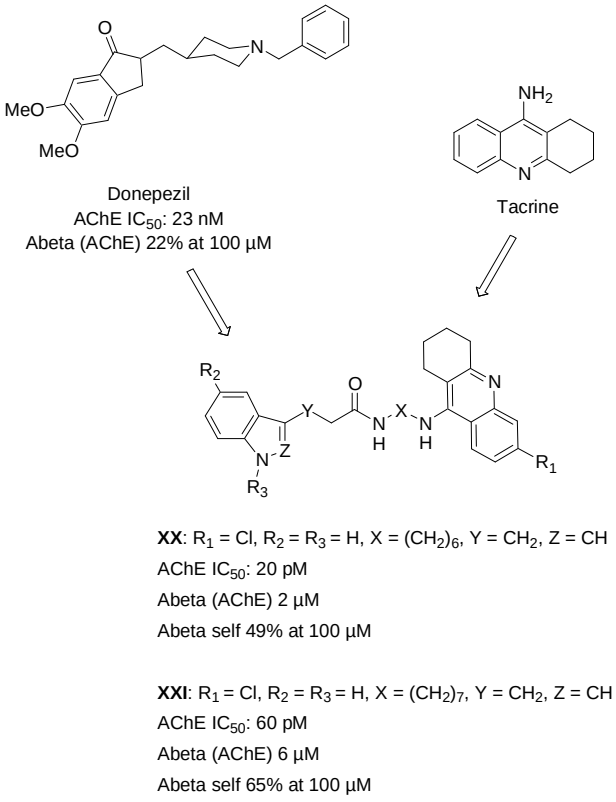

Figure 48. Design strategy leading to dual binding site AChEIs.

AChEIs Targeting Other Neurotransmitter Systems

There is a well-documented link between neurotransmitter systems changes occurring in the brain of AD patients and clinically observed symptoms, such as cognitive decline and neuropsychiatric abnormalities. However, behavioural change is related not only with the severity of cholinergic loss but also to alterations in the serotoninergic and noradrenergic systems.

Ladostigil is an important example of multimodal drug which combines in a single molecule the neuroprotective effects of a selective monoamine oxidase (MAO)-B inhibitor (rasagiline), with the AChE inhibitory activity of the anti-Alzheimer drug rivastigmine. Ladostigil is now finishing phase II clinical studies for the treatment of dementia with PD-like symptoms and depression[171] . It was rationally designed by assuming that the ability to inhibit AChE activity might be conferred by the introduction of a carbamate moiety in the structure of rasagiline, which is a MAO-B inhibitor with *in vitro* and *in vivo* neuroprotective activity (Figure 49). MAO inhibition is an interesting property to be taken into account when designing MTDLs against AD. Indeed, MAOs during their catalytic activity of deamination of neurotransmitters (noradrenaline, dopamine, and serotonin), produces hydrogen peroxide, which represents a source of ROS for vulnerable neurons affected by AD[172].

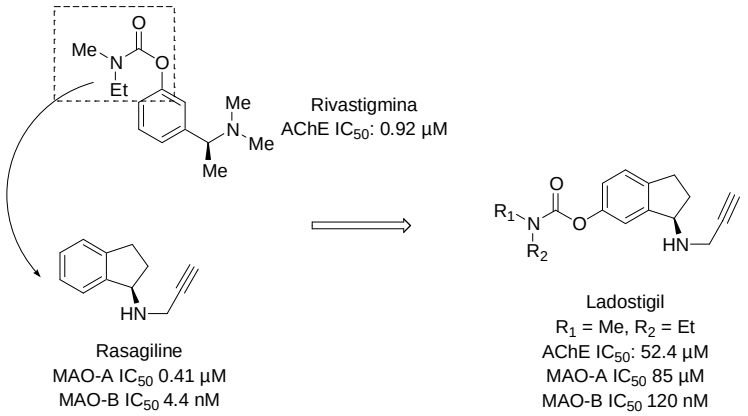

Figure 49. Drug design leading to Ladostigil.

In addition to MAO inhibitors, depression in AD patients has been successfully treated with inhibitors of serotonin transporter (SERT), antidepressants that lack anticholinergic action. Thus, it was reasoned that combining SERT and AChE inhibitory activities could offer greater therapeutic benefits in AD. Successful design strategy was based on coupling rivastigmine (AChEI) and fluoxetine (SERT inhibitor), which were chosen as lead compounds to design AChE/SERT inhibitors (Figure 50)[173]. Compounds of the A series were designed by linking the methyleneoxyphenyl moiety of fluoxetine to the ethylamine function of rivastigmine[174], whereas ring-closed compounds of the B series were designed to explore the effect of the conformational restriction[175]. Between the obtained compounds, (*S*)-RS-1259 exhibited potent inhibitory *in vitro* activities against AChE and SERT (IC_{50} values of 101 and 42 nM, respectively) and, following oral administration in mice, in the brain as well.

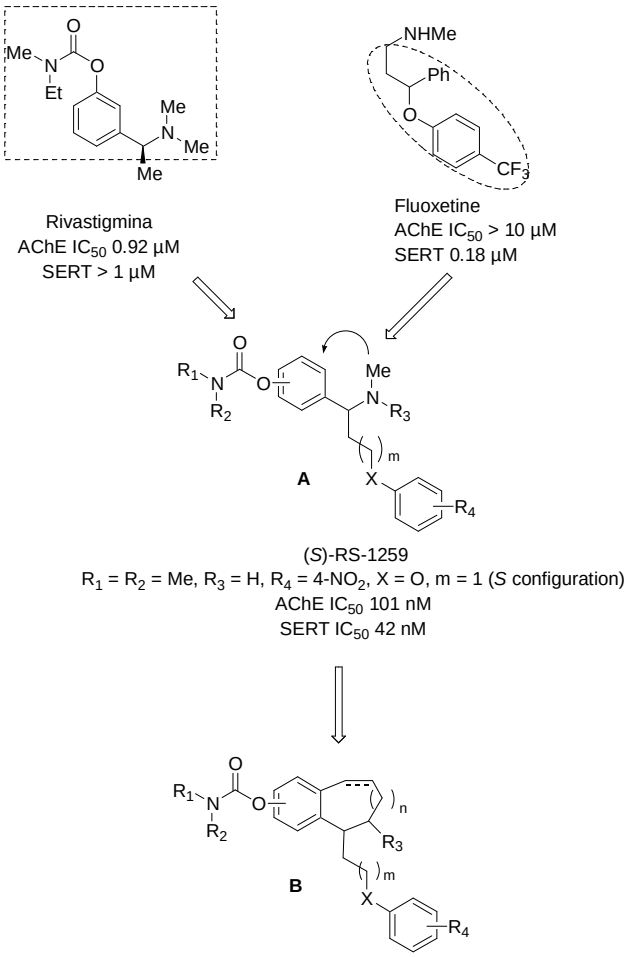

Figure 50. Drug design leading to dual inhibitors of AChE and SERT.

Oxidative stress is recognized as a central feature of AD pathogenesis. Treatments that specifically target sources of ROS have, therefore, attracted particular attention. On this purpose, the structure of Lipoic acid (LA), an antioxidant, was combined with that of an inhibitor of the AChE catalytic site, such as tacrine; moreover, it has argued that the cyclic moiety of LA could interact with AChE PAS, which is associated with Aβ aggregation. Thus, this strategy allowed to combine the antioxidant properties of LA with the AChE inhibition ability of tacrine to improve cholinergic transmission, inhibit Aβ aggregation, and control oxidative damage[176]: this led to a new class of compounds whose prototype was Lipocrine (Figure 51).

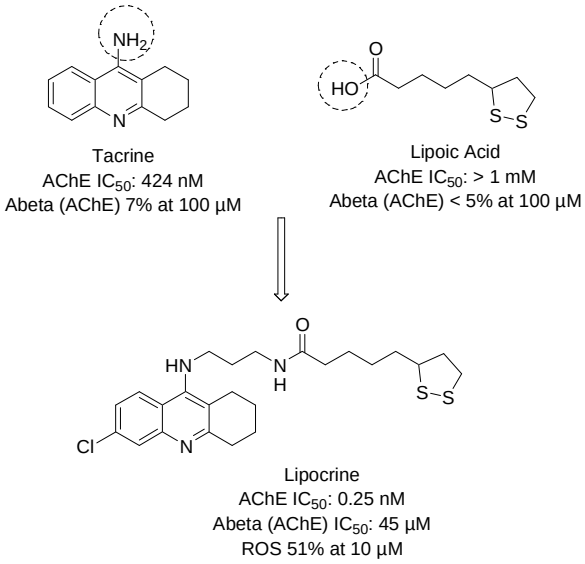

Figure 51. Design strategy leading to Lipocrine.

Lipocrine is a potent, mixed-type AChE inhibitor, exhibiting an IC_{50} value of 0.25 nM. It also inhibits AChE-induced Aβ aggregation with an IC_{50} at 45 µM and, as expected, the fragment of LA confers antioxidant properties, as revealed by the ability of 50 µM, to inhibit ROS formation in a cellular assay[177].

Dishomeostasis of cerebral metals in brain is another clear-cut factor contributing to the neuropathology of AD. On the basis of a novel "pharmacophore conjugation" concept, the bifunctional molecule **XXII** (Figure 52) has been reported as an innovative metal-complexing agent that specifically targets amyloid. **XXII** contains in its structure one metal-chelating and two amyloid-binding moieties and it reduced Zn^{2+}-induced Aβ precipitation and *in vitro* APP expression and attenuated cerebral Aβ amyloid pathology in PS1/APP transgenic mouse model[178].

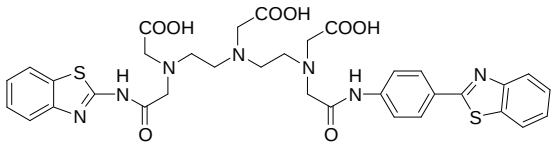

Figure 52. Structure of **XXII**.

In 2007, Melchiorre and coworkers reported on a strategy to convert dual-binding AChEI, bis-(7)-tacrine, in triple function agents. The inner polymethylene spacer of bis-(7)-tacrine, a well known AChEI, has been replaced by the inner spacer characteristic of bw284c51 and ambenonium. These spacers have been choosing because they are endowed with carbonyl and oxamide functions characterized by metal-chelating properties.

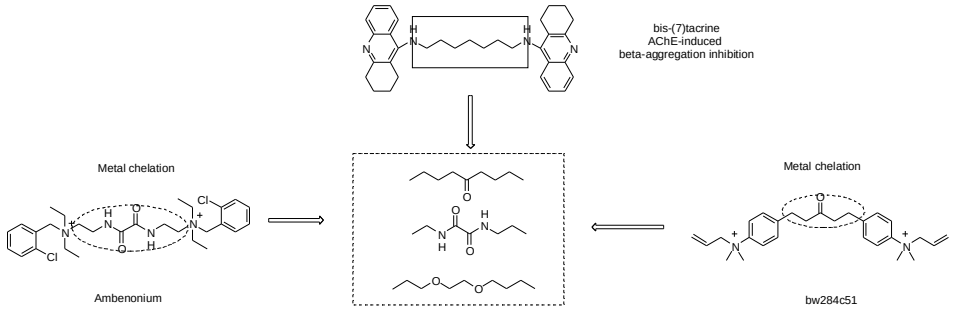

Figure 53. Design strategy leading to bis-tacrine metal-chelating.

Indeed, the designed compounds, beyond their biological properties mediate by AChE-inhibition, have additional properties by acting as metal-chelators[179].

A very promising MTDL developed in the Melchiorre's group is Memoquin. It derives from the incorporation of the benzoquinone fragment of coenzyme Q10 into the flexible chain of caproctamine (Figure 54). The selection of this moiety was based on the finding that coenzyme Q10 has been reported to have two different beneficial actions against AD. Not only coenzyme Q10 scavenges ROS, but it might also directly inhibit the deposition of Aβ in the brain[180].

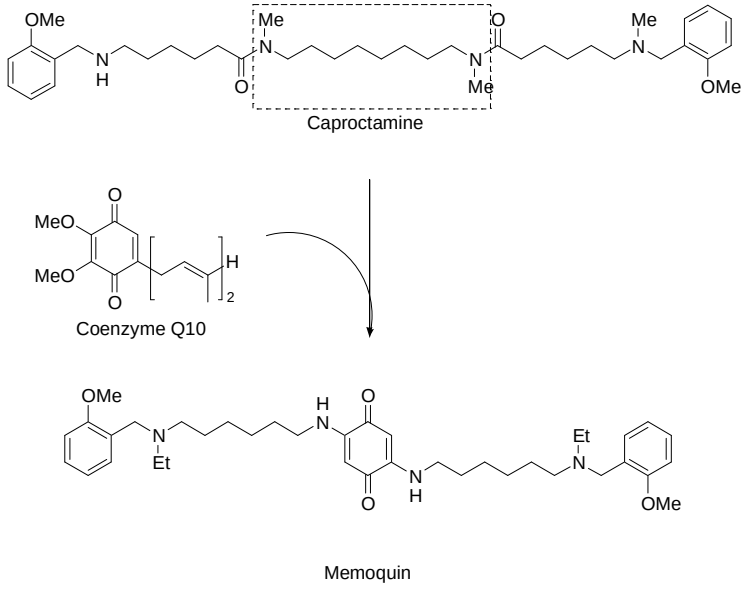

Figure 54. Drug design for Memoquin.

The biological profile of Memoquin was then widely explored by means of both *in vitro* and *in vivo* assays to assess its therapeutic potential as MTDL for combating AD. The antioxidant activity of Memoquin was confirmed by its *in vitro* ability to neutralize radicals and to act as a substrate for the NADPH quinone oxidoreductase 1 (NQO1), an enzyme responsible for the *in vivo* transformation of Memoquin into the more antioxidant hydroquinone form. Memoquin maintained a nanomolar inhibitory potency against human

AChE, and it was able to inhibit the AChE-induced Aβ aggregation, inhibited self-assembly of Aβ. Moreover, the antiamyloidogenic profile of Memoquin was also investigated by testing its ability to act as an inhibitor of BACE-1. The compound was found to have an IC_{50} value of 108 ±23 nM. In addition, Memoquin has been tested *in vivo* in an AD 11 transgenic mouse model: it was able to ameliorate the cholinergic and cognitive impairment, and to reduce Aβ deposition and τ hyperphosphorylation at three different stages of neurodegeneration (2, 6, and 15 months of age). Moreover, Memoquin showed other promising properties, such as good oral bioavailability, efficacy in crossing the blood-brain barrier, and a favourable safety profile in preclinical non-regulatory acute and chronic toxicology studies[181,182].

1.1.4 Caproctamine and derivatives

In 1998, Melchiorre and coworkers published a study aimed to produce novel ligands based on a polyamine backbone having affinity for both AChE active and PAS sites and for M_2 AChR receptor, as well, useful for the treatment of AD[169].

This study started from the observation that Benextramine[183], a tetraamine disulfide developed as an irreversible α-adrenoreceptor antagonist, displayed also a significant affinity for cardiac muscarinic M_2 receptor and potentiate the effect of ACh on the frog rectus muscle, as well.

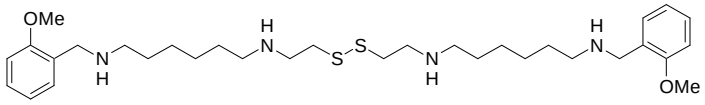

Benextramine

Structure-Activity Relationships studies on Benextramine have been performed by studying the effect of the disulfide bridge, the distance between the two nitrogen atoms and the conversion of the secondary central amines into amide functions.

Table 1. Biological activities of compounds **XIII**-**XXX**.

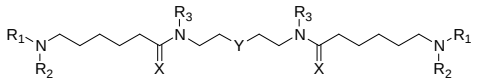

XXIII-XXX

						pIC$_{50}$		pA$_2$		
no	R_1	R_2	R_3	X	Y	AChE	BChE	M_1	M_2	M_3
Benextramine	2-MeOC$_6$H$_5$CH$_2$	H	H	H_2	S-S	5.14	5.21	nd	nd	nd
XXIII	H	H	H	H_2	S-S	3.30	3.19	nd	nd	nd
XXIV	2-MeOC$_6$H$_5$CH$_2$	H	H	H_2	CH_2	5.14	5.06	nd	6.67	5.89
XXV	2-MeOC$_6$H$_5$CH$_2$	H	H	H_2	$(CH_2)_2$	5.19	5.86	nd	6.98	5.76
XXVI	2-MeOC$_6$H$_5$CH$_2$	H	H	H_2	$(CH_2)_3$	5.35	5.43	nd	7.64	5.92
XXVII	2-MeOC$_6$H$_5$CH$_2$	H	H	H_2	$(CH_2)_4$	5.27	6.01	6.85	7.92	6.06
XXVIII	2-MeOC$_6$H$_5$CH$_2$	H	H	O	$(CH_2)_4$	5.73	4.94	nd	6.30	5.35
XXIX	2-MeOC$_6$H$_5$CH$_2$	H	Me	O	$(CH_2)_4$	6.51	5.22	nd	6.67	5.21
XXX	2-MeOC$_6$H$_5$CH$_2$	Me	Me	O	$(CH_2)_4$	6.77	4.93	5.66	6.39	5.55
tacrine						6.66	6.44	nd	nd	nd

All the polyamines designed were effective inhibitors of AChE and BChE with the exception of **XXIII** suggesting that the 2-methoxybenzyl group on the terminal nitrogen of benextramine contribute significantly to the binding with the enzyme. Replacement of the disulfide bridge of benextramine with two methylene

units led to **XXV** that was more potent than benextramine in inhibiting both enzymes. Chain length modification between the two inner nitrogen of **XXV**, affording **XXIV**-**XXVII**, did not affect significantly the affinity for AChE. Transforming the inner amine functions of **XXVII** (methoctramine) into amide groups affording **XXVIII** resulted in a reduced affinity for M_1 and M_3 muscarinic receptors and an increase potency as AChEI. Furthermore, N-methylation of **XXVIII**, affording **XXIX** and **XXX** (caproctamine) resulted in a further increase in affinity for AChE. Caproctamine resulted 42-fold more potent at AChE than benextramine and a weak antagonist at both M_1 and M_3 receptors while displaying an affinity towards muscarinic M_2 receptor similar to the affinity for AChE.

Caproctamine is a mixed type inhibitor able to inhibit both sites of AChE. Docking studies showed that caproctamine was able to simultaneously contact both sites and to establish favourable interactions with a number of residues in the gorge. At one end of the molecule, the 2-methoxybenzylamine moiety can interact with a set of residues near Trp84, while, at the opposite end, the second *2*-methoxybenzylamine group can reach the peripheral binding site that was postulated to correspond to Trp279[167].

SAR studies on caproctamine structure were performed in order to determine the effect of different substituents on the phenyl rings and the *N*-substituents on the four nitrogen atoms of **XXX**:

- the 2-methoxy groups have been replaced with several other groups in order to determine the influence of the steric and the electronic effects on AChE inhibition. Their replacement with halogen atoms, such chlorine (**XXI**) or bromine (**XXXII**), do not increase the affinity towards AChE suggesting that variations of electronic density on the aromatic rings are not important in the interaction with AChE. In order to determine the possibility of establish H-bond with the enzyme, the methoxy group has been shifted from 2- position to 3- and 4- position leading to derivative **XXXIII, XXXIV** respectively. Compound **XXXV**, without any substituent on the phenyl ring is slightly more active than **XXXIII** and **XXXIV**.
- in order to investigate the role of the methyl substituents on the two basic functions, they were substituted with ethyl groups obtaining an ethyl series of derivatives (**XXXVII**-**XLI**) in which the most potent resulted **XLI**. The relative free base **XL** was chosen as lead compound thanks to its better pharmacokinetic profile.

Table 2. Biological activities of compounds **XXXI**-**XL**.

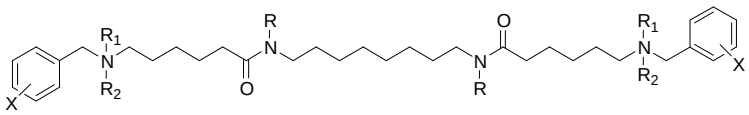

XXX-LX

No.	R	R_1	R_2	X	pIC_{50} AChE
caproctamine	Me	Me	H	2-OMe	6.77
XXXI	Me	Me	H	2-Cl	6.68
XXXII	Me	Me	H	2-Br	6.57
XXXIII	Me	Me	H	3-OMe	6.30
XXXIV	Me	Me	H	4-OMe	5.34
XXXV	Me	Me	H	H	6.97
XXXVI	H	Me	H	2-OMe	6.06
XXXVII	H	Et	H	2-OMe	6.66
XXXVIII	Me	Et	H	H	7.15
XXXIX	Me	Et	Me	H	7.77
XL	Me	Et	H	2-OMe	7.73
XLI	Me	Et	Me	2-OMe	7.92

Further optimization studies were performed on **XL** by replacing the amide groups by an oxygen atom, leading to **XLII** and **XLIII** that were less potent toward AChE. Furthermore, the replacement of the ethyl group on the two basic amine nitrogen atoms with an *i*-propyl residue did not affect the AChE inhibition activity (**XLIV**).

Finally, to verify whether the 2-methoxy functions of **XL** have a role in the interaction with the enzyme, they were replaced by selected groups that have different values of π and σ parameters based on the liphophilic (π) and electronic (σ) characteristic of the substituent, respectively. Once again the most potent compound resulted **XL**, indicating the important role of the two aromatic substituents to improve the basicity of the two amide functions. This property allows the protonation of the two basic functions at physiological pH, for an optimal interaction with AChE, as confirmed by a directed correlation between AChE inhibiting activity and the pK_a of different substituted compounds. The better substituent was found to be 2-methoxy, probably because it increases the percentage of protonate amine at physiologically pH by increasing the basicity of nitrogen through mesomeric and inductive effects. Indeed, a direct correlation between pK_a and AChE-inhibitory activity has been found for compounds **XLV**-**LI**[184].

Table 3. Biological activities of compounds **XLII**-**LVIII**.

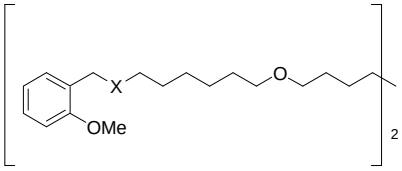

LII-XLIII

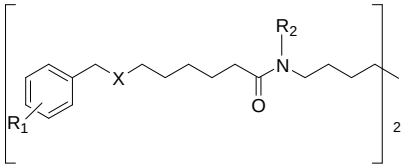

XLIV-LVIII

no	R_1	X	R_2	pIC_{50} AChE	pIC_{50} BChE	AChE/BChE
caproctamine	2-OMe	NMe	Me	6.77	4.93	68
XL (**1**)	2-OMe	NEt	Me	7.73	5.65	121
XLII		NEt		6.69	5.58	13
XLIII		N^+(Me)Et		7.11	6.12	10
XLIV	2-OMe	NEt	*i*Pr	7.74	5.67	118
XLV	H	NEt	Me	7.31	5.97	21
XLVI	2-Cl	NEt	Me	6.95	5.39	37
XLVII	2-CF_3	NEt	Me	5.34	3.78	36
XLVIII	2-O*n*Pr	NEt	Me	7.47	6.78	5
XLIX	2-Me	NEt	Me	7.25	5.13	132
L	2-NO_2	NEt	Me	6.10	4.26	69
LI	H	N^+(Me)Et	Me	7.43	5.60	69
LII	2-Cl	N^+(Me)Et	Me	7.71	5.59	133
LIII	2- CF_3	N^+(Me)Et	Me	7.93	5.12	640
LIV	2-OMe	N^+(Me)Et	Me	7.92	5.85	118
LV	2-O*n*Pr	N^+(Me)Et	Me	7.76	7.08	5
LVI	2-Me	N^+(Me)Et	Me	7.78	5.19	388
LVII	2-NO_2	N^+(Me)Et	Me	7.91	5.62	196
LVIII	2-OMe	N^+(Me)Et	*i*Pr	8.09	5.78	204

A previous docking study carried out on the diprotonated form of caproctamine revealed that it is able to interact simultaneously with both active and peripheral sites of AChE and to establish favourable interactions with a number of residues in the gorge thanks to the flexibility of the molecule, which allows it to assume many conformations. To reduce the conformational freedom of the polymethylene chain of polyamines, a series of compounds have been designed in which the inner octamethylene chain of **XL** is incorporated partially or totally into a more constrained moiety as shown in Figure 55.

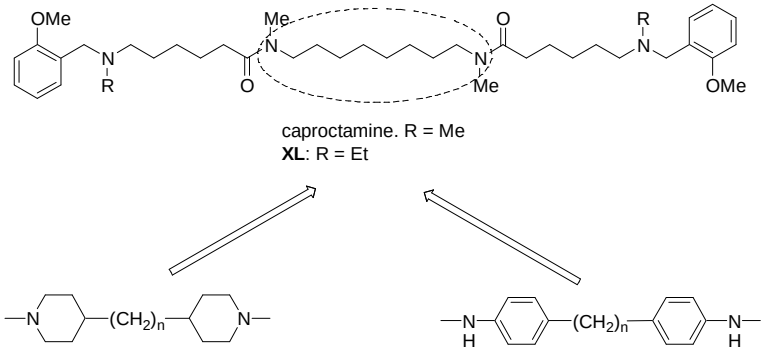

Figure 55. Design strategy leading to less flexible derivatives of **XL**.

These structural modifications would afford compounds in which the inner diamide moiety is forced to assume a more definite arrangement that would allow the two basic terminal chains to orient themselves in different spatial regions relative to each other. Therefore, the highly flexible polymethylene chain connecting the two amide functions of **XL** was replaced by the less flexible dipiperidine or dianiline moieties, affording **LIX-LXII** or **LXIII-LXV**, respectively.

Table 4. Biological activities of compounds **LIX**-**LXV**.

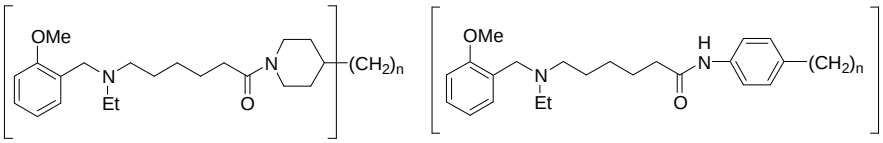

LIX-LXII **LXIII-LXV**

no	n	pIC_{50} AChE	pIC_{50} BuChE	% inhibition Aβ (AChE)
caproctamine		6.77	4.93	<5
LX		7.73	5.65	<5
LIX (**2**)	0	8.48	5.07	41
LX	1	8.48	5.19	nd
LXI	2	8.13	5.44	15
LXII	3	8.18	5.47	nd
LXIII	0	7.55	5.73	35
LXIV	1	7.20	5.74	nd
LXV	2	6.77	5.77	nd

Replacements of the octamethylene inner spacer of caproctamine with bicyclic moieties lead to an increase of activity towards AChE. In particular, the most active compounds were the dipiperidino derivatives **LIX** and **LX** and the dianiline derivative **LXIII**. All the new compounds designed inhibited both catalytic and peripheral binding sites, but only the less flexible **LIX** and **LXIII** were able to inhibit AChE-induced Aβ-aggregation. In addition, **LXI** also inhibited the self-induced Aβ-aggregation[185].

Caproctamine is able to interact with PAS but it does not inhibit AChE-induces Aβ-aggregation. Therefore, the authors hypothesized that the inhibition of PAS is not sufficient condition to inhibit AChE-induced Aβ-aggregation and the insertion of less flexible moieties in the structure of caproctamine is required to gain the ability to inhibit Aβ-aggregation induced by AChE.

1.2 Drug Design

The "one-molecule-multiple-targets" paradigm suggests that a single molecule could hit several targets responsible for the onset and/or progression of AD[7,186]. To this end, the design and synthesis of several examples of MTDLs for combating neurodegenerative diseases have been published[187]. This seems to be the more appropriate approach for addressing the complexity of AD and may provide new drugs for tackling the multifactorial nature of AD, and hopefully stopping its progression.

In 1998, Melchiorre and coworkers reported on derivatives displaying affinity for (i) AChE active and peripheral binding sites and (ii) muscarinic M_2 receptors. The prototypes caproctamine and its ethyl analogue (**1**) directly derived from methoctramine, an irreversible muscarinic M_2 antagonist. The methoctramine-structure was modified in order to improve its lipophilicity, by replacing the two inner amine functions with amide groups and by introducing a methyl substituent on the four nitrogen atoms. These studies led to the discovery of caproctamine, a new lead in the research of MTDLs because endowed with the ability to inhibit AChE and M_2 muscarinic subtype receptors, in order to improve the release of ACh in the synaptic cleft by blocking the presynaptic M_2 muscarinic receptor respectively[167]. Further studies carried out on caproctamine demonstrated that the AChE inhibitory potency was enhanced by the replacement of the methyl groups located on the two side nitrogen atoms with two ethylene groups leading to **1**. In the same study, was also demonstrated that a 2-methoxy group on the two phenyl rings of **1** conferred the highest AChE inhibition potency by improving the basicity of the two basic nitrogen atoms[184,188].

Because AChE may act as a chaperone in inducing Aβ aggregation through the interaction of its peripheral anionic site (PAS) with the peptide, the inhibition of PAS might be relevant to the search for AChEIs endowed with Aβ antiaggregating properties[189]. Although caproctamine and **1** contacted PAS and active AChE binding sites, they did not inhibit the AChE-induced Aβ aggregation. To verify whether this failure was due to their high structural flexibility, their inner octamethylene spacer was partially or totally incorporated into a more constrained moiety. This led to the discovery of the dipiperidino derivative **2**, which displayed improved AChE inhibitory potency and the ability to partially inhibit AChE-induced Aβ aggregation, suggesting that inhibition of Aβ aggregation is achieved by polyamines incorporating a constrained spacer between the two inner nitrogen atoms rather than a flexible polymethylene chain[185]. It is known that aromatic residues may give additional interactions with the aromatic rings lined in AChE gorge[190] and may confer β-sheet-breaking properties that might lead to the inhibition of self-mediated Aβ aggregation[191]. Thus, to obtain new AChE-inhibiting MTDLs endowed with additional properties such as inhibition of AChE-induced Aβ aggregation and β-sheet-breaking ability[192], the dipiperidino moiety of **3** has been replaced with less flexible cyclic systems, leading to **3**-**15** (Figure 56). Monoamine **15** was included in this study to verify the importance, if any, of the two aminoalkyl side chains in the interaction with AChE and Aβ.

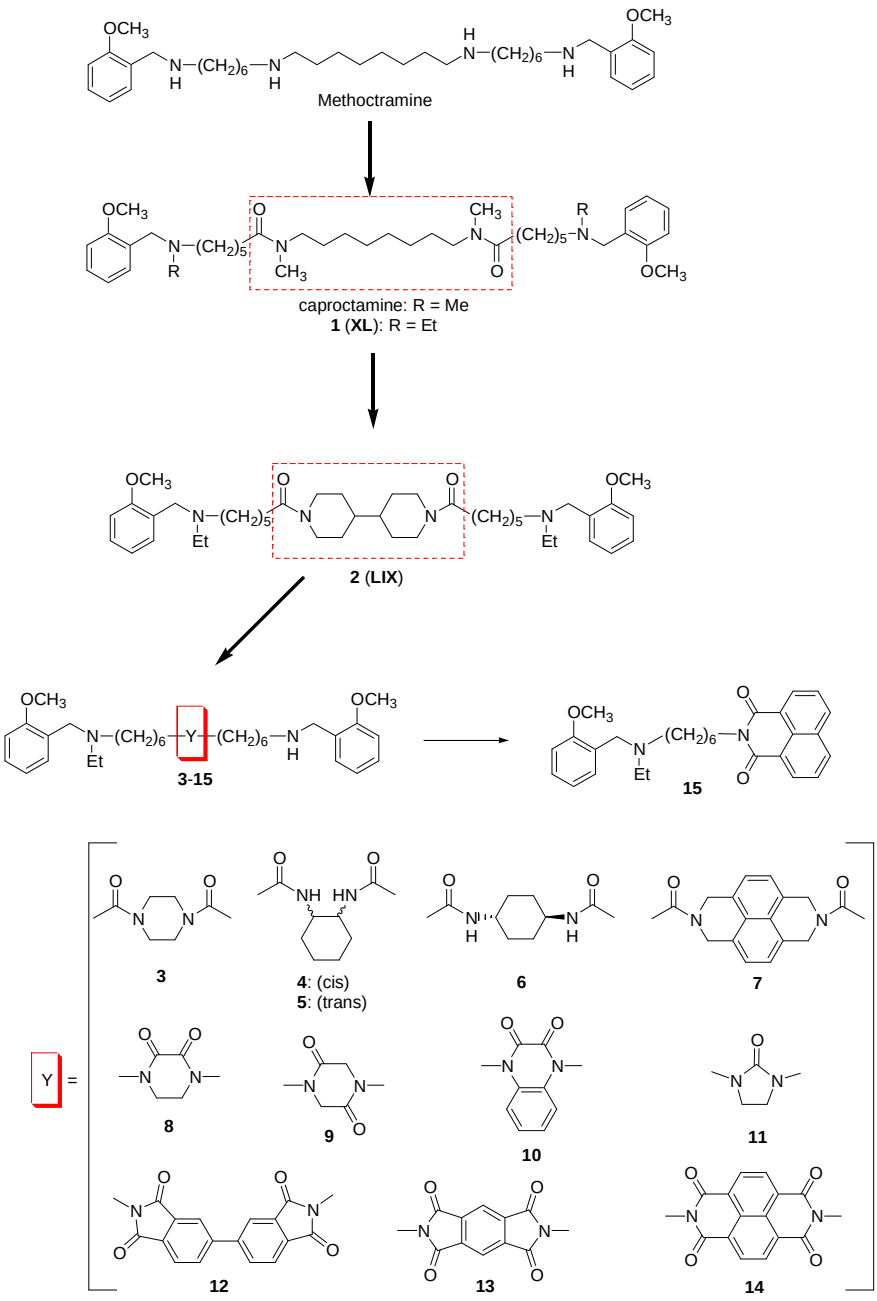

Figure 56. Drug design leading to compounds **3-15**.

1.3 Methods

1.3.1 Synthesis

Diamine diamides **34**-**38** were obtained by reacting *N*-[(benzyloxy)carbonyl]-6-aminocaproic acid with piperazine, *cis*-cyclohexane-1,2-diamine, (±)-*trans*-cyclohexane-1,2-diamine, *trans*-cyclohexane-1,4-diamine, and ethane-1,2-diamine, respectively. Removal of the *N*-(benzyloxy)carbonyl group by acidic hydrolysis gave diamine diamides **39**-**43**, which were treated with 2-methoxybenzaldehyde followed by reduction with $NaBH_4$ of the formed Schiff base to the corresponding dibenzyl derivatives **44**-**48**. Diethylation of **44**-**48** with diethyl sulphate gave **3**-**6** and **49** (Figure 56). Reduction of **49** afforded **50**, which was condensed with diethyloxalate to give **8** (Scheme 1).

Acylation of 1,2,3,6,7,8-hexahydrobenzo[*lmn*][3,8]phenanthroline[193] with 6-bromohexanoyl chloride gave **51**, whereas N-alkylation of piperazine-2,5-dione, 1,4-dihydroquinoxaline-2,3-dione, and imidazolidin-2-one with the appropriate dibromoderivative afforded intemediates **52**-**54**, which were diaminated with ethyl-(2-methoxybenzyl)amine to give **7**, **9**-**11**, respectively (Scheme 2).

Finally, **12**-**15** were obtained through the condensation of the commercially available anhydrides [5,5′]biisobenzofuranyl-1,3,1′,3′-tetraone, benzo[1,2-*c*;4,5-*c*′]difuran-1,3,5,7-tetraone, isochromeno[6,5,4-*def*]isochromene-1,3,6,8-tetraone,benzo[*de*]isochromene-1,3-dione, respectively, with *N*-ethyl-*N*-(2-methoxybenzyl)hexane-1,6-diamine[181] (Scheme 3). Different salts (dioxalates for **2**-**9**, **11**, and **14** and di-*para* toluenesulfonates for **11**, **12**, **13** and **15**) were prepared to obtain derivatives easier to handle.

Scheme 1

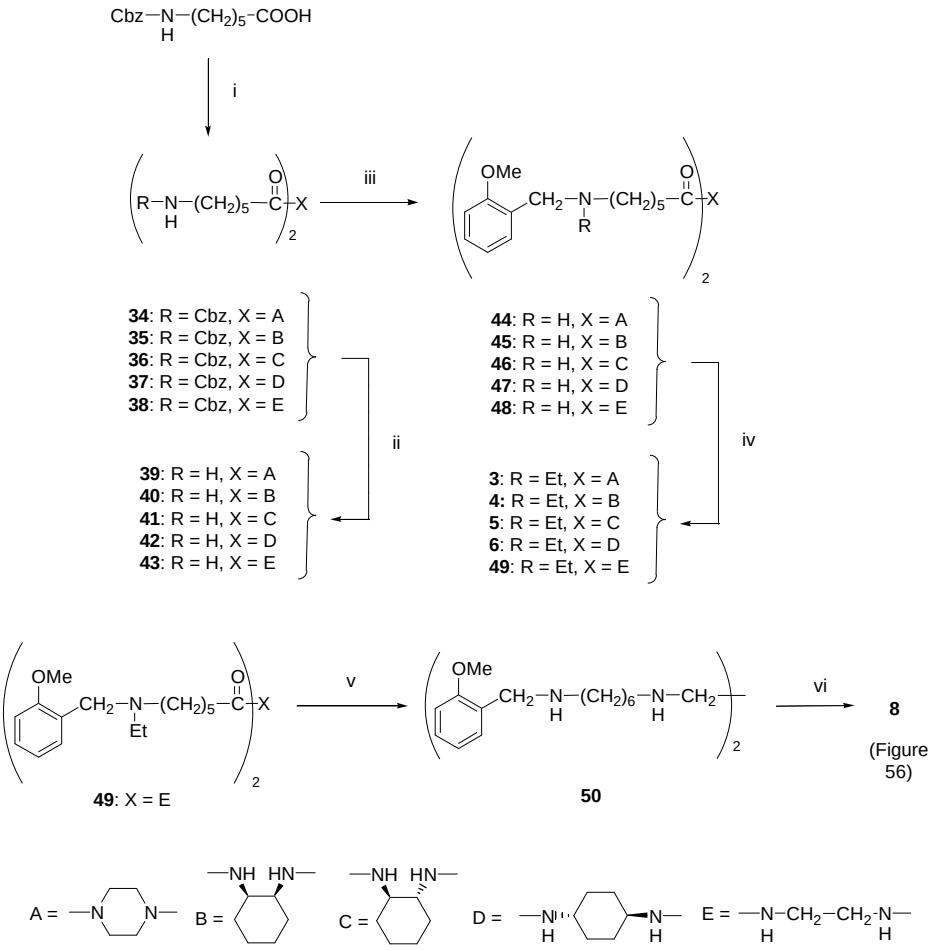

Conditions: Cbz = $C_6H_5CH_2OCO$-; (i) Et_3N, EtOCOCl, dioxane, room temp, 72 h; (ii) 30% HBr in CH_3COOH, CH_3COOH, room temp, 4 h; (iii) (a) 2-$MeOC_6H_4CHO$, toluene, reflux, 6 h; (b) $NaBH_4$, EtOH, room temp, 6 h; (iv) $(EtO)_2SO_2$, toluene, reflux, 48 h; (v) a) borane-N-ethyl-N-isopropylaniline complex, diglyme, reflux, 4 h; (b) 6 N HCl, reflux, 1 h; (vi) diethyloxalate, EtOH, reflux, 12 h.

Scheme 2

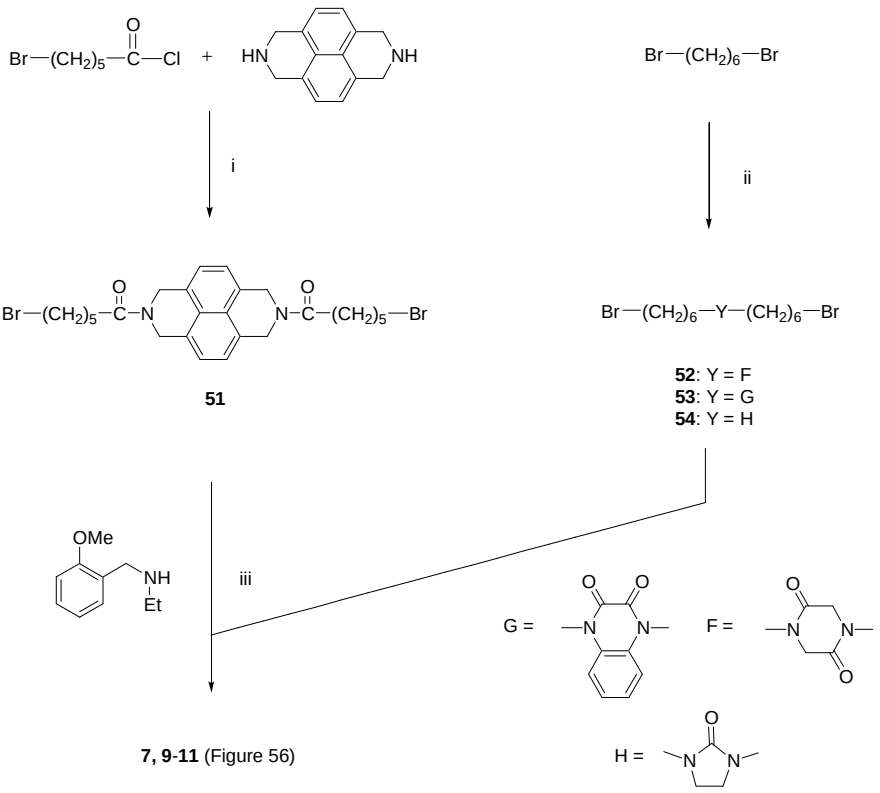

Conditions: (i) Et_3N, CH_2Cl_2, room temp, 96 h; (ii) 60% NaH, anhydrous DMF, piperazine-2,5-dione or 1,4-dihydroquinoxaline-2,3-dione or imidazolidin-2-one, room temp for **36** and **51** and reflux for **52**, 24 h; (iii) for **9** and **10**, KI, K_2CO_3, 1-pentanol, reflux, 40 h; for **7** and **11**, CH_3CN and Et_3N, reflux, 64 h.

Scheme 3

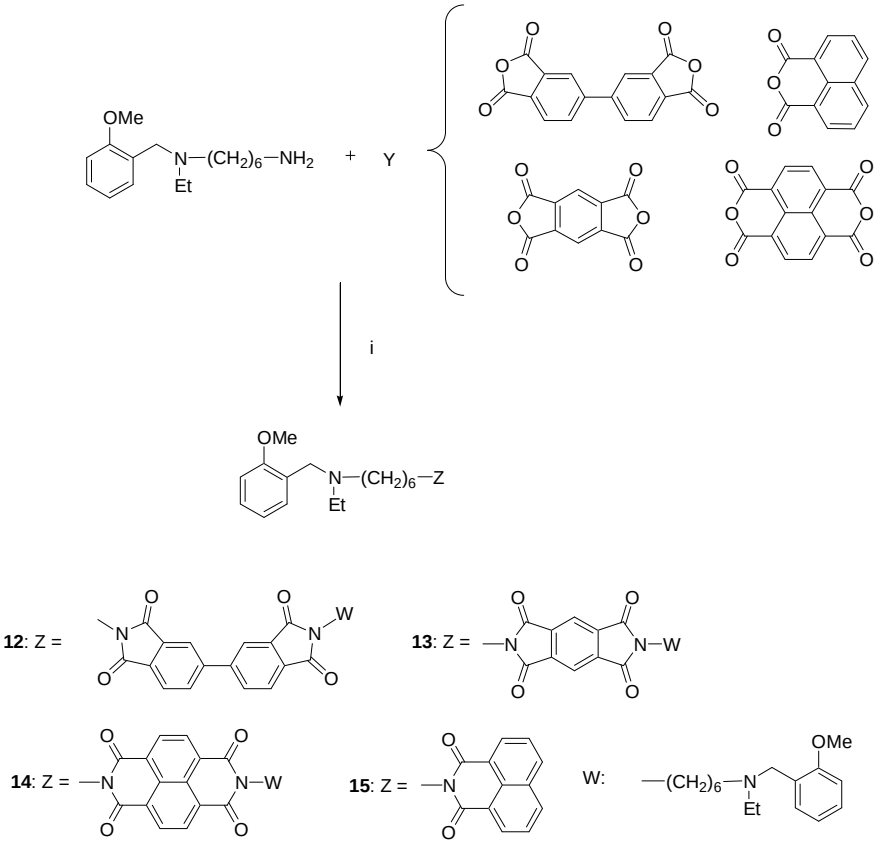

Conditions: (i) amine and anhydride molar ratio, 2:1 for **12**-**14** and 1:1 for **15**, EtOH, reflux, 60 h.

1.3.2 Biology

To determine the potential interest of compounds **3-15** for the treatment of AD, their inhibitory potency against recombinant human AChE and BChE was evaluated by studying the hydrolysis of acetylthiocholine (ATCh) following the method of Ellman *et al*. The inhibitory potency was expressed as IC_{50} values, which represent the concentration of inhibitor required to decrease enzyme activity by 50%. To allow comparison of the results, caproctamine **1**, **2**, donepezil, galantamine, and donepezil were used as the reference compounds. The nature of AChE inhibition caused by these compounds was investigated by the comparison of the graphical analysis of steady-state human AChE inhibition data of the most potent compound of this series (**14**).

The ability of such compounds to inhibit both self-induced and AChE-induced Aβ-aggregation was assessed by purposely optimized Thioflavin T-based fluorimetric assay[194,195].

The ability of some compounds to inhibit BACE-1 was assesses through FRET-assay[112].

1.3.3. Computational studies

To disclose a possible binding mode of **14** at the AChE, BChE, and BACE-1 binding pockets, docking simulations were performed using the available crystallographic structures of the three enzymes (PDB codes 1B41 for AChE[196], 1P0M for BChE[197], and 1FKN for BACE-1[53]. Furthermore, calculation of electrostatic potential maps for compounds **8** and **14** have been performed[198].

1.4 Results and Discussion

To determine the potential interest of **3**-**15** for AD treatment, their inhibitory potency was evaluated on recombinant human AChE and isolated BChE from human serum in comparison with caproctamine, **1**-**2** and the marketed drugs donepezil and galantamine.

An analysis of the results (Table 5) reveals that replacement of the dipiperidino moiety of **2** with constrained moieties strongly influenced the ability to inhibit AChE and BChE. The new derivatives inhibited AChE activity in the nanomolar range with the exception of **4**-**6**. The low affinity of **4**-**6** for AChE might be due to the difficulty of the two amide functions to assume a planar arrangement to each other, as is probably possible for **3**, **8**, **9**, and **11**, which were only slightly less potent than **1**. The most potent compounds of the present series (**7**, **10**, **12**-**14**) were characterized by an aromatic residue in the middle of their structure. This suggests the possibility of establishing more π-π interactions with several aromatic residues located in the AChE gorge. In particular, **14**, endowed with a 1,4,5,8-naphthalenetetracarboxylic diimide (NTD) moiety, showed a very high AChE inhibitory activity and a 9-fold improvement in potency in comparison with **2**. All the synthesized compounds showed a selective inhibitory activity for AChE relative to BChE, and **14** was the most selective and potent of the series with an AChE/BChE selectivity ratio greater than 5000, perhaps relevant when considering the emerging role of BChE in AD[199] and the importance of selectivity toward AChE in AD treatment[200]. Finally, **15**, characterized by only one side chain, was 144-fold less potent than **14**, highlighting the importance of the presence of two side chains for an optimal interaction with both sites of AChE.

PAS is well-established as important for β-fibrils formation mediated by AChE[189,201]; thus, compounds able to interact with amino acids located in the PAS area may reduce the formation of neurotoxic Aβ fibrils. PAS may thus be an attractive target when developing potential AD-modifying drugs. A Lineweaver-Burk plot obtained at increasing concentrations of substrate and inhibitor showed that **14** interacted with the catalytic site and PAS (Figure 57). Therefore, the ability of **3** and **6**-**15** to inhibit AChE-induced Aβ (1-40) aggregation was assessed through a thioflavin T-based fluorometric assay[188]. **4** and **5** were not evaluated because of their poor AChE inhibitory activity. **3**, **7**, and **8** were as active as **2** (Table 5), while **9**-**14** were more potent than **2**. It appears that an inner spacer bearing aromatic residues may be optimal for inhibiting AChE-induced Aβ aggregation.

Table 5. Inhibition of AChE and BChE Activities and of AChE-Mediated and Self-Induced Aβ Aggregation by **3-15** and Reference Polyamines **1-2**

Compound[a]	IC_{50} (nM)[b]		Inhibition of Aβ aggregation (%)		AChE/BChE[m]
	AChE	BChE	AChE-induced[c]	self-induced[d]	
caproctamine[e]	170 ± 2[e]	11600 ± 300[e]	<5[f]	20.3 ± 1.9	69
1 (**XL**)	16.1 ± 0.5[e]	2250 ± 60[e]	<5	nd[h]	138
2 (**LIX**)	3.32 ± 0.12[g]	8490 ± 610[g]	41.2 ± 2.0	13.7 ± 6	2570
3	25.7 ± 1.9	10700 ± 1900	38.9 ± 4.0	<5[f]	417
4	4160 ± 200	30800 ± 2300	nd[h]	nd[h]	7.0
5	5470 ± 240	36800 ± 3300	nd[h]	nd[h]	6.7
6	8550 ± 40	25300 ± 4200	25.6 ± 4.6	nd[h]	3
7	4.83 ± 0.16	1040 ± 30	42.1 ± 2.2	12.7 ± 2.9	219
8	68.9 ± 2.4	10300 ± 400	47.5 ± 1.6	nd[h]	148
9	15.9 ± 0.6	2090 ± 130	61.4 ± 4.4	4.8 ± 1.3	132
10	1.41 ± 0.03	95.8 ± 1.5	70.8 ± 3.2	8.8 ± 2.9	68
11	72.4 ± 3.2	876 ± 24	53.8 ± 3.7	<5	12
12	14.0 ± 0.6	293 ± 23	70.2 ± 4.83	16.5 ± 1.3	21
13	7.70 ± 0.27	3000 ± 200	51.1 ± 0.3	<5	389
14	0.37 ± 0.02	1910 ± 120	>90[i]	54.5 ± 5.4[j]	5129
15	53.5 ± 5.7	416 ± 32	19.5 ± 2.8	<5	8
donepezil	23.1 ± 4.8	7420 ± 390	22[k]	<5	
galantamine	2010 ± 150[l]	20700 ± 1500[l]	17.9 ± 0.1[l]	<5	
propidium	32300[l]	13200[l]	82.0 ± 2.5[k]	61.1 ± 4.6[l]	
Congo Red	nd[h]	nd[h]	nd[h]	78.8 ± 0.9	

[a] **1**, dihydrochloride; **1-9**, **11**, and **14**, dioxalate; **10**, **12**, **13**, di-*para* toluenesulfonate; **15**, *para*-toluenesulfonate. See Figure 56 for structures. [b] Human recombinant AChE and BChE from human serum were used. IC_{50} values represent the concentration of inhibitor required to decrease enzyme activity by 50% and are the mean of two independent measurements, each performed in triplicate. [c] Inhibition of AChE-induced Aβ (1-40) aggregation. The concentrations of the tested inhibitor and Aβ (1-40) were 100 and 230 μM, respectively, whereas the Aβ (1-40)/AChE ratio was equal to 100:1. [d] Inhibition of self-induced Aβ (1-42) aggregation (50 μM) produced by the tested compound at 10 μM concentration. [e] Data from ref 167. [f] Not significant. [g] Data from ref 168. [h] nd, not determined. [i] IC_{50} = 8.13 ± 0.97μM. [j] IC_{50} = 9.69 ± 1.09 μM. [k] Data from ref 189. [l] Data from ref 196.[m] The AChE/BChE selectivity ratio is the antilog of difference between pIC_{50} values at AChE and BChE.

14 was the most potent inhibitor with an IC_{50} lower than that of the reference compound propidium[189]. Notably, neither **2** nor any of the marketed AChE inhibitors, when tested in the same conditions, showed comparable antiaggregating activity[189,202]. The most potent published compounds acting as AChE-induced Aβ aggregation inhibitors display a potency in the same range as **14**[170,169,203]. The low inhibitory activity shown by **14** emphasizes the importance of the two aminoalkyl side chains for an optimal interaction with the two AChE binding sites.

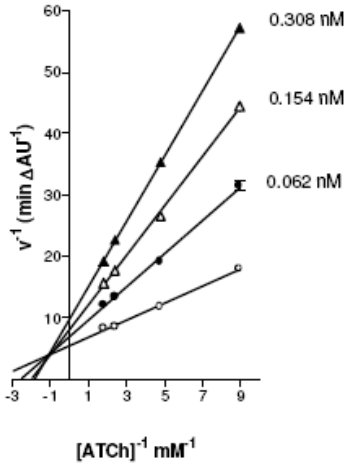

Figure 57. Steady-state inhibition by **14** of AChE hydrolysis of acetylthiocholine. Lineweaver-Burk reciprocal plots of initial velocity and substrate concentrations are presented. Reciprocal plots of initial velocity in the absence of inhibitor gave an estimate k_{app} for acetylthiocholine of 170 ± 15 μM (four experiments). Lines were derived from a weighted least-squares analysis of the data points.

Since it was previously reported that compounds endowed with a polyamine scaffold may interfere with Aβ polymerization and aggregation[204], the ability of **3**, **7**, **9, 10, 12**, **14** to inhibit self-promoted Aβ (1-42) aggregation was also determined (Table 5)[189]. Again, **14**, although less potent that the reference compound Congo red, displayed an IC_{50} comparable with that of propidium. This activity might be due to the ability of **14** to behave as a β-sheet breaker because of its planar and constrained aromatic system[201]. Unfortunately, because of its low solubility, the contribution, if any, of the NTD moiety benzo[*lmn*][3,8]phenanthroline-1,3,6,8-tetraone[193] and, consequently, its possible contribution to the different biological properties of **14** could not be determined.

Moreover the ability of some compounds to inhibiting BACE1 was also investigated. The founded value for **14** was 392 ± 31 nM, whereas the most known BACE inhibitors, based on peptide structure, showed higher potency in the same range[205]. The other compounds tested, **3**, **7**, **9**, showed inhibition values in micromolar range (**3**, 6% inhibition at 500 nM, **7**, 8% inhibition at 500 nM and **9**, 16% inhibition at 500 nM).

To disclose a possible binding mode of **14** at AChE and BChE binding pockets, docking simulations were performed using the available crystallographic structures of the two enzymes (PDB codes: 1B41 for AChE[196], 1P0M for BChE[197]). Because of **14**'s flexibility, several docking runs were carried out with

GOLD[206]. The outcomes were clusterized by AClAP[207]. In Figure 58 a low energy pose representative of a statistically populated cluster is reported for binary complexes of AChE and **14** (Figure 58A) and of BChE and **14** (Figure 58B). The binding mode of **14** at the AChE gorge shows that the ligand can interact with Trp86 of the internal anionic site and with Trp286 of PAS. The latter could explain **14**'s ability to inhibit AChE-induced Aβ aggregation. **14** might also interact with several aromatic residues of the enzyme mid-gorge[208]. In particular, the NTD moiety could establish favourable π-π stacking or simple hydrophobic interactions with Tyr341, Phe338, and Phe295.

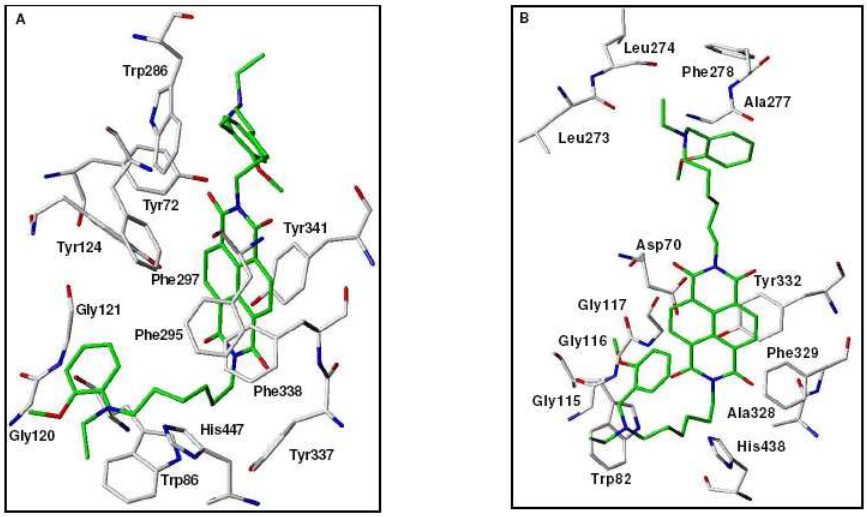

Figure 58. Docking model of **14** at the binding sites of AChE (A), and BChE (B). The residues relevant for the interaction between **15** and the biological counterparts are reported.

Moreover, Tyr72 may interact by H-bonding with the methoxy substituent of one of the benzylammonium ends. This could account for the high inhibitory potency of **14** against human AChE. Conversely, although **14** could favourably interact with several BChE amino acids (Figure 58A), the lack of the same pool of aromatic residues at the BChE mid-gorge may explain **14**'s AChE/BChE selectivity. Indeed, besides a cation-π interaction between **14** and the Trp82 indole ring of BChE, the only other striking interaction was between **14** and Tyr332. Moreover, **14** seemed unable to interact with Phe278, a fundamental residue for inhibiting BChE activity[208]. The presence of BChE Asp70 close to one of the two imide moieties of the NTD scaffold may further decrease the molecule's affinity toward this target.

To identify a possible binding mode of **14** in BACE-1 docking simulation were performed (Figure 59). It can be seen that **14** was actually able to interact with Asp32, one of the aspartic acids of the catalytic dyad of the enzyme. In particular one carbonyl oxygen of **14** could accept a proton H-bond interaction with the residue. Moreover the naphtalentetracarboxylic diimide moiety could establish H-bond interaction with Thr231 and Thr72 side chains. Finally the benzylamonium groups could interact with Phe47 and Tyr198.

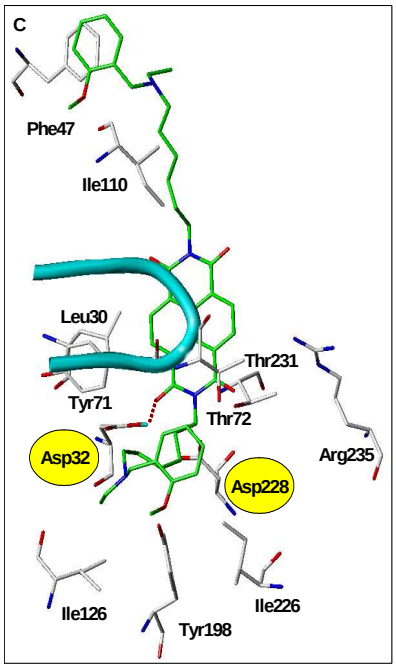

Figure 59. Docking model of **14** at the binding sites of BACE-1. The residues relevant for the interaction between **14** and the biological counterparts are reported.

Furthermore, electrostatic potential study has been carried out on **14** and **7** in order to explain their different inhibitory activity on BACE-1[198](Figure 60). It has been observed a different charge density in the two aromatic moieties, in particular the naphtalentetracarboxylic diimide moiety seemed to present a more positive charge density thanks to the presence of the four carbolyl groups which exerted an inductive electron withdrawing effect. This different potential charge could facilitate the interaction between the negative charged aspartic residue of BACE-1 and **14**. The same did not happen for **7** which is characterized by a more negative charge density. Finally, the higher inhibition potency of **14** in comparison with **7** might be due by the complete planar disposition of the central nucleus which could better fit in the enzyme cavity.

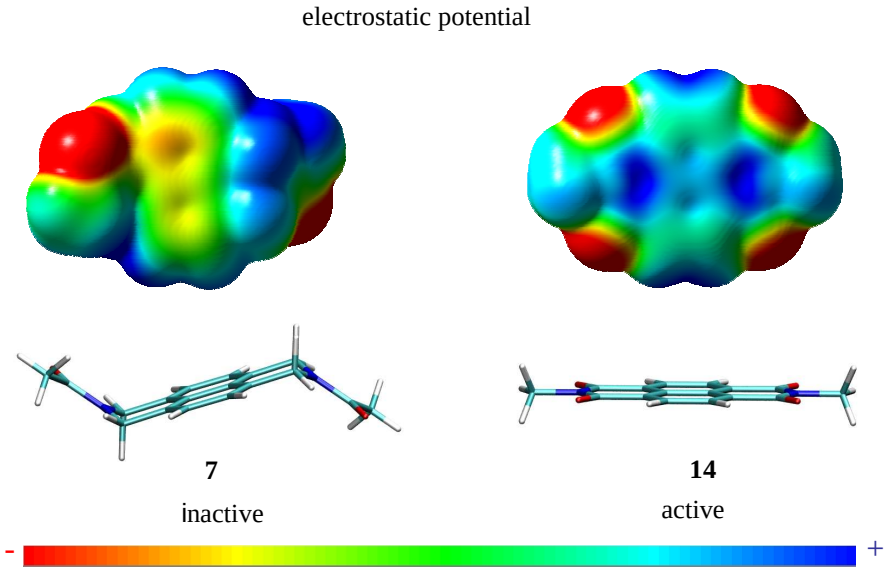

B3LYP/6-31G* electrostatic potential mapping an electron density isosurface

Figure 60. Electrostatic potential study carried out on **14** and **7**.

1.5 Conclusion

In this work it has been demonstrated that constraining the dipiperidino moiety of **2** led to derivatives with a better biological profile. The most potent was **14**, endowed with an NTD moiety. It inhibited AChE in the subnanomolar range, AChE induced and self-promoted Aβ-aggregation in micromolar concentration and BACE1 in nanomolar concentration. Thus, **14** emerges as an MTDL able to hit several targets of the AD pathogenesis cascade.

However, the rational design of compounds that simultaneously modulate different protein targets at a comparable concentration for each target remains a challenging task. In the present case, proof of the concept of the biological profile of **14** *in vivo* is needed to confirm the relevance of the NTD moiety in the design of new derivatives for AD treatment.

1.6 Experimental section

1.6.1 Chemistry

Melting points were taken in glass capillary tubes on a Buchi SMP-20 apparatus and are uncorrected. ESI-MS spectra were recorded on Perkin-Elmer 297 and WatersZQ 4000. ^{1}H NMR and ^{13}C NMR were recorded on Varian VRX 200 and 300 instruments. Chemical shift are reported in parts per millions (ppm) relative to peak of tetrmethylsilane (TMS) and spin multiplicities are given as s (singlet), br s (broad singlet), d (doublet), t (triplet), q (quartet) or m (multiplet) Although IR spectral data are not included (because of the lack of unusual features), they were obtained for all compounds reported, and they were consistent with the assigned structures. The elemental compositions of the compounds agreed to within ±0.4% of the calculated value. Where the elemental analysis is not included, crude compounds were used in the next step without further purification. Chromatographic separations were performed on silica gel columns by flash (Kieselgel 40, 0.040-0.063 mm, Merck) or gravity (Kieselgel 60, 0.063-0.200 mm, Merck) column chromatography. Reactions were followed by thin layer chromatography (TLC) on Merck (0.25 mm) glass-packed precoated silica gel plates (60 F254) and then visualized in an iodine chamber or with a UV lamp.The term “dried” refers to the use of anhydrous sodium sulfate.

General Procedure for the Synthesis of 34-38. Ethyl chloroformate (0.95 mL, 10 mmol) in dry dioxane (20 mL) was added dropwise to a stirred and cooled (5 °C) solution of *N*-[(benzyloxy)carbonyl]-6-aminocaproic acid (2.65 g, 10 mmol) and Et_3N (1.4 mL, 10 mmol) in dioxane (30 mL), followed after standing for 30 min by the addition of the suitable diamine (5 mmol) in dioxane (20 mL). After the mixture was stirred at room temperature for 72 h, the solvent was evaporated, affording a residue that was suspended in water (100 mL). The solid residue was filtered off and washed with 2 N NaOH, 2 N HCl, and brine, to afforded the desired crude products **34-38**.

{6-[4-(6-Benzyloxycarbonylamin-hexanoyl)piperazin-1-yl]-6-oxohexyl}carbamic acid benzyl ester (34): from anhydrous piperazine as starting diamine; pink solid; 93% yield; mp 123-125 °C; ^{1}H NMR (200 MHz, $CDCl_3$) δ 1.24-1.79 (m, 10H + 2H exchangeable with D_2O), 2.34 (t, *J*= 6.0, 4H), 3.14-3.28 (q, *J* = 9.0, 4H), 3.39-3.54 (m, 4H), 3.64-3.76 (m, 4H), 4.64-4.74 (br s, 2H), 5.10 (s, 4H), 7.29-7.42 (m, 10H).

***cis*-{5-[2-(6-Benzyloxycarbonylamino-hexanoylamino)-cyclohexylcarbamoyl]-pentyl}carbamic acid benzyl ester (35)**: from *cis*-cyclohexane-1,2-diamine as starting diamine; whitesolid; 49% yield; mp 103-105 °C; ^{1}H NMR (200 MHz, $CDCl_3$) δ 1.22-1.73 (m, 20H), 1.85 (br s, exchangeable with D_2O, 2H), 2.19 (t, *J* = 6.0, 4H), 3.18 (q, *J* = 4.0, 4H), 4.08 (br s, exchangeable with D_2O, 2H), 4.96 (br s, 2H), 5.20 (s, 4H), 7.22-7.38 (m, 10H).

(±)-*trans*-{5-[2-(6-Benzyloxycarbonylaminohexanoylamino)cyclohexylcarbamoyl]pentyl}carbamic acid benzyl ester (36): from (±)-*trans*-cyclohexane-1,2-diamine as starting diamine; white solid; 60% yield; mp 112-115 °C; ^{1}H NMR (200 MHz, CDCl3) δ 1.16-1.90 (m, 20H), 1.97-2.20 (m, 4H + 2H exchangeable with

D_2O), 3.16 (q, *J* = 6.0, 4H), 3.60-3.78 (m, 2H), 5.18 (s, 4H), 5.88-5.95 (m, exchangeable with D_2O, 2H), 7.29-7.42 (m, 10H).

***trans*-{5-[4-(6-Benzyloxycarbonylaminohexanoylamino)cyclohexylcarbamoyl]pentyl}-carbamic acid benzyl ester (37)**: from *trans*-cyclohexane-1,4-diamine as starting diamine; red solid; 89% yield; mp 123-125 °C; ^{1}H NMR (300 MHz, DMSO) δ 1.12-1.52 (m, 16H + 2H, exchangeable with D_2O), 1.63-1.82 (m, 4H), 2.03 (t, *J* = 6.0, 4H), 2.98 (q, *J* = 4.0, 4H), 3.45 (br s,2H), 3.88 (br s, exchangeable with D_2O, 1H), 4.52 (br s, exchangeable with D_2O, 1H), 5.03 (s, 4H), 7.25-7.43 (m, 10H); MS (ESI^+) *m/z* = 631 $(M+Na)^+$.

{5-[2-(6-Benzyloxycarbonylaminohexanoylamino)ethylcarbamoyl]pentyl}carbamic acid benzyl ester (38): from ethane-1,2-diamine as starting diamine; white solid; 64% yield; mp 172-174 °C; ^{1}H NMR (200 MHz, DMSO) δ 1.10-1.62 (m, 12H + 2H exchangeable with D_2O), 2.15-2.19 (t, *J* = 6.0, 4H), 2.89-3.15 (m, 8H), 5.02 (s, 4H), 7.17.7.42 (m, 10H), 7.76-7.84 (br s, exchangeable with D_2O, 2H).

General Procedure for the Synthesis of 39-43. A solution of 30% HBr in acetic acid (25 mL) was added to a solution of **34-38** (3.1 mmol) in acetic acid, and the resulting mixture was stirred for 4 h at room temperature. Ether (100 mL) was then added, yielding a solid, which was washed with ether (3 x 20 mL) and dissolved in water (50 mL). The solution was made basic with KOH pellets and extracted with CH_2Cl_2 (3 x 30 mL). Removal of the dried solvent gave compounds **39-43** in quantitative yields.

6-Amino-1-[4-(6-aminohexanoyl)piperazin-1-yl]hexan-1-one (39): white solid; mp 109-111°C; ^{1}H NMR (300 MHz, $CDCl_3$) δ 1.08-1.27 (br s, 4H), 1.38-1.76 (m, 8H + 4H exchangeable with D_2O), 2.39 (t, *J* = 6.0, 4H), 2.70 (t, *J* = 7.0, 4H), 3.43-3.54 (m, 4H), 3.61-3.73 (m, 4H).

***cis*-6-Aminohexanoic acid [2-(6-aminohexanoylamino)cyclohexyl]amide (40)**: yellow foam solid; ^{1}H NMR (200 MHz, $CDCl_3$) δ 1.25-1.71 (m, 20H + 4H exchangeable with D_2O), 2.19 (t, *J* = 6.0, 4H), 2.69 (t, *J* = 7.1, 4H), 3.87-4.08 (m, 2H), 6.19-6.31 (br s, exchangeable with D_2O, 2H).

(±)-*trans*-6-Aminohexanoic acid [2-(6-aminohexanoylamino)cyclohexyl]amide (41): white powder; mp 75-77 °C; ^{1}H NMR (200 MHz, $CDCl_3$) δ 1.18-1.82 (m, 20H + 2H exchangeable with D_2O), 2.05 (br s, exchangeable with D_2O, 2H), 2.18 (t, *J* = 6.3 4H), 2.68 (t, *J* = 7.2, 4H), 3.58-3.71 (m, 2H), 6.31 (br s, exchangeable with D_2O, 2H).

***trans*-6-Aminohexanoic acid [4-(6-aminohexanoylamino)cyclohexyl]amide (42)**: grey powder; mp 87-89 °C; ^{1}H NMR (300 MHz, $CDCl_3$) δ 1.05-1.72 (m, 20H + 4H exchangeable with D_2O), 2.18 (t, *J* = 6.2, 4H), 2.70 (t, *J* = 7.1, 4H), 3.75 (m, 2H), 5.38 (br s, exchangeable with D_2O, 2H).

6-Aminohexanoic acid [2-(6-aminohexanoylamino)ethyl]amide (43): foam solid; ^{1}H NMR (200 MHz, $CDCl_3$) δ 1.18-1.47 (m, 4H), 1.56-1.77 (m, 8H + 4H exchangeable with D_2O), 2.16-2.21 (t, *J* = 6.3, 4H), 2.70-2.81 (t, *J* = 7.2, 4H), 3.35-3.47 (m, 4H), 6.38-6.45 (br s, exchangeable with D_2O, 2H).

General Procedure for the Synthesis of 44-48. A mixture of **39-43** and 2-methoxybenzaldehyde (in a 1:2.2 molar ratio) in toluene (50 mL) was stirred at the refluxing temperature in a Dean-Stark apparatus for 6 h. Following solvent removal, the residue was taken up in EtOH (30 mL), $NaBH_4$ (0.19 g, 5 mmol) was added,

and the stirring was continued at room temperature for 6 h. The mixture was then made acidic with 3 N HCl, filtered, and evaporated. The residue was dissolved in water, and the resulting solution was washed with ether, made basic with 2N NaOH, and extracted with CH_2Cl_2 (3 x 30 mL). Removal of the dried solvent gave the desired crude products **44-48**, which were purified by flash chromatography.

6-(2-Methoxybenzylamino)-1-{4-[6-(2-methoxybenzylamino)hexanoyl]piperazin-1-yl}hexan-1-one (44): yellow oil; 66% yield; eluting solvent, toluene/MeOH/EtOAc/aqueous 33%ammonia (2:6:2:0.15); ^{1}H NMR (300 MHz, $CDCl_3$) δ 1.20-1.75 (m, 12H), 2.10-2.22 (br s, exchangeable with D_2O, 2H), 2.30 (t, *J* = 6.0, 4H), 2.57 (t, *J* = 7.1, 4H), 3.29-3.40 (m, 4H), 3. 49-3.60 (m, 4H), 3.74 (s, 4H), 3.81 (s, 6H), 6.77-6.94 (m, 4H), 7.11-7.24 (m, 4H); MS (ESI$^+$) *m/z* = 553 $(M+H)^+$.

***cis*-6-(2-Methoxybenzylamino)hexanoic acid-{2-[6-(2-methoxybenzylamino) hexanoylamino]cyclohexyl}amide (45)**: yellow oil; 84% yield; eluting solvent, $CHCl_3$/petroleum ether/MeOH/toluene/aqueous 33% ammonia (5:2:2:1:0.15); ^{1}H NMR (200 MHz, $CDCl_3$) δ 1.28-1.91 (m, 20H), 2.08-2.28 (m, 4H + 2H exchangeable with D_2O), 2.62 (t, *J* = 6.0, 4H), 3.78 (s, 4H),3.84 (s, 6H), 3.95-4.08 (m, 2H), 6.56 (br s, exchangeable with D_2O, 2H), 6.82-6.96 (m, 4H), 7.15-7.32 (m, 4H).

(±)-*trans*-6-(2-Methoxybenzylamino)hexanoic acid {2-[6-(2-methoxybenzylamino)hexanoylamino]cyclohexyl}amide (46): yellow oil; 82% yield; eluting solvent, $CHCl_3$/petroleum ether/MeOH/toluene/aqueous 33% ammonia (5:2:2:1:0.15); ^{1}H NMR (200 MHz, $CDCl_3$) δ 1.18-1.72 (m, 20H), 1.82-1.98 (m, exchangeable with D_2O, 2H), 2.06 (t, *J* = 6.0, 4H), 2.52 (t, *J* = 6.0, 4H), 3.42-3.61 (m, 2H), 3.68 (s, 4H), 3.73 (s, 6H), 6.67-6.85 (m, 4H + 2H exchangeable with D_2O), 7.06-7.18 (m, 4H).

***trans*-6-(2-Methoxybenzylamino)hexanoic acid {4-[6-(2-methoxybenzylamino) hexanoylamino]cyclohexyl}amide (47)**: yellow oil; 71% yield; gravity column chromatography, eluting solvent, $CHCl_3$/petroleum ether/MeOH/toluene/aqueous 33% ammonia (5:2:2:1:0.15); ^{1}H NMR (200 MHz, $CDCl_3$) δ 1.18-1.71 (m, 20H), 1.82 (br s, exchangeable with D_2O, 2H), 2.07-2.32 (t, *J* = 6.0, 4H), 2.53 (t, *J* = 6.0 4H), 3.75(s, 4H), 3.82 (s, 6H), 3.95-4.06 (m, 2H), 6.22 (br s, exchangeable with D_2O, 2H), 6.81-6.93 (m, 4H), 7.13-7.28 (m, 4H); MS (ESI$^+$) m/z = 581 $(M+H)^+$.

6-(2-Methoxybenzylamino)hexanoic acid {2-[6-(2-methoxybenzylamino) hexanoylamino]ethyl}amide (48): yellow oil; 65% yield; gravity column chromatography, eluting solvent, toluene/MeOH/CH_2Cl_2/aqueous 33% ammonia (3:3:4:0.05); ^{1}H NMR (300 MHz, $CDCl_3$) δ 1.35-1.66 (m, 12H), 1.93-1.99 (br s, exchangeable with D_2O, 2H), 1.15-2.2 (t, *J* = 7.0, 4H), 2.58- 2.63 (t, *J* = 7.0, 4H), 3.31-3.33 (m, 4H), 3.78 (s, 4H), 3.85 (s, 6H), 6.75-6.82 (br s, exchangeable with D_2O, 2H), 6.87 (m, 4H), 7.22-7.26 (m, 4H).

General Procedure for the Synthesis of 3-6, and 49. A mixture of **44**, **45**, **46**, **47** or **48** and diethylsulfate (1:2.5 ratio) was heated at the refluxing temperature for 48 h in toluene. Following removal of the solvent, the residue was taken up in water and made basic with KOH pellets and immediately extracted with $CHCl_3$ (3 x 20 mL) or directly purified by column chromatography to avoid the quaternarization of amine functions.

Removal of the dried solvent gave a residue that was purified by gravity column chromatography, providing the desired compound **3-6**, and **49**. **3-6** were finally converted into the dioxalate salt (foam solid).

6-[Ethyl-(2-methoxybenzyl)amino]-1-(4-{6-[ethyl-(2-methoxybenzyl) amino] hexanoyl} piperazin-1-yl)hexan-1-one (3): yellow oil; 54% yield; eluting solvent, MeOH/toluene/EtOAc/aqueous 33% ammonia (6:2:2:0.2); ^{1}H NMR (free base, 300 MHz, $CDCl_3$) δ 1.08 (t, *J* = 5.4, 6H), 1.21-1.77 (m, 12H), 2.29 (t, *J* = 7.4, 4H), 2.20-2.44 (m, 8H), 3.25-3.4 (m, 8H), 3.60 (s, 4H), 3.82 (s, 6H), 6.79-7.01 (m, 4H), 7.10-7.25 (m, 2H), 7.39-7.48 (m, 2H); ^{13}C NMR (free base, 300 MHz, $CDCl_3$) δ 11.95, 25.37, 27.11, 27.55, 33.52, 41.62, 45.45, 47.85, 51.51, 53.58, 55.49, 105.32, 120.27, 127.58, 128.16, 130.09, 162.53, 172.95; MS (ESI^+) m/z = 609 $(M+H)^+$. Anal. ($C_{40}H_{60}N_4O_{12}$) C, H, N.

***cis*-6-[Ethyl-(2-methoxybenzyl)amino]hexanoic acid (2-{6-[ethyl-(2-methoxybenzyl)amino] hexanoylamino}cyclohexyl)amide (4)**: yellow oil; 30% yield; eluting solvent, $CHCl_3$/petroleum ether/toluene/MeOH/aqueous 33% ammonia (4:3:2:1:0.10); ^{1}H NMR (free base, 300 MHz, $CDCl_3$) δ 1.08 (t, *J* = 6.3, 6H), 1.22-1.83 (m, 20H), 2.18 (t, *J* = 7.0, 4H), 2.42-2.58 (m, 8H), 3.58 (s, 4H), 3.78 (s, 6H), 4.01 (br s, 2H), 6.71-6.67 (br s, exchangeable with D_2O, 2H), 6.78-6.93 (m, 4H), 7.1 (m, 2H), 7.41 (d, *J* = 6.0, 2H); MS (ESI^+) m/z = 637 $(M+H)^+$. Anal. ($C_{42}H_{64}N_4O_{12}$) C, H, N.

(±)-*trans*-6-[Ethyl-(2-methoxybenzyl)amino]hexanoic acid (2-{6-[ethyl-(2-methoxybenzyl)amino]hexanoylamino}cyclohexyl)amide (5): yellow oil; 41% yield; eluting solvent, $CHCl_3$/petroleum ether/toluene/MeOH/aqueous 33% ammonia (4:3:2:1:0.10); ^{1}H NMR (free base, 300 MHz, $CDCl_3$) δ 1.08 (t, *J* = 6.3, 6H), 1.21-1.79 (m, 20H), 2.15 (t, *J* = 7.0, 4H), 2.41-2.60 (m, 8H), 3.60 (s, 4H), 3.81 (s, 6H), 4.04 (br s, 2H), 6.05-6.12 (br s, exchangeable with D_2O, 2H), 6.78-6.93 (m, 4H), 7.18 (m, 2H), 7,41 (d, *J* = 6.0, 2H); ^{13}C NMR (free base, 300 MHz, $CDCl_3$) δ 13.70, 24.97, 26.02, 27.09, 27.44, 32.60, 37.13, 47.89, 51.58, 53.66, 53.87, 55.58, 110.46, 120.53, 127.75, 128.47, 130.30, 157.92, 174.05; MS (ESI^+) m/z = 637 $(M+H)^+$. Anal. ($C_{42}H_{64}N_4O_{12}$) C, H, N.

***trans*-6-[Ethyl-(2-methoxybenzyl)amino]hexanoic acid (4-{6-[ethyl-(2-methoxybenzyl) amino]hexanoylamino}cyclohexyl) amide (6)**: colorless oil; 26% yield; eluting solvent, $CHCl_3$/petroleum ether/EtOAc/MeOH/ aqueous 33% ammonia (4:3:2:1:0.05); ^{1}H NMR (free base, 200 MHz, CD_3OD) δ 1.12 (t, *J* = 6.3, 6H), 1.18-1.71 (m, 16H), 2.18 (t, *J* = 7.0, 4H), 2.41-2.62 (m, 8H), 3.52-3.64 (m, 6H), 3.82 (s, 6H), 4.12 (q, 4H), 6.31 (br s, exchangeable with D_2O, 2H), 6.82-7.02 (m, 4H), 7.18-7.38 (m, 4H); ^{13}C NMR (free base, 200 MHz, CD_3OD) δ 9.87, 13.23, 25.15, 26.38, 30.52, 30.80, 35.25, 48.66, 50.27, 52.24, 53.88, 59.59, 109.57, 119.26, 125.49, 127.57, 130.15, 157.40, 173.20. MS (ESI^+) m/z = 637 $(M+H)^+$. Anal. ($C_{42}H_{64}N_4O_{12}$), C, H, N.

6-[Ethyl-(2-methoxybenzyl)amino-hexanoic acid (2-{6-[ethyl-(2-methoxybenzyl)amino] hexanoylamino}ethyl)amide (49): yellow oil; 30% yield; eluting solvent, MeOH/EtOAc/toluene/aqueous 33% ammonia (4:3:3:0.08); ^{1}H NMR (free base, 300 MHz, $CDCl_3$) δ 1.09-1.14 (t, *J* = 7.2, 6H), 1.28-1.36 (m, 4H), 1.57-1.67 (m, 8H), 2.18-2.23 (t, *J* = 7.5, 4H), 2.53-2.58 (t, *J* = 7.5, 4H), 2.60-2.67 (q, *J* = 6.0, 4H), 3.36-3.38 (m, 4H), 3.71 (s, 4H), 3.85 (s, 6H), 6.31-6.42 (br s, 2H), 6-81-6.98 (m, 4H), 7.16-7.20 (m, 2H), 7.44-

7.47 (m, 2H); ^{13}C NMR (free base, 300 MHz, $CDCl_3$) δ 11.2, 25.3, 26.1, 26.8, 36.3, 40.1, 47.5, 51.1, 53.1, 55.3, 110.3, 120.4, 128.2, 129.1, 130.5, 157.8, 174.2; MS (ESI^+) m/z = 583 $(M+H)^+$.

Synthesis of *N*-Ethyl-*N'*-(2-{6-[ethyl-(2-methoxybenzyl)amino]hexylamino}ethyl)-*N*-(2-methoxybenzyl)hexane-1,6-diamine (50). A solution of 2 M borane-*N*-ethyl-*N*-isopropylaniline complex (BACH-EI) in tetrahydrofuran (2 mL) was added dropwise at room temperature to a solution of **32** (0.160 mg, 0.27 mmol) in dry diglyme (10 mL) under a stream of dry nitrogen. When the addition was completed, the reaction mixture was heated at the refluxing temperature for 4 h. After cooling at room temperature, excess borane was destroyed by cautious dropwise addition of water (10 mL) and 6 N HCl (12 mL). The resulting mixture was then heated at the refluxing temperature for 1 h. After solvent evaporation, the crude product was washed with ethyl ether (3 x15 mL), then the mixture was made basic with aqueous 35% NaOH and extracted with $CHCl_3$ (4 x50 mL). Removal of the dried solvent gave a residue that was purified by gravity column chromatography, eluting with MeOH/EtOAc/toluene/aqueous 33% ammonia (4:3:3:0.1), to give **33** as colorless oil (0.035 g, 23% yield); ^{1}H NMR (200 MHz, $CDCl_3$) δ 1.09-1.14 (t, *J* = 7.2, 6H), 1.27-1.51 (m, 16H), 1.96-2.09 (m, 2H), 2.43-2.65 (m, 12H), 2.75 (s, 4H), 3.61 (s, 4H), 3.84 (s, 6H), 6.89-6.95 (m, 4H), 7.11-7.31 (m, 2H), 7.40-7.45 (m, 2H); ^{13}C NMR (300 MHz, $CDCl_3$) δ 11.7, 26.8, 27.2, 27.4, 29.4, 47.5, 48.3, 49.5, 51.3, 53.4, 55.3, 110.1, 120.1, 127.5, 130.1, 157.6; MS (ESI^+) m/z = 555 $(M+H)^+$.

1,4-Bis-{6-[ethyl-(2-methoxybenzyl)amino]hexyl}piperazine-2,3-dione (8). Diethyloxalate (9 μl, 0.063 mmol) was added to a solution of **50** (0.035 g, 0.063 mmol) in EtOH and the resulting mixture was heated at the refluxing temperature for 12 h. The crude material obtained, after the evaporation of the solvent, was purified by flash cromatography eluting solvent, MeOH/EtOAc/toluene/aqueous 33% ammonia (3:4:3:0.05) to give **8** as colorless oil, which was finally converted into the dioxalate salt; 42% yield; ^{1}H NMR (300 MHz, $CDCl_3$) δ 1.09-1.14 (t, *J* =7.2, 6H), 1.35-1.63 (m, 16H), 2.53-2.58 (t, *J* = 7.5, 4H), 2.60-2.67 (q, *J* = 6.0, 4H), 3.45-3.53 (m, 8H), 3.81 (s, 4H), 3.87 (s, 6H), 6.90-6.99 (m, 4H), 7.29-7.31 (m, 2H), 7.50-7.53 (m, 2H); ^{13}C NMR (300 MHz, $CDCl^3$) δ 10.9, 25.9, 26.4, 26.9, 27.1, 44.4, 47.3, 50.8, 52.8, 55.4, 110.4, 120.5, 128.6, 131.0, 157.3, 157.8; MS (ESI^+) m/z = 609 (M+H)+. Anal. ($C_{40}H_{60}N_4O_{12}$) C, H, N.

6-Bromo-1-[7-(6-bromo-hexanoyl)-3,6,7,8-tetrahydro-1H-benzo[*lmn*][3,8]phenanthrolin-2-yl]-hexan-1-one (51): 6-Bromohexanoyl chloride (1.627 g, 7.6 mmol) was added dropwise at 0 °C to a solution of 1,2,3,6,7,8-hexahydrobenzo[*lmn*][3,8]phenanthroline[1] (0.800 g, 3.80 mmol) and Et_3N (0.771 g, 7.6 mmol) in CH_2Cl_2. The resulting reaction mixture was stirred at room temperature for 96 h. The solution was washed with 2 N HCl, H_2O, 2 N $NaHCO_3$ and then the solvent was removed under vacuum. The obtained crude material was washed several time with petroleum ether/ether 7:3 and then purified by flash chromatography eluting solvent, ethyl acetate/petroleum ether (8:2) to afford **51** as yellow foam solid (0.2 g, 9% yield); ^{1}H NMR (200 MHz $CDCl_3$) δ 1.16-1.30 (m, 4H), 1.35-1.53 (m, 4H), 1.60-1.77 (m, 4H), 2.45 (t, *J* = 6.0, 4H), 3,38 (t, *J* = 6.4, 4H), 4.90(s, 4H), 5.12 (s, 4H), 7.07-7.40 (m, 4H).

General Procedure for the Synthesis of 52-54. Powdered 60% NaH (1.6 g, 20 mmol) was added to a cooled (0 °C) solution of piperazine-2,5-dione (10 mmol), 1,4-dihydroquinoxaline-2,3-dione (10 mmol), and imidazolidin-2-one (10 mmol), respectively, in 10 ml of anhydrous DMF under nitrogen atmosphere. The resultant solution was stirred for 30 min at room temperature, then, the 1,6-dibromohexane (9.75 g, 40 mmol) was added dropwise and the solution was stirred for 24 h at room temperature (or at refluxing temperature for **54**). After evaporation of the solvent, the resulting crude material was washed with ether and purified by flash chromatography.

1,4-Bis-(6-bromohexyl)piperazine-2,5-dione (52): foam solid; 46% yield; eluting solvent,EtOAc/petroleum ether (8:2); ^{1}H NMR (200 MHz, $CDCl_3$) δ = 1.27-1.62 (m, 16H), 3.32-3.51 (m, 8H), 3.97 (s, 4H).

1,4-Bis-(6-bromohexyl)-1,4-dihydroquinoxaline-2,3-dione (53): yellow oil; 18% yield; eluting solvent, EtOAc/petroleum ether (8:2); ^{1}H NMR (300 MHz, $CDCl_3$) δ 1.48-1.58 (m, 8H), 1.78-1.92 (m, 8H), 3.42 (t, *J* = 6.6, 4H), 4.23 (t, *J* = 7.5, 4H), 7.16-7.26 (m, 2H), 7.44-7.48 (m, 2H); MS (ESI$^+$) m/z = 511 $(M+Na)^+$.

1,3-Bis-(6-bromohexyl)imidazolidin-2-one (54): yellow oil; 22% yield; eluting solvent, EtOAc/petroleum ether (5:5); ^{1}H NMR (300 MHz, $CDCl_3$) δ 1.27-1.83 (m, 16H), 3.03-3.20 (m, 4H), 3.35-3.47 (m, 4H), 3.60-3.65 (t, *J* = 6.0, 4H); 13C NMR (200 MHz, CDCl3) δ 25.8, 27.4, 27.8, 33.5, 33.7, 42.6, 44.0, 161.3.

General Procedure for the Synthesis of 7 and 11. A mixture of ethyl(2-methoxybenzyl)amine (0.125 g, 0.76 mmol) and triethylamine (0.077 g, 0.76 mmol) was added to a solution of the dibromoderivative **51** or **54** (0.38 mmol) in CH_3CN (20 mL). The reaction mixture was stirred at the refluxing temperature for 64 h. After solvent evaporation, the crude material was poured in water, made basic, and extracted with CH_2Cl_2 (3 × 50 mL). After evaporation of the solvent, the crude material was purified by flash chromatography.

The two purified compounds were converted into the dioxalate salts as described for **3-6**.

2,7-Bis-{6-[ethyl-(2-methoxy-benzyl)-amino]-hexyl}-benzo[lmn][3,8]phenanthroline-1,3,6,8-tetraone (7): It was synthesized from **51**: yellow oil; 27% yield; eluting solvent, toluene/EtOAc/MeOH/CH2Cl2/aqueous 33% ammonia (4:4:1:1:0.05); ^{1}H NMR (free base, 200 MHz, $CDCl_3$) *δ* 1.01 (t, *J*=5.4, 6H), 1.17-1.68 (m, 12H), 1.68-2.51 (m, 12H), 3.38 (s, 6H), 3.58 (s, 4H), 4.88 (s, 4H), 5.06 (s, 4H), 6.68-6.96 (m, 4H), 7.17-7.42 (m, 8H); 13C NMR (200 MHz, CDCl3) *δ* 11.9, 25.3, 27.0, 27.5, 44.7, 47.8, 48.8, 51.4, 53.5, 55.4, 110.3, 120.3, 127.6, 127.9, 128.2, 130.2, 157.7, 198.1; MS (ESI$^+$) *m/z* 733 $(M+H)^+$. Anal. ($C_{50}H_{64}N_4O_{12}$), C, H, N.

1,3-Bis-{6-[ethyl-(2-methoxybenzyl)amino]hexyl}imidazolidin-2-one (11). It was synthesized from **54**; yellow oil; 30 % yield; eluting solvent, EtOAc/MeOH/toluene/aqueous 33% ammonia (5:1:4:0.05); ^{1}H NMR (free base, 300 MHz, $CDCl_3$) δ 1.51-1-93 (t, *J* = 7.2, 6H), 1.29-1.56 (m, 16H), 2.48-2.57 (m, 8H), 3.18-3.21 (m, 4H), 3.29 (s, 4H), 3.61-3.64 (m, 4H), 3.85 (s, 6H), 6.82-6.98 (m, 4H), 7.17-7.26 (m, 2H), 7.39-7.48 (m, 2H); MS (ESI$^+$) *m/z* = 581 $(M+H)^+$. Anal. ($C_{39}H_{60}N_4O_{11}$), C, H, N.

General Procedure for the Synthesis of 9 and 10. KI (1.6 g,10 mmol), K_2CO_3 (4.7 g, 17 mmol), and ethyl(2-methoxybenzyl)amine (0.313 g, 1.9 mmol) were added to a solution of the dibromoderivative **52** or

53 (0.38 mmol) in *n*-pentanol (20 mL). The resulting mixture was heated at the refluxing temperature for 40 h. After evaporation of the solvent the crude product was washed with water and taken up with a 1:1 mixture of ether and ethyl acetate (50 mL). The organic phase was dried and the solvent evaporated. The crude mixture was purified by flash chromatography to afford the desired compound. **8** was converted into the dioxalate salt as described for **3-6**, and **9** was converted into the di-*p*-toluenesulfonate salt by adding 2 equiv of *p*-toluenesulfonic acid in ether to an ether solution of the free base.

1,4-Bis-{6-[ethyl-(2-methoxybenzyl)amino]hexyl}piperazine-2,5-dione (9). It was synthesized from **52**; yellow oil; 57% yield; eluting solvent, toluene/EtOAc/MeOH/CH_2Cl_2/aqueous 33% ammonia (4:4:1:1:0.05); ^{1}H NMR (free base, 200 MHz, $CDCl_3$) δ 1.08 (t, *J* = 6.8, 6H), 1.28-1.34 (m, 8H), 1.52-1.56 (m, 8H), 2.49 (t, *J* = 7.4, 4H), 2.55-2.59 (m, 4H), 3.38 (t, *J* = 7.4, 4H), 3.60 (s, 4H), 3.84 (s, 6H), 3.95 (s, 4H), 6.85-6.96 (m, 4H), 7.23-7.26 (m, 2H), 7.42-7.44 (m, 2H); ^{13}C NMR (200 MHz, $CDCl_3$) δ 11.6, 24.6, 26.5, 26.6, 46.1, 47.7, 50.0, 51.3, 53.1, 55.4, 110.4, 120.5, 126.9, 127.4, 130.1, 157.8, 163.5; MS (ESI^+) m/z = 631 $(M+Na)^+$. Anal. ($C_{40}H_{60}N_4O_{12}$), C, H, N.

1,4-Bis-{6-[ethyl-(2-methoxy-benzyl)-amino]-hexyl}-1,4-dihydro-quinoxaline-2,3-dione (10). It was synthesized from **53**: yellow oil; 11% yield; eluting solvent, toluene/EtOAc/MeOH/ aqueous 33% ammonia (4:5:1:0.03); ^{1}H NMR (free base, 200 MHz, $CDCl_3$) *δ* 1.07 (t, *J*) 6.0, 6H), 1.38-1.77 (m, 16H), 2.50 (t, *J*) 15, 4H), 2.55 (q, *J*) 7.5, 4H), 3.61 (s, 4H), 3.83 (s, 6H), 4.19 (t, *J*) 7.8, 4H), 6.85-7.44 (m, 12H); ^{13}C NMR (200 MHz, $CDCl_3$) *δ* 11.7, 26.8, 26.9, 43.2, 47.6, 51.3, 53.2, 55.3, 110.2, 115.1, 120.3, 124.0, 126.7, 127.6, 130.1, 151.0, 154.1, 157.6; MS (ESI^+) *m*/*z* 657 $(M + Na)^+$. Anal. ($C_{54}H_{72}N_4O_{10}S_2$) C, H, N.

General Procedure for the Synthesis of 12-15. A solution of *N*1-ethyl-*N*1-(2-methoxybenzyl)hexane-1,6-diamine (0.08 mmol, for **15** 0.04 mmol) and the appropriate anhydride (0.4 mmol) in ethanol (40 mL) was heated at the refluxing temperature for 60 h. After the mixture was cooled to room temperature, the solvent was evaporated to give a crude material which was purified by flash chromatography. **12** and **13** were converted into the di-*p*-toluenesulfonate salts, whereas **14** and **15** were converted into the dioxalate and *p*-toluenesulfonate salt, respectively.

2,2'-Bis-{6-[ethyl-(2-methoxybenzyl)amino]hexyl}-[5,5']biisoindolyl-1,3,1',3'-tetraone (12). It was synthesized from [5,5']biisobenzofuranyl-1,3,1',3'-tetraone; yellow oil; 51% yield; eluting solvent, CH2Cl2/MeOH/aqueous 33% ammonia (9:1:0.1); ^{1}H NMR (free base, 200 MHz, $CDCl_3$) δ 1.45-1.22 (t, *J* = 7.0, 6H), 1.27-1-70 (m, 16H), 2.58-2.73 (m, 8H), 3-68-3.75 (t, *J* = 7.4, 4H), 3.81 (s, 4H), 3.85 (s, 6H), 6.87-7.01 (m, 4H), 7.24-7.30 (m, 2H), 7.50-7.53 (d, *J* = 5.8, 4H), 7.97-7.98 (d, *J*= 1, 2H), 8.10 (s, 2H); MS (ESI^+) m/z = 787 $(M+H)^+$. Anal. ($C_{62}H_{74}N_4O_{12}S_2$), C,H,N.

2,6-Bis-{6-[ethyl-(2-methoxybenzyl)amino]hexyl}pyrrolo[3,4-*f*]isoindole-1,3,5,7-tetraone (13). It was synthesized from benzo[1,2-*c*;4,5-*c'*]difuran-1,3,5,7-tetraone; yellow oil; 35% yield; eluting solvent, CH_2Cl_2/MeOH/aqueous 33% ammonia (9:1:0.02); ^{1}H NMR (free base, 200 MHz, $CDCl_3$) δ 1.22 (t, *J* = 6.8, 6H), 1.36-1.43 (m, 8H), 1.68-1.71 (m, 8H), 2.67-2.78 (m, 8H), 3.74 (t, *J* =7.0, 4H), 3.86 (s, 10H), 6.88-7.03

(m, 4H), 7.27-7.35 (m, 4H), 7.53-7.57 (m, 2H); MS (ESI+) m/z =711 (M+H)+. Anal. ($C_{56}H_{70}N_4O_{12}S_2$), C, H, N.

2,7-Bis-{6-[ethyl-(2-methoxy-benzyl)-amino]-hexyl}-benzo[lmn][3,8]phenanthroline-1,3,6,8-tetraone (14). It was synthesized from isochromeno[6,5,4-*def*]isochromene-1,3,6,8-tetraone: colorless oil; 43% yield; eluting solvent, toluene/EtOAc/CH_2Cl_2/MeOH/aqueous 33% ammonia (4:4:1:1:0.05); ^{1}H NMR (free base, $CDCl_3$) δ 1.05 (t, J) 7.4, 6H), 1.43-1.76 (m, 16H), 2.43-2.59 (m, 8H), 3.58 (s, 4H), 3.82 (s, 6H), 4.19 (t, J) 7.6, 4H), 6.18-6.96 (m, 4H), 7.15-7.28 (m, 2H), 7.89-7.43 (m, 2H), 8.77 (s, 4H); ^{13}C NMR (free base, $CDCl_3$) δ 1.12, 11.96, 27.07, 27.16, 27.37, 28.22, 41.02, 47.74, 51.44, 53.58, 55.41, 110.25, 120.35, 125.38, 126.69, 127.52, 128.29, 128.40, 129.10, 130.13, 130.94, 157.73, 162.85; MS (ESI^+) *m/z* 761 $(M + H)^+$. Anal. ($C_{50}H_{60}N_4O_{14}$) C, H, N

2-{6-[Ethyl-(2-methoxybenzyl)amino]hexyl}benzo[*de*]isoquinoline-1,3-dione (15). It was synthesized from benzo[*de*]isochromene-1,3-dione; yellow solid; 41% yield; eluting solvent, toluene/$CHCl_3$/MeOH/aqueous 33% ammonia (4:0.5:0.5:0.01); ^{1}H NMR (200 MHz, $CDCl_3$) δ 1.06-1.13 (t, J = 7.0, 3H), 1.41-1.75 (m, 8H), 2.48-2.62 (m, 4H), 3.67 (s, 2H), 3.84 (s, 3H), 4.15-4.23 (t, J= 7.4, 2H), 6,84-6.99 (m, 2H), 7.16-7.20 (m, 1H), 7.45-4.48 (d, J = 6.6, 1H), 7.78 (t, J = 7.6, 2H), 8.21-8.25 (d, J = 7.4, 2H), 8.61-8.64 (d, J = 7.2, 2H); MS (ESI^+) m/z = 445 $(M+H)^+$. Anal. ($C_{35}H_{40}N_2O_6S$) C, H, N.

1.6.2 Biology

Determination of the Inhibitory Effect on AChE and BChE Activities

The method of Ellman *et al.*[209] was followed. Prototypes caproctamine, **1**, and **2** and the AChEIs donepezil, galantamine, and propidium were used as reference compounds. Five different concentrations of each compound were used to obtain inhibition of AChE or BChE activity comprised between 20% and 80%. The assay solution consisted of a 0.1 M phosphate buffer, pH 8.0, with the addition of 340 μM 5,5'-dithiobis(2-nitrobenzoic acid), 0.02 unit/mL human recombinant AChE or human serum BChE (Sigma Chemical), and 550 μM substrate (acetylthiocholine iodide or butyrylthiocholine iodide). Test compounds were added to the assay solution and preincubated at 37 °C with the enzyme for 20 min followed by the addition of substrate. Assays were done with a blank containing all components except AChE or BChE to account for nonenzymatic reaction. The reaction rates were compared, and the percentage of inhibition due to the presence of test compounds was calculated. Each concentration was analyzed in triplicate, and IC50 values were determined graphically from log concentration-inhibition curves.

Determination of the Mode of Action

To obtain estimates the mode of action of **14**, reciprocal plots of 1/V versus 1/[S] were constructed at relatively low concentration of substrate (below 0.5 mM). The plots were assessed by a weighted least square analysis that assumed the variance of V to be a constant percentage of V for the entire data set. Data analysis was performed with GraphPad Prism 4.03 software (GraphPad Software Inc.). Reciprocal plots involving **15** inhibition show both increasing slopes (decreased Vmax at increasing inhibitor's concentrations) and

increasing intercepts (higher *K*m) with higher inhibitor concentration. This pattern indicates mixed-type inhibition, arising from a significant inhibitor interaction with both the free enzyme and the acetylated enzyme.

Determination of the Inhibitory Effect on Aβ Aggregation Induced by AChE

Aliquots of 2 μL of Aβ(1-40) (Bachem AG, Switzerland), lyophilized from 2 mg/mL HFIP and dissolved in DMSO at a final concentration of 230 μM, were incubated for 24 h at room temperature in 0.215 M sodium phosphate buffer (pH 8.0). For coincubation experiments, aliquots of AChE (2.30 μM, ratio 100:1) and AChE in the presence of the tested compound (100 μM) were added. Blanks containing Aβ, AChE, Aβ plus the tested compound, and AChE plus the tested compound in 0.215 M sodium phosphate buffer (pH 8.0) were prepared. The final volume of each vial was 20 μL. To quantify amyloid fibril formation, the thioflavin T fluorescence method was used[210,211,201]. Thioflavin T binds to amyloid fibrils, giving rise to an intense specific emission band at 490 nm in its fluorescent emission spectrum. Therefore, after incubation, the samples were diluted to a final volume of 2 Ml with 50 mM glycine-NaOH buffer (pH 8.5) containing 1.5 μM thioflavin T. A 300 s time scan of fluorescence intensity was carried out (λexc = 446 nm, λem = 490 nm), and values at the plateau were averaged after subtraction of the background fluorescence of the 1.5 μM thioflavin T solution.

Determination of the Inhibitory Effect on the Self-Mediated A*β*(1-42) Aggregation

HFIPpretreated Aβ(1-42) samples (Bachem AG) were resolubilized with a CH_3CN/Na_2CO_3/NaOH (48.4:48.4:3.2) to have a stable stock solution ([Aβ] = 500 μM). Experiments were performed by incubating the peptide in 10 mM phosphate buffer (pH 8.0) containing 10 mM NaCl at 30 °C for 24 h (final Aβ concentration 50 μM) with and without the tested compound at 10 μM. To quantify amyloid fibril formation, the thioflavin T fluorescence method was used. After incubation, the samples were diluted to a final volume of 2.0 mL with 50 mM glycine-NaOH buffer (pH 8.5) containing 1.5 μM thioflavin T. A 300 s time scan of fluorescence intensity was carried out (λexc = 446 nm, λem = 490 nm) 490 nm), and values at the plateau were averaged after subtraction of the background fluorescence of the 1.5 μM thioflavin T solution.

Inhibition of BACE-1 activity

Purified Baculovirus-expressed BACE-1 (α-secretase) and rhodamine derivative substrate were purchased from Panvera (Madison, WI, U.S). Sodium acetate and DMSO were from Sigma Aldrich (Milan, Italy). Purified water from Milli-RX system (Millipore, Milford, MA, USA) was used to prepare buffers and standard solutions. Spectrofluorometric analyses were carried out on a Fluoroskan Ascent multiwell spectrofluorometer (excitation: 544 nm; emission: 590 nm) by using black microwell (96 wells) Cliniplate plates (Thermo LabSystems, Helsinki, Finland).

Stock solutions of the tested compounds were prepared in DMSO and diluted with 50 mM sodium acetate buffer pH=4.5.

Specifically, 20 μL of BACE-1 enzyme (25 nM) were incubated with 20 μL of test compound for 60 minutes. To start the reaction, 20 μL of substrate (0.25 μM) were added to the well. The mixture was incubated at 37 °C for 60 minutes. To stop the reaction, 20 μL of BACE-1 stop solution (sodium acetate 2.5 M) were added to each well. Then the spectrofluorometric assay was performed by reading the fluorescence signal at 590 nm.

Assays were done with a blank containing all components except BACE-1 in order to account for non enzymatic reaction. The reaction rates were compared and the percent inhibition due to the presence of test compounds was calculated. Each concentration was analyzed in triplicate. The percent inhibition of the enzyme activity due to the presence of increasing test compound concentration was calculated by the following expression: $100-(v_i/v_o \times 100)$, where v_i is the initial rate calculated in the presence of inhibitor and v_o is the enzyme activity. To demonstrate inhibition of BACE-1 activity, statine-derived inhibitor (Calbiochem, Darmstadt, Germany) was used as reference inhibitor (IC_{50}=18 nM)[112].

1.6.3 Computational studies

Docking simulations were carried out by means of the GOLD software[212] (v. 3.0.1) and using the crystallographic structures of AChE, BChE, and BACE-1 obtained by the Protein Data Bank (PDB codes 1B41 for AChE[196], 1P0M for BChE[197] and 1FKN for BACE-1[53]). BACE-1 was always simulated in the monoprotonated state, namely with a proton on one aspartic acid of the catalytic dyad. Therefore, docking simulations were carried out either with BACE-1 Asp32 inner oxygen or with BACE-1 Asp228 inner oxygen protonated. **14** was built in Sybyl 7.1.1 (Tripos Associates; Inc: St. Louis; MO 2001, USA) and then geometry optimized optimized at density functional level of theory (B3LYP/6-31G**) by means of the Gaussian03 software[213,214]. **14** was always modeled and docked in the diprotonated state. **14** was docked 100 times at the active site of the three enzymes and the poses ranked according two scoring functions: GOLDSCORE and CHEMSCORE. As suggested by the GOLD[212] authors, genetic algorithm default parameters were set: the population size was 100, the selection pressure was 1.1, the number of operations was 10, the number of islands was 5, the niche size was 2, migrate was 10, mutate was 95, and crossover was 95.

Both sets of poses (i.e., those ranked with GOLDSCORE and those ranked with CHEMSCORE) were then clustered with AClAP v.1.0[207,215]. Briefly, AClAP is a newly developed clustering protocol implemented in a MATLAB metalanguage program, which combines a hierarchical agglomerative cluster analysis with a clusterability assessment method and a user independent cutting rule. In particular, when applied to docking outcomes, we demonstrated that the combination of the average linkage rule with the cutting function developed by Sutcliffe and co-workers[216] turned out to be an approach that meets all of the criteria required for a robust clustering protocol.

Finally, a low energy docking pose representative of a statistically populated cluster was taken into account to identify a possible binding mode of **14** at AChE, BChE, and BACE-1 active sites.

All molecular modeling studies were performed on a dualcore Intel(R) Xeon(TM) CPU 3.00GHz running Linux Fedora Core 5.

1.6.4 Elemental Analysis of Reported Compounds

No.	Formula	Calcd, %			Found, %		
		C	H	N	C	H	N
3	$C_{40}H_{60}N_4O_{12}$	60.90	7.67	7.10	60.95	7.61	7.06
4	$C_{42}H_{64}N_4O_{12}$	61.75	7.90	6.86	61.79	7.95	6.81
5	$C_{42}H_{64}N_4O_{12}$	61.75	7.90	6.86	61.80	7.85	6.82
6	$C_{42}H_{64}N_4O_{12}$	61.75	7.90	6.86	61.77	7.87	6.80
7	$C_{50}H_{64}N_4O_{12}$	65.77	7.07	6.14	65.78	7.04	6.12
8	$C_{40}H_{60}N_4O_{12}$	60.90	7.67	7.10	60.85	7.65	7.06
9	$C_{40}H_{60}N_4O_{12}$	60.90	7.67	7.10	60.86	7.68	7.05
10	$C_{54}H_{72}N_4O_{10}S_2$	64.77	7.25	5.60	64.78	7.23	5.58
11	$C_{39}H_{60}N_4O_{11}$	61.56	7.95	7.36	61.57	7.94	7.33
12	$C_{62}H_{74}N_4O_{12}S_2$	65.82	6.59	4.95	65.80	6.60	4.93
13	$C_{56}H_{70}N_4O_{12}S_2$	63.73	6.69	5.31	63.74	6.68	5.30
14	$C_{50}H_{60}N_4O_{14}$	63.82	6.43	5.95	63.93	6.45	5.90
15	$C_{35}H_{40}N_2O_6S$	68.16	6.54	4.54	68.15	6.53	4.52

Section 2

2.1 Introduction

Cancer is a term generally used to describe a group of diseases characterized by uncontrolled cell-growth. Cancer is a leading cause of death worldwide: it is responsibly for 7.9 million deaths, around 13% of all death, in 2007 and deaths from cancer worldwide are projected to continue rising, with an estimated value of 12 million in 2030. The main types of cancer leading to overall cancer mortality each year are lung cancer (1.4 million deaths/year), stomach cancer, (866,000 deaths/year), liver cancer (653, 99 deaths/year), colon (677, 00 deaths/year) and breast cancer (548,000 deaths/year). In Italy, in 2005 cancer killed approximately 157,000 people, 57,000 of them were under the age of 70 and it is predicted that it is going to rise from 26.5% of all death in 2005 to 26.8% of all death in 2009[217].

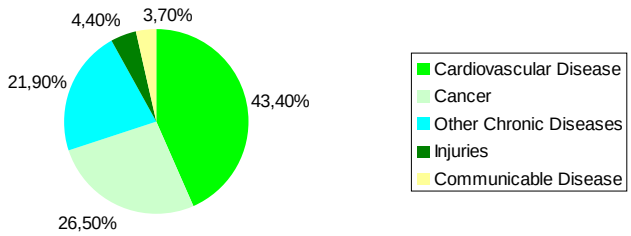

Figure 61. Main causes of death in Italy in 2005[217].

Cancer arises when cells escape from their normal control mechanisms and being to grow and to spread in different part of the organism through a process called metastasis. Cancer begins from one single cell and the transformation from a normal cell into a tumour cell is a multistage process that involved several biochemical pathways.

Cancer therapy is based on surgery, radiotherapy and chemotherapy. Killing cancer cells with chemical agents is a very difficult challenge because such transformed cells do not present different biochemical characteristics from normal cells. Treatment of cancer has mainly involved the use of agents directed to target that are not specific and, therefore, chemotherapeutic agents are in most of the cases aspecific and this lead to a wide spectrum of side effects in patients.

The drug resistance is another problem associate with cancer chemotherapy. Cancer cells are able to develop many mechanisms that make them resistant to anticancer drugs, by increasing the efflux of the drug, and/or the enzyme-mediated deactivation of the drug, and/or by altering the binding site or the metabolic pathways. Furthermore, many drugs which showed promising activity in preclinical *in vitro* studies did not confirm the same results in clinical trials. This is associate with the difficult to find clinical relevant preclinical models.

Along time, many different classes of antiproliferative drugs have been developed and they are able to hit several biochemical pathways implicated in the cancer development.

Cancer is a multifactorial disease and, therefore, a single medicine is not sufficient to effectively treat it. Among different therapeutically approaches useful for cancer treatment, an emerging strategy is represented by the so called “Multi-Target Direct Ligand” approach (MTDL). This approach is base on the assumption that a single drug may simultaneously modulate targets involved in the cascade of a pathological events leading to a multifactorial disease. This approach seems to be the more adequate for cancer treatment.

Herein, it is reported on the development of potential new MTDLs as anticancer drugs able to hit different target involved in cancer pathogenesis. In particular, the MTDLs described in the present study should be able, in principle, to act as:

- intercalator agents;
- apoptosis activators:
- PIN1 inhibitors.

2.1.1 Polyamines

Polyamines are simple organic compounds having low-molecular weight and two or more amino groups charged at physiologically conditions. Natural polyamines, such as putrescine (Put), spermine (Spm) and spermidine (Spd) are widely distributed in living organism and they are involved in several ways in cell proliferation and in homeostasis preserving[218,219,220,221].

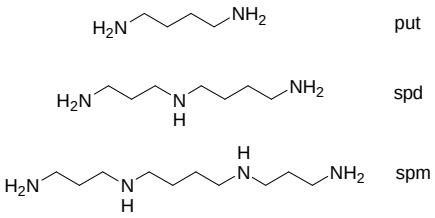

Figure 62. Chemical structure of Putrescine (Put), Spermidine (Spd) and Spermine (Spm).

Metabolism of Polyamines and their involvement in cellular homeostasis

In mammalian cells, the natural polyamines are found in millimolar concentration and their intracellular concentration is tightly regulated by multiple pathways such as synthesis from amino acids precursor, cellular uptake which provide polyamines from diet and intestinal microorganism as well as degradation and efflux. In eukaryotic cells, Put, Spd and Spm are synthesized from the amino acids L-ornithine and L-

methionine. Put derives from decarboxylation of ornithine by ornithine decarboxylase (ODC); this is the rate-limiting step in the polyamine's biosynthesis. Both Spd and Spm derived from Put; Spd is synthesized by the addition of an aminopropyl group thanks to Spermidine synthase. Adding another aminopropyl group to Spd yields to Spm by the action of Spermine synthase. The two aminopropyl groups used in this biosynthetic pathway directly derived from decarboxylated S-adenosylmethionine; such compound comes from methionine that is firstly transformed in S-adenosylmethionine and then decarboxylated by S-adenosylmethionine decarboxylase to give decarboxylated S-adenosylmethionine (Figure 63)[222].

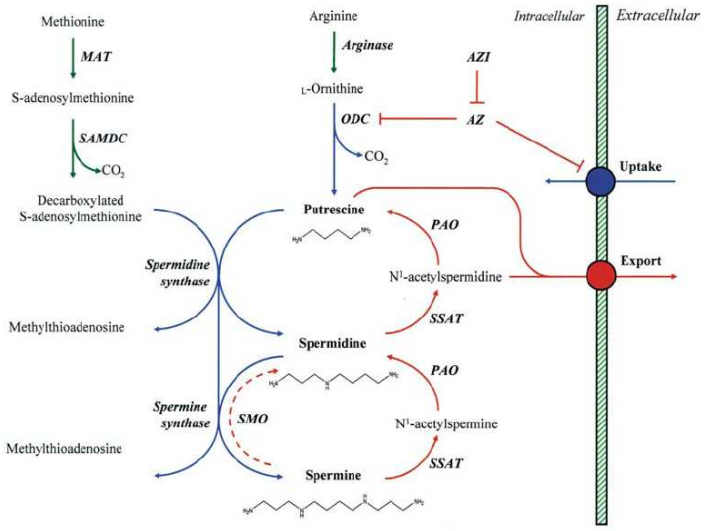

Figure 63. Polyamines metabolism[222].

Polyamines catabolism is driven by Spd/Spm N^1-acetyltransferase (SSAT). Such enzyme system use acetyl-CoA as acetyl source to obtain N^1-acetylspermine and N^1-acetylspermidine. The acetylation removes the positive charge on the amino group and, therefore, acetylated polyamines are less potent than non-acetylated compounds. These two acetylderivatives could be either extracted from the cell or oxidized by FAD-dependent polyamine oxidase (PAO): acetylated Spm is cleaved into Spd and acetylated Spd is cleaved into Put[223]. Polyamines could also be degradated by oxidative deamination catalyzed by a copper dependent amino-oxidase. Oxidation of acetylated polyamines leads to a great quantities of γ-aminobutiric acid, 3-acetamidopropanal, hydrogen peroxide and ammonia. In particular, hydrogen peroxide and aminoaldehydes are very toxic compounds and could lead to oxidative stress and apoptotic-induction; moreover, hydrogen peroxide positively modulates the enzymatic activity of SSAT (Figure 64)[224,225].

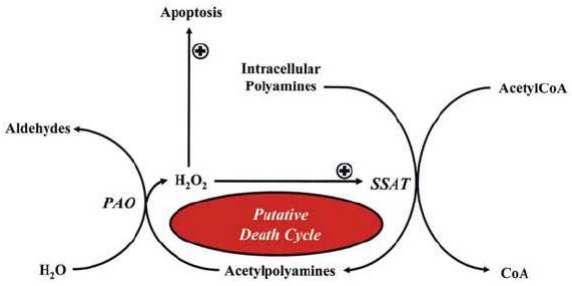

Figure 64. Polyamine metabolism and cell death[222].

Furthermore, cells possess uptake and efflux systems for polyamines. It has been suggested that the Polyamine Transporter (*PAT*) is carrier-mediated, energy-dependent and saturable. Moreover, despite some cells posses just one carrier for all three natural polyamines, some other cells are characterized by two classes of carrier: one for Put and the other for Spd and Spm[222,226]. *PAT* are more expressed in rapidly growing cells, such as cancers cells. *PAT* is not so selective and, therefore, different polyamines analogues could use such carrier to get into the cells[227]. Furthermore, cells posses systems able to transport polyamines outside the cells. This system is tightly regulated by the growth status of the cell[228].

Concerning all the enzymes involved in polyamines metabolism ODC resulted one of the most interesting. It is a highly inducible enzyme with an extremely short half-life. It requires for its activity pyridossal 5`-phosphate as cofactor which binds at Lys69; moreover, a thiol-group reducing agents are necessary for the enzyme activity[229]. ODC activity is dependent by the formation of a dimer and critical residues in the active site were Lys169 and His197[230]. ODC's expression could be regulated by oncogenes and its activity is controlled by polyamines through positive or negative feedback: high polyamines concentration reduces its activity while low polyamines levels increase it. Furthermore, different studies show an increase in ODC activity after inducing apoptosis and this suggest its involvement in programmed cell death[231]. ODC binds to a small regulatory protein induced by an increase of polyamines level, called Antyzime AZ.[232].

SSAT is a homotetramer of molecular mass about 80 KDa; it is induced by a number of stimuli including various toxic agents, hormones, growth factors and polyamines themselves[233]. SSAT acetylates specifically primary amino group and its substrates are Spd and Spm but not Put. Acetyl-CoA is used as acetyl-donor and its binding site is located in a highly conservated region of 20 AA and Arg142 and Arg148 play a critical role for its binding[234].

Polyamines are deeply involved in regulation of cellular functions and they are able to modulate cell growth and death. During cell cycle, changing in polyamines and ODC levels has been observed. In Chinese Hamster Ovary (CHO) during the progression of the cell cycle, Put levels are increased in S and G_2 phases, Spm concentrations are increased for the period of S and G_1 phase and Spd is increased during all the cell cycle[222].

Cellular growth is critically regulated by the rising or the reduction of proteins and kinase-proteins known as cyclin and cyclin-dependent kinase (Ckds) and many evidences show a link between such proteins and polyamines. Growth factors and hormones cause an acceleration of cell cycle by increasing the level of cyclins. Different cyclins have been identified and they act on specific phases of the cell cycle; for example, in the G_1 phase, cyclin D1, D2, D3 and E activate the appropriate Cdk that is responsible for the phosphorylation of particular substrates leading to cell cycle progression[235]. Polyamines have a critical role in cell growth and, therefore, interaction occurs between them and cyclin/Cdks. Changes in expression of the cyclin and Cdks take place during the different phases of cell cycle together with changes in ODC and polyamines concentration (Figure 65).

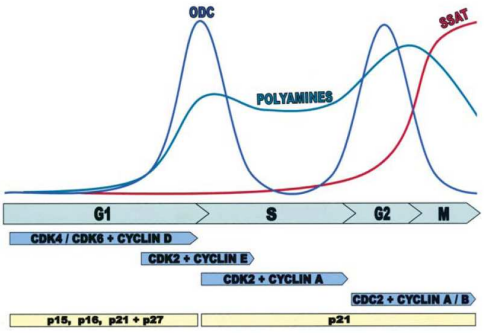

Figure 65. Effect of polyamines on cell cycle[222].

The exact mechanism of how polyamines affect the cyclin/Cdks system is still not completely defined but seems that polyamines regulated cyclin degradation[236]. Thomas and coworkers showed as polyamines were able to modulate cyclin D1. They treated MCF-7 cells with polyamine analogues causing a decrease in Put, Spd and Spm levels. Such decrease has been associated with a decrease in cyclin D1 level and cell cycle arrest in G_1. Furthermore, they valuated the effect of difluoromethylornithine (DMFO), an inhibitor of ODC, and CGP 48664, an S-adenosylmethionine decarboxylase inhibitor, on cyclin D1 and E in MCF-7 cells (Figure 66). In this study, DMFO induces a decrease of cyclin D1 whereas CGP 48664 led to an increase of two-fold in Cyclin D1: these results suggested a possible regulation of cyclin D1 by Put. Moreover, DMFO had no effect on cyclin E while CGP 48664 increased its level suggesting that Spm has a role in cyclin E regulation[220].

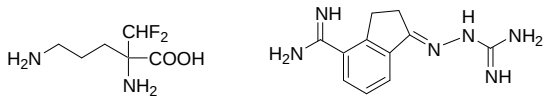

Difluoromethylornithine (DMFO)

CGP 48664

Figure 66. Chemical structure of DMFO and CGP 48664.

This and other studies[237] demonstrated a strictly link between polyamines and cell cycle regulation and how polyamines could be involved in cell growth desregulation. Therefore, it is not surprising that in the last decades many efforts have been performed to determine relationships between polyamines and cellular proliferation in order to develop drugs able to act on polyamines-mediated biochemical pathways.

In the early 70's, several studies revealed the presence of high levels of polyamines in serum and urine of people affected by leukaemia, melanoma, adenocarcinome and myeloma and, therefore, polyamines have been suggested as biochemical cancer marker. Furthermore, an increase in polyamines level have been notice in patients having cystic fibrosis, psoriasis and in pregnant girls; all these evidences point out that almost every pathological condition leading to a cellular death or pathological growth, such as inflammation, yield to an increase in polyamines concentration[238]. Polyamines and cancer are deeply connected and this address the research in finding new therapeutical entities that, inhibiting enzymes involved in polyamines biosynthesis could reduce their intracellular concentration leading to a cytostatic effect.

In addition to their connection with cell cycle regulation, polyamines, being generally charged at physiological pH, can interact with nucleic acids and, in particular, with DNA in non-sequence specific manner[239]. Polyamines are able to stabilize duplex and triplex B-DNA structure[240] and to promote B- to Z-DNA transition in recombinant plasmid[241]. Furthermore, it has been demonstrated that polyamines have an important role in the formation of nucleosome[242].

Beyond their interaction with DNA, polyamines interact also with phospholipids, and membrane protein[243]. In addition, natural and synthetic polyamines can interact with several important receptor systems, such as muscarinic, nicotinic and glutamate receptors[244,245].

Recently, it has been demonstrated that polyamines can act as protector agents against ROS by acting directly as free radical scavenger[246,247,248].

An increasing number of evidences are linking polyamines with programmed cell death. Nevertheless, the biochemical pathways that connect such compounds with increasing or decreasing of the apoptotic process is quite complex and some results appear contradictory[249].

Apoptosis is a programmed cell death that involved just a single cell and polyamines are important factors in its control. Packham and Cleveland discovered a marked increase of ODC activity after inducing apoptotic cell death suggesting a direct role of ODC as mediator of apoptosis. Furthermore, they suggested that ODC is an effector of c-Myc induced apoptosis (c-Myc is a gene which encodes for transcription factors; a mutated version of c-Myc is found in many cancers). Increase of ODC activity will lead to an increase in polyamine synthesis and, therefore, in their metabolism leading to an increase of ROS formation (Figure 67)[250].

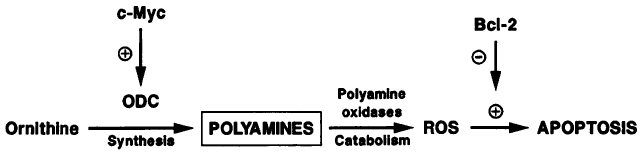

Figure 67. Model for c-Myc-induced apoptosis[250].

On the other hand, in human leukaemia cells HL-60 apoptotic induction has been blocked by using DMFO whereas adding exogenous polyamines restore the apoptotic process; therefore, an increase of polyamines could revert the inhibitory effect of DMFO on ODC[251]. Moreover, addition of exogenous polyamines prevens the apoptotic induction by DNA-fragmentation caused by etoposide (apoptotic-inductor); these evidences support the hypothesis that polyamines act as apoptotic-inhibitors. In studies on HL-60 cells treated with etoposide, an increased of ODC's activity has been observed, in the first 2-4 hours, followed by an almost completely inhibition of its activity; this may indicate that an increase of ODC is necessary for apoptosis induction while its decreasing is fundamental for holding the apoptotic process.

The *in vitro* cytotoxicity of Spm and Spd is well documented; in several experiments it is shown how they could be metabolized by a serum amine oxidase lead to cytotoxic compounds such as amino aldehydes, ammonia and hydrogen peroxide[252]. Moreover, the oxidation of polyamines catalyzed by PAO lead to hydrogen peroxide which is implicated in the induction of apoptosis; however, in several rat tissues PAO has been localized only in peroxisome where hydrogen peroxide could be reduced by the action of peroxisomal peroxide and other detoxifying enzymes[253]. Recent studies suggested that polyamines themselves could exert cytotoxic effects. Spm at millimolar concentration is cytotoxic to baby-hamster kidney cells; this effect is not due to the formation of toxic amino aldehydes because serum amino-oxidases were not present. It has been observed that inhibitors of amino-oxidase, such as aminoguanidine, could partially prevent the observed toxicity while treatment of the cells with MDL 72527, a PAO inhibitor, enhances the toxicity[254].

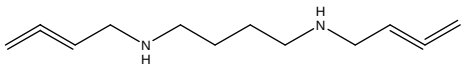

MDL 72527

p53 is the major tumor suppressor protein of the body. It is a transcription factor involved in cell cycle regulation, the initiation of apoptotic death and DNA repairing[255].

Li *et al.* investigated the mechanism of regulation of p53 gene expression by polyamines. In intestinal mucosal epithelial cells, they found that polyamines negatively regulated post-transcription of p53. In particular, depletion of polyamines enhances expression of p53 gene. Moreover, accumulation of p53 activates the transcription of cell cycle arrest genes leading to growth-inhibition (Figure 68)[256].

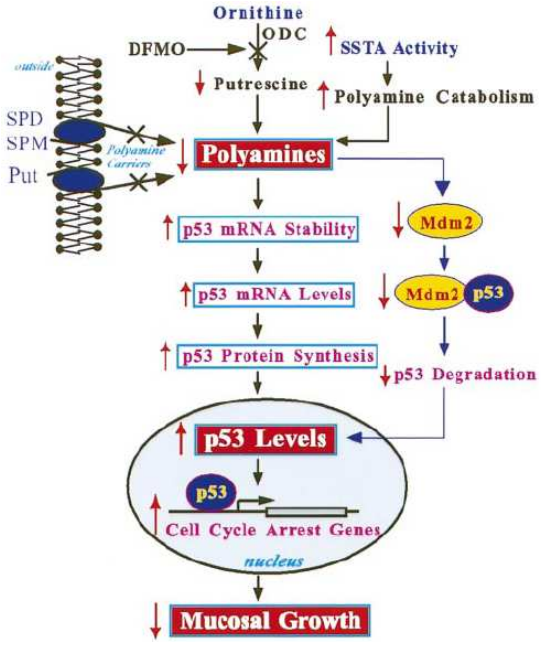

Figure 68. Regulation of expression of the p53 gene by cellular polyamines[256].

Some authors reported the influence of polyamines on the activity of nuclear factor κB (NF-κB). Such factor could have either pro- and anti-apoptotic effects depending on cell type and kind of death stimuli. They found that polyamines depletion induced an increase in NF-κB activity probably due the decrease of IKBα protein levels (IKBα bound NF-κB in the cytoplasm keeping it in an inactive form)[257]. In contrast, in another study, Shah *et al.* reported that Spm has a stimulatory effect on NF-κB MCF-7 breast cancer cells[258].

Nowdays, it is clear that polyamines and caspases are strictly connected[259,260,261]. Caspases are proteases that play a fundamental role in signalling and executing apoptosis[262,263,264]. They posses in their active site a cysteine residue which cleaved substrates at Asp-Xxx bound and acted in concert in a cascade triggered by apoptotic signalling. At least 14 distinct mammalian caspases have been identified and 11 of them are humans (Figure 69). Of these 11 caspases not all are involved in apoptotic cascade: caspases-1, -4 and -5 are mediator of inflammation and cleaved proinflammatory cytokines. The other seven caspases are apoptotic and generally are divided in two classes:

- initiator caspases, which includes caspases-2, -8, -9 and -10;
- effector caspases, which includes caspases-3, -6 and -7.

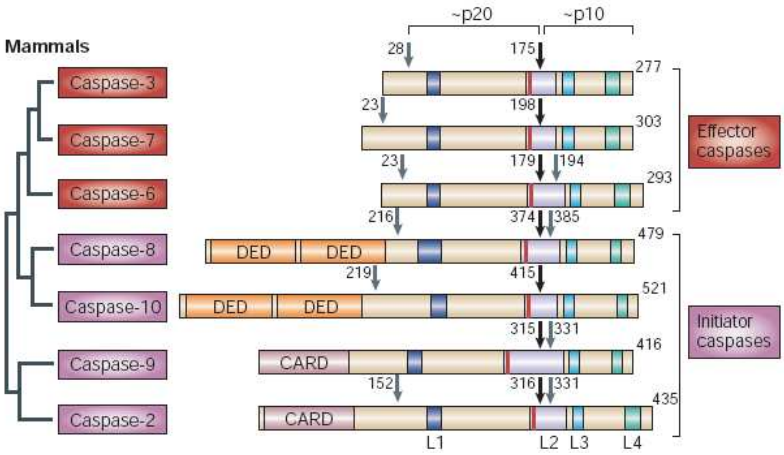

Figure 69. Apoptotic caspases in mammalian[264].

The initiator caspases activate the effectors which are able to degrade several substrates such as nuclear protein and cytoplasm. The activation of caspase effectors could be carried out also by non-caspase proteases such as catepsin and calpains[265].

All caspases are produced in cells as inactive proenzymes that contain three domains: an NH_2-terminal domain, a large subunit (~20 KDa) and a small subunit (~10 KDa). Proteolytic cleavage of the caspases precursor results in the separation of large and small subunit.

The caspases-cascade may initiate by different pathways depending on the origin of the death stimuli. The extrinsic pathway is initiated by the binding of a death ligand such as Fas-I to the respective death receptor. This pathway is receptor-dependent and several death receptors family has been identified such as TNF-R1, Fas and NGF-R. Among these families the Fas is the best characterized. Fas activates procaspase-8 and the active caspase-8 can activate caspase-3, hydrolyzing several apoptotic substrates.

Alternatively, caspases-cascade could be triggered in a receptor-independent pathway by different stimuli including chemotherapeutic agents.

The intrinsic pathway is mediated by mitochondria: apoptotic signals can influence the permeability of mitochondrial membrane inducing release of some pro-apoptotic proteins into the cytoplasm, such cytochrome C[259]. Cytochrome C released in the cytoplasm becomes part of the apoptosome which mediates activation of caspases-9; this pathway is strictly regulated by Bcl-2 family protein. In addition, another pro-apoptotic factor released by mitochondria is the apoptotic inducing factor (AIP) which can activate caspase-3 or can move into the nucleus and induces DNA fragmentation[266]. Both receptor-dependent and mitochondrial pathways converge at level of caspases-3 (Figure 70).

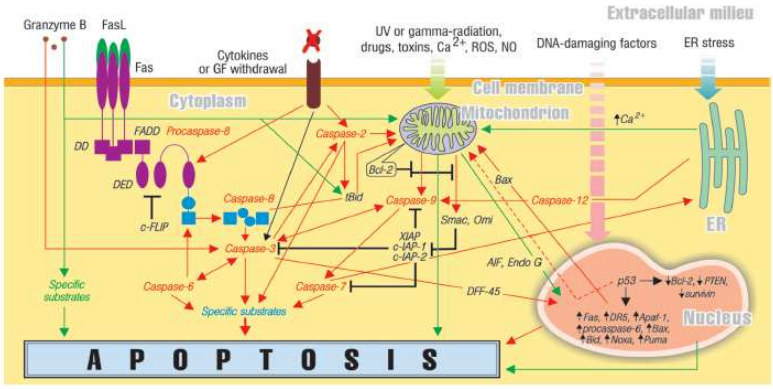

Figure 70. Involvement of caspases in apoptosis[259].

How caspases kill cells is not fully understood but seems that they could inactivate proteins that protect cells from apoptosis or they could destroy important cell structures as nuclear lamina.

Due to their fundamental role in homeostasis maintenance, caspases could represent an attractive pharmacological target for the treatment of pathologies caused by cell growth desregulation. For example, caspases inhibition could be helpful in all the diseases triggered by an excessive apoptosis such as neurodegenerative diseases. On the other hand, caspases activation could be useful in cancer treatment where an excessive cell proliferation occurs. Therefore, they may be promising biochemical target for designing new therapeutical instrument for the treatment of such diseases[267].

Stefanelli and coworkers studying the link between polyamines and caspases observed that in HL60 cells polyamines induce activation of caspases; in particular, they showed that Spm was more efficient than Spd in activation of caspases-3 while Put resulted inactive. Moreover, they observed that Spm is able to bind to mitochondria and to induce the release of cytochrome C[268,269,270] . On the other hand, Nitta *et al.* showed that in different cell lines depletion of intracellular polyamines caused disruption of mitochondrial membrane potential leading to caspases activation[271].

As above discussed, many evidences link polyamines to different apoptotic pathways; nevertheless, the exact role of such molecules in these biochemical cascades is still controversial. The overall picture is quite complicate and seems that polyamines may behave as pro-apoptotic or anti-apoptotic agents depending on the particular physiopathological condition.

Biochemical and Medicinal Chemistry aspects of polyamines

Polyamines are essential in maintaining homeostasis and variation in their concentration is associated with different pathological conditions. Therefore, several groups have focused their research in discovering new molecular structures able to interfere with all the biochemical pathways in which polyamines are involved. For example, agents able to inhibit polyamines biosynthetic enzymes will prevent cell growth and, therefore, could be used as antiproliferative agents. Moreover, polyamines analogues have been developed in order to induce apoptosis in transformed cells. In addition, polyamine residues could be used as delivering

agents by using *Polyamines Transporter System* (*PAT*) to facilitate the entreance of different drugs into the cells[272,273].

The discover of molecules targeting the enzymes involved in polyamines metabolic pathways has been the first approach used in order to developed potential therapeutic agents (Figure 71).

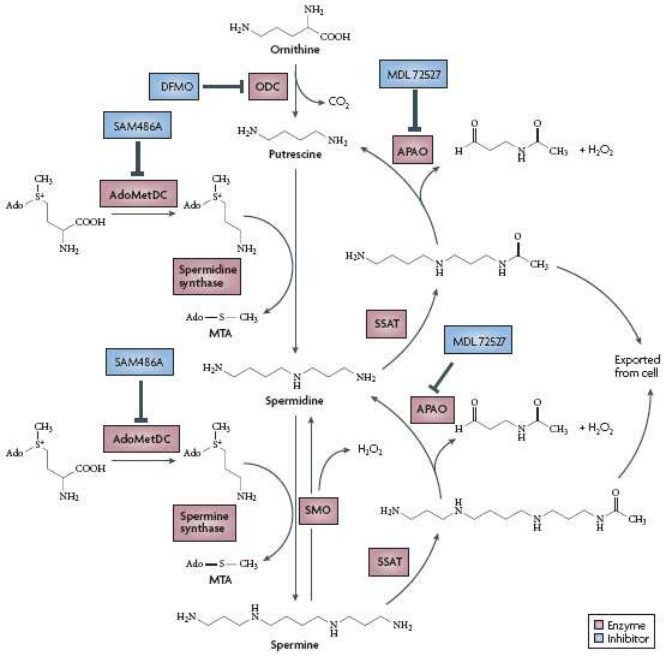

Figure 71. Targets in the polyamine metabolic pathway[272].

Perhaps the most known enzyme involved in polyamines metabolism is ODC and one of the most important inhibitor of such enzyme is 2-difluromethylornithine (DMFO) that acting as suicide inhibitor induces the arrest of cell growth[274]. DMFO is an enzyme-activated irreversible inhibitor: it first competes with ornithine for the binding site and then it is decarboxylated by the enzyme to create a highly reactive intermediate that forms a covalent bind with Cys360 or Lys69 leading to enzyme inactivation[275]. In *vitro*, DMFO induces arrest of cell growth by depletion of Put and Spd even if the levels of Spm are variable. However, *in vivo* DMFO was found to display cytostatic effect and not cytotoxic effect; nevertheless, it is under investigation as chemopreventive agent in prostate and colon cancer in combination with non-steroidal anti-inflammatory drugs.

Moreover, several inhibitor of S-adenosylmethionine (SAM) decarboxylase have been developed. One of the earliest inhibitor developed is methylglyoxal bis -guanylhydrazone (MGBG). It has been reported that it is active as antileukemic agent but its clinical use has been limited due to its severe toxicity[276]. MGBG is a competitive inhibitor of SAM and, moreover, it seems to be able to interact with mitochondria. Nevertheless, MGBG could be considered as lead compound for the development of additional agents. For example, SAM486A developed by Novartis is a potent inhibitor of AdoMetDC and it does not present any mitochondrial activity and its possible use as therapeutic agent is currently under investigation[276]. In

addition, some S-adenosyl methionine (AdoMet) analogues have been developed but, unfortunately, these compounds could not be used *in vivo* due their insufficient methabolic stability[277].

Other target enzymes are Spd and Spm-synthasse for which analogues of the transition state have been designed. S-adenosyl-3-thio-1,8-diaminooctane (AdoDATO) is a specific inhibitor of Spd synthase; unfortunately, it causes depletion of Spd but increases Put and Spm leading to few growth-inhibitory effect (Figure 72)[278,279].

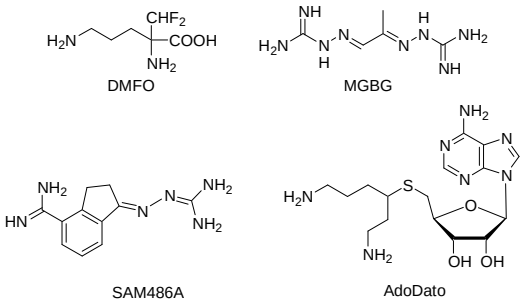

Figure 72. Chemical structure of DMFO, MGBG, SAM 486A and AdoDato.

A more recent approach to inhibith polyamine biosynthesis is based on the design and synthesize new polyamines analogues. Such compounds should be able to entry into the cells using the *PAT*, downregulate biosynthetic enzymes and/or upregulate catabolic enzymes[272,273].

The first generation of these polyamines analogues were the N,N^1-bis(ethyl)polyamines; they are terminally alkylated analogues of Spd and Spm (Figure 73). The more active of these polyamines analogue are BESpd (N^1,N^8bis(ethyl)spermidine), BESpm (N^1,N^{12}bis(ethyl)spermine), DENSpm (N^1,N^{11}bis(ethyl)norspermine) and BEHSpm (N^1,N^{14}bis(ethyl)homospermine) which induce depletion of intracellular polyamines and exhibit several anticancer activities against cancer cells. These analogues get into the cells through *PAT* and induce depletion of polyamines by acting on ODC, AdoMetDC and SSAT. For example, BESpd was found to be active on DMFO-resistant human non-small-cell lung-cancer line, NCI H157[280]. Very important was the discovery that the respond to these agents was dependent by phenotype of the cell: DMFO-sensitive human non-small-cell lung-cancer line NCI H82 is more resistant to BESpd than NCI H157 cells[281]. In NCI H157 cells, bis-ethylpolyamines have shown to increase the activity of SSAT in dose- and time-dependent manner and, in addition, they cause down-regulation of ODC and AdoMetDC[282]. In particular, SSAT induction seems to be strictly linked with cell death even if such connection depend on the type of polyamines analogues and of cell lines: for example, DMSpm (1,12-dimethylspermine) in human large-cell lung carcinoma cells is a very potent SSAT inducer but it shows no-toxicity[283]. How the induction of SSAT leads to cytotoxicity is not totally clear; it seems that a high induction of SSAT causes production of substrates for PAO whose activity is responsible of cytotoxic concentration of hydrogen peroxide.

Among the different analogues synthesized, DENSpm is a very active SSAT-inducer, it is taken up by the polyamines transporter, it downregulates ODC and S-adenosyl methionine decarboxylase (AdoMetDC) and

it upregulated polyamines catabolism; for these reasons it has been recognized to be a good candidate for clinical trials but, in such tests, unfortunately it showed an unacceptable neurotoxicity[284,285].

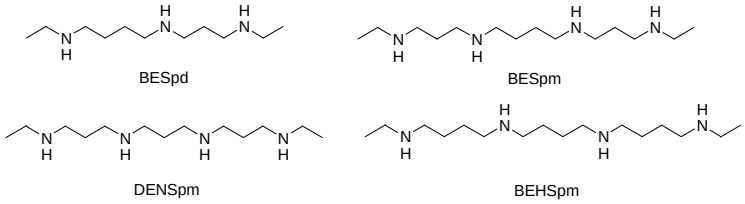

Figure 73. Chemical structure of N,N^1-bis(ethyl)polyamines: BESpd, BESpm, DENSpm, BEHSpm.

Furthermore, asymmetrically substituted polyamines analogues have been synthesized and tested (Figure 74). Derivatives such as PENSpm (N^1-propargyl-N^{11}-ethylnorspermine), CPENSpm (N^1-cyclopropylmethyl-N^{11}-ethylnorspermine), CHENSpm (N^1-cycloheptylmethyl-N^{11}-ethylnorspermine) and IPENSpm ((*S*)-N^1-(2-methyl-1-butyl)-N^{11}-ethyl-4,8-diazaundecane) exert significant antiproliferative activity by inducing SSAT, downregulating ODC and AdoMetDC[286,287]. Among these compounds, CHENSpm, despite its low SSAT-inducing activity, induces apoptosis in non-small-cell lung cancer producing G_2/M block by interfering with normal tubulin polymerization[288,289].

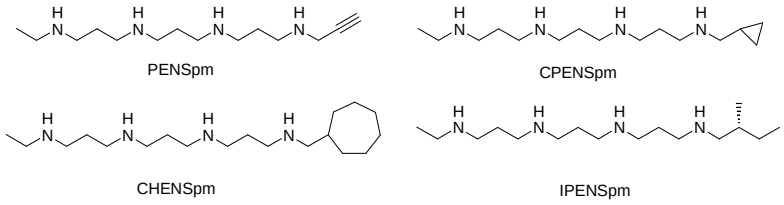

Figure 74. Chemical structure of asymmetrically substituted polyamines: PENSpm, CPESpm, CHESpm, IPENSpm.

In addition, several derivatives have been developed by replacing the polymethylene chain between the amine functions with conformational restricted group able to reduce the free rotation around the C-C bound (Figure 75)[290]. Two "frozen" polyamines analogues are CGC-11047 and CGC-11093 in which the replacement of the polymethylene chain with a more rigid double bond and cyclopropane moiety affects both the activity and the toxicity[291,292]. Despite the similar structure, only CG-11047 is able to induce SSAT and SMO; moreover, CGC-11093 is in phase-1 trial as antiproliferative agent while CGC-11047 is in phase-1 as single agent and in phase-1b in association with Bevacizumab, docetaxel or gemcitabin.

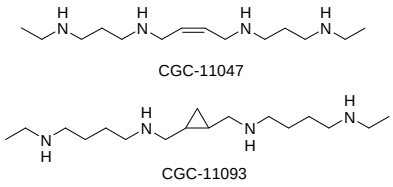

Figure 615. Structure of "frozen" polyamines analogues: CGC-11047 and CGC-11093

Despite their effect on their own metabolism, polyamines are able to interact DNA and chromatine and, therefore, many efforts have been made in order to develop compounds able to target them. Oligoamines with many amine functions in the side chains have been developed and they displaied antiproliferative activity in submicromolar range in human prostate cell line (Figure 76)[293] In particular, CGC-11444 was active also against human breast cancer cells *in vitro* and *in vivo* by inducing cytochrome C release and caspase-3 activation and, in addition, it seemed to alter the expression of estrogen receptor[294].

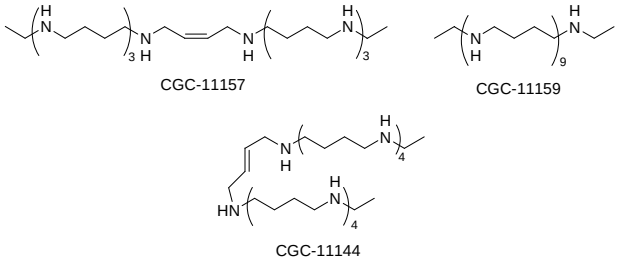

Figure 76. Oligoamines CGC-11157, CGC-11159, CGC-11144.

Bis(benzyl)polyamine MDL 27695 showed the ability to inhibit proliferation of HeLa cells. Interestingly, no correlation between DNA binding properties and antitumor activities of MDL 27695 and its analogues was detected[295].

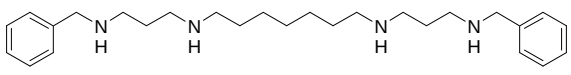

In addition, MDL 27695 seems able to gain into cells using PAT or some other specific polyamine transporter.

Recently, it has been demonstrated that different types of cancers showed an increased activity of the *PAT* due to the increased requirement of polyamines. Moreover, several studies reveal that many polyamines analogues use *PAT* to enter into cells and such transport system lacks of selectivity. Therefore, such system

could be used to selectively deliver polyamine-anticancer drug conjugate preferentially into cancer cells avoiding the side toxic effects towards normal cells normally exerted by anticancer agents.

Unfortunately, not only cancer cells but also some normal cells system such as bone marrow, intestinal epithelium and hair folliculi, are rapidly growing cells; however, the real therapeutic effectiveness of this strategy needs to be verify.

Both Spd and Spm have an high affinity toward DNA and the development of conjugate between polyamine and structure able to interact with DNA could lead to an increase of affinity toward DNA thanks to the establishment of additional electrostatic interactions. One of the first example of application of this strategy is represented by the conjugate clorambucile-Spd (Figure 77); this derivative showed a DNA affinity 10000 times higher than clorambucile alone suggesting the role of polyamines chain to establish additional interactions with phosphate moieties of DNA: in addition, it penetrates into cells through *PAT* system[296,297].

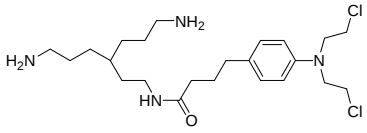

Figure 77. Conjugate clorambucile-Spd.

In 2000, Phanstiel and coworkers developed a series of conjugate polyamines-DNA intercalator in order to target DNA and/orTopoisomerase II (TOPOII) activity. Such derivatives have a Spm fragment covalented linked at its N4 position to an acridine (**LXVI**, **LXVII**) or to an anthracene (**LXVIII**, **LXIX**) moiety.

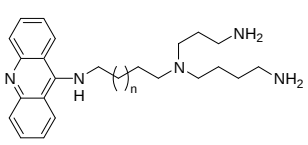

LXVI: n=1
LXVII: n=2

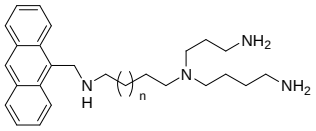

LXVIII: n=1
LXIX: n=2

All these derivatives showed the ability to interfere with TOPOII in a dose- and time-dependent manner and acridine-derivatives are more active in inhibit TOPOII than anthracene-derivatives. In contrast, in L1210 (murine leukaemia cell line) anthracene derivatives were more potent than the acridine-based conjugate. Concerning their ability to use *PAT* to gain into cells, this study revealed that spermidine-based ligands may not represent the right architecture to use *PAT* whereas the activity of **LXX**, which is based on spermine moiety, was more efficacious *PAT* ligand.

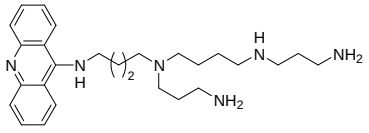

LXX

Soon later, the same authors reported on the synthesis and the biological evaluation of a new series of polyamine-DNA intercalator agents (**LXXI-LXXVI**).

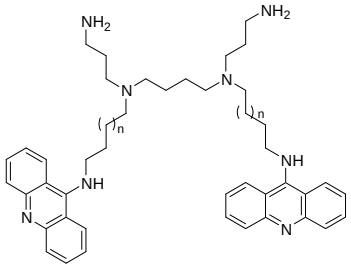

LXXI: n=1
LXXII: n=2

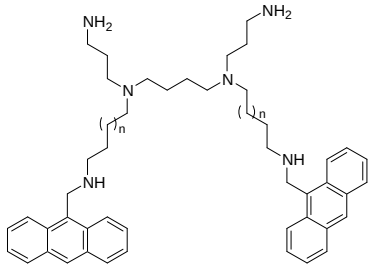

LXXIII: n=1
LXXIV: n=2

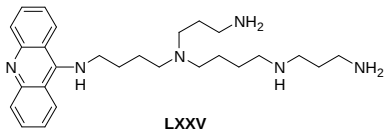

LXXV

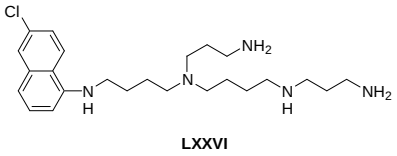

LXXVI

Such compounds have been tested in order to evaluate their inhibitory activity towards DNA-TOPOII: the bis-Spm derivatives, **LXXI-LXXIV** are more efficient at 5 μM than mono-Spm derivatives. Moreover, bis-derivatives containing the C5 tether length, **LXXII** and **LXXIV**, were more active than the corresponding containing the C4 tether length, **LXXI** and **LXXIII**. Concerning the possibility to gain into cells by *PAT*, the mono-intercalator-Spm moiety, **LXXV**, had the highest affinity for the L1210 *PAT*[298]. Basing on the high cytotoxicity of anthracene moiety over the acridine analogue, a series of tetraamine-anthracene derivatives have been synthesized and evaluated for their intracellular uptake via *PAT*. Furthermore, in this study it has been evaluated also the affinity of unsubstituted polyamines system for the *PAT*.

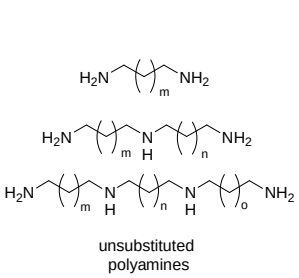

unsubstituted polyamines

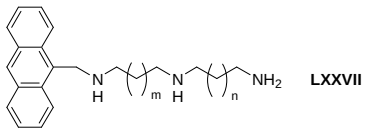

LXXVII

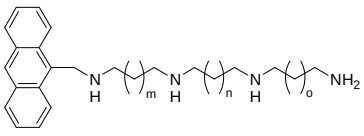

LXXVIII

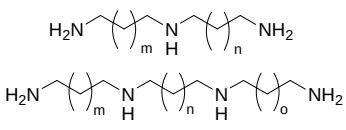

LXXIX: m=1, n=1 IC_{50}= 5120 nM
LXXX: m=1, n=2 IC_{50}= 2460 nM
LXXXI: m=2, n=2 IC_{50}= 2300 nM
LXXXII: m=1, n=1, o=1 IC_{50}=1510 nM
LXXXIII: m=1, n=2, o=1 IC_{50}= 1340 nM
LXXXIV: m=2, n=2, o=2 IC_{50}= 730 nM

From this evaluation appeared that in L1210 cells, tetraamines showed more affinity to *PAT* than triamine and diamines; moreover, it was observed that the better distance between two nitrogens atoms corresponded to 4 carbon atoms.

However, such cell line results to be more susceptible to triamines conjugate **LXXVII** than tetraamines **LXXVIII**. Of course, these results depend on polyamine architecture; in particular in terms of vector design, the 4,4-triamine motif was found to be optimal chemical signal to gain into cells via *PAT*. That could be explain considering that tetraamines are high-affinity *PAT* ligands that slowly dissociate from the receptor while triamines have lower binding affinity and dissociate rapidly from *PAT* to exert the cytotoxic effect. Indeed, a deconvolution microscopy study in A375 melanoma cells reveled a rapid internalization for the intercalator-4,4 triamine conjugate whereas the intercalator-4,4,4 tetraamine remained mostly at the cell surface[299].

In addition, in 2004 Phanstiel *et al.* synthesized a new series of anthracene-polyamine conjugate in order to prove the sensibility of *PAT* to small changes in its substrates. Based on these compounds and previous works, they presented a model which related polyamine-anthracene conjugate to *PAT*-mediated cytotoxicity (Figure 78).

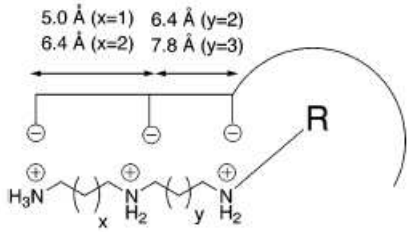

Figure 78. Architecture of PAT[299].

They showed that the best results were obtained when x is equal to 1 or 2 and when y is 2 or 3; increasing y value from 3 to 4 in anthracenyl-containing conjugate lead to a dramatically decrease of selectivity for *PAT*. This decreasing in uptake and cytotoxicity reveals that the hydrophobic cavity cannot accommodate groups bigger than the anthracenyl ones. In addition, if R is a smaller group then antracenyl, as napthyl moiety, it is possible to increase the length of N1-tether from methyl to ethyl holding a good selectivity toward *PAT*. Furthermore, based on a computational model developed studying compounds **LXXXV**, **LXXXVI** and **LXXXVII** they proposed a two-step model, "where first the conjugate binds primarily through its polyamine portion to *PAT* and then hydrophobic substituent seeks out its associated pocket to initiate the receptor-mediated endocytosis event[300].

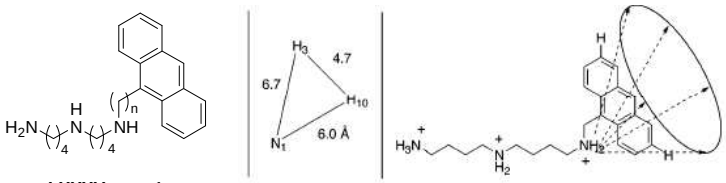

LXXXV: n = 1
LXXXVI: n = 2
LXXXVII: n = 3

compound	n	N^1-H^{10} (Å)	N^1-H^3 (Å)
LXXXV	1	6.0	6.7
LXXXVI	2	7.5	7.9
LXXXVII	3	8.4	8.7

Figure79. Model for polyamines-*PAT* interaction[300].

2.1.2 Peptidil-prolyl *cis/trans* isomerase (PIN1)

PIN1 is a member of evolutionarily conserved enzymes, peptidyl-prolyl isomerase (PPIase family) and catalyze the *cis/trans* isomerisation of peptidyl-prolyl amide bonds. PPIases, by changing the conformation of the peptide bond, may alter the conformation of their substrates and, therefore, their function. PPIases are highly expressed and have been divided in three groups differing in the amino acids sequences of their catalytic domain and their substrate specificity:

1. cyclophilins, which bind the immunosuppressant drug cyclosprin A;
2. FK506 binding proteins, which bind the immunosuppressant drugs FK506 and Rapamycin;
3. parvulins, which do not bind any immunosuppressant drugs[301].

PIN1 belongs to a parvulin subfamily of PPIases to this subfamily belong also PAR10 in bacteria, PAR14 and PAR10 in eukaryotic[302].

PIN1 is an 18 kDa protein form by 163 AA; it is composed by two domain organized around a hydrophobic cavity: an amino-terminal WW domain (amino acids 1-39) and a carboxylic-terminal domain (amino acids 45-163) (Figure 80). The amino-terminal domain is involved in protein-protein interaction while the carboxylic-terminal domain represented the PPIase domain which catalyzed the isomerisation of the proline peptide bond between the *cis-trans* conformations.

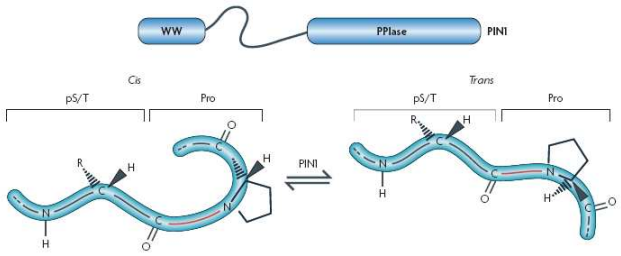

Figure 80. Stucture of PIN1[301].

The crystal structure of PIN1 reveals that the active site is located at the surface of the enzyme; it is a hydrophobic pocket composed by Leu122, Met130, and Phe134 which binds the cyclic side chain of the prolyl residue. The peptide bond undergoing the catalyzed *cis*/*trans* isomerisation is surrounded by His59, Cys113, Ser154, and His157; Lys63, Arg68, and Arg69 form a basic cluster, which binds the phosphorylated Ser/Thr of the substrate (Figure 81)[303].

a) b)

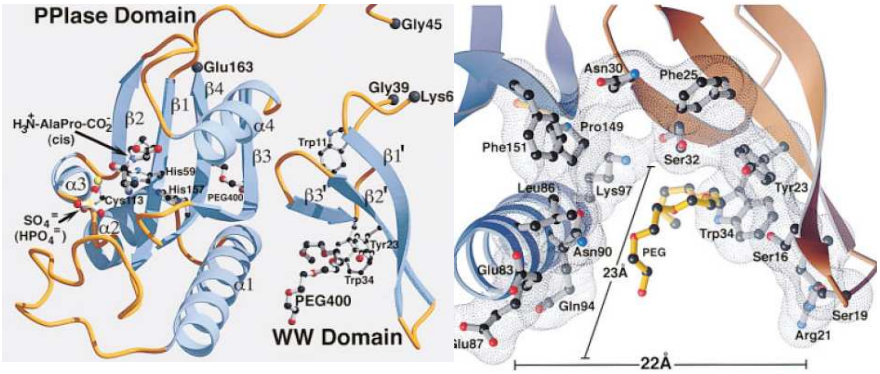

Figure 81. a) Ribbon representation of PIN1. b) Ribbon and molecular surface representation of the PIN1 interdomain cavity. The WW domain is orange and the PPIase domain is light blue[303].

A closer look to the crystal structure of PIN1 with an Ala-Pro dipeptide shows an important role for two structural motifs: the loop between residues 66 and 77 and Cysteine113. This loop is involved in binding the phosphate moiety of the substrate[303] and, in yeast, Lys63 is essential for the anchoring function of the phosphorylated substrate. Cys113 is spatially close to the Ala-Pro bound; this suggested a possible catalytic mechanism through a nucleophilic attack on the carboxylic carbon of the substrate by the sulphur of Cys113. Later, it has been shown that Cys113 has a very low pKa suggesting that this residue is ionized under physiologically conditions. Moreover, the local environment around Cys113, particularly Ser111 and Ser115, would maintain Cys113 with a negative, full or partially, charge; therefore, Cys113 will present its negative charge to the carbonyl atom of the substrate when it is bound to the *cis*-conformation. This negative charge would weaken the double bound character of the substrate pSer-Pro peptide bond allowing rotation from 0˚ (*cis*) to 180˚ (*trans*)[304,305].

The peptide bond linking two amino acids can either adopt *cis* or *trans* conformation but for all amino acids except proline *trans* conformation is thermodynamically more favoured than *cis* conformation; moreover, rotation around the peptide bond is energetically disfavoured due its partial double bond character. For proline the energy difference between the two conformations is far smaller and therefore the motifs Xxx-Pro could exist in both conformations. Both *cis* and *trans* conformation are substrates and product and, therefore, PIN1 acts catalysing the *cis-trans* and the *trans-cis* conversion[306].

The WW domain only recognizes phosphorylated Ser/Thr motifs followed by a Proline; PIN1 is the only PPIase having the WW domain and therefore it exclusively bind Ser/Thr-Pro motifs. Due to its affinity to phosphorylated Ser/Thr-Pro motifs, PIN1 works in concert with kinase and phosphatases proteins; the phosphorylation is carried out by different proteins which play important roles in many important biological processes such as cell-cycle regulation and cellular stress response. Kinases involved in these phosphorylation processes are i.e. the mitogen-activated protein kinase (MAPK), cycline-

dependent kinase (CDK), extracellular signal-regulated protein kinase (ERK) and glycogen synthase kinase 3β (GSK-3).

Role of PIN1 in cellular biochemical pathways

PIN1 is involved in several different biological events and it plays important roles in many pathological condition such as cancer, Alzheimer's disease, microbial infection, asthma and so on (Figure 82). The reversible phosphorylation of Ser/Thr-Pro motifs is a key regulatory mechanism for the control of cellular processes.

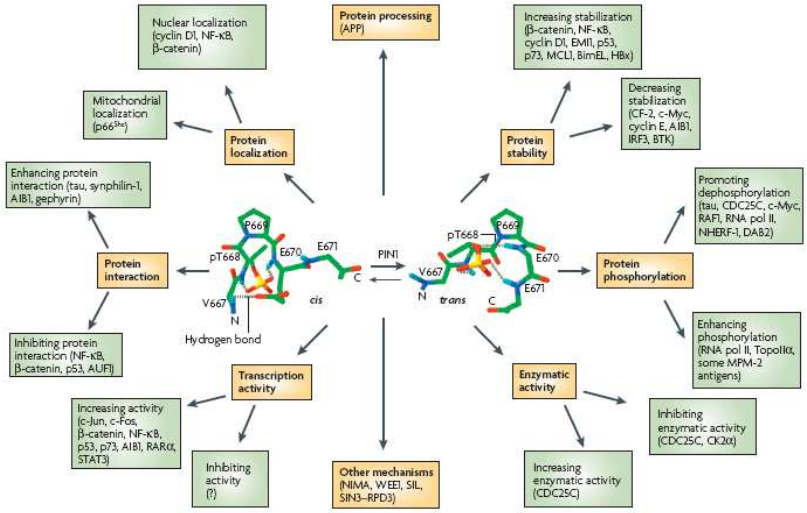

Figure 82. PIN1 regulates a spectrum of target activities[322].

PIN1 has been first identified in yeast as protein able to interact with *never in mitosis gene a* (NIMA) an essential mitotic kinase found in *Aspergillus nidulans*. NIMA overexpression induces cell death and therefore it was suggested that PIN1 has an important role in mitosis regulation acting as negative modulator. Moreover, depletion of its homologue in *Saccaromyces cerivisiae* ESS1 induces mitotic arrest[301].

Several evidences show that PIN1 acts on various mitotic-specific phosphoproteins. Cell cycle is regulated by many protein kinases known as Cdks which drive cells through different phases of the cell cycle. These kinases alter the function of proteins triggering the mitotic process by phosphorylating hundreds of proteins such as cyclin B-cdc2. PIN1 binds Cdc25 *in vitro* and *in vivo* which is the activating phosphatases of cyclin B-cdc2 and inhibits its activity; the activation of cyclin B-cdc2 is important for the progression from G_2 to mitosis and such interaction between Cdc25 and PIN1 partially explains the ability of PIN1 to inhibit the G_2/M transition[307].

Moreover, PIN1 inhibits the function of mitosis-inhibitory kinase Wee1 that inactivates cyclin B/cdc2 through phosphorylation by interacting with Wee box[308]. In addition, PIN1 interacts with the early-mitotic inhibitor Emi1; Emi1 inhibits the activity of anaphase-promoting complex APC that controls the cell

division acting on various regulatory proteins. Emi1, required to induce S-phase and M-phase entry by stimulating cyclin B accumulation, is synthesized at G_1-S transition and is degraded by ubiquitin-ligase $SCF^{\beta trpc}$ pathway at prometaphase; PIN1 stabilize Emi1 by preventing its association with $SCF^{\beta trpc}$.[309]

PIN1 also plays an important role in mitotic chromosome condensation; it interacts with chromatin during G_2/M phase and modulates the mitotic protein at phosphorylation level[310].

All these results suggest that PIN1 is deeply involved in cell cycle regulation and therefore it is not surprising that it could have an impact on diseases caused by uncontrolled cells proliferation such as cancer. Many oncogenes and suppressor are regulated by Proline-directed phosphorylation and several evidences show that PIN1 is overexpressed in many human cancers such as breast, prostate, cervical, brain, lung and colon cancer[311].

PIN1 overexpression is correlated with the overexpression of two of its substrates, cyclin D1 and β-catenin. PIN1 plays a critical role in regulation of cyclin D1. Overexpression of cyclin D1 has been found in 50% of patients with breast cancer and it is involved in oncogenesis; furthermore, inhibition of cyclin D1 expression causes growth arrest of tumor cells while its overexpression induce cell transformations. PIN1 increases levels of cellular cyclin D1 mRNA and protein, and activates its promoter through the AP-1 site. The AP-1 complex is formed by c-Jun and c-Fos protein and c-Jun activity is modulated by phosphorylation induced by growth-factors, oncogenic proteins or stress (for example, c-Jun could be phosphorylated by JNKs, c-Jun N-terminal kinases, which could be also activated by oncogenic Ras). PIN1 binds phosphorylated c-Jun and increases its ability to activate cyclin D1 promoter (Figure 83)[312].

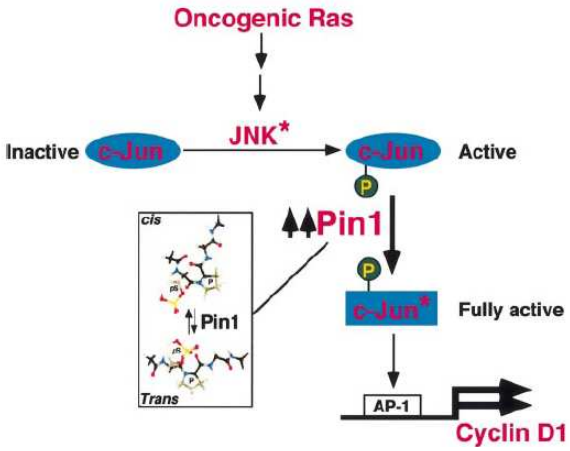

Figure 83. Role of PIN1 in regulating cyclin **D1**[312]**.**

Moreover, it has been demonstrated that cyclin D1 may be phosphorylated at Thr286 and PIN1 could bind this Thr286/Pro motif stabilizing it by preventing its nuclear export and following cytoplasmatic degradation[313].

PIN1 is also able to stabilize β-catenin; it is involved in cancer development thanks to its ability to induce several genes critical for the cancerogenetic process such as those for cyclin D1, c-Myc and peroxisome-proliferator-activated receptor-δ (PPAR-δ). β-catenin is regulated by different proteins such

as *adenomatus polyposis coli* protein (APC) which is a nuclear-cytoplasmatic shuttling protein that can export β-catenin to cytoplasm where it is degradated; β-catenin contains different Ser/Pro motifs and, therefore, after phosphorylation of such sites it could be bind by PIN1. Such interaction takes place both *in vitro* and *in vivo.* The phosphorylation of β-catenin occurs at Ser246/Pro which is next to the APC-binding site and PIN1 isomerizes this peptide bond preventing the ability of β-catenin to bind APC, thus, increasing the nuclear fraction of β-catenin. In addition, PIN1 transactivates several β-catenin target genes[314].

Another example of how PIN1 is linked to cell growth pathways derives from its interaction with the transcription factor NF-κB. It is an ubiquitous transcription factor that controls the expression of genes involved in immune responses, apoptosis, and cell cycle. NF-κB is a dimer of proteins belonging to the Rel family, including p65 (RelA), p50, p52, c-Rel, and the most abundant activated form consists of a p65 and p60. It is normally sequestered in the cytoplasm by interacting with protein known as IkBs and it could be activated by a variety of stimuli, as cytokines, viral proteins and stress inducers; degradation of IkBs activates NF-κB allowing its nuclear translocations. It has been observed that after cytokine treatment, PIN1 binds to pThr254/Pro motif in p65 inhibiting its bond with IkBα (a type of IkBs) increasing therefore NF-κB's nuclear accumulation and activity[315].

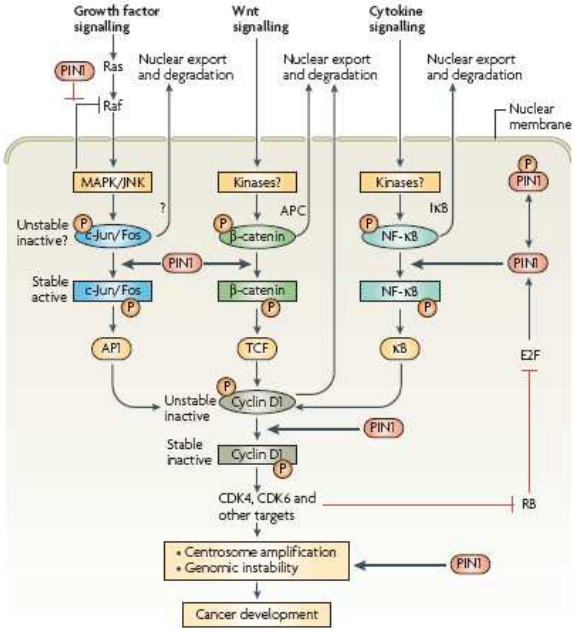

Figure 84. PIN1 regulates multiple oncogenic signalling[322].

PIN1 plays a critical role in regulating centrosome duplication. Deregulation of centrosome duplications leadsto abnormal centrosome numbers and aberrant mitosis. This duplication is modulate by multiple proteins such as Cdk-2 which are Pro-directed kinases. Suizu *et al.* reported that PIN1 is involved in regulation of centrosome duplications and its deregulation lead to centrosome amplifications,

chromosome instability and oncogenesis. It is believed that PIN1 could modulate centrosome duplications thought cyclin D1[316].

PIN1 also modulates the function of different proteins involved in cellular response to stress injury; for example, PIN1 is able to stabilize p53 and p73 following genotoxic stress. Several stresses could activate kinases, such as members of MAP kinase and CDKs, able to phosphorylate p53. Such p53 phosphorylation occurs at Ser33, Ser46, Thr81 and Ser315 generating sites for PIN1 recognition. The binding of PIN1 generates conformational changes in p53 "leading to activation of genes required to cell-cycle checkpoint or promote apoptosis"[317,318]. Moreover, the activity of p53 is also controlled by the apoptosis inhibitor iASPP which blocks p53 binding to cell-death related promoter: in presence of cytotoxic stress PIN1 induces dissociation of iASPP from p53[319].

Furthermore, PIN1 is able to bind che-1, an RNA polymerase II-binding protein that plays an important role in transcriptional activity of p53, which is down-regulated during the apoptotic process. In response to various stimuli che-1 is phosphorylated and it could be negatively modulated by HDM2/MDM2 proteins. The interaction between HDM2/MDM2and che-1 is regulated by PIN1; che-1 interacts with PIN1 following apoptotic DNA damage and it increases che-1 degradation[320].

PIN1 seems to be able also to regulate phospho-Ser77 Retinoic Acid Receptors α (RAR α). RARα activity is regulated by phosphorylation that can occur at different sites:

1. Ser369: protein kinase A phosphorylates Ser369 promoting heterodimerization and DNA binding;
2. Ser157: Ser157 is phosphorylated by protein kinase C leading to destabilization of heterodimer-DNA complex;
3. Ser77: Ser 77 is phosphorylated by cdk7 leading to receptor stabilization in presence of the ligand.

The latter AA is located in a region whit several Pro residues and represents a substrate of PIN1; phosphorylation of Ser77 is moreover important for RARα stability; indeed, RARα is able to activate the fibroblast growth factor promoter *fgf8* which is a gene involved in cancerogenesis. Therefore, PIN1 is able to modulate RARα degradation and so it is able to down regulate RARα activity on *fgf8*[321].

In addition to all above presented connections with cell growth regulation and desregulation processes, PIN1 is deeply involved in neuronal function[322]. PIN1 is expressed in neurons and although its physiological functions are still not totally elucidated, it is clear that PIN1 interacts with several proteins involved in the neuronal homeostasis, such as τ protein and Amyloid Precursor Protein APP[323,324]; τ phosphorylation precedes the formation of neurofibrillary tangles while from the phosphorylation of APP derived the Aβ peptide which leads to the formation of senile plaques. Extracellular senile plaques and intracellular neurofibrillary tangles are the neuropathological hallmarks of Alzheimer's Disease (AD) and therefore PIN1, targeting τ and APP, results to be involved in AD. PIN1 binding pThr231-τ restore the functions of phosphorylated τ to bind microtubules and to promote microtubule assembly. Moreover,

PIN1 binding to pThr231 induces τ dephosphorylation by promoting the action of PP2A which is the physiological τ phosphatase[325]. Furthermore, PIN1 is involved in the A*β* production acting on phosphorylated APP[326]. APP is a transmembrane protein that could be processed by two distinct pathways; the non-amyloidogenic pathway which involves a proteolytic cleavage by α-secretase and leads to non-toxic product and an amyloidogenic pathway which consists a sequential cleavage by β- and γ-secretase which leads to production of peptides, mainly of 40 or 42 amino acids in length, called Aβ_{40} and Aβ_{42} respectively. Of the two released products, Aβ_{42} is the more toxic even if both have been found in senile plaques. APP could be phosphorylated at Thr668 by different kinases, such as stress-activated protein kinase 1b, cyclin-dependent kinase and Cdc2 kinase, and such phosphorylation increases A*β* secretion *in vitro*. The effect of PIN1 on APP cascade is more complicated. In 2005 Akiyama and coworkers demonstrated, by studying the production of A*β* in both wild-type and PIN1-null mice, that PIN1 promotes A*β* production *in vivo*. This is because the levels of Aβ_{40} and Aβ_{42} were reduced in PIN1-null mice compared with wild-type[327]. Soon later, Pastorino and coworkers showed that PIN1 is able to bind pThr668 both *in vitro* and *in vivo* experiments. Moreover, it has been shown that Thr668-Pro APP is largely in *trans*-conformation with a small amount of *cis*-conformation that could increase after the phosphorylation of Thr668. The "*trans*-conformation is more susceptible to non-amyloidogenic process while the *cis*-conformation favours the amyloidogenic process. The presence of PIN1 keeps the fraction of *cis*-Thr668-Pro APP low whereas a loss of PIN1 function leads to an accumulation of *cis*-Thr668-Pro APP and promotes amyloidogenic production of A*β*" (Figure 85)[328].

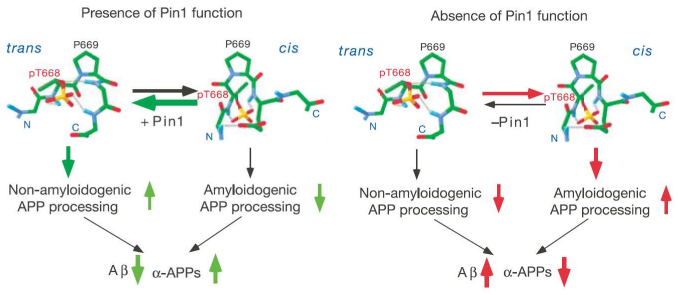

Figure 85. Effect of the presence and the absence of PIN1 in APP processing[328].

Moreover, oxidative stress may play an important role in the pathogenesis and in the progression of AD. Such oxidative stress is manifested by nucleic acids oxidation, proteins oxidation, lipids peroxidations and ROS formation[329]. Butterfield *et al* showed that protein oxidation was increased in the hippocampi of Mild Cognitive Impairment (MCI) subjects (MCI is a transition zone between normal cognitive aging and early dementia), suggesting that such protein oxidation is important in AD development. Specifically they found that α-enolase, glutamine-synthetase, pyruvate kinase M2 and PIN1 were more oxidized in the hippocampi of MCI subject[330] PIN1 activity was found to be reduced in AD

hippocampus due to its oxidative modification. PIN1 could be oxidazed both *in vitro* and *in vivo* and the resulting reduced activity seems to be responsible of the increased concentration of phospho-τ in AD[331].

PIN1 inhibitors

An increasing number of evidences suggest that PIN1 could be an attractive new target for anticancer drug development[332]; as above discussed PIN1 is overexpressed in many human cancers, it acts as critical catalyst for multiple oncogenic pathways and in several cancer cell lines depletion of PIN1 determines arrest of mitosis followed by apoptosis-induction. Moreover, it has been shown that PIN1 knockout mice developed normally suggesting that an anti-PIN1 therapy could not generate toxic effecta[333].

Up to now the only successful strategy leading to PIN1 inhibition *in vitro* and *in vivo* derived from the use of antisense strategies, dominant negative strategies, RNA interference and gene knockout[333,334,335,336]. Not so many small-molecule PIN1 inhibitors have been identified, and unfortunately none of them is clinically useful.

The most known PIN1 inhibitor is the natural product Juglone (5-hydroxy-1,4-Naphtoquinone) which specifically inactivates the activity of parvulin-like PPIase from *E. coli*, the homologous PPIase Ess1 in yeast and the human PIN1 while it does not affect the other families of PPIase, cyclophilins and FK506BPs.

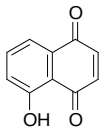

Juglone

Juglone covalently bind to the side chain of Cys41 probably by a Michael addition which occurs between the sulfhydryl group of the Cys and the α,β-unsaturated carbonyl system of the juglone[337]. Juglone induces apoptosis in Hela cells in dose-dependent manner and prevents cells from entering in apoptosis (Figure 86)[333, 338].

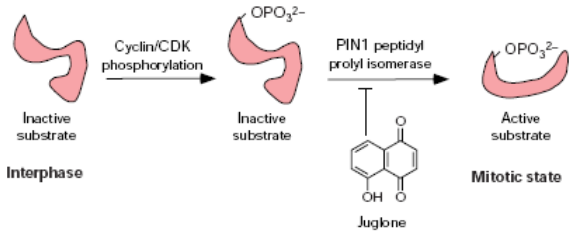

Figure 86. Ability of Juglone to inhibit PIN1[338].

Moreover, Juglone blocks transcription by interacting with RNA polymerase II but the results show that such effect is not mediated by the inhibition of PIN1[339]; furthermore, Juglone inhibits also other enzymes such as pyruvate carboxylase and glutathione S-transferase[337].

In 2003 Uchida *et al.* identified new PIN1 inhibitors by screening a chemical library of compounds with double ring structure and compounds previously developed as potential anticancer (Figure 87). Among the different compounds tested, three of them resulted potent PIN1 competitive inhibitors: PiA which inhibits PIN1 with an IC_{50} of 2.0 μM, PiB and PiJ with both an IC_{50} of 1.5 μM. These derivatives are more potent than Juglone which showed an IC_{50} of 5 μM and they did not bind DNA or other target protein such as Topoisomerase I. Moreover, the effects of PiB and PiJ on cancer cell proliferation were tested in many cancer cells, such as HSC2, HCT116, OVK2, SKOV3, and they were the most potent inhibitor of cell proliferation showing an IC_{50} in μM range.

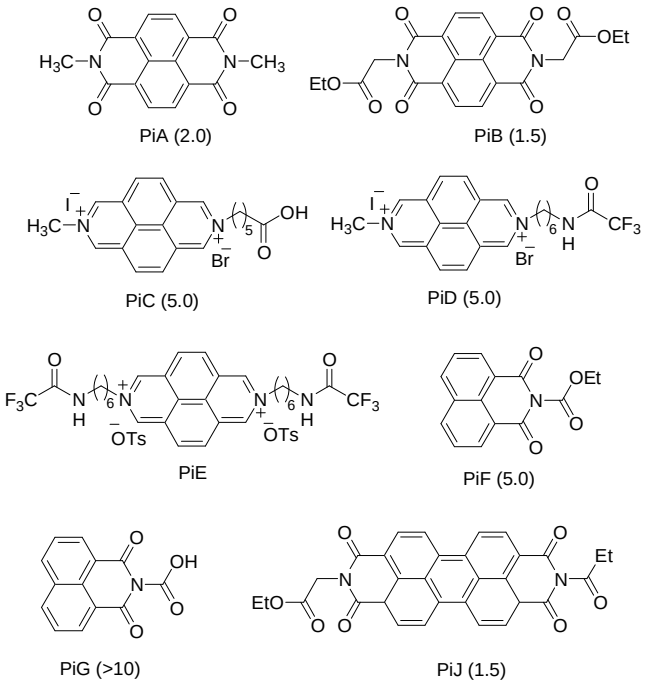

Figure 87. PIN1 inhibitors developed by Uchida *et al.*; in brackets are reported their IC_{50} expressed in μM[340].

Most of the compounds tested have symmetrical structure and this might lead to an increase in potency; moreover, docking studies on PiB have been performed showing how PiB inhibits PIN1: the aromatic rings of PiB may establish π-π interaction with the protein's amino acids while the hydrogen atom of Arg69 and His157 and the backbone amide hydrogen of Lys57 form an H-bond with the oxygen atoms of PIN1 suggesting that the aromatic rings and the oxygen atoms are crucial for the PIN1-PiB interaction (Figure 88)[340].

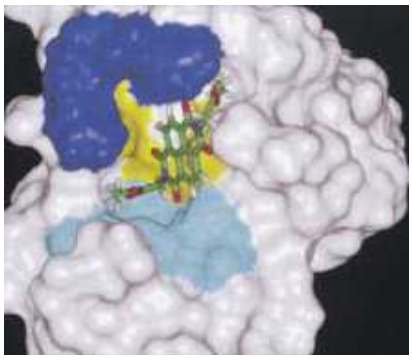

Figure 88. Docking model of PiB in PIN1[340].

In 2005, Bayer *et al.* discovered new peptidomimetic PIN1 inhibitors derived from the natural product Pepticinnamin E, an inhibitor of farnesyltransferase. These new derivatives synthesized by combinatorial synthesis were able to induce apoptosis but in some cases the connection between apoptosis-induction and farnesyltransferase inhibition was not clear; however, many evidences suggested a possible involvement of PIN1. Among all the Pepticinnamin analogues synthesized, the most potent resulted compounds **LXXXVIII-XC** which showed an IC_{50} values in micromolar range (Figure 89). These compounds seem to inhibit *h*PIN1 by decreasing the thermodynamic stability of the protein and/or lowering its solubility in aqueous media and are able to induce apoptosis in mammalian transformed cell line[341].

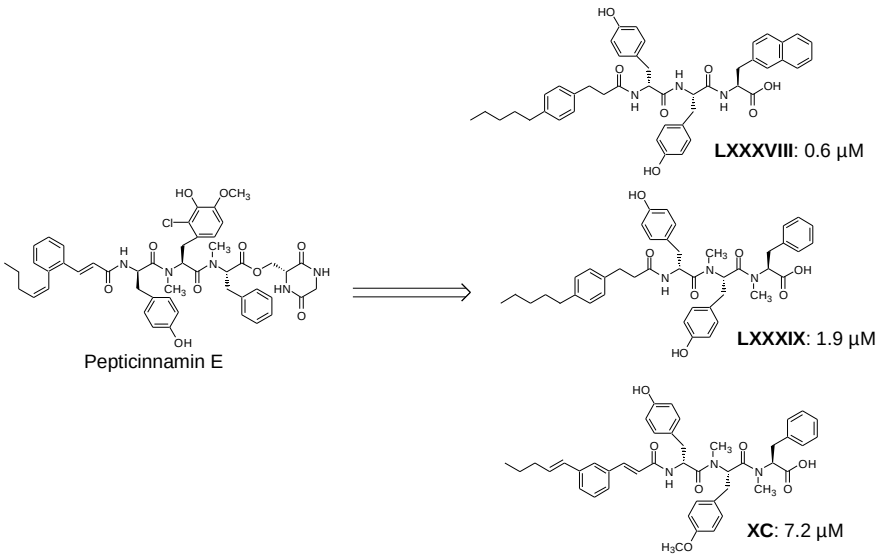

Figure 89. PIN1 inhibitors derived from Pepticinnamin E[341].

In 2006 Wildemann and coworkers reported the screening of a combinatorial peptide library leading to the discovery of very potent PIN1 inhibitors. Starting from the structure of PIN1 bound to Ala-Pro dipeptide, they generated fifteen compounds having the following general structure: Ac-Lys(N^{ε}-biotinoyl)-Ala-Ala-Xaa-Thr(PO_3H_2)-Yaa-Zaa-Glm-NH_2 where Xaa, Yaa, Zaa could be either natural amino acids, non-natural

amino acids or N-alkyl amino acids. The most potent compound of the series was the peptide Ac-Lys(N^{ε}-biotinoyl)-Ala-Ala-Bht-Thr(PO_3H_2)-Pip-Nal-Glm-NH_2 which showed an IC_{50} value of 0.21 µM (Bth, *β*-(3-benzothienyl)alanine; Nal, *β*-(2-naphthyl)alanine; Pip, piperidine-2-carboxylic acid).

Another group of peptidomimetics able to inhibit PIN1 has been developed by Wang *et al.* using alkenes as amide isosters (Figure 90). This approach has been previously used by the same research group in order to obtain hCyPA inhibitors: for example, they showed that the peptidomimetic Ala-*cis*-Pro (Z)-alkene inhibited hCyPA with an IC_{50} of 6.5 µM[342]; moreover, the dipeptide Leu-trans-Pro (E)-alkene was able to inhibit FKPB with an IC_{50} of 8.6 µM[343]. Therefore, Wang and coworkers developed three conformationally locked PIN1 substrate isosters: Ac-Phe-Phe-pSer-ψ[(*Z* and *E*)CH=C]-Pro-Arg-NH_2, **XCI** and **XCII**, and *N*-methylamide **XCIII**.

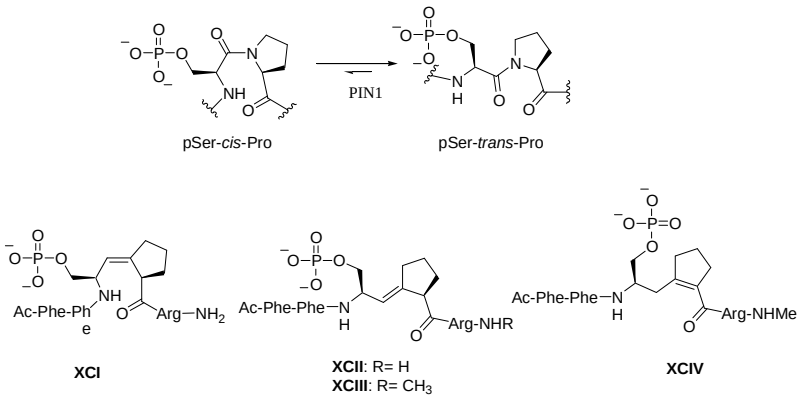

Figure 90. PIN1-mediated pSer-Pro amide isomerisation and inhibitors *cis*-isoster **XCI**, trans-isoster **XCII** and **XCIII** and endocyclic isomer of **XCIV**[344].

Both peptidomimetics **XCI** and **XCII** are competitive inhibitors of PIN1 and the *cis*-isostere **XCI** (IC_{50} 1.3 µM, competitive inhibitor constant K_{is} 1.74 µM) was more potent than *trans*-isostere **XCII** (IC_{50} 28 µM, K_{is} 40 µM respectively). These results suggested that PIN1 catalytic domain binds the *cis*-isostere stronger than the *trans*-isostere and that PIN1 preferentially binds the *cis*-isostere in acqueous solution. Moreover, **XCIII** which is more hydrophobic derivative of **XCII** did not improve the biological activity as well as the endocyclic isomer **XCIV** is a very poor inhibitor showing that the location of the double bond is fundamental in the protein-substrate recognition. In addition, **XCI** and **XCII** has been tested again A2780 ovarian cancer cells displaying an IC_{50} of 8.3 and 140 µM, respectively[344].

In 2006 Daum and coworkers designed a series of Aryl Indanyl Ketones as transition-state analogues of PIN1: they assert that the aryl 1-indanyl ketones motif could mimicked the “twisted-amide” transition states and the change of hybridization about the ring nitrogen atom (Figure 91).

All the aryl indanyl ketones synthesized **XCV-C** showed K_i values in the micromolar range. The methoxy group in a adjacent position to the carbonyl group, **XCV**, was better than the hydroxy group, **XCVI**, leading to the more potent derivative (K_i 8.7 µM for **XCV** and 15.0 µM for **XCVI**); moreover the introduction of a

nitro group on the phenyl ring, **XCIX**, caused an improvement of PIN1 inhibition to sub-micromolar range while the reduction of the nitro group to amino group, **C**, did not influence the inhibition values (K_i 0.5 µM for **XCIX** and 0.4 µM for **C**). The two enantiomers of **XCVIII** showed different K_i values (K_i 5.6 µM for (*R*)-**XCVIII** and 51.0 µM for (*S*)-**XCVIII**). (*R*)-**XCVIII,** (*S*)-**XCVIII** and *rac*-**XCVIII** have been found able to reduce the activity of p53 reporter gene in etoposide treated MCF-7 cells (human breast adenocarcinome); moreover, these compounds were able to decrease the level of β-catenin (in tumor cells, PIN1 regulates the β-catenin turnover) in SH-SY5Y cell lines (human neuroblastoma)[345].

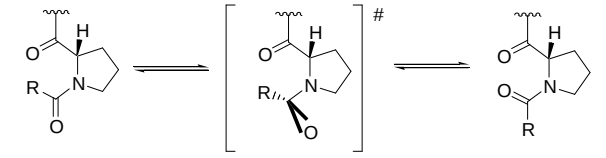

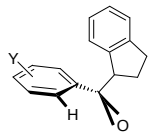

aryl 1-indanyl ketones

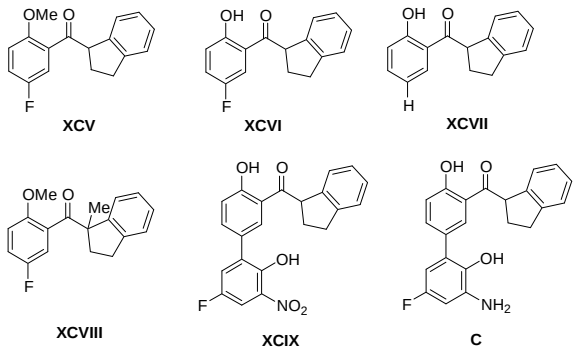

Figure 91. Selected aryl 1-indanyl ketones designed by Daum *et al*[345].

Some of the PIN1 inhibitors showed above are phosphorylated compounds that penetrate with difficulty the cellular membrane due to the negative charge located on the phosphate group. In 2007, Zhao and Ezkorn presented PIN1 inhibitor **CI** and its prodrug form **CII**; the phosphate group was masked by bis (bis-pivalyloxymethyl) (POM) group that is enzymatically removed after its entry in the cell to give its active form (Figure 92).

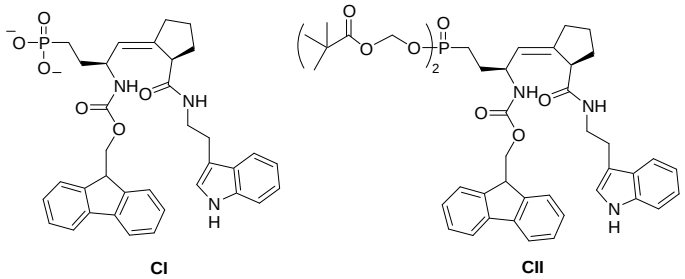

Figure 92. PIN1 inhibitor **CI** and its prodrug form **CII**[346]**.**

CI inhibits PIN1 in µM range and both compounds have been tested in A2780 ovarian cells; **CI** shows an IC_{50} of 46.2 µM and **CII** shows an IC_{50} of 26.9 µM suggesting that the introduction of POM on phosphate group of **CI** may help the entry into the cells by improving the hydrophobicity of the inhibitor[346].

2.1.3 DNA as Target for anticancer drugs

DNA plays a fundamental role in cell proliferation and cancerogenetic processes and therefore a large percentage of anticancer agents are molecules that are able to interact with it. Based on their possible interaction with DNA, such molecules have been classified in four wide groups:

- Alkylating agents, which are able to covalently bound DNA;
- Agents able to truncate DNA double helix;
- Agents that reversibly interact with double helix of DNA;
- Agents that intercalate between the DNA bases.

Among decades many efforts have been made in order to discover new molecules and new biochemical pathways which could be targeted by these molecules. One of the most important reported anticancer compounds is represented by the intercalator agents. Such kinds of molecules are typically characterized by a planar heterocycle of approximately the size and shape of DNA base pair. They insert perpendicularly into the DNA without forming any covalent bonds and the formed complex is stabilized by hydrophobic, Van der Walls , hydrogen bonding and charge transfer forces. It has been reported that these interactions may affect the cells replication processes leading to cellular death[347].

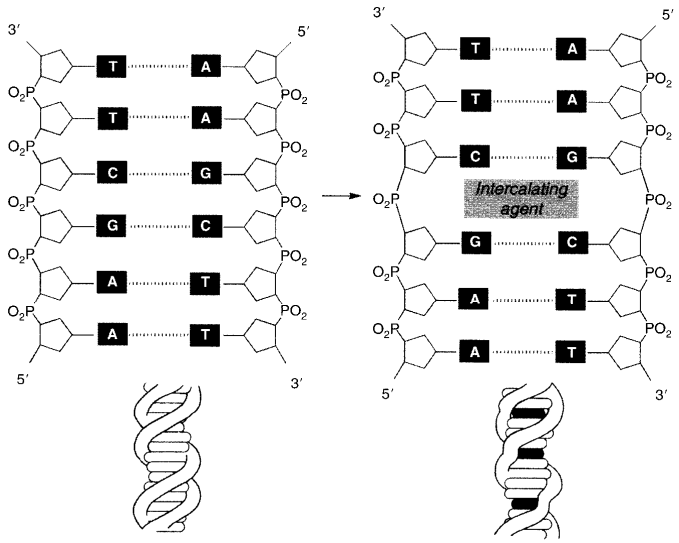

Figura 93. Deformation of DNA by an intercalating agent[347].

Although their ability to insert directly into the molecular structure of DNA, this is just the first mechanisms used by this molecule to induce cytotoxicity. Indeed, many DNA-intercalators are able to induce changes in DNA-associated proteins, such as DNA-polymerase, transcription factors and

Topoisomerase[347]. The latter interaction is probably the most important mechanism of cytotoxicity induces by such molecules. They are able to stabilize the ternary complex DNA-drug-Topoisomerase, therefore, blocking the action of this important enzyme; once the ternary complex is detected by the cell as damage it will triggers a series of events, such as p53 activation, leading to apoptosis[348].

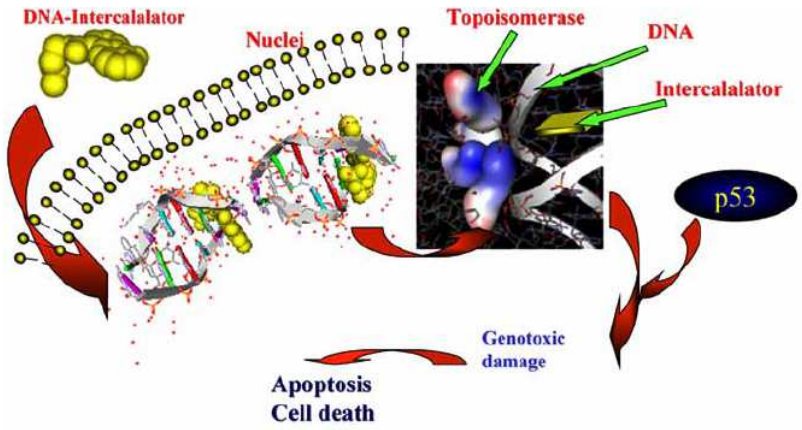

Figure 94. Schematic representation of the mechanism of cytotoxicity of a DNA-Intercalator[348].

Intercalators represent a wide group of compounds that could be classified in two main groups:

- Classical intercalators, which display their cyctoxicity by inhibiting Topoisomerase II;
- Non-classical intercalators, developed more recently.

The most important differences between these two classes of intercalator concern the chemical structures: classical-intercalators contains bi- or tri-cyclic rings fused while non-classical intercalators present non fused rings system[349].

Classical intercalators could further be classificated in subfamily, based on the nature of their chromophore unit, in:

- Naphthalimide and related compounds, such as Mitonafide, Amonafide, Azonafide and Elinafide;
- Intercalators based on the pyridocarbazole system, such as Ellipticine and 9-methoxyellipticine;
- Anthracycline, such as Doxorubicine, Daunomicine and Mitoxantrone;
- Antibiotics of the Echinomycin family, such as Echinominine and Triostina;
- Acridine and related compounds, such ad Amsacrine;
- Actinomycin;
- Analogues of Benzimidazo-[1,2,c]quinazoline[350].

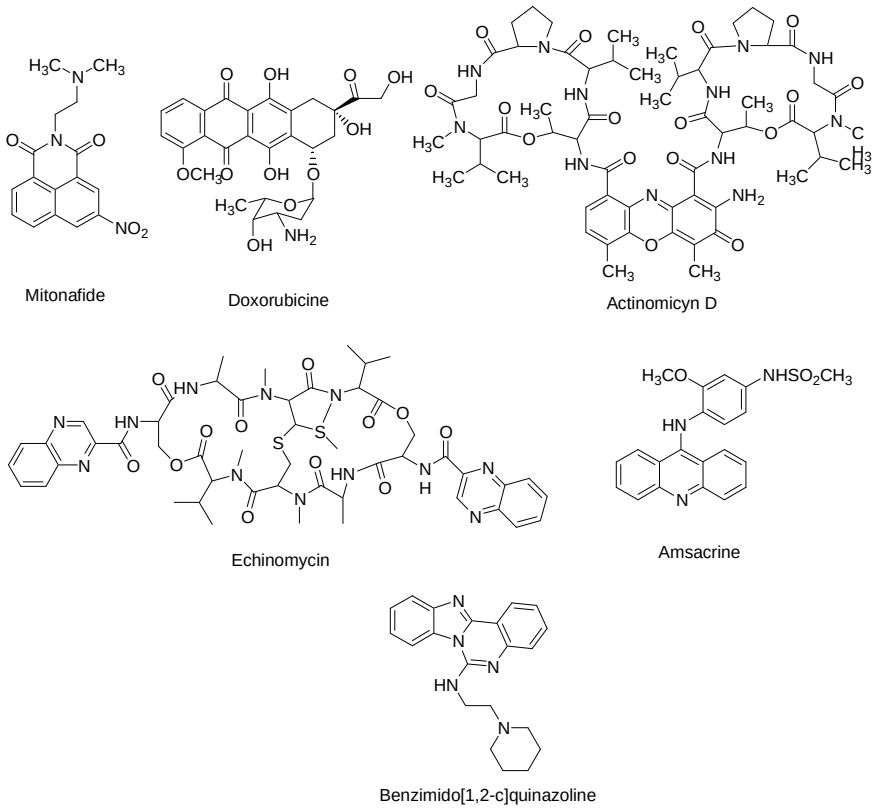

Figure 95. Selected examples of classical intercalators.

These compounds so different from the chemical point of view, exert their cytotoxic effect by intercalating into DNA and by inhibiting TopoII; moreover, some of them could have different mechanism of action: for example, Anthracyclin thanks to their oxidoreductive properties are able to induce DNA-damage through ROS-formation or Acridine could inhibit either TOPOI and TOPOII.

Non-classical intercalators are characterized by the presence of a huge aromatic planar system able to intercalate and to stabilize triple-helix DNA more than duplex-helix. Also non-classical intercalators are divided in different groups:

- Threading intercalators;
- Tris-interacalator, such as triacridines.

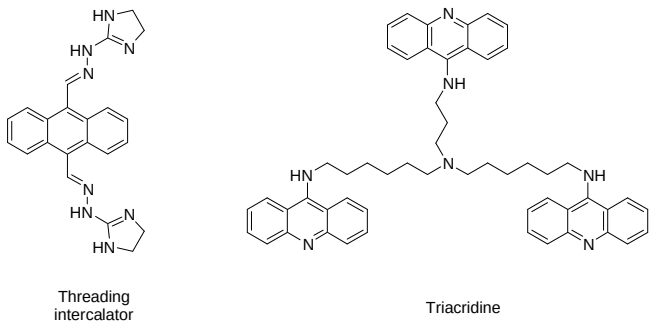

Figure 96. Chemical structure of non-classical intercalators.

Among all the intercalators developed, Braña and coworkers in 1970s published a series of Naphthalimides as anticancer agents[351]. SAR studies carried out on these structures showed that the presence of a basic terminal group is essential for activity and that such activity is maximal when the nitrogen atom on the side chain is two methylene units far from the aromatic ring; furthermore, it has been discovered that the better substituent on the nitrogen atom is a dimethyl ones and substitution in position 5 on the naphthalic ring is resulted the best for the activity; the prototypes of this series are Amonafide and Mitonafide (Figure 97)[352,353].

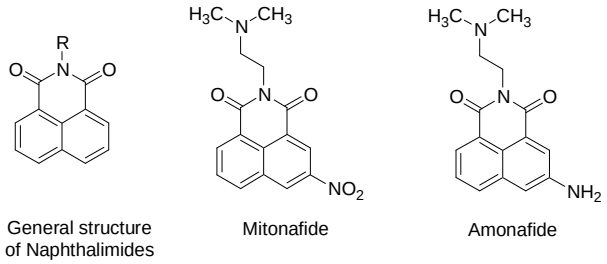

Figure 97. Naphtalimides developed by Braña and coworkers.

The chemical structure of such compounds derived from the combination of chemical motifs that characterized other anticancer compounds: β-nitronaphthalene from Aristocholic Acid, the ring of CG-630 and the basic chain of Tilorone (Figure 98).

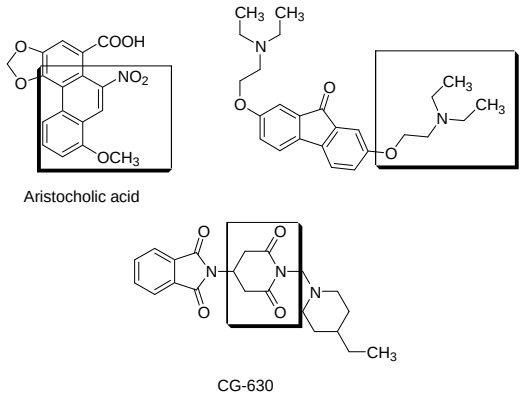

Figure 98. Chemical motifs included in the anticancer drug design.

Both Amonafide and Mitonafide have been tested in clinical trials; Amonafide is active against murine lymphocytic leukemia (P338) cells and lymphocytic mouse leukemic L1210 cells while Mitonafide is active against human epidermoid carcinoma KB cells and cervical cancer HeLa cells[354,355]. Both compounds intercalated into DNA[356] and are able to induce a TOPOII-mediated DNA cleavage at Nucleotide No 1830 on pBR322 DNA[357]. In particular, it has been seen that such cleavage is not observed in compounds without the basic side chain.

Amonafide is substrate of a specific metabolic enzyme, *N*-acetyltransferase 2 (NAT2) that catalyzed the acetylation of a wide range of amines, including arylamines and heteroaromatic amines. Substrates of NAT2 are also isoniazide, procainamide, hydralazine and sulfonamides. Amonafide could be metabolized through two different pathways: the first one by cytochrome CYP1A2 leading to a formation of oxidized derivative and the second one by NAT2 leading to N-acetylamonafide which is still metabolically active. Recently, it has been demonstrated that the most important side effects of Amonafide are caused by its acetylated metabolites (Figure 99)[358].

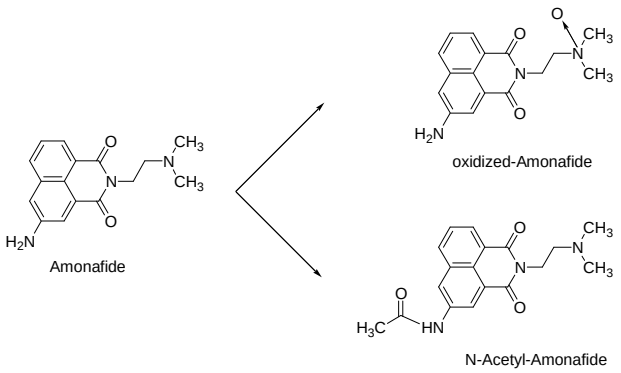

Figura 99. Metabolization of Amonafide.

Amonafide and Mitonafide are the most active compounds in the series of Naphthalimides and the only difference between them is constituted by the substituent on the aromatic ring: Mitonafide presents an

electron-donating amino group while Amonafide presents an electron-withdrawing nitro group. It has been suggested that the nitro-group promotes the formation of a charge transfer complex with DNA-bases while the amino-group promotes the stabilization of DNA-drug complex through the formation of hydrogen bond with the phosphate group of the DNA-backbone. Therefore, a number of SAR studies carried outon the ring-substituent have been carried out leading to the compounds having an amino-group in 8 and a nitro-group in 5; such derivatives were more active than Mitonafide and Amonafide on Human colon carcinoma cell line CX-1 and human hepatic stellate cell line LX-1. Moreover, a series of dinitro- and diamino-derivatives of Amonafide and Mitonafide, **CIII** and **CIV** have been described and they showed both *in vitro* and *in vivo* antileukemia and antimelanoma activities[359].

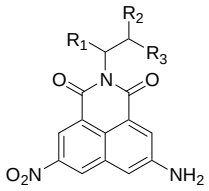

General formula
of 5-amino-8-naphthalimides

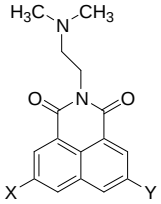

CIII: X = Y = NH_2 5,8-diaminonaphthalimides
CIV: X = Y = NO_2 5,8-dinitronaphthalimides

Another modification is represented by the replacement of the naphthalene moiety by an anthracene obtaining Azonafide, which result more active than Amonafide on the cell lines of human melanoma UACC375, human ovarian cancer OVCAR3 and L1210[360]. Analogues of Azonafide have been synthesized by replacing the anthracene moiety with phenanthrene (**CV)** and azaphenanthrene (**CVI**, **CVII**): unfortunately these compounds were less potent than Azonafide pointing out that linear anthracene chromophore is better than other rings system[361].

.

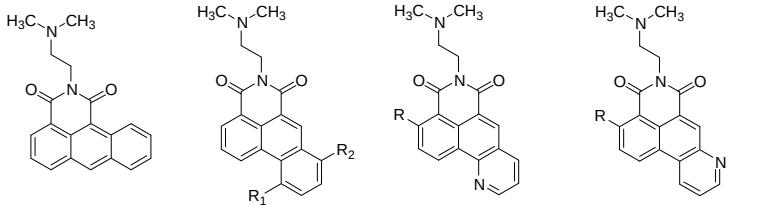

Azonafide

CV: Phenanthrene derivative

CVI: Azaphenanthrene derivative

CVII: Azaphenanthrene derivative

In order to improve the antiproliferative activity of these compounds, other analogues have been designed where the naphthalene rings were fused to other heteroaromatic systems. Despite the introduction of an imidazolic ring did not lead to any improvement, the introduction of a π-deficient pyrazine ring lead to a new series, Pyrazinonaphthalimmides **CVIII** and **CIX**, endowed with a more potent intercalating activity; such compounds have been screened against human colon adenocarcinome HT-29, HeLa and human prostate

cancer PC-3 cell lines showing an IC_{50} in micromolar range. Compound **CIX** having a -CF_3 group is less active than **CVIII**: this result could be explained by the steric hindrance of the trifluoromethyl group[362,352].

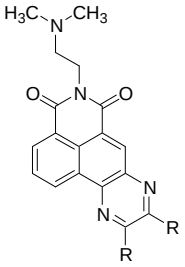

CVIII: R = H
CIX: R = CF_3

Based on these promising results given by the introduction of a pyrazine ring, other similar compounds have been synthesized in which the aromatic system of Amonafide has been conjugated with a π-deficient ring, such as furane and thiophene (**CX-CXIII)**.

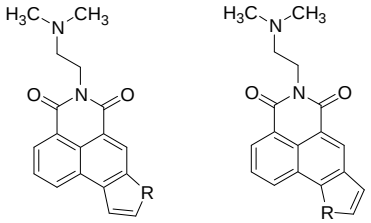

CX: R = O
CXI: R = S

CXII: R = O
CXIII: R = S

All these compounds have been screened against HT-29, HeLa and PC-3 cell lines resulting to be more potent than Amonafide; in particular **CX** is active in a submicromolar concentration. In order to explain the activity of **CX**, Braña and coworkers proposed a model to clarify the interaction between it and DNA (Figure 100). This model calculates four different possible orientations of **CX** into DNA:

a. orientation with the side chain in the major groove and the furan ring stacking between the bases T and G;
b. orientation with the side chain in the major groove and the furan ring stacking between A and C;
c. orientation with the side chain in the minor groove and the furan stacking between T and G;
d. orientation with the side chain in the minor groove and the furan ring stacking between A and C.

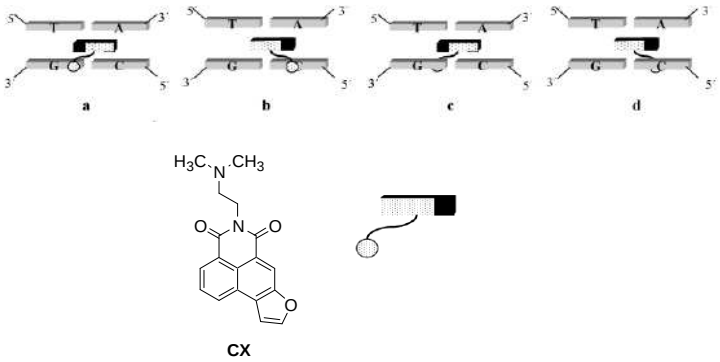

Figure 100. Possible interaction model of **CX** with DNA; the black square represents the orientation of the furan ring, and the sphere represents the protonated dimethylamino group of the side chain[363].

The more stable orientation is the one where the side chain remains in the major groove of the DNA and the furan ring is stacked between the bases A and C[363].

Furthermore, a series of molecules derived from the fusion of the aromatic rings of Amonafide and thiazolidine rings, calledThioazonaphthalimides, showed a very potent activity as intercalator (**CXI-CXIII)**. In this case, the better length of the side chain has been found to correspond to three methylenes groups which allowed the nitrogen atom to stay at the right distance from DNA in order to establish H-bond, outlining the importance of the basic side chain.

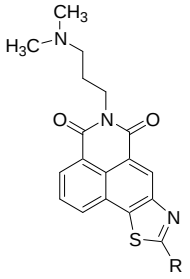

CXI: R = H
CXII: R = CH_3
CXIII: R = CF_3

All these compounds result to be more active than Amonafide against different cancer cell lines, such as A-549 human lung adenocarcinome and P388 lymphoblastic cell lines. In particular, **CXII** is more active against P388 and **CXIII** is more active against A-549 cell lines[364].

In order to improve the binding activity toward DNA a new series of bisintercalating agents have been designed basing on the structure of Amonafide and Mitonafide. Such compounds, called bis-naphthalimides, are structurally characterized by the presence of two naphthalimide units bound together by a chain containing at least one nitrogen atom and with different substituent on the aromatic rings.

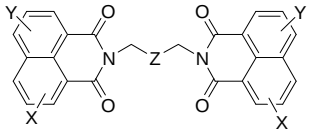

Y = H, 6-NO_2, 6-NH_2
X = H, 3-NO_2, 3-NH_2, 3-$NHCOCH_3$,
3-Br, 2-OH, 3-OH, 4-OH
Z = aminoalkylic chain

In HT-29 cell lines all the bis-naphthalimides resulted more potent than Amonafide and Mitonafide; the susbstituent on the aromatic rings sensibly influenced the antiproliferative activity: 3-$NHCOCH_3$ < 3-NH_2 < 3-NO_2. However, the more active compound was that without substituents on the aromatic rings; such compound called Elinafide showed an excellent antiproliferative activity against HT-29; moreover, *in vivo* Elinafide has shown to be able not only to inhibit the cellular growth but also to induce regression of the cancer cell mass; furthermore, the absence of the nitro group on the aromatic ring seemed to reduce the neurotoxicity associate with Mitonafide[365.366].

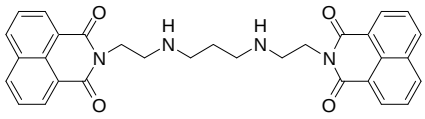

Elinafide

Elinafide acts by forming a sequence-specific complex with an exanucleotide $d(ATGCAT)_2$ portion where two naphtalimide units bisintercalate at TpG and CpA steps of the DNA, stacking with G and A. Moreover, the *N*,*N*-bis(ethylene)-1,3-propylenediamine linker lies in the major groove; furthermore, one of the protonated amino groups of Elinafide is hydrogen-bonded to O6 of guanine in the major groove while the other one could form an hydrogen-bond to guanine O6 of the opposite strand or establishes a weaker hydrogen-bond with N7 of the same base (Figure 101)[367,368].

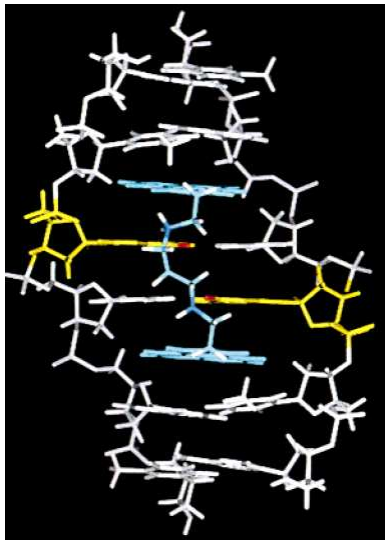

Figure 101. Stereoview of the complex elinafide-d(ATGCAT)$_2$; Elinafide is in blue, guanine in yellow and the oxygen atom is in red[368].

Moreover, a series of symmetrically and non-symmetrically Linefeed derivatives have been developed by replacing the naphthalene system with an acenaphthene one. However, the latter compounds were less active than the symmetric homologues[369,370].

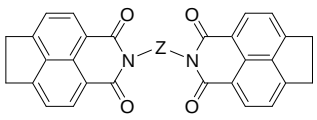

Symmetrical bis-derivatives of Elinafide

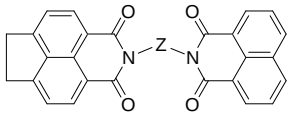

Asymmetrical bis-derivatives of Elinafide

In order to find compounds more potent than Elinafide, compound DMP-840 has been developed and it displaied biological effects similar to those of Elinafide; it binds DNA forming a stable ternary complex with DNA and TOPOII but it did not poison TOPOII[371].

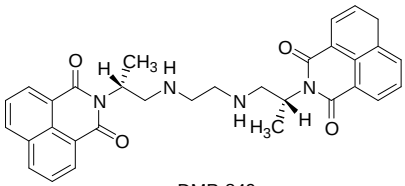

DMP-840

A further development of this series of derivatives is represented by the replacement of the naphthalendiimide structure with the 1,4,5,8-tetracarboxylicnaphthalendiimide (NDI) moiety to obtain new and more active intercalator agents. Indeed, both these features posses a big aromatic system and two co-

planar carbonyl groups. Therefore, new intercalator moiety has been esigned (N-BDMPrNDI, DMe-NDI,Phen-NDI) and, in addition, such compounds with NDI structure, beside their ability to intercalate into DNA, stabilize the triple helix DNA. Instability of triple-helix DNA is due to the repulsion between the nucleotides of these triple helix and such structure are strictly implicated in the genes regulation. Several studies point out that an increase in the stability of these structure could be useful in anti-genes and antisense therapy[372].

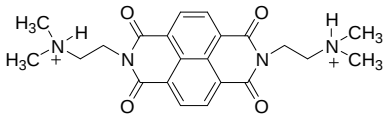

N-BDMPrNDI

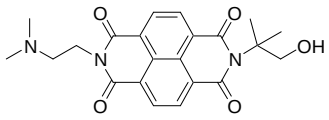

DMe-NDI

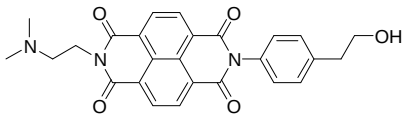

Phen-NDI

2.2 Drug Design

Design and synthesis of new anticancer agents represents one of the most challenging field in medicinal chemistry. Cancer is one of the main causes of death worldwide and despite several efforts have been made by scientists, anticancer drugs currently in therapy present a wide range of side effects due to their lack of selectivity[159].

One of the most interesting group of antiproliferative compounds used in therapy is represented by molecules targeting DNA, such as intercalators. These compounds, thanks to their chemical structures, are able to intercalate into the double helix of DNA and trigger different biochemical cascades leading to cell death.

Furthermore, it is known that natural polyamines are extremely important as regulator of cell growth because they control the progression of the cell cycle and regulate the cellular entry in apoptosis. In particular, their strictly relationship with apoptosis is emerging as an important target to focus on. Indeed, it has been demonstrated that natural polyamines, such as spermine and spermidine, are able to trigger apoptosis acting on caspases and mitochondrial-mediated apoptotic pathway. Moreover, given their importance in maintaining cellular homeostasis, polyamines are widely distributed in all kind of cells. Polyamines could be either synthesized by cells or could be provided from outside sources by using a specific transport system (*PAT*). This active transport system is more expressed in cancer cells, because, thanks to their fast reproduction, they need high levels of polyamines. Therefore, *PAT* represents an ideal target to hit selectively cancer cells and to deliver specific anticancer drugs. As reported before several polyamines-intercalators conjugate have been developed and are actually under clinical investigation.

Another recent and important cancer cell target is constituted by the enzyme called prolyl-peptidyl *cis-trans* isomerase (PIN1). Current experimental evidences show that PIN1 is deeply involved in the development of carcinogenesis process. In particular, PIN1 is able to recognize specific phosphorylated Thr/Ser-Pro motifs of several proteins and to induce isomerisation of the peptide bound leading to change in protein structure and function. It has been shown that PIN1 inhibition prevents entry into mitosis and cell division and it is overexpressed in numerous human cancers. Therefore, PIN1 is proposed as a therapeutic target for cancer treatment and PIN1-inhibitors may represent promising anticancer agents[332]. The aim of this work is to design and synthesize new molecular entities acting as Multi-Target-Directed Ligands (MTDLs)[7,156] able to hit different biochemical targets involved in cancerogenesis. Cancer can be considered a multifactorial disease and a single drug hitting a single target (one molecule-one target approach) may be inadequate for the treatment of such disease. Otherwise, compounds able to hit more than one therapeutic targets could be effective in treating of this complex disease (one molecule-multiple targets approach). The rational design of new MTDLs, that is compounds that simultaneously modulate different protein targets, either positively or negatively, at a comparable concentration for each target, remains a challenging task. Normally, the starting point to design new MTDLs is represented by a scaffold endowed with a particular

biological profile which can be widened by inserting new pharmacophoric units responsible of additive pharmacological properties.

In literature there are several examples of synthetic polyamines characterized by antiproliferative activity, one of them is represented by MDL 27695[295]. This compound showed a good antiproliferative activity against HeLa and MCF-7 cell lines, probably due to its ability to interfere with intracellular polyamines pathways. Although its basic functions, protonated at physiological pH, it is capable to entry into cells by using *PAT* or other alternative transport systems. This compound, although investigated some years ago, called our attention for its particular chemical features very similar to many other polyamines synthesized by Melchiorre and coworkers. It is structurally characterized by a polyamine backbone endowed with two benzylic groups inserted on the outer nitrogen atoms. We thought to design new anticancer MTDLs by applying the "universal template approach"[244] on the MDL 27695 structure with the aim to enlarge its biological profile. This approach has been successfully applied in the past and it asserts that the insertion of different pharmacophores onto the polymethylene tetraamine backbone can tune both affinity and selectivity for any given receptor and/or enzyme systems[244]. With this in mind, we searched some pharmacophores to introduce on the template, represented by the polyamine backbone, of MDL 27695. Two structures called our attention: N-BDMPrNDI and PiB. The first one is known as DNA intercalator, the second one represents a PIN1 inhibitor discovered by random screening by Uchida and coworkers. Both structures seem very similar, and in particular are characterized by a 1,4,5,8-naphthalenetetracarboxylic diimide (NTD) moiety. With the aim to widen the biological properties of MDL 27695, in order to obtain new MTDLs endowed with antiproliferative activity together with the ability to intercalate in DNA structure and to inhibit Pin1, we inserted the NTD moiety, peculiar chemical feature of N-BDMPrNDI and PiB, on the template structure of MDL 27695, obtaining **16**-**24**, which differ by side chains length (Figure 102). The presence of the methoxy groups in *orto* positions on the two aromatic rings is justified by electronic effects exerted by these two substituents which contribute to increase the basicity of the two basic nitrogen atoms and the relative protonation at physiological pH, facilitating their binding with the phosphate groups of DNA[167].

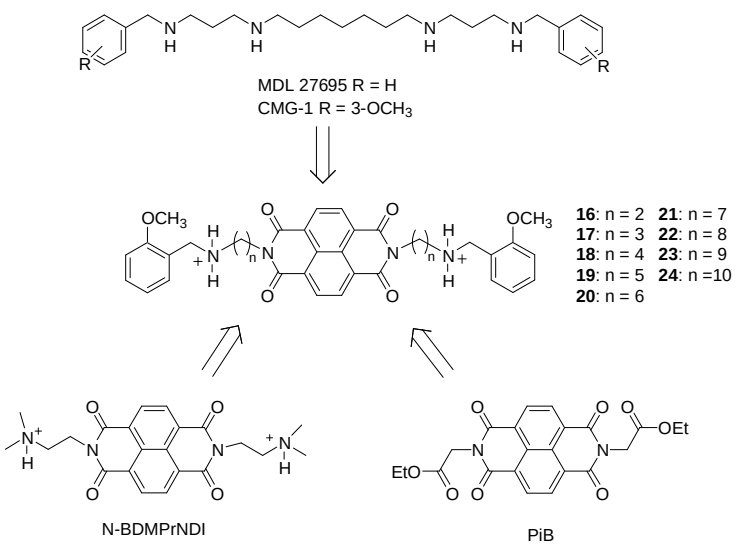

Figure 102. Drug design of compounds **16**-**24**.

Finally, the molecular simplification approach has been applied to **16**-**24** structures, obtaining **25**-**33**, in order to verify the importance of the two basic side chains. To note that these derivatives resemble the structure of mitonafide, a well known anticancer drug in phase II of clinical trials (Figure 103).

:

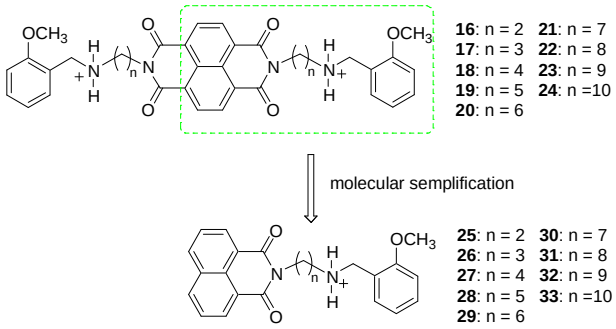

Figura 103. Drug design for compounds **25**-**33.**

2.3 Methods

2.3.1 Synthesis

Compounds **16** and **17** have been synthesized following the procedure showed in scheme 4. The appropriate diamine, **55** and **56**, have been monoprotected at the nitrogen atom with *tert*-Buthoxycarbonyl group obtain amines **57** and **58** as reported in literature[373]. **61** and **62** have been synthesized following the procedure reported in literature[374]: **57** and **58** were directly condensated with naphthalenetetracarboxylic dianhydride to give conjugate **59** and **60**; removal of the protecting group by acidic hydrolisys led to diamines **61** and **62**. These diamines were treated with 2-methoxybenzaldehyde followed by reduction with sodium borohydride of the formed Schiff base to the corresponding dibenzyl derivatives **16** and **17**.

Compounds **18-24** have been synthesized following the procedure showed in scheme 5. Naphthalenetetracarbocylic dianhydride was condensed with the corresponding diamines **63-69** to obtain the derivatives **70-76**; such compounds were treated with 2-methoxybenzaldehyde to form the Schiff base that is then reduced by sodium borohydride to give the corresponding diamine diimides **18-24**.

Finally, **25-33** were obtained by reacting 1,8-Naphthalic anhydride with the corresponding diamines **63-69** leading to **77-85** following the procedure reported in literature[375]; then, **77-85** were condensate with 2-methoxybenzaldehyde and then reduced by sodium borohydride giving the products **25-33.**

Salt *p*toluenesulfonates of all compounds were prepared to obtain derivatives easier to handle.

Scheme 4

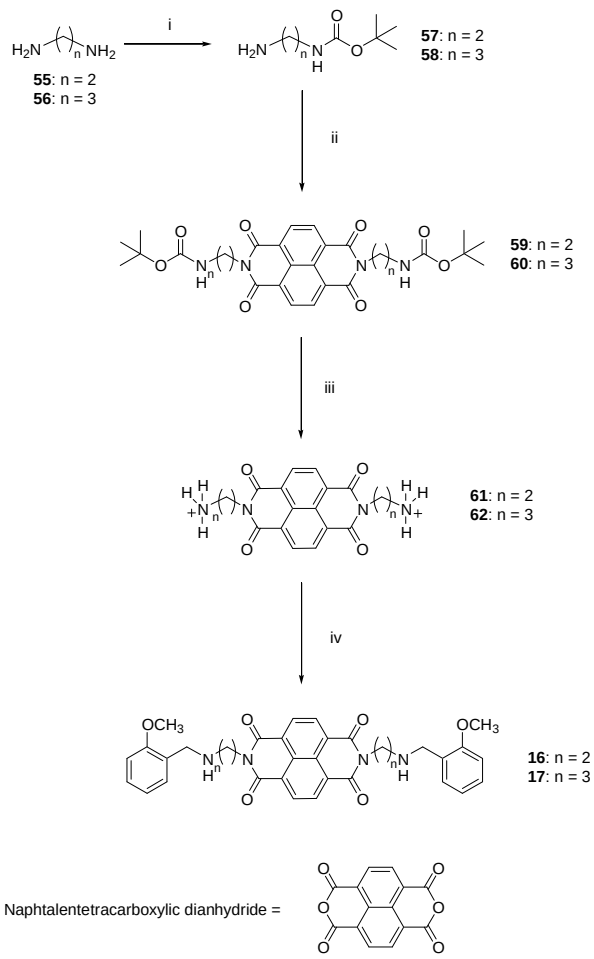

Condition: (i) Boc_2O, $CHCl_3$, room temperature; (ii) Naphtaletetracarboxylic dianhydride Et_3N, *i*-PrOH, reflux; (iii) CF_3COOH, CH_2Cl_2 ; iv) (a) Et_3N, 2-$MeOC_6H_4CHO$, MeOH, reflux, (b) $NaBH_4$, MeOH, room temperature

Scheme 5

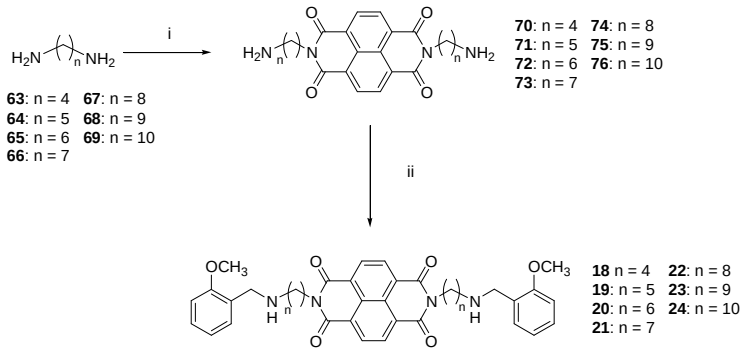

63: n = 4 **67**: n = 8
64: n = 5 **68**: n = 9
65: n = 6 **69**: n = 10
66: n = 7

70: n = 4 **74**: n = 8
71: n = 5 **75**: n = 9
72: n = 6 **76**: n = 10
73: n = 7

18 n = 4 **22**: n = 8
19: n = 5 **23**: n = 9
20: n = 6 **24**: n = 10
21: n = 7

Condition: (i) Naphtalenetetracarboxylic dianhydride, EtOH-Toluene 1:1, reflux; (ii) 2-$MeOC_6H_4CHO$, MeOH, reflux, (b) $NaBH_4$, MeOH, room temperature.

Scheme 6

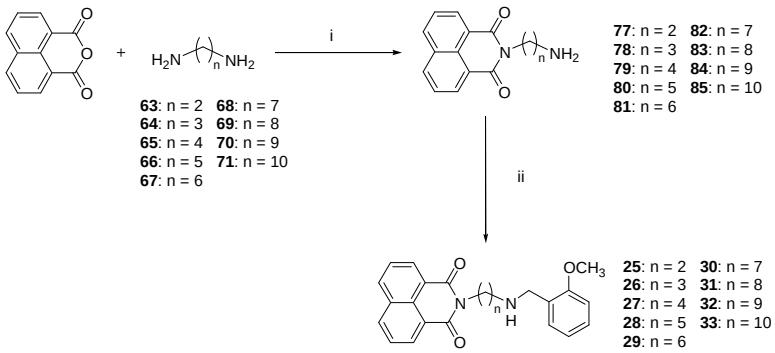

Condition: (i) EtOH, reflux; (ii) 2-$MeOC_6H_4CHO$, Toluene, reflux, (b) $NaBH_4$, EtOH, room temperature.

2.3.2 Biology

Derivatives were tested for *in vitro* antiproliferative activity in human breast cancer (SKBR-3) and leukemia (CEM) cell lines. Growth inhibition induced by tested compounds was evaluated by the MTT [3-(4,5-dimethylthiazolyil-2)-2,5-diphenyltetrazolium bromide] assay.

The DNA-binding activity of the strongly cytotoxic compounds **16**, **17** and mitonafide was determined using a fluorometric intercalator displacement method[376] and it s expressed as the drug concentration reducing by 50% the fluorescence of DNA-bound Ethidium bromide. From these data, an apparent binding constant (K_{app}) can be calculated, that roughly estimate the affinity of the drug for calf thymus DNA[376.377].

All the experimental part of the biology assays has been reported in other PhD thesis. However, it will be described in a paper which will be published as soon as possible.

2.4 Results and Discussion

Derivatives **16-33** were firstly evaluated by *in vitro* assays for their antiproliferative activity in human breast cancer (SKBR-3) cell and leukemia cell (CEM) lines to identify the lead compound of the series. Growth inhibition induced by tested compounds was assessed by the 3-(4,5-dimethylthiazolyil-2)-2,5-diphenyltetrazolium bromide (MTT) assay, based on the assessment of mitochondrial dehydrogenase activities. In particular, the cells were treated with the test compounds at concentration ranging from 0.1 to 10 μM for 24 h, 48 h and 72 h. Each quoted value is the mean of sextuple experiments. To compare the antiproliferative potencies in terms of concentrations required for 50% of the effect, all analogues were tested in dose-dependent manner, and the observed IC_{50} values are listed in Table 6.

From an analysis of the results **17** (n=3) emerged as the most potent compound of the entire series on the two cells lines (IC_{50} values of 0.2 and 0.4 μM, respectively). From the general point of view, the bis substituted derivatives are generally more potent than the related mono substituted derivatives, with the exception of **22** and **23** which showed comparable activity values with that of corresponding **31** and **32**. It can be observed that in the first series of the bis substituted derivatives, the growing homologation of the side chains influenced the cytotoxic activity. Indeed, the cytotoxic activity on the two cells lines, starting from **17**, which was the most potent, showed a minimum level for **21** (n = 7), raising again with the increase of the chain length from 8 (**22**) to 10 (**23**) methylene units. To note that **24** showed a comparable biological profile with the most potent **17** on SKBR-3 cell line, but not on CEM one, where it displayed however a notable value of 0.7 μM. The same pattern was not observed in the mono substituted series, in which the only notable derivative was **32** endowed with an IC_{50} value on SKBR-3 of 0.5 μM.

Table 6. Cytotoxyc activity of **16**-**33** on SKBR-3 breast cancer and leukemia cells (CEM) after 72 hours compounds exposure.

Compound[a]	IC_{50} SKBR-3 (μM)[b]	IC_{50} CEM (μM)[b]
16	0.7	1.3
17	0.2	0.4
18	0.7	0.8
19	1.1	1.1
20	1.2	2.2
21	1.7	2.5
22	1.0	1.6
23	0.4	1.4
24	0.2	0.7
25	2	N.A.
26	N.A.	N.A.
27	1.7	3.2
28	N.A.	N.A.
29	N.A.	N.A.
30	N.A.	N.A.
31	1.4	1.2
32	0.5	1.3
33	2	8

[a] **16**-**33** *para*-toluensulfonate[b] IC_{50} values represent the concentration causing 50% growth inhibition. They were determined by linear regression method.

After this first screening investigation, **16** and **17** were selected for further investigation about their cytotoxic molecular mechanisms. Derivative **17** because was the most potent of the series, and **16** because characterized by similar chemical features, in particular for the same chain length, of mitonafide. To confirm the cytotoxic action of **16** and **17**, their effects against HL60 leukemia cells were assessed. In particular, **16** and **17** confirmed their antiproliferative activity (**16**, IC_{50} = 0.93 μM; **17**, IC_{50} = 1.21 μM) toward this cell line with a comparable pattern with that of mitonafide (IC_{50} = 1.60 μM). (Figure 104).

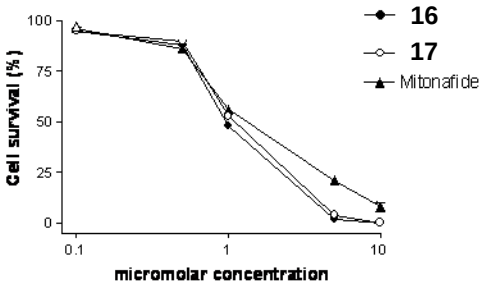

Figure 104. Toxicity of **16** and **17** against HL60 leukemia cells. The cells were incubated 24 h in the presence of the indicated concentration of compound, afterward cell death was determined by dye exclusion.

As reported in the introduction part, mitonafide and diimides derivatives, are well known intercalators. To verified if **16** and **17** are able to interact with DNA, DNA-binding studies were carried out using mitonafide as reference compound. For this purpose the DNA-binding activities of **16** and **17** were determined by applying a fluorometric intercalator displacement method and it is expressed as the drug concentration reducing by 50% the fluorescence of DNA-bound Ethidium bromide. From these data, an apparent binding constant (K_{app}) can be calculated, that roughly estimate the affinity of the drug for calf thymus DNA. Table 7shows the ability of **16**, **17** and mitonafide to bind DNA by Ethidium displacement assays. Both synthesized derivatives showed a more potent activity in comparison with the reference compound mitonafide. In particular **16** (EC_{50} about 90 nM) resulted 100 times more potent than mitonafide.

Table 7. Determination of binding to DNA by Ethidium displacement assay.

Compound[a]	EC_{50} (nM)[b]	K_{app} (M^{-1})[c]
Mitonafide	11500 ± 320	2.20×10^6
16	93 ± 4	2.07×10^8
17	122 ± 6	2.72×10^8

[a] **16**, **17**, *para*-toluensulfonate.[b] EC_{50} values are defined as the drug concentrations which reduce the fluorescence of the DNA-bound ethidium by 50%, and are reported as the mean of three determinations ± sem. [C] Apparent binding constant (K_{app}) values have been calculated taking as 10^7 M^{-1} the ethidium binding constant.

To verify if the cytotoxic effects of **16** and **17** were caused by apoptosis induction caspase activation experiments were carried out. To this aim the cells were treated with a 5 µM concentration of the compounds and after 4 and 24 h the activity of caspase proteases acting on the substrate sequence Asp-Glu-Val-Asp (DEVD), i.e. mainly effector caspases, were measured. Caspases activation represents a marker of apoptotic

cell death. Figure 105A shows that **16** and **17**, as well as mitonafide, triggered caspase activation. The analysis by Western blotting of protein extracted from cells treated 4 h with the aforementioned compounds, confirmed the activation of caspase-3, the main caspase effector (Figure 105B). Actually, in treated cells, it can be observed a reduction of the inactive precursor procaspase 3 (32 kDa), associated with the appearance of the proteolytic fragments, costitutive of the active enzyme (Figure 105B). It is noteworthy that the novel compounds trigger caspase activation rapidly, and after a few hours of treatment a large part of the procaspase 3 is processed into the active form, leading to apoptosis. The caspases activation carried out by **16** was confirmed by further assays on different cell lines. These results reported in Figure 105C, show that **16** caused caspase activation in different cell lines, such as SH-SY5Y neuroblastoma cells, H9c2 heart cells, and Jurkat T-cells. To note the behaviour of mitonafide which caused, quite surprisingly, caspases activation.

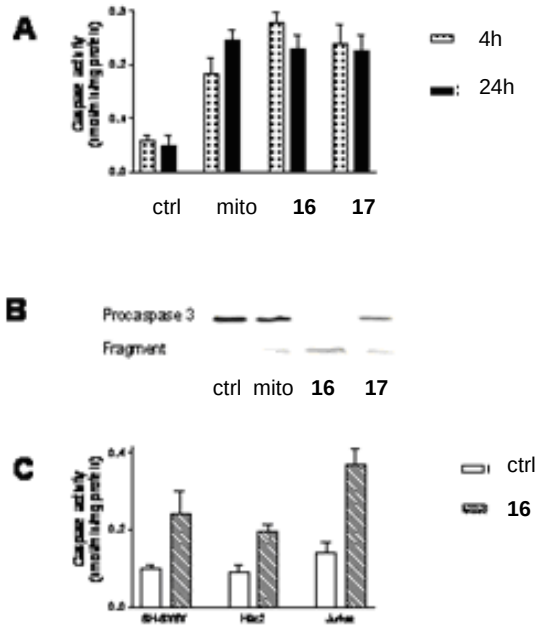

Figure 105. 16, **17** and mitonafide trigger caspase-dependent cell death.

The involvement of some putative signal transduction pathways involved in apoptosis induction by the strongly cytotoxic compounds **16** and **17** and by reference compound mitonafide, was examined in SH-SY5Y neuroblastoma cells (Figure 106). The treatment of the cells with **16** or **17** (5 µM) for 20 hours caused a large accumulation of p53 protein, that was observed also in mitonafide-treated cells. At the same time, **16**, **17** and mitonafide caused a profound down regulation of the survival kinase Akt and also abolished its phosphorylation. In the case of the ERK1/2 mitogen-activated protein kinases, the effects of **16** and **17** were completely different with respect to mitonafide. Indeed, mitonafide caused a decrease of the p42 and p44

ERK proteins, but did not block their phosphorylation. On the other hand, **16** and **17** caused a decrease of the p42 ERK2 protein, and completely inhibited the phosphorylation of both p42 and p44 ERKs.

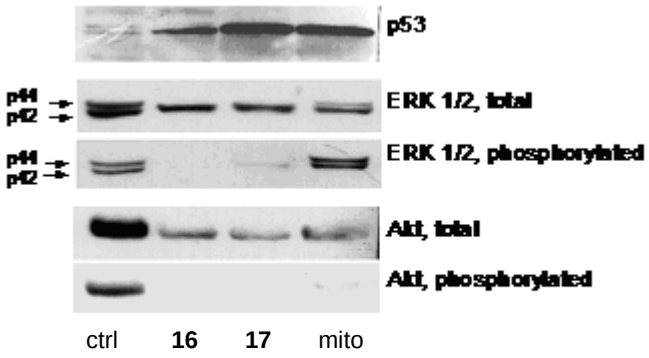

Figure 106. Effect of **16** and **17** on signal transduction pathway correlated to cell survival.

Furthermore, compounds **16**, **17** and juglone, a well known PIN1-inhibitor, have been tested on HCT116 (colon carcinoma cell line) and MDA-MB-231 (human breast adenocarcinome) (Table 8).

Table 8. IC_{50} values of compound **1**, **2** and **4** and juglone on HCT116 and MDA-MB-231 cell lines.

Compound	IC_{50} HCT116 (μM)	IC_{50} MDA-MB-231(μM)
Juglone	n.d	5.48
16	1.11	1.27
17	1.01	0.84

Both compounds confirmed antiproliferative activity in these cell lines in micromolar range; in particular, **16** and **17** were more active than Juglone on MDA-MB-231 cell lines.

In order to determine a possible interaction with Pin1, **16** and **17** have been tested in murine embrional fibroblasts PIN1+/+ and PIN1-/-. Figure 107 shows that PiB, **16** and **17** determine an effect on cell growth stronger in cells PIN+/+, in comparison with PIN1 -/- cell line, suggesting that their effects on cell growth could be dependent by PIN1 inhibition.

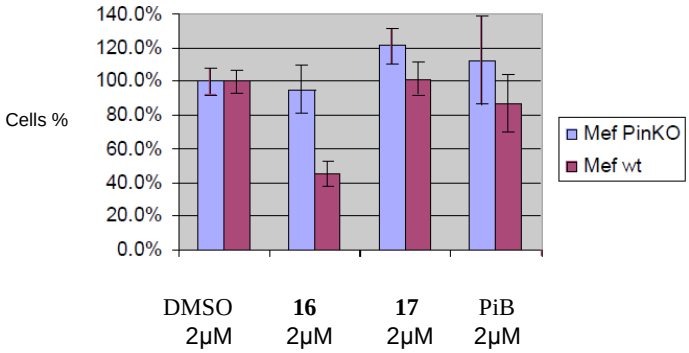

Figure 107.

This last experiment experiment points out, in very preliminary fashion, that **16** and **17** could interact with PIN1. However, to confirm the direct activity on PIN1 by **16** and **17**, further additional experiments are necessary.

2.5 Conclusion

This study allowed us to discover of new MTDLs endowed with different biological activities as anticancer agents. All the compounds designed displayed a citotoxic activity against SKBr-3 and CEM cell lines in micromolar range. In particular, compounds **16** and **17** emerged as the most potent of the series showing a profile of activity similar to that of Mitonafide, choose as reference compound. They showed an affinity toward DNA (**16**, EC_{50} = 93 nM; **17**, EC_{50} = 122 nM) nearly 100 times higher than that of Mitonafide. Furthermore, **16** and **17** were able to rapidly trigger caspases activation in different cell lines (SH-SY5Y, H9c2, and Jurkat T-cells). During this study was discovered that Mitonafide is also able to trigger caspase activation: such biological property of Mitonafide was not reported in literature until now. Moreover, **16** and **17** caused a large accumulation of p53 protein in SH-SY5Y cells. In addition, they seemed able to interact with the protein PIN1 as suggested by preliminary assays performed in murine embrional fibroblasts PIN1+/+ and PIN1-/-. However, further tests should be performed in order to elucidate a possible interaction between **16** and **17** compounds and PIN1.

All together these data point out that 16 and 17 interact/activate several targets involved in vcancer development, therefore this study may represent a promising starting point for the development of new MTDLs hopefully useful for the cancer treatment.

2.6 Experimental Section

2.6.1 Chemistry

Melting point were taken in glass capillary tubes on a Buchi SMP-20 apparatus and are uncorrected. ESI-MS spectra were recorded on Perkin-Elmer 297 and WatersZQ 4000. ^{1}H NMR and ^{13}C NMR were recorded on Varian VRX 200 and 300 instruments. Chemical shift are reported in parts per millions (ppm) relative to peak of tetrmethylsilane (TMS) and spin multiplicities are given as s (singlet), br s (broad singlet), d (doublet), t (triplet), q (quartet) or m (multiplet) Although IR spectral data are not included (because of the lack of unusual features), they were obtained for all compounds reported, and they were consistent with the assigned structures. The elemental compositions of the compounds agreed to within ±0.4% of the calculated value. Where the elemental analysis is not included, crude compounds were used in the next step without further purification. Chromatographic separations were performed on silica gel columns by flash (Kieselgel 40, 0.040-0.063 mm, Merck) or gravity (Kieselgel 60, 0.063-0.200 mm, Merck) column chromatography. Reactions were followed by thin layer chromatography (TLC) on Merck (0.25 mm) glass-packed precoated silica gel plates (60 F254) and then visualized in an iodine chamber or with a UV lamp.The term “dried” refers to the use of anhydrous sodium sulfate.

General procedure for the synthesis of derivatives 16, **17**: the appropriate diamine **61**, **62**(1.15mmol) was dissolved in MeOH at 0˚ C and the solution was made basic adding Et_3N; the 2-methoxybenzaldehyde (2.3 mmol) was added and resulting mixture was refluxed for 4h and the formation of a yellow solid was observed. After cooling down, $NaBH_4$ (23 mmol) was added at 0˚ C and stirred overnight. The mixture was then made acidic with 3 N HCl and the solvent was removed under vacuum. The residue was dissolved in water, and the resulting solution made basic with K_2CO_3, and extracted with CH_2Cl_2 (3 x 30 mL); the organic phase was dried and the solvent was evaporated. The crude product was purified by flash chromatography to afford the desired compound **16** and **17**. The two purified compounds were converted in di-*p*-toluen-sulfonate (foam solids).

2,7-bis(2-(2-methoxybenzylamino)ethyl)benzo[lmn][3,8]phenanthroline-1,3,6,8(2H,7H)-tetraone (16): yellow oil, 26% yield from **61** as starting diamine, purified by flash chromatography eluting with toluene/EtOAc/CH_3OH/aqueous 28% ammonia (5:4.5:0.5:0.01); ^{1}H NMR (free base, 300MHz $CDCl_3$) δ 1.83 (br s, 2H exchangeable with D_2O), 3.02 (t, J = 6.3, 4H), 3.85 (s, 4H), 3.88(s, 6H), 4.40 (t, J = 6.6, 4H), 6.84-6.92 (m, 4H), 7.19-7.25(m, 4H), 8.78 (s, 4H); MS (ESI^+) m/z = 593 $(M+H)^+$. Anal. ($C_{34}H_{32}N_4O_6$), C, H, N.

2,7-bis(3-(2-methoxybenzylamino)propyl)benzo[lmn][3,8]phenanthroline-1,3,6,8(2H,7H)-tetraone (17): yellow oil, 27% yield from **62** as starting diamine, purified by flash chromatography eluting with toluene/EtOAc/CH_2Cl_2/CH_3OH/aqueous 28% ammonia (4:4:1:1:0.03); ^{1}H NMR (free base, 300MHz $CDCl_3$) δ 1.99-2.07 (m, 4H + 2H exchangeable with D_2O), 2.77 (t, J = 6.9, 4H), 3.83 (s, 4H), 3.87 (s, 6H), 4.33 (t, J

= 7.2, 4H), 6.86-6.91 (m, 4H), 7.20-7.25 (m, 4H), 8.76 (s, 4H); MS (ESI^+) *m/z* = 621 $(M+H)^+$. Anal. ($C_{36}H_{36}N_4O_6$), C, H, N.

General procedure for the synthesis of derivatives 70-76: the appropriate diamine **63-69** (25 mmol) was dissolved in a mixture of toluene/ethanol 1:1 under a stream of dry nitrogen and a solution of isochromeno[6,5,4-def]isochromene-1,3,6,8-tetraone (5 mmol) dissolved in toluene/ethanol 1:1 was added; the mixture was refluxed for 24h. Then, the solvent was evaporated, affording a residue that was suspended in water. The solid residue was filtered off and washed several times with water to afforded the desired crude product**70-76**.

2,7-bis(4-aminobutyl)benzo[lmn][3,8]phenanthroline-1,3,6,8(2H,7H)-tetraone (70): was synthesized from **63**; brown solid; quantitative yield; m.p 213-215°C;

2,7-bis(5-aminopentyl)benzo[lmn][3,8]phenanthroline-1,3,6,8(2H,7H)-tetraone (71): was synthesized from **64**; red solid; quantitative yield; m.p 213-215°C;

2,7-bis(6-aminohexyl)benzo[lmn][3,8]phenanthroline-1,3,6,8(2H,7H)-tetraone (72): was synthesized from **65**; red solid; quantitative yield; m.p 216-219°C;

2,7-bis(7-aminoheptyl)benzo[lmn][3,8]phenanthroline-1,3,6,8(2H,7H)-tetraone (73): was synthesized from **66**; red solid; quantitative yield; m.p 203-206°C;

2,7-bis(8-aminooctyl)benzo[lmn][3,8]phenanthroline-1,3,6,8(2H,7H)-tetraone (74): was synthesized from **67**; red solid; quantitative yield; m.p 144-147°C;

2,7-bis(9-aminononyl)benzo[lmn][3,8]phenanthroline-1,3,6,8(2H,7H)-tetraone (75): was synthesized from **68**; red solid; quantitative yield; m.p 115-118°C;

2,7-bis(10-aminodecyl)benzo[lmn][3,8]phenanthroline-1,3,6,8(2H,7H)-tetraone (76): was synthesized from **69**; red solid; quantitative yield; m.p 110:112°C.

General procedure for the synthesis of 18-24: a mixture of the appropriate diamine **70-76** and 2-methoxybenzaldehyde (in a ratio 1:2.4) in toluene was refluxed in a Dean-Stark apparatus for 3 h. Following solvent removal, the residue was taked up in EtOH, $NaBH_4$ (in a 1:5 molar ratio) was added, and the stirring was continued at room temperature for 4 h. The mixture was then made acidic with 6N HCl and the solvent removed. Then, the residue was dissolved in water and the resulting solution was washed with ether, made basic with KOH and extracted with CH_2Cl_2 (3 x 30 mL). Removal of the dried solvent gave the desired products **18-24** which were finally converted in the *para*-toluenesulfonate salts (foam solid).

2,7-bis(4-(2-methoxybenzylamino)butyl)benzo[lmn][3,8]phenanthroline-1,3,6,8(2H,7H)-tetraone (18): it was synthesized from **70**; brown solid; 25% yield; ^1H NMR (free base, 300 MHz, $CDCl_3$) δ 1.46-1.77 (m, 8H+ 2H exchangeable with D_2O), 2.62 (t, *J* = 6.7, 4H), 3.82 (s, 4H), 3.86(s, 6H), 4.21(t, *J* = 7.2, 4H), 6.86-6.96(m, 4H), 7.27-7.31(m,4H), 8.77(s, 4H); MS (ESI^+) *m/z* = 649 $(M)^+$

2,7-bis(5-(2-methoxybenzylamino)pentyl)benzo[lmn][3,8]phenanthroline-1,3,6,8(2H,7H)-tetraone (19): it was synthesized from **71**; brown solid; 37% yield; ^1H NMR (free base, 300 MHz, $CDCl_3$) δ 1.41-1.82

(m, 12H+ 2H exchangeable with D_2O), 2.57 (t, *J* = 6.9, 4H), 3.87 (s, 4H), 3.92(s, 6H), 4.27(t, *J* = 7.2, 4H), 6.73-6.91(m, 4H), 7.29-7.33(m,4H), 8.74(s, 4H); MS (ESI^+) *m/z* = 677 $(M)^+$

2,7-bis(6-(2-methoxybenzylamino)hexyl)benzo[lmn][3,8]phenanthroline-1,3,6,8(2H,7H)-tetraone (20): it was synthesized from **72**; brown solid; 23% yield; ^1H NMR (free base, 300 MHz, $CDCl_3$) δ 1.35-1.87 (m, 16H+ 2H exchangeable with D_2O), 2.85 (t, *J* = 6.7, 4H), 3.79 (s, 4H), 3.88(s, 6H), 4.30(t, *J* =7.1, 4H), 6.84-6.99(m, 4H), 7.30-7.37(m,4H), 8.78(s, 4H); MS (ESI^+) *m/z* = 705 $(M)^+$

2,7-Bis-[7-(2-methoxy-benzylamino)-heptyl]-benzo[lmn][3,8]phenanthroline-1,3,6,8-tetraone (21): it was synthesized from **73**; brown solid; 27% yield; ^1H NMR (free base, 300 MHz, $CDCl_3$) δ 1.29-1.72 (m, 20H+ 2H exchangeable with D_2O), 2.93 (t, *J* = 6.6, 4H), 3.83 (s, 4H), 3.90(s, 6H), 4.26(t, *J* = 7.2, 4H), 6.80-6.99(m, 4H), 7.28-7.42(m,4H), 8.75(s, 4H); MS (ESI^+) *m/z* = 733 $(M)^+$

2,7-Bis-[8-(2-methoxy-benzylamino)-octyl]-benzo[lmn][3,8]phenanthroline-1,3,6,8-tetraone (22): it was synthesized from **74**; brown solid; 21% yield; ^1H NMR (free base, 300 MHz, $CDCl_3$) δ 1.37-1.73 (m, 24H+ 2H exchangeable with D_2O), 2.79 (t, *J* = 6.8, 4H), 3.87 (s, 4H), 3.94 (s, 6H), 4.31(t, *J* = 7.3, 4H), 6.75-6.97(m, 4H), 7.29-7.41(m,4H), 8.71(s, 4H); MS (ESI^+) *m/z* = 761 $(M)^+$

2,7-bis(9-(2-methoxybenzylamino)nonyl)benzo[lmn][3,8]phenanthroline-1,3,6,8(2H,7H)-tetraone (23): It was synthesized from **75**; brown solid; 30% yield; ^1H NMR (free base, 300 MHz, $CDCl_3$) δ 1.25-1.63 (m, 28H+ 2H exchangeable with D_2O), 2.69 (t, *J* = 6.9, 4H), 3.85 (s, 4H), 3.96 (s, 6H), 4.27(t, *J* = 7.3, 4H), 6.75-7.01(m, 4H), 7.28-7.47(m,4H), 8.78(s, 4H); MS (ESI^+) *m/z* = 790 $(M)^+$

2,7-bis(10-(2-methoxybenzylamino)decyl)benzo[lmn][3,8]phenanthroline-1,3,6,8(2H,7H)-tetraone (24): It was synthesized from **76**; yellow solid; 70% yield; ^1H NMR (free base, 300 MHz, $CDCl_3$) δ 1.19-1.75 (m, 32H+ 2H exchangeable with D_2O), 2.76 (t, *J* = 6.7, 4H), 3.93 (s, 4H), 4.01 (s, 6H), 4.29(t, *J* = 7.2, 4H), 6.83-6.97(m, 4H), 7.29-7.45(m,4H), 8.74(s, 4H); MS (ESI^+) *m/z* = 818 $(M)^+$

General procedure for the synthesis of 77-85: compounds **77-85** have been synthesized following the procedure reported in literature[375].

2-(6-aminohexyl)-1H-benzo[de]isoquinoline-1,3(2H)-dione (81): it was synthesized from **65**; yellow oil; 77% yield; ^1H NMR (200 MHz, $CDCl_3$) δ 1.45-1.77 (m, 8H), 2.71 (t, *J* = 7.0, 2H), 4.21 (t, *J* = 7.6, 2H), 7.78 (t, *J* = 7.9, 2H), 8.22-8.26 (d, *J* = 8.0, 2H) 8.61-8.65 (d, *J* = 7.4, 2H).

2-(7-aminoheptyl)-1H-benzo[de]isoquinoline-1,3(2H)-dione (82): It was synthesized from **66**; yellow oil; 85% yield; ^1H NMR (200 MHz, $CDCl_3$) δ 1.42-1.77 (m, 10H), 2.71 (t, *J* = 7.1, 2H), 4.21 (t, *J* = 7.2, 2H), 7.79 (t, *J* = 7.6, 2H), 8.23-8.27 (d, *J* = 8.0, 2H) 8.62-8.66 (d, *J* = 7.4, 2H).

2-(8-aminooctyl)-1H-benzo[de]isoquinoline-1,3(2H)-dione (83): It was synthesized from **67**; yellow oil; 20% yield; ^1H NMR (200 MHz, $CDCl_3$) δ 1.35-1.65 (m, 12H), 2.69 (t, *J* = 6.6, 2H), 4.20 (t, *J* = 6.6, 2H), 7.78 (t, *J* = 7.2, 2H), 8.22-8.26 (d, *J* = 8.0, 2H) 8.61-8.65 (d, *J* = 7.4, 2H).

2-(9-aminononyl)-1H-benzo[de]isoquinoline-1,3(2H)-dione (84): It was synthesized from **68**; yellow oil; 55% yield; ^1H NMR (200 MHz, $CDCl_3$) δ 1.32-1.64 (m, 14H), 2.69 (t, *J* = 7.0, 2H), 4.20 (t, *J* = 7.8, 2H), 7.78 (t, *J* = 7.6, 2H), 8.22-8.26 (d, *J* = 8.0, 2H) 8.61-8.65 (d, *J* = 7.4, 2H).

2-(10-aminodecyl)-1H-benzo[de]isoquinoline-1,3(2H)-dione (85): It was synthesized from **69**; yellow oil; 82% yield; ^{1}H NMR (200 MHz, $CDCl_3$) δ 1.30-1.64 (m, 16H), 2.69 (t, *J* = 7.0, 2H), 4.19 (t, *J* = 7.8, 2H), 7.77 (t, *J* = 7.8, 2H), 8.21-8.25 (d, *J* = 8.0, 2H) 8.61-8.64 (d, *J* = 7.4, 2H).

General procedure for the synthesis of derivatives 25-33: a mixture of **77-85** and 2-methoxybenzaldehyde (in a ratio 1:1.2) in toluene was refluxed in a Dean-Stark apparatus for 3 h. Following solvent removal, the residue was taked up in EtOH, $NaBH_4$ (in a 1:2.5 molar ratio) was added, and the stirring was continued at room temperature for 12 h. The mixture was then made acidic with 6N HCl and the solvent removed. Then, the residue was dissolved in water and the resulting solution was washed with ether, made basic with K_2CO_3 and extracted with $CHCl_3$ (3 x 30 mL). Removal of the dried solvent gave the desired products **25-33** which were purified by flash chromatography. **25-33** were finally converted into the *para*-toluensulfonate salt (foam solid).

2-(2-(2-methoxybenzylamino)ethyl)-1H-benzo[de]isoquinoline-1,3(2H)-dione (25): was synthesized from **77**; yellow oil; 24% yield; eluting solvent petroleum ether/$CHCl_3$/MeOH/ aqueous 33% ammonia (6:3.5:0.5/0.1); ^{1}H-NMR (free base, 200 MHz, $CDCl_3$) δ 1.92 (br s, 1H exchangeable with D_2O), 2.97 (t, *J* = 6.6,2H), 3.77 (s, 3H), 3.84 (s, 2H), 4.32 (t, *J* = 8.0, 2H), 6.76-6.88 (m, 2H), 7.12-7.24 (m, 2H), 7.62-7.70 (m, 2H), 8.08-8.13 (m, 2H), 4.48-8.52 (m,2H); MS (ESI^+) m/z = 361 $(M+H)^+$.

2-(3-(2-methoxybenzylamino)propyl)-1H-benzo[de]isoquinoline-1,3(2H)-dione (26): was synthesized from **78**; yellow oil; 24% yield; eluting solvent petroleum ether/$CHCl_3$/MeOH/ aqueous 33% ammonia (6:3.5:0.5/0.1); ^{1}H-NMR (free base, 200 MHz, $CDCl_3$) δ 1.91-2.05 (m, 2H), 2.36 (br s, 1H exchangeable with D_2O), 2.73 (t, *J* = 7.0, 2H), 3.81 (s, 3H), 3.84 (s, 2H), 4.25 (t, *J* = 7.0, 2H), 6.82-6.90 (m, 2H), 7.15-7.25 (m, 2H), 7.65-7.74 (m, 2H), 8.13-8.17 (m, 2H), 8.52-8.55 (m, 2H); MS (ESI^+) m/z = 375 $(M+H)^+$.

2-(4-(2-methoxybenzylamino)butyl)-1H-benzo[de]isoquinoline-1,3(2H)-dione (27): was synthesized from **79** yellow oil; 29% yield; eluting solvent petroleum ether/$CHCl_3$/MeOH/ aqueous 33% ammonia (6:3.5:0.5/0.1); ^{1}H-NMR (free base, 200 MHz, $CDCl_3$) δ 1.60-1.82 (m, 4H), 2.45 (br s, 1H exchangeable with D_2O), 2.67 (t, *J* = 7.0, 2H), 3.79 (s, 3H), 3.83 (s, 2H), 4.17 (t, *J* = 7.4, 2H), 6.81-6.92 (m, 2H), 7.16-7.25 (m, 2H), 7.69 (t, *J* = 8.0, 2H), 8.12-8.17 (m, 2H), 8.51-8.55 (m, 2H); MS (ESI^+) m/z = 389 $(M+H)^+$.

2-(5-(2-methoxybenzylamino)pentyl)-1H-benzo[de]isoquinoline-1,3(2H)-dione (28): was synthesized from **80**; yellow oil; 34% yield; eluting solvent petroleum ether/$CHCl_3$/MeOH/ aqueous 33% ammonia (6:3.5:0.5/0.1); ^{1}H-NMR (free base, 200 MHz, $CDCl_3$) δ 1.27-1.80 (m, 6H+1H exchangeable with D_2O), 2.65 (t, *J* = 7.4, 2H), 3.81 (s, 2H), 3.84 (s, 3H), 4.17 (t, *J* = 7.8, 2H), 6.84-6.94 (m, 2H), 7.19-7.30 (m, 2H), 7.72 (t, *J*= 8.2, 2H), 8.15-8.19 (m, 2H), 8.53-8.57 (m, 2H); ^{13}C NMR (free base, $CDCl_3$) δ 24.76, 27.91, 29.18, 40.19, 48.57, 48.76, 55.15, 110.11, 120.32, 122.57, 126.58, 127.18, 127.98, 128.35, 130.02, 131.02, 131.45, 133.72, 157.55, 164.02;MS (ESI^+) m/z = 403 $(M+H)^+$.

2-(6-(2-methoxybenzylamino)hexyl)-1H-benzo[de]isoquinoline-1,3(2H)-dione (29): was synthesized from **81**; yellow oil; 25% yield; eluting solvent petroleum ether/$CHCl_3$/MeOH/ aqueous 33% ammonia (6:3.5:0.5/0.1); ^{1}H-NMR (free base, 200 MHz, $CDCl_3$) δ 1.22-1.74 (m, 8H+1H exchangeable with D_2O),

2.68 (t, *J* = 7.3, 2H), 3.85 (s, 2H), 3.89 (s, 3H), 4.18 (t, *J* = 7.9, 2H), 6.89-6.99 (m, 2H), 7.15-7.26 (m, 2H), 7.73 (t, *J* = 8.0, 2H), 8.13-8.19 (m, 2H), 8.50-8.55 (m, 2H); MS (ESI^+) m/z = 417 $(M+H)^+$.

2-(7-(2-methoxybenzylamino)heptyl)-1H-benzo[de]isoquinoline-1,3(2H)-dione (30): was synthesized from **82** yellow oil; 27% yield; eluting solvent petroleum ether/$CHCl_3$/MeOH/ aqueous 33% ammonia (6:3.5:0.5/0.1); ^{1}H-NMR (free base, 300 MHz, $CDCl_3$) δ 1.22-1.74 (m, 10+1H exchangeable with D_2O), 2.68 (t, *J* = 7.3, 2H), 3.85 (s, 2H), 3.89 (s, 3H), 4.18 (t, *J* = 7.9, 2H), 6.89-6.99 (m, 2H), 7.15-7.26 (m, 2H), 7.73 (t, *J* = 8.0, 2H), 8.13-8.19 (m, 2H), 8.50-8.55 (m, 2H); MS (ESI^+) m/z = 431 $(M+H)^+$.

2-(8-(2-methoxybenzylamino)octyl)-1H-benzo[de]isoquinoline-1,3(2H)-dione (31): was synthesized from **83**; yellow oil; 36% yield; eluting solvent petroleum ether/$CHCl_3$/MeOH/ aqueous 33% ammonia (6:3.5:0.5/0.1); ^{1}H-NMR (free base, 200 MHz, $CDCl_3$) δ 1.27-1.73 (m, 12H+1H exchangeable with D_2O), 2.63 (t, *J*= 7.7, 2H), 3.86 (s, 2H), 3.88 (s, 3H), 4.18 (t, *J* = 7.8, 2H), 6.85-6.96 (m, 2H), 7.22-7.29 (m, 2H), 7.76 (t, *J* = 8.0, 2H), 8.19-8.23 (m, 2H), 8.58-8.62 (m, 2H); MS (ESI^+) m/z = 445 $(M+H)^+$.

2-(9-(2-methoxybenzylamino)nonyl)-1H-benzo[de]isoquinoline-1,3(2H)-dione (32): was synthesized from **84**; yellow oil; 25% yield; eluting solvent petroleum ether/$CHCl_3$/MeOH/ aqueous 33% ammonia (6:3.5:0.5/0.1); ^{1}H-NMR (free base, 300 MHz, $CDCl_3$) δ 1.32-1.81 (m, 14H+1H exchangeable with D_2O), 2.62 (t, *J* = 7.5, 2H), 3.83 (s, 2H), 3.87 (s, 3H), 4.20 (t, *J*=7.8, 2H), 6.88-6.97 (m, 2H), 7.24-7.30 (m, 2H), 7.78 (t, *J* = 8.1, 2H), 8.21-8.25 (m, 2H), 8.61-8.64 (m, 2H); MS (ESI^+) m/z = 459 $(M+H)^+$.

2-(10-(2-methoxybenzylamino)decyl)-1H-benzo[de]isoquinoline-1,3(2H)-dione (33): was synthesized from **85**; yellow oil; 32% yield; eluting solvent petroleum ether/$CHCl_3$/MeOH/ aqueous 33% ammonia (6:3.5:0.5/0.1); ^{1}H-NMR (free base, 300 MHz, $CDCl_3$) δ 1.28-1.77 (m, 16H+1H exchangeable with D_2O), 2.59 (t, *J* = 6.6, 2H), 3.80 (s, 2H), 3.84 (s, 3H), 4.18 (t, *J* =7.8, 2H), 6.85-6.95 (m, 2H), 7.20-7.28 (m, 2H), 7.75 (t, *J* = 7.8, 2H), 8.18-8.22 (m, 2H), 8.58-8.61 (m, 2H); MS (ESI^+) m/z = 473 $(M+H)^+$.

Bibliography

[1] Mount, C.; Downton, C. *Nature Med.* **2006**, *12*, 780-784.
[2] Alzheimer, A.; Stelzmann, R.A.; Schnitzlein, H.N.; Murtagh, F.R. *Clin. Anat.* **1995**, *8*, 429-431.
[3] Jellinger, K.A. *J. Neural. Transm.* **2006**, *113*, 1603-1623.
[4] Bartus, R.T.; Dean, .L.; Beer, B.; Lippa, A.S. *Science*, **1982**, *217*, 408-414
[5] Eckman, C.B.; Eckman, E.A. *Neurol. Clin*, ***2007***, *25*, 669-682.
[6] Melnikova, I. Nat. Rev. Drug Discovery **2007**, 6, 341-342.
[7] Cavalli, A.; Bolognesi, M.L.; Minarini, A.; Rosini, M.; Tumiatti, V.; Recanatini, M.; Melchiorre, C. *J. Med. Chem.* **2008**, *51*, 347-372.
[8] Holtzman, D.M.; Bales, K.R.; Tenkova, T.; et.al. *Proc. Natl. Acad. Sci. USA*, **2000**, 97, 2892-2897.
[9] Drachman, D.A. *Neurology **1977**, 27*, 783-790.
[10] Ellis, K.A.; Nathan, O.J. *Int. J. Neuropshycopharmacol.* **2001**, 4, 299-313.
[11] Buccafusco, J.J. *Cognitive Enhancing Drugs* **2004**, 1-10.
[12] Lipton, S.A. *Nat. Rev. Drug Discovery* **2006**, *5*, 160-70.
[13] Schmitt, B.; Bernhardt, T.; Moeller, H.J.; Heuser, I.; Frolich, L. *CNS Drugs* **2004**, *18*, 827-844.
[14] Shi Q, Gibson GE.*Alzheimer Dis. Assoc. Disord.* **2007**, *21*, 276-91.
[15] Moreira, P.I.; Santos, M.S.; Oliveira, C.R. *Antioxid. Redox Signal.* **2007**, *9*, 1621–1630.
[16] Bartus, R.T. *Recent Advances in Gerontology* (H. Orimo, Ed.) **1978**, 225-228.
[17] Bartus, R.T. *Science* **1979**, *270*, 1087-1089.
[18] Francis, P.T.; Palmer, A.M.; Snape, M.; Wilcock, G.K. *J. Neurol. Neurosurg. Psychiatry.* **1999**, *66*, 137-147.
[19] Whitehouse, P.J.; Martion, A.M.; Marcus, K.A. et al. *Arch. Neurol.* **1988**, *45*, 722–724.
[20] Nordberg, A.; Alafuzoff, I.; Winblad, B. *J. Neurosci. Res.* **1992**, *31*, 103–111.
[21] Warpman, U.; Alafuzoff, I.; Nordberg, A. *Neurosci. Lett.* **1993**, *150*, 39–43.
[22] Bartus, R.T. *Exp. Neurol.* **2000**, *163*, 495-529.
[23] Oddo, S.; Laferla, F. M.; *J. Physiol.* **2006**, *99*, 172-179.
[24] Wess, J.; Eglen, R.M.; Gautam, D. *Nat. Rev. Drug Disc.* **2007**, *6*, 721.
[25] Buccafusco, J.J.; Terry, A.V. *Persp. Pharmacol.* **2003**.
[26] Taylor, R.; Radic, Z. *Ann. Rev. Pharmacol. Toxicol.* **1994**, *34*, 281-320.
[27] Diamant, S.; Podoly, E.; Friedler, A.; Ligumsky, H.; Livnah, O.; Soreq, H. *Proc Natl Acad Sci USA* **2006**, *103*, 8628-8633.
[28] Weik, M.**;** Ravelli, R.B.**;** Kryger, G.**;** McSweeney, S.**;** Raves, M.L.**;** Harel, M.**;** Gros, P.**;** Silman, I.**;** Kroon, J.**;** Sussman, J.L**.** *Proc. Natl. Acad. Sci. U S A.* **2000**, *97*,623-628.
[29] Sussman, J.L.; Harel, M.; Frolow, F.; Oefner, C.; Goldman, A.; Toker, L.; Silman, I. *Science* **1991**, *253*, 872-879.
[30] Sussman, J.L.; Harel, M.; Silman, I. *Chem. Biol. Interact.* **1993**, *87*, 187-197.
[31] Volicer, L.; Crino, P.B. *Neurobiol Aging* **1990**, *11*, 567-571.
[32] Inestrosa, N.C.; Alvarez, A.; Perez, C.A.; Moreno, R.D.; Vicente, M.; Linker, C.; Casanueva, O.I.; Soto, C; Garrido, J. *J. Neuron* **1996**, *16*, 881-891.
[33] Bartolini, M.; Bertucci, C., Cavrini, V., Andrisano, V. *Biochem. Pharmacol.* **2003**, *65*, 407-416.
[34] Alvarez, A.; Opazo, C.; Alacorn, R.; Garrido, J:; Inestrosa, N.C. *J Mol Biol* **1997**, *272*, 348-361.
[35] De Ferrari, G.V.; Canales, M.A.; Shin, I., Weiner, L.M. Silman, I; Inestrosa, N.C. *Biochemistry* **2001**, *40*, 10447-10457.
[36] Glenner, G.G.; Wong, C.W. *Biochem. Biophys. Res. Commun.* **1984**, *120*, 885-890.
[37] Masters, C.L.; Simms, G.; Weinman, N.; Multhaup, G.; McDonal, B.L.; Beyreuther, K.; *Proc. Natl. Acad. Sci. USA* **1985**, *82*, 4245-4249.
[38] Lambert, M.P.; Barlow, A.K.; Chromy, B.A.; Edwards, C.; Freed, R.; Liosatos, M.; Morgan, T.E.; Rozovsky, I.; Trommer, B.; Viola, K.L.; Wals, P.; Zhang, C.; Finch, C.E.; Krafft, G.A.; Klein, W.L. *Proc. Natl. Acad. Sci. U.S.A* **1998**, *95*, 6448-6453.
[39] Hartley, D. M.; Walsh, M.D.; Ye, C.P.; Diehl,T.; Vasquez, S.; Vassilev, P.M.; Teplow, D.B.; Selkoe, D.J. *J. Neurosci.* **1999**, *19*, 8876-8884.
[40] Hsia, A.Y.; Masliah, E.;McConlogue, L.;Yu, G.Q.;Tatsuno, G.;Hu, K.; Kholodenko, D.; Malenka, R.C.; Nicoll, R.A., Mucke, L. *Proc. Natl. Acad. Sci. U.S.A* **1999**, *96*, 3228-3233.
[41] Iwatsubo, T., Odaka, A.; Suzuki, N.; Mizusawa, H.; Nukina, N.; Ihara, Y. *Neuron* **1994**, *13*, 45-53.
[42] Verdile. G.; Fuller, S.; Atwood, C.S.; Laws, S.M.; Gandy, S.E.; Martins, R.N. *Pharmacol. Res.* **2004**, *50*, 397-409.
[43] Pastorino. L.; Lu. K.P. *Eur. J. Pharmacol.* **2006**, *545*, 29-38.
[44] Mattson, M.P. *Nature* **2004**, *430*, 631-639.
[45] Esler, W.P.; Wolfe, M.S. *Science* **2001,** *293*, 1449–1454.
[46] Citron, M. *Nature Rev. Neurosci.* **2004**, *5*, 677-685.
[47] Kimberly, W.T.; Zheng, J.B.; Guernette, S.Y.; Seolkoe, D.J. *J. Biol. Chem.* **2001**, *276*, 40288-40292.

[48] Leissring, M.A.; Murphy, M.P.; Mead, T.R.; Akbari, Y.; Sugarman, M.C.; Jannatipour, M.; Anliker, B.; Müller, U.; Saftig, P., De Strooper, B.; Wolfe, M.S.; Golde, T.E.; LaFerla, F.M. *Proc. Natl. Acad. Sci. U S A.* **2002**, *99*, 4697-4702.
[49] Puglielli, L.; Konopka, G.; Pack-Chung, E.; Ingano, L.A.; Berezovska, O.; Hyman, B.T.; Chang, T.Y.; Tanzi, R.E.; Kovacs, D.M. *Nat. Cell. Biol.* **2001**, *3*, 905-912.
[50] Vassar, R.; Bennett, B.D.; Babu-Khan, S.; Kahn, S.; Mendiaz, E.A.; Denis, P.; Teplow, D.B., Ross, S.; Amarante, P.; Loeloff, R.; Luo, Y.;Fisher, S.; Fuller, J.; Edenson, S.; Lile, J.; Jarosinski, M.A.; Biere, A.L.; Curran, E.; Burgess, T.; Louis, J.C.; Collins, F.; Treanor, J.; Rogers, G.; Citron, M. *Science* **1999**, *286*, 735-741.
[51] Yan, R.; Bienkowski, M.J.; Shuck, M.E.; Miao, H.; Tory, M.C.; Pauley, A.M.; Brashier, J.R.; Stratman, N.C.; Mathews, W.R.; Buhl, A.E.; Carter, D.B.; Tomasselli, A.G.; Parodi, L.A.; Heinrikson, R.L.; Gurney, M.E. *Nature* **1999**, *402*, 533-537.
[52] Gosh, A.; Gemma, S.; Tang, J. *Neuroterapeutics* **2008**, *5*, 388-408.
[53] Hong, L.; Koelsch, G.; Lin, X.; Wu, S.; Terzyan, S.; Ghosh, A.K.; Zhang, X.C.; Tang, J. *Science* **2000**, *290*, 150–153.
[54] De Strooper, B.; Saftig, P.; Craessaerts, K.; Vanderstichele, H.; Guhde, G.; Annaert, W.; Von Figura, K.; Van Leuven, F. *Nature* **1998**, *391*, 387-390.
[55] Mastrangelo, P.; Mathews, P.M.; Chishti, M.A.; Schmidt, S.D.; Gu, Y.;Yang, J.; Mazzella, M.J.; Coomaraswamy, J.; Horne, P.; Strome, B.; Pelly, H.; Levesque, G.; Ebeling, C.; Jiang, Y.; Nixon, R.A.; Rozmahel, R.; Fraser, P.E.; St George-Hyslop, P.; Carlson, G.A.; Westaway, D. *Proc. Natl. Acad. Sci. U S A* **2005**, *102*, 8972-8977.
[56] Wolfe, M.S.*Nat. Rev. Drug Discov.* **2002**, *1*, 859-866.
[57] Shah, S.; Lee, S.F.; Tabuchi, K.; Hao, Y.H.; Yu, C.; LaPlant, Q.; Ball, H.; Dann, C.E.; Südhof, T.; Yu, G. *Cell* **2005**, *122*, 435-447.
[58] Steiner, H.; Winkler, E.; Edbauer, D.; Prokop, S.; Basset, G.; Yamasaki, A.; Kostka, M.; Haass, C. *J. Biol. Chem.* **2002**, *277*, 39062-39065.
[59] Strooper, B.D.; Annaert, W. *Nat. Cell. Biol.* **2001**, *3*, E221-225.
[60] Wong, G.T.; Manfra, D.; Poulet, F.M.; Zhang, Q.; Josien, H.; Bara, T.; Engstrom, L.; Pinzon-Ortiz, M.; Fine, J.S.; Lee, H.-J.J.; Zhang, L.; Higgins, G.A.; Parker, E.M. *J. Biol. Chem.* **2004**, *279*, 12876-128829.
[61] Lu, D.C.; Rabizadeh, S.; Chandra, S.; Shayya, R.F.; Ellerby, L.M.; Ye, X.; Salvesen, G.S.; Koo, E.H.; Bredesen, D.E. *Nat. Med.* **2000**, *6*, 397-404.
[62] Suh, Y.H.; Checler, F. *Pharmacol. Rev.* **2002**, *54*, 469-525.
[63] Varadarajan, S.; Yatin, S.; Aksenova, M.; Butterfield, D.A. *J. Struct. Biol. 2000*, **130**, 184-208.
[64] Johnson, G.V.; Stoothoff, W.H. *J. Cell. Sci.* **2004**, *117*, 5721-5729.
[65] Goedert, M.; Spillantini, M.G.; Jakes, R.; Rutherford, D.; Crowther, R.A. *Neuron.* **1989**, *3*, 519-526.
[66] Lee, V.M.; Goedert, M.; Trojanowski, J.Q. *Annu. Rev. Neurosci.* **2001**, *24*, 1121-1159.
[67] Alonso, A.D.; Zaidi, T.; Novak, M.; Barra, H.S.; Grundke-Iqbal, I.; Iqbal, K. *J. Biol. Chem.* **2001**, *276*, 37967-37973.
[68] Salehi, A.; Delcroix, J.D.; Mobley, W.C.*Trends Neurosci.* **2003**, *26*, 73-80.
[69] Lee, H.G.; Perry, G.; Moreira, P.I.; Garrett, M.R.; Liu, Q.; Zhu, X.; Takeda, A.; Nunomura, A.; Smith, M.A. *Trends Mol. Med.* **2005**, *11*, 164-169.
[70] Sayre, L.M.; Perry, G.; Smith, M.A. *Chem. Res. Toxicol.* **2008,** *21*, 172-188.
[71] Colombres, M.; Sagal, J.P.; Inestrosa, N.C. *Curr. Pharm. Des.* **2004**, *10*, 3167-3175.
[72] Barnham, K.J.; Masters, C.L.; Bush, A.I. *Nat. Rev. Drug Discov.* **2004**, *3*, 205-214.
[73] Liu, G.; Huang, W.; Moir, R.D.; Vanderburg, C.R.; Lai, B.; Peng, Z.; Tanzi, R.E.; Rogers, J.T.; Huang, X. *J. Struct. Biol.* **2006**, *155*, 45-51.
[74] Zhu, X.; Su, B.; Wang, X.; Smith, M.A.; Perry, G. *Cell. Mol. Life Sci.* **2007**, *64*, 2202-2210.
[75] Huang, X.; Atwood, C.S.; Moir, R.D.; Hartshorn, M.A.; Vonsattel, J.P.; Tanzi, R.E.; Bush, A.I. *J. Biol. Chem.* **1997**, *272*, 26464-26470.
[76] Atwood, C.S.; Moir, R.D.; Huang, X.; Scarpa, R.C.; Bacarra, N.M.; Romano, D.M.; Hartshorn, M.A.; Tanzi, R.E.; Bush, A.I. *J. Biol. Chem.* **1998**, *273*, 12817-12826.
[77] Curtain, C.C.; Ali, F.; Volitakis, I.; Cherny, R.A.; Norton, R.S.; Beyreuther, K.; Barrow, C.J.; Masters, C.L.; Bush, A.I.; Barnham, K.J. *J. Biol. Chem.* **2001**, *276*, 20466-20473.
[78] Liu, G.; Huang, W.; Moir, R.D.; Vanderburg, C.R.; Lai, B.; Peng, Z.; Tanzi, R.E.; Rogers, J.T.; Huang, X. *J. Struct. Biol.* **2006**, *155*, 45-51.
[79] Butterfield, D.A.; Castegna, A.; Lauderback, C.M.; Drake, *J. Neurobiol. Aging* **2002**, *23*, 655-664.
[80] Lauderback, C.M.; Hackett, J.M.; Huang, F.F.; Keller, J.N.; Szweda, L.I.; Markersbery, W.R.; Butterfield, D.A. *J. Neurochem.* **2001**, *78*, 413-416.
[81] Klafki, H.W.; Staufenbiel, M.; Kornhuber, J.; Wiltfang, J. *Brain* **2006**, *129*, 2840-2855.
[82] Hynd, M.R.; Scott, H.L.; Dodd, P.R. *Neurochem. Int.* **2004**, *45*, 583-595.
[83] Lipton, S.A. *Nat. Rev. Drug Discov.* **2006**, *5*, 160-170.
[84] Stys, P.K.; Lipton, S.A. *Trends Pharmacol. Sci.* **2007**, *28*, 561-566.
[85] Mattson, M.P.; Cheng, B.; Davis, D.; Bryant, K.; Lieberburg, I.; Rydel, R.E. *J. Neurosci.* **1992**, *12*, 376-389.

[86] Harkany, T.; Abrahám, I.; Timmerman, W.; Laskay, G.; Tóth, B.; Sasvári, M.; Kónya, C.; Sebens, J.B.; Korf, J.; Nyakas, C.; Zarándi, M.; Soós, K.; Penke, B.; Luiten, P.G. *Eur. J. Neurosci.* **2000**, *12*, 2735-2745.
[87] Couratier, P.; Lesort, M.; Sindou, P.; Esclaire, F.; Yardin, C.; Hugon, J. *Mol. Chem. Neuropathol.* **1996**, *27*, 259-273.
[88] Bachurin, S.O. *Med. Res. Rev.* **2002**, *23*, 48-88.
[89] Terry, A.V.; Buccafusco, J.J. *J. Pharmacol. Exp. Ther.* **2003**, *306*, 821-827.
[90] Ferris, S.H. *Expert Opin. Pharmacother.* **2003**, *4*, 2305-2313.
[91] Kumar, V.; Calache, M. *Int. J. Clin. Pharmacol. Ther. Toxicol.* **1991**, *29*, 23-37.
[92] Caccamo, A.; Oddo, S.; Billings, L.M.; Green, K.N., Martinez-Coria, H.; Fisher, A.; LaFerla, F.M. Neuron. 2006, 49, 671-682.
[93] Eglen, R.M. *Prog. Med. Chem.* **2005**, *43*, 105-136.
[94] Zhang, W.; Basile, A.S.; Gomeza, J.; Volpicelli, L.A.; Levey, A.I.; Wess, J. *J. Neurosci.* **2002**, *22*, 1709-1717.
[95] Quirion, R.; Wilson, A.; Rowe, W.; Aubert, I.; Richard, J.; Doods, H.; Parent, A.; White, N.; Meaney, M.J. *J. Neurosci.* **1995**, *15*, 1455-1462.
[96] Quirion, R.; Wilson, A.; Rowe, W. *J. Neurosci.* **1995**, *15*, 1455-1462
[97] Billard, W.; Binch, H.; Bratzler, K.; Chen, L.Y.; Crosby, G.; Duffy, R.A.; Dugar, S; Lachowicz, J.; McQuade, R.; Pushpavaman, P., Ruperto, V.B.; Taylor, L.A.; Clader, J.W. *Bioorg. Med. Chem. Lett.* **2000**, 10, 2209-2211.
[98] McCombie, S.W.; Lin, S.I.; Tagat, J.R.; Nazareno, D.; Vice, S.; Ford, J.; Asberom, T.; Leone, D.; Kozlowski, J.A.; Zhou, G., Ruperto, V.B.; Duffy, R.A.; Lachowicz, J.E. *Bioorg. Med. Chem. Lett.* **2002**, 12, 795-798.
[99] Potter, A.; Corwin, J.; Lang, J.; Piasecki, M.; Lenox, R.; Newhouse, P.A. P*sychopharmacology* **1999**, *142*, 334-342.
[100] Vernier, J.M.; El-Abdellaoui, H.; Holsenback, H.; Cosford, N.D.; Bleicher, L.; Barker, G.; Bontempi, B.; Chavez-Noriega, L.; Menzaghi, F.; Rao, T.S.; Reid, R.; Sacaan, A.I.; Suto, C.; Washburn, M.; Lloyd, G.K.; McDonald, I.A. *J. Med. Chem.* **1999**, *42*, 1684-1686.
[101] Cummings, J.L.; Doody, R.; Clark, C. Neurology 2007, 69, 1622-1634.
[102] Racchi, M.; Mazzucchelli, M.; Porrello, E.; Lanni, C.; Govoni, S. *Pharmacol. Res.* **2004**, *50*, 441-451.
[103] Wilcock, G.K.; Scott, M.; Pearsall, T. *Lancet* **1994**, *343*, 294.
[104] Sugimonto, H.; Yamanishi, Y., Ogura, H. *Yakugaku Zasshi* **1999**, *119*, 101-113.
[105] Raskid, M.A.; Peskind, E.R.; Wessel, T. *Neurology* **2000**, *54*, 2261-2268.
[106] Bowen, D.M.; Benton, J.S.; Spillane, J.A. *J. Neurol. Sci.* **1982**, *57*, 191-202.
[107] Inestrosa, N.C.; Alvarez, A, Perez, C.A.; Moreno, R.D.; Vicente, M.; Linker, C.; Casanueva, O.I.; Soto, C.; Garrido, J. *Neuron* **1996**, *16*, 881-891.
[108] Dominguez, D.I.; De Strooper, B. *Trends Pharmacol. Sci.* **2002**, *23*, 324-330.
[109] Luo, Y.; Bolon, B.; Kahn, S.; Bennett, B.D.; Babu-Khan, S.; Denis, P.; Fan, W.; Kha, H.; Zhang, J.; Gong, Y.; Martin, L.; Louis, J.C.; Yan, Q.; Richards, W.G.; Citron, M.; Vassar, R. *Nat. Neurosci.* **2001**, *4*, 231-232.
[110] John, V.; Beck, J.P.; Bienkowski, M.J.; Sinha, S.; Heinrikson, R.L. *J. Med. Chem.* **2003**, *46*, 4625-4630.
[111] Ghosh, A.K.; Bilcer, G.; Harwood, C.; Kawahama, R.; Shin, D.; Hussain, K.A.; Hong, L.; Loy, J.A.; Nguyen, C.; Koelsch, G.; Ermolieff, J.; Tang, J. *J. Med. Chem.* **2001**, *44*, 2865-2868.
[112] Sinha, S.; Anderson, J.P.; Barbour, R.; Basi, G.S.; Caccavello, R.; Davis, D.; Doan, M. *Nature* **1999**, *402*, 537-540.
[113] Tung, J.S.; Davis, D.L., Anderson, J.P.; Walker, D.E.; Mamo, S.; Jewett, N.; Hom, R.K.; Sinha, S.; Thorsett, E.D.; John, V. *J. Med. Chem.* **2002**, *45*, 259-262.
[114] Hom, R.K.; Fang, L.Y.; Mamo, S.; Tung, J.S.; Guinn, A.C.; Walker, D.E.; Davis, D.L.; Gailunas, A.F.; Thorsett, E.D.; Sinha, S.; Knops, J.E.; Jewett, N.E.; Anderson, J.P.; John, V. *J. Med. Chem.* **2003**, *46*, 1799-1802.
[115] Kimura, T.; Hamada, Y.; Stochaj, M.; Ikari, H.;Nagamine, A.; Abdel-Rahman, H.; Igawa, N.; Hidaka, K.; Nguyen, J.T.; Saito, K.; Hayashi, Y.; Kiso, Y. *Bioorg. Med. Chem. Lett.* **2006**, *16*, 2380-2386.
[116] Maillard, M.C.; Hom, R.K.; Benson, T.E.; Moon, J.B.; Mamo, S.; Bienkowski, M.; Tomasselli, A.G.; Woods, D.D.; Prince, D.B.; Paddock, D.J.; Emmons, T.L.; Tucker, J.A.; Dappen, M.S.; Brogley, L.; Thorsett, E.D.; Jewett, N.; Sinha, S.; John, V. *J. Med. Chem.* **2007**, *50*, 776-819.
[117] Silvestri, R. *Med. Res. Rev.* **2009**, *29*, 295-338.
[118] Miyamoto, M.; Matsui, J.; Fukumoto, H., Tarui, N. Patent WO01/00665, 2001.
[119] Qiao, L.; Etcheberrigaray, R. Patent WO 02/96897, 2002.
[120] Baxter, E.W.; Conway, K.A.; Kennis, L.; Bischoff, F.; Mercken, M.H.; Winter, H.L.; Reynolds, C.H.; Tounge, B.A.; Luo, C.; Scott, M.K.; Huang, Y.; Braeken, M.; Pieters, S.M.; Berthelot, D.J.; Masure, S.; Bruinzeel, W.D.; Jordan, A.D.; Parker, M.H.; Boyd, R.E.; Qu, J.; Alexander, R.S.; Brenneman, D.E.; Reitz, A.B. *J. Med. Chem.* **2007**, *50*, 4261-4264.
[121]Wolfe, M.S. *Neurotherapeutics* **2008**, *5*, 391-398.
[122] Dovey, H.F.; John, V.; Anderson, J.P.; Chen, L.Z.; de Saint Andrieu, P.; Fang, L.Y.; Freedman, S.B.; Folmer, B.et al *J. Neurochem.* **2001**, *76*, 173-181.
[123] Anderson, J.J.; Holtz, G.; Baskin, P.P.; Turner, M.; Rowe, B.; Wang, B.; Kounnas, M.Z.; Lamb, B.T.; Barten, D.; Felsenstein, K.; McDonald, I.; Srinivasan, K.; Munoz, B.; Wagner, S.L. *Biochem. Pharmacol.* **2005**, *69*, 689-698.

[124] Best, J.D.; Jay, M.T.; out, F.; Ma, J.; Nadin, A.; Ellis,S.;Lewis, H.D.; Pattison, C.; Reilly, M.; Harrison, T.; Shearman, M.S.; Williamson, T.L.; Atack, J.R. *J. Pharmacol. Exp. Ther.* **2005**, *313*, 902-908.
[125] Wong, G.T., Manfra, D.; Poulet, F.M.; Zhang, Q.; Josien, H.; Bara, T.; Engstrom, L.; Pinzon-Ortiz, M.; Fine, J.S.; Lee, H.J.; Zhang, L.; Higgins, G.A.; Parker, E.M. *J. Biol. Chem.* **2004**, *279*, 12876-12829.
[126] Weggen, S.; Eriksen, J.L.; Das, P.; Sagi, S.A.; Wang, R.; Pietrzik, C.U.; Findlay, K.A.; Smith, T.E.; Murphy, M.P.; Bulter, T.; Kang, D.E.; Marquez-Sterling, N.; Golde, T.E.; Koo, E.H. *Nature* **2001**, *414*, 212-216.
[127] Okochi, M.; Fukumori, A.; Jiang, J.; Itoh, N.; Kimura, R.; Steiner, H.; Haass, C.; Tagami, S.; Takeda, M. *J. Biol. Chem.* **2006**, *281*, 7890-7898.
[128] Eriksen, J.L.; Sagi, S.A.; Smith, T.E.; Weggen, S.; Das, P.; McLendon, D.C.; Ozols, V.V.; Jessing, K.W.; Zavitz, K.H.; Koo, E.H.; Golde, T.E. *J. Clin. Invest.* **2003**, *112*, 440-449.
[129] Netzer, W.J.; Dou, F.; Cai, D.; Veach, D.; Jean, S.; Li, Y.; Bornmann, W.G.; Clarkson, B.; Xu, H.; Greengard, P. *Proc. Natl. Acad. Sci. U S A* **2003**, *100*, 12444-12449.
[130] Adessi, C.; Soto, C. *Drug Dev. Res.* **2002**, *56*, 184–193.
[131] Soto, C.; Sigurdsson, E.M.; Morelli, L.; Kumar, R.A.; Castaño, E.M.; Frangione, B. *Nat. Med.* **1998**, *4*, 822-826.
[132] Howlett, D.R.; George, A.R.; Owen, D.E.; Ward, R.V.; Markwell, R.E. *Biochem. J.* **1999**; *343*, 419–423.
[133] Wolozin, B. *Neuron.* **2004**, 41, 7–10.
[134] Refolo, L.M.; Pappolla, M.A.; LaFrancois, J.; Malester, B.; Schmidt, S.D.; Thomas-Bryant, T.; Tint, G.S.; Wang, R.; Mercken, M.; Petanceska, S.S.; Duff, K.E. *Neurobiol. Dis.* **2001**, *8*, 890-899.
[135] Fassbender, K.; Simons, M.; Bergmann, C.; Stroick, M.; Lutjohann, D.; Keller, P.; Runz, H.; Kuhl, S.; Bertsch, T.; von Bergmann, K.; Hennerici, M.; Beyreuther, K.; Hartmann, T. *Proc. Natl. Acad. Sci. U S A* **2001**, *98*, 5856-5861.
[136] Schenk, D.; Barbour, R.; Dunn, W.; Gordon, G.; Grajeda, H.; Guido, T.; Hu, K.; Huang, J.; Johnson-Wood, K.; Khan, K.; Kholodenko, D.; Lee, M.; Liao, Z.; Lieberburg, I.; Motter, R.; Mutter, L.; Soriano, F.; Shopp, G.; Vasquez, N.; Vandevert, C.; Walker, S.; Wogulis, M.; Yednock, T.; Games, D.; Seubert, P. *Nature* **1999**, *400*, 173-177.
[137] Solomon, B.; Koppel, R.; Frankel, D.; Hanan-Aharon, E. *Proc. Natl. Acad. Sci. U S A.* **1997**, *94*, 4109-4112
[138] DeMattos, R.B.; Bales, K.R.; Cummins, D.J.; Paul, S.M.; Holtzman, D.M. *Science* **2002**, *295*, 2264-2267.
[139] Lee, V.M. *Proc. Natl. Acad. Sci. USA* **2001**, *98*, 8931-8932.
[140] Orgogozo, J.M.; Gilman, S.; Dartigues, J.F.; Laurent, B.; Puel, M.; Kirby, L.C.; Jouanny, P.; Dubois, B.; Eisner, L.; Flitman, S.; Michel, B.F.; Boada, M.; Frank, A.; Hock, C. *Neurology* **2003**, *61*, 46-54.
[141] Ferrer, I.L; Boada Rovira, M.; Sánchez Guerra, M.L.; Rey, M.J.; Costa-Jussá, F. *Brain Pathol.* **2004**, *14*, 11-20.
[142] Cherny, R.A.; Legg, J.T.; McLean, C.A.; Fairlie, D.P.; Huang, X.; Atwood, C.S.; Beyreuther, K.; Tanzi, R.E.; Masters, C.L.; Bush, A.I. *J. Biol. Chem.* **1999**, *274*, 23223-23228.
[143] Huang, X.; Atwood, C. S.; Hartshorn, M. A.; Multhaup, G.; Goldstein, L. E.; Scarpa, R. C.; Cuajungco, M. P.; Gray, D. N.; Lim, J.; Moir, R. D.; Tanzi, R. E.; Bush, A. I. *Biochemistry* **1999**, *38*, 7609.
[144] Fraser, F.W.; Kim, Y.; Huang, X.; Goldstein, L.E.; Moir, R.D.; Lim, J.T.; Beyreuther, K.; Zheng, H.; Tanzi, R.E. Masters, C.L.; Bush, A.I. *Neuron* **2001**, *30*, 665-676.
[145] Li, L.; Sengupta, A.; Haque, N.; Grundke-Iqbal, I.; Iqbal, K. *FEBS Lett.* **2004**, *566*, 261-269.
[146] Bulic, B.; Pickhardt, M.; Schmidt, B.; Mandelkow, E.M.; Waldmann, H.; Mandelkow, E. *Angew. Chem. Int. Ed.* **2009**, *48*, 1740-1752.
[147] Bulic, B.; Pickhardt, M.; Khlistunova, I.; Biernat, J.; Mandelkow, E.M.; Mandelkow, E.; Waldmann, H. *Angew. Chem. Int. Ed.* **2007**, *46*, 9215-9219.
[148] Taniguchi, S.; Suzuki, N.; Masuda, M.; Hisanaga, S.; Iwatsubo, T.; Goedert, M.; Hasegawa, M. *J. Biol. Chem. 2005*, *280*, 7614-7623.
[149] Necula, M.; Chirita, C. N.; Kuret, J. *Biochemistry* **2005**, *44*, 10227-10237.
[150] Chen, H.S.; Lipton, S.A. *J. Neurochem.* **2006**, *97*, 1611-1626.
[151] Behl, C.; Davis, J.; Cole, G.M.; Schubert, D. *Biochem. Biophys. Res. Commun.* **1992**, *186*, 944–950.
[152] Xu, H.;Gouras, G.K.; Greenfield, J.P.; Vincent, B.; Naslund J.; Mazzarelli, L.; Fried, G.; Jovanovic,. J.N.; Seeger, M.; Relkin, N.R.; Liao, F.; Checler, F.; Buxbaum, J.D.; Chait, B.T.; Thinakaran, G.; Sisodia, S.S.;Wang, R.; Greengard, P.; Gandy, S. *Nat. Med.* **1998**, *4*, 447–451.
[153] Reiter, R. *Oxidative Progr. Neurobiol.* **1998**, *56*, 359–384.
[154] Pappolla, M.A..; Chyan, Y.J.; Poeggeler, B.; Frangione, B.; Wilson, G.; Ghiso, J.; Reiter, R.J.; *J. Neural. Transm.* **2000**, *107*, 203–231.
[155] Bachurin, S.; Oxenkrug, G.; Lermontova, N.; Afanasiev, A.; Beznosko, B.; Vankin, G.; Shevtzova; E.; Mukhina, T.; Serkova, T. *Ann. N.Y. Acad. Sci.* **1999**, *890*,155–166.
[156] Morphy, R.; Rankovic, Z. *J. Med. Chem.* **2005**, *48*, 6523-6543.
[157] Recanatini, M.; Valenti, P. *Curr. Pharm. Des.* **2004**, *10*, 3157-3166.
[158] Alvarez, A.; Bronfman, F.; Pérez, C.A.; Vicente, M.; Garrido, J.; Inestrosa, N.C. *Neurosci. Lett.* **1995**, *201*, 49-52.
[159] De Ferrari, G.V.; Canales, M.A.; Shin, I.; Weiner, L.M.; Silman, I.; Inestrosa, N.C. *Biochemistry*. **2001**, *40*, 10447-10457.
[160] Muñoz-Torrero, D. *Curr. Med. Chem.* **2008**, *15*, 2433-2455.

[161] Pang, Y.P.; Quiram, P.; Jelacic, T.; Hong, F.; Brimijoin, S. *J. Biol. Chem.* **1996**, **271**, 23646-23649.
[162] Li, W.; Xue, J.; Niu, C.; Fu, H.; Lam, C.S.; Luo, J.; Chan, H.H.; Xue, H.; Kan, K.K.; Lee, N.T.; Li, C.; Pang, Y.; Li, M.; Tsim, K.W.; Jiang, H.; Chen, K.; Li, X.; Han, Y. *Mol. Pharmacol.* **2007**, *71*, 1258-1267.
[163] Fu, H.; Li, W.; Luo, J.; Lee, N.T.; Li, M.; Tsim, K.W.; Pang, Y.; Youdim, M.B.; Han, Y. *Biochem. Biophys. Res. Commun*. **2008**, *366*, 631-636.
[164] Lewis, W.G.; Green, L.G.; Grynszpan, F.; Radić, Z.; Carlier, P.R.; Taylor, P.; Finn, M.G.; Sharpless, K.B. *Angew. Chem. Int. Ed.*, **2002**, *41*, 1053-1057.
[165] Manetsch, R.; Krasiński, A.; Radić, Z.; Raushel, J.; Taylor, P.; Sharpless, K.B.; Kolb, H.C. *J. Am. Chem. Soc.* **2004**, *126*, 12809-12818.
[166] Krasiński, A.; Radić, Z.; Manetsch, R.; Raushel, J.; Taylor, P.; Sharpless, K.B.; Kolb, H.C. *J. Am. Chem. Soc.* **2005**, *127*, 6686-6692.
[167] Melchiorre, C.; Andrisano, V.; Bolognesi, M. L.; Budriesi, R.; Cavalli, A.; Cavrini, V.; Rosini, M.; Tumiatti, V.; Recanatini, M. *J. Med. Chem.* **1998**, *41*, 4186–4189.
[168] Piazzi, L.; Rampa, A.; Bisi, A.; Gobbi, S.; Belluti, F.; Cavalli, A.; Bartolini, M.; Andrisano, V.; Valenti, P.; Recanatini, M. *J. Med. Chem.* **2003**, *46*, 2279–2282.
[169] Bolognesi, M. L.; Andrisano, V.; Bartolini, M.; Banzi, R.; Melchiorre, C. *J. Med. Chem.* **2005**, *48*, 24–27.
[170] Munoz-Ruiz, P.; Rubio, L.; Garcia-Palomero, E.; Dorronsoro, I.; del Monte-Millan, M.; Valenzuela, R.; Usan, P.; de Austria, C.; Bartolini, M.; Andrisano, V.; Bidon-Chanal, A.; Orozco, M.; Luque, F. J.; Medina, M.; Martinez, A. *J. Med. Chem.* **2005**, *48*, 7223–7233.
[171] Youdim, M. B.; Amit, T.; Bar-Am, O.; Weinreb, O.; Yogev-Falach, M. *Neurotoxic. Res.* **2006**, *10*, 181–192.
[172] Alper, G.; Girgin, F. K.; Ozgonul, M.; Mentes, G.; Ersoz, B. *Eur. Neuropsychopharmacol.* **1999**, *9*, 247–252.
[173] Kogen, H.; Toda, N.; Tago, K.; Marumoto, S.; Takami, K.; Ori, M.; Yamada, N.; Koyama, K.; Naruto, S.; Abe, K.; Yamazaki, R.; Hara, T.; Aoyagi, A.; Abe, Y.; Kaneko, T. *Org. Lett.* **2002**, *4*, 3359–3362.
[174] Toda, N.; Tago, K.; Marumoto, S.; Takami, K.; Ori, M.; Yamada, N.; Koyama, K.; Naruto, S.; Abe, K.; Yamazaki, R.; Hara, T.; Aoyagi, A.; Abe, Y.; Kaneko, T.; Kogen, H. *Bioorg. Med. Chem.* **2003**, *11*, 1935–1955.
[175] Toda, N.; Tago, K.; Marumoto, S.; Takami, K.; Ori, M.; Yamada,N.; Koyama, K.; Naruto, S.; Abe, K.; Yamazaki, R.; Hara, T.; Aoyagi, A.; Abe, Y.; Kaneko, T.; Kogen, H. *Bioorg. Med. Chem.* **2003**, *11*, 4389–4415.
[176] Bolognesi, M. L.; Minarini, A.; Tumiatti, V.; Melchiorre, C. *Mini-Re*V. *Med. Chem.* **2006**, *6*, 1269–1274.
[177] Rosini, M.; Andrisano, V.; Bartolini, M.; Bolognesi, M. L.; Hrelia, P.; Minarini, A.; Tarozzi, A.; Melchiorre, C. *J. Med. Chem.* **2005**, *48*,360–363.
[178] Dedeoglu, A.; Cormier, K.; Payton, S.; Tseitlin, K. A.; Kremsky, J. N.; Lai, L.; Li, X.; Moir, R. D.; Tanzi, R. E.; Bush, A. I.; Kowall, N. W.; Rogers, J. T.; Huang, X. *Exp. Gerontol.* **2004**, *39*, 1641–1649.
[179] Bolognesi, M.L.; Cavalli, A.; Valgimigli, L.; Bartolini, M.; Rosini, M.; Andrisano, V.; Recanatini, M.; Melchiorre, C. *J. Med. Chem.* **2007**, *50*, 6446-6449.
[180] Gutzmann, H.; Hadler, D. *J. Neural. Transm.* 1998, 54, 301–310.
[181] Cavalli, A.; Bolognesi, M.L.; Capsoni, S.; Andrisano, V.; Bartolini, M.; Margotti, E.; Cattaneo, A.; Recanatini, M.; Melchiorre, C. *Angew. Chem. Int. Ed.* **2007**, *46*, 3689-3692.
[182] Bolognesi, M.L.; Cavalli, A.; Melchiorre, C. *Neurotherapeutics* 2009, 6, 152-162.
[183] Melchiorre, C.; Yong, M. S.; Benfey, B. G.; Belleau, B. *J. Med. Chem.* **1978**, *21*, 1126-1132.
[184] Tumiatti, V.; Rosini, M.; Bartolini, M.; Cavalli, A.; Marucci, G.; Andrisano, V.; Angeli, P.; Banzi, R.; Minarini, A.; Recanatini, M.; Melchiorre, C. *J. Med. Chem.* **2003**, *46*, 954-966.
[185] Tumiatti, V., Andrisano, V.; Banzi, R.; Bartolini, M.; Minarini, A.; Rosini, M.; Melchiorre, C. *J. Med. Chem.* **2004**, *47*, 6490-6498.
[186] Van der Schyf, C. J.; Geldenhuys, W. J.; Youdim, M. B. *J. Neurochem.* **2006**, *99*, 1033–1048.
[187] Decker, M. *Mini-Rev. Med. Chem.* **2007**, *7*, 221–229
[188] Bartolini, M.; Bertucci, C.; Gotti, R.; Tumiatti, V.; Cavalli, A.; Recanatini, M.; Andrisano, V. *J. Chromatogr. A* **2002**, *958*, 59-67.
[189] Bartolini, M.; Bertucci, C.; Cavrini, V.; Andrisano, V. *Biochem. Pharmacol.* **2003**, *65*, 407–416.
[190] Axelsen, P. H.; Harel, M.; Silman, I.; Sussman, J. L. *Protein Sci.* **1994**, *3*, 188–197.
[191] Nesterov, E. E.; Skoch, J.; Hyman, B. T.; Klunk, W. E.; Bacskai, B. J.; Swager, T. M. *Angew. Chem., Int. Ed.* **2005**, *44*, 5452–5456.
[192] Adessi, C.; Soto, C. *Drug De*v. *Res.* **2002**, *56*, 184–193.
[193] Sotiriou-Leventis, C.; Mao, Z. *J. Heterocycl. Chem.* **2000**, *37*, 1665–1667.
[194] Inestrosa, N. C.; Alvarez, A.; Calderon, F. *Mol. Psychiatry* **1996**, *1*, 359-361.
[195] Bartolini, M.; Bertucci, C.; Bolognesi, M.L.; Cavalli, A.; Melchiorre, C.; Andrisano, V. *Chembiochem* **2007**, *8*, 2152-2161.
[196] Kryger, G.; Harel, M.; Giles, K.; Toker, L.; Velan, B.; Lazar, A.; Kronman, C.; Barak, D.; Ariel, N.; Shafferman, A.; Silman, I.; Sussman, J. L. *Acta Crystallographica Section D-Biological Crystallography* **2000**, *56*, 1385-1394.
[197] Nicolet, Y.; Lockridge, O.; Masson, P.; Fontecilla-Camps, J. C.; Nachon, F. *J. Biol. Chem.* 2003, *278*, 41141-41147.

[198] Mecozzi, S.; West, A.P.; Dougherty, D.A. *Proc. Natl. Acad. Sci. U S A.* **1996**, *93*, 10566-10571.
[199] Diamant, S.; Podoly, E.; Friedler, A.; Ligumsky, H.; Livnah, O.; Soreq, H. *Proc. Natl. Acad. Sci. U.S.A.* **2006**, *103*, 8628–8633
[200] Liston, D. R.; Nielsen, J. A.; Villalobos, A.; Chapin, D.; Jones, S. B.;Hubbard, S. T.; Shalaby, I. A.; Ramirez, A.; Nason, D.; White, W. F. *Eur. J. Pharmacol.* **2004**, *486*, 9–17.
[201] Inestrosa, N. C.; Alvarez, A.; Perez, C. A.; Moreno, R. D.; Vicente, M.; Linker, C.; Casanueva, O. I.; Soto, C.; Garrido, J. *Neuron* **1996**, *16*, 881–891.
[202] Bolognesi, M. L.; Bartolini, M.; Cavalli, A.;And risano, V.; Rosini, M.;Minarini, A.; Melchiorre, C. *J. Med. Chem.* **2004**, *47*, 5945–5952.
[203] Xie, Q.; Wang, H.; Xia, Z.; Lu, M.; Zhang, W.; Wang, X.; Fu, W.; Tang, Y.; Sheng, W.; Li, W.; Zhou, W.; Zhu, X.; Qiu, Z.; Chen, H. *J. Med. Chem.* **2008**, *51*, 2027–2036.
[204] Bolognesi, M. L.; Banzi, R.; Bartolini, M.; Cavalli, A.; Tarozzi, A.; Andrisano, V.; Minarini, A.; Rosini, M.; Tumiatti, V.; Bergamini, C.; Fato, R.; Lenaz, G.; Hrelia, P.; Cattaneo, A.; Recanatini, M.; Melchiorre, C. *J. Med. Chem.* **2007**, *50*, 4882–4897.
[205] Thompson, L.A.; Bronson, J.J.; Zusi, F.C. *Curr. Pharm. Des.* **2005**, *11*, 3383-3404.
[206] Jones, G.; Willett, P.; Glen, R. C.; Leach, A. R.; Taylor, R. *J. Mol. Biol.* **1997**, *267*, 727–748.
[207] Bottegoni, G.; Cavalli, A.; Recanatini, M. *J. Chem. Inf. Model.* **2006**, *46*, 852–862.
[208] Campiani, G.; Fattorusso, C.; Butini, S.; Gaeta, A.; Agnusdei, M.; Gemma, S.; Persico, M.; Catalanotti, B.; Savini, L.; Nacci, V.; Novellino, E.; Holloway, H. W.; Greig, N. H.; Belinskaya, T.; Fedorko, J. M.; Saxena, A. *J. Med. Chem.* **2005**, *48*, 1919–1929.
[209] Ellman, G. L.; Courtney, K. D.; Andres, V., Jr.; Feather-Stone, R. M. *Biochem Pharmacol* **1961,** *7*, 88-95.
[210] Naiki, H.; Higuchi, K.; Nakakuki, K.; Takeda, T. *Laboratory Investigation* **1991,** 65, 104-110.
[211] LeVine, H., 3rd. *Protein Sci* **1993,** *2*, 404-10.
[212] Jones, G.; Willett, P.; Glen, R. C. *J. Mol. Biol.* **1997**, *267*, 727-748.

[213] Gaussian, I. Pittsburgh, PA, **2003**.
[214] Gaussian 03, R. C., Frisch, M. J.; Trucks, G. W.; Schlegel, H. B.; Scuseria, G. E.; Robb, M. A.; Cheeseman, J. R.; Montgomery, Jr., J. A.; Vreven, T.; Kudin, K. N.; Burant, J. C.; Millam, J. M.; Iyengar, S. S.; Tomasi, J.; Barone, V.; Mennucci, B.; Cossi, M.; Scalmani, G.; Rega, N.; Petersson, G. A.; Nakatsuji, H.; Hada, M.; Ehara, M.; Toyota, K.; Fukuda, R.; Hasegawa, J.; Ishida, M.; Nakajima, T.; Honda, Y.; Kitao, O.; Nakai, H.; Klene, M.; Li, X.; Knox, J. E.; Hratchian, H. P.; Cross, J. B.; Bakken, V.; Adamo, C.; Jaramillo, J.; Gomperts, R.; Stratmann, R. E.; Yazyev, O.; Austin, A. J.; Cammi, R.; Pomelli, C.; Ochterski, J. W.; Ayala, P. Y.; Morokuma, K.; Voth, G. A.; Salvador, P.; Dannenberg, J. J.; Zakrzewski, V. G.; Dapprich, S.; Daniels, A. D.; Strain, M. C.; Farkas, O.; Malick, D. K.; Rabuck, A. D.; Raghavachari, K.; Foresman, J. B.; Ortiz, J. V.; Cui, Q.; Baboul, A. G.; Clifford, S.; Cioslowski, J.; Stefanov, B. B.; Liu, G.; Liashenko, A.; Piskorz, P.; Komaromi, I.; Martin, R. L.; Fox, D. J.; Keith, T.; Al-Laham, M. A.; Peng, C. Y.; Nanayakkara, A.; Challacombe, M.; Gill, P. M. W.; Johnson, B.; Chen, W.; Wong, M. W.; Gonzalez, C.; and Pople, J. A.; Gaussian, Inc., Wallingford CT, **2004**.
[216] Bottegoni, G.; Rocchia, W.; Recanatini, M.; Cavalli, A. *Bioinformatics* **2006**, *22*, e58-65.
[216] Kelley, L. A.; Gardner, S. P.; Sutcliffe, M. J. *Protein Eng.* **1997**, *10*, 737-741.
[217] Source World Health Organization.
[218] Tabor, C.W.; Tabor, H. *Annu. Rev. Biochem.* **1984**, *53*, 749-790.
[219] Bachrach, U; Wang, Y.C.; Tabib, A. *News Physiol. Sci.* **2001**, *16*, 106-109.
[220] Thomas, T.; Thomas, T.J. *Cell. Mol. Life Sci.* **2001**, *58*, 244-258.
[221] Pegg, A.E. *Cancer Res.* **1988**, *48*, 759-774.
[222] Wallace, H.M.; Fraser, A.V.; Hughes, A. *Biochem. J.* **2003**, *376*, 1-14.
[223] Morgan, D.M.; *Mol. Biotechnol.* **1999**, *11*, 229-250.
[224] Parchment, R.E.; Pierce, G.B. *Cancer Res.* **1989**, *49*, 6680-6686.
[225] Bonneau, M.J. ; Poulin, R. *Exp. Cell. Res.* **2000**, *259*, 23-34.
[226] Seiler, N.; Delcros, J.G.; Moulinoux, J. P. *Int. J. Biochem. Cell. Biol.* **1996**, *28*, 843–861.
[227] Wallace, H.M.; Keir, H.M. *Biochim. Biophys. Acta* **1981**, *676*, 25–30.
[228] Wallace, H.M. *Med. Sci. Res.* **1987**, *15*, 1437–1440.
[229] McCann, P.P.; Pegg, A.E. *Pharmacol. Ther.* **1992**, *54*, 195-215.
[230] Lu, L.; Stanley, B.A.; Pegg, A.E. *Biochem. J.* **1991**, *277*, 671–675.
[231] Packham, G.; Porter, C.W.; Cleveland, J.L. *Oncogene* **1996**, *13*, 461-9.
[232] Nilsson, J.; Grahn, B.; Heby, O. *Biochem. J.* **2000**, *346*, 699–704.
[233] Lasero, R.A.; Pegg, A.E.; *The FASEB Journal* **1993**, 7, 653-661.
[234] Coleman, C.S.; Huang, H.; Pegg, A.E. *Biochem. J.* **1996**, *316*, 697-701.
[235] Pestell, R.G.; Albanese, C.; Reutens, A.T.; Segall, J.E.; Lee, R.J.; Arnold, A. *Endocr. Rev.* **1999**, *20*, 501-534.
[236] Thomas, T.; Thomas, T.J. *Cancer Res.* 1994, 54, 1077-1084.

[237] Ackermann, J.M.; Pegg, A.E.; McCloskey, D.E. *Prog. Cell. Cycle Res.* **2003**, *5*, 461-468.
[238] Fallace, H.M.; Fraser, A.V. *Biochem. Society* **2003**, *31*, 393-396.
[239] Burton, D.R.; Forsén, S.; Reimarsson, P. *Nucleic Acids Res.* **1981**, *9*. 1219-1228.
[240] Musso, M.; Thomas, T.; Shirahata, A.; Sigal, L.H.; Van Dyke, M.W.; Thomas, T.J. *Biochemistry* **1997**, *36*, 1441-1449.
[241] Thomas, T.J.; Gunnia, U.B.; Thomas, T. *J. Biol. Chem.* **1991**, *266*, 6137-6141.
[242] Basu, H.S.; Smirnov, I.V.; Peng, H.F.; Tiffany, K.; Jackson, V. *Eur. J. Biochem.* **1997**, *243*, 247-258.
[243] Bachrach, U. *Curr. Protein Pept. Sci.* **2005**, *6*, 559-566.
[244] Melchiorre, C.; Antonello, A.; Banzi, R.; Bolognesi, M.L.; Minarini, A.; Rosini, M.; Tumiatti, V. *Med. Res. Rev.* **2003**, *23*, 200-233.
[245] Usherwood, P.N. *Farmaco* **2000**, *55*, 202-205.
[246] Khan, A.U.; Mei, Y.H.; Wilson, T. *Proc. Natl. Acad. Sci. USA* **1992**, *89*, 11426-11427.
[247] Khan, A.U.; Di Mascio, P.; Medeiros, M.H.; Wilson, T. *Proc. Natl. Acad. Sci. USA* **1992**, *89*, 11428-11430.
[248] Ha, H.C.; Sirisoma, N.S.; Kuppusamy, P.; Zweier, J.L.; Woster, P.M.; Casero, R.A. *Proc. Natl. Acad. Sci. USA* **1998**, *95*, 11140-11145.
[249] Seiler, N.; Raul, F. *J. Cell. Mol. Med.* **2005**, *9*, 623-642.
[250] Packham, G.; Cleveland, J.L. *Mol. Cell. Biol.* **1994**, *14*, 5741-5747.
[251] Monti, M.G.; Ghiaroni, S.; Pernecco, L.; Barbieri, D.; Marverti, G.; Franceschi, C. *Life Sci*. **1998**, *62*, 799-806.
[252] Seiler, N. *Can. J. Physiol. Pharmacol.* **1987**, *65*, 2024-2035.
[253] Van-den-Munckhof, R.J.; Denyn, M.; Tigchelaar, G.W.; Schipper, R.G.; Verhofsad, A.A.J.; Van-Noorden, C.J.; Frederiks, W.M. *J. . Histochem. Cytochem.* **1995**, *43*, 1155-1162.
[254] Brunton, V.G.; Grant, M.H.; Wallace, H.M. *Biochem. J.* **1991**, *280*, 193-198.
[255] Römer,L.; Klein,C.; Dehner,A.;Kessler, H.;Buchne, J. *Angew. Chem. Int. Ed.* **2006**, *45*, 6440–6460
[256] Li, L.; Rao, J.N.; Guo, X.; Liu, L.; Santora, R.; Bass, B.L.; Wang, J.Y. *Am. J. Physiol. Cell Physiol.* **2001**, *281*, C941-953.
[257] Li, L.; Rao, J.N.; Bass, B.L.; Wang, J.Y. *Am. J. Physiol. Gastrointest. Liver Physiol.* **2001**, *280*, G992-G1004.
[258] Shah, N.; Thomas, T.; Shirahata, A.; Sigal, L.H.; Thomas, T.J. *Biochemistry* **1999**, *38*, 14763-14774.
[259] Philchenkov, A. *J. Cell. Mol. Med.* **2004**, *8*, 432-44.
[260] Seiler, N.; Raul, F. *J. Cell. Mol. Med.* **2005**, *9*, 623-624.
[261] Pignatti, C.; Tantini, B.; Stefanelli, C.; Flamigni, F. *Amino Acids* **2004**, *27*, 359-65.
[262] Thornberry, N.A.; Lazebnik, Y. *Science* **1998**, *281*, 1312-1316.
[263] Thornberry, N.A. *Chem. Biol.* **1998**, *5*, R97-103.
[264] Riedl, S.J.; Shi, Y. *Nat. Rev. Mol. Cell. Biol.* **2004**, *5*, 897-907.
[265] Johnson, D.E. *Leukemia* **2000**, *4*, 1695-703.
[266] Loeffler, M.; Kroemer, G. *Exp. Cell. Res.* **2000**, *256*, 19-26.
[267] Thornberry, N.A.; Lazebnik, Y. *Science* **1998**, *281*, 1312-1316.
[268] Stefanelli, C.; Bonavita, F.; Stanic, I.; Mignani, M.; Facchini, A.; Pignatti, C.; Flamigni, F.; Caldarera, C.M.; *FEBS Lett.* **1998**, *437*, 233-236.
[269] Stefanelli, C.; Bonavita, F.; Stanic, I.; Pignatti, C.; Flamigni, F.; Guarnieri, C.; Caldarera, C.M. *FEBS Lett.* **1999**, *451*, 95-98.
[270] Stefanelli, C.; Stanic, I.; Zini, M.; Bonavita, F.; Flamigni, F.; Zambonin, L.; Landi, L.; Pignatti, C.; Guarnieri, C.; Caldarera, C.M. *Biochem. J.* **2000**, *347*, 875-880.
[271] Nitta, I.; Igarashi, K.; Yamamoto, N. *Exp. Cell. Res.* **2002**, *276*, 120-128.
[272] Casero, R.A.; Marton, L.J. *Nat. Rev. Drug Discov.* **2007**, *6*, 373-390.
[273] Wallace, H.M.; Fraser, A.V. *Biochem. Soc. Trans.* **2003**, *31*, 393-396.
[274] Metcalf, B.W.; Bey, B.; Danzin, C.; Jung, M.J.; Casara, P.; Vevert, J.P. *J. Am. Chem. Soc.* **1978**, *100*, 2551-2553.
[275] Poulin, R.; Lu, L.; Ackermann, B.; Bey, P.; Pegg, A.E. *J. Biol. Chem.* **1992**, *267*, 150-158.
[276] Williams-Ashman, H.G.; Seidenfeld, J. *Biochem. Pharmacol.* **1986**, *35*, 1217-1225.
[277] Pegg, A.E. *Cancer Res.* **1988**, *48*, 759-774.
[278] Tang, K.C.; Pegg, A.E.; Coward, J.K. *Biochem. Biophys. Res. Commun.* **1980**, *96*, 1371-1377.
[279] Pegg, A.E.; Tang, K.C.; Coward, J.K. *Biochemistry* **1982**, *21*, 5082-5089.
[280] Casero, R.A.; Go, B.; Theiss, H.W.; Smith, J.; Baylin, S.B.; Luk, G.D. *Cancer Res.* **1987**, *47*, 3964-3967.
[281] Casero, R.A.; Ervin, S.J.; Celano, P.; Baylin, S.B.; Bergeron, R.J. *Cancer Res.* **1989**, *49*, 639-643.
[282] Casero, R.A.; Celano, P.; Ervin, S.J.; Porter, C.W.; Bergeron, R.J.; Libby, P.R. *Cancer Res.* **1989**, *49*, 3829-3833.
[283] Yang, J.; Xiao, L.; Berkey, K.A.; Tamez, P.A.; Coward, J.K.; Casero, R.A. *J. Cell. Physiol.* **1995**, *165*, 71-76.
[284] Gabrielson, E.W.; Pegg, A.E.; Casero, R.A. *Clin. Cancer Res.* **1999**, *5*, 1638-1641.
[285] Creaven, P.J.; Perez, R.; Pendyala, L.; Meropol, N.J.; Loewen, G.; Levine, E.; Berghorn, E.; Raghavan, D. *Invest. New Drugs.* **1997**, *15*, 227-234.

[286] Saab, N.H.; West, E.E.; Bieszk, N.C.; Preuss, C.V.; Mank, A.R.; Casero, R.A. Woster, P.M. *J. Med. Chem.* **1993**, *36*, 2998-3004.
[287] Casero, R.A.; Mank, A.R.; Saab, N.H.; Wu, R.; Dyer, W.J.; Woster, P.M. *Cancer Chemother. Pharmacol.* **1995**, *36*, 69-74.
[288] Ha, H.C.; Woster, P.M.; Casero, R.A. *Cancer Res.* **1998**, *58*, 2711-2714.
[289] Webb, H.K.; Wu, Z.; Sirisoma, N.; Ha, H.C.; Casero, R.A.; Woster, P.M. *J. Med. Chem.* **1999**, *42*, 1415-1421.
[290] Reddy, V.K.; Valasinas, A.; Sarkar, A.; Basu, H.S.; Marton, L.J.; Frydman, B. *J. Med. Chem.* **1998**, *41*, 4723-4732.
[291] Waters, W.R.; Frydman, B.; Marton, L.J.; Valasinas, A.; Reddy, V.K.; Harp, J.A.; Wannemuehler, M.J.; Yarlett, N. *Antimicrob. Agents Chemother.* **2000**, *44*, 2891-2894.
[292] Frydman, B.; Porter, C.W.; Maxuitenko, Y.; Sarkar, A.; Bhattacharya, S.; Valasinas, A.; Reddy, V.K.; Kisiel, N.; Marton, L.J.; Basu, H.S. *Cancer Chemother. Pharmacol.* **2003**, **51**, 488-492
[293] Valasinas, A.; Reddy, V.K.; Blokhin, A.V.; Basu, H.S. Bhattacharya, S.; Sarkar, A.; Marton, L.J.; Frydman, B. *Bioorg. Med. Chem.* **2003**, *11*, 4121-4131.
[294] Huang, Y.; Hager, E.R.; Phillips, D.L.; Dunn, V.R.; Hacker, A.; Frydman, B.; Kink, J.A.; Valasinas, A.L.; Reddy, V.K.; Marton, L.J.; Casero, R.A., Davidson, N.E. *Clin. Cancer Res.* **2003**, *9*, 2769-2777.
[295] Bitonte, A.J.; Bush, T.L.; McCann, P.P. *Biochem, J.* **1989**, *257*, 769-774.
[296] Cohen, G.M.; Cullis, P.M.; Hartley J.A.; Mather, A.; Symons M.C.R.; Wheelhouse, R.T, *J. Chem. Soc. Chem. Commun.* **1992**, 298-300.
[297] Cullis, P.M.; Merson-Davies, L.; Weaver, R. *Chem. Commun.* **1998**, *16*, 1699-1700.
[298] Wang, L.; Price, H.L.; Juusola, J.; Kline, M.; Phanstiel, O. IV; *J. Med. Chem.* **2001**, *44*, 3682-3691.
[299] Wang, C.; Delcros, J.G.; Biggerstaff, J.; Phanstiel, O. IV *J. Med. Chem.* **2003**, **46**, 2672-2682.
[300] Gardner, R.A.; Delcros, J.G.; Konate, F.; Breitbeil, F. III, Martin, B.; Sigman, M.; Huang, M.; Phanstiel, O. IV *J. Med. Chem.* **2004**, *47*, 6055-6069.
[301] Yeh, E.S.; Means, A. *Nat. Rev. Cancer* **2007**, *7*, 381-388.
[302] Lu, K.P.; Hanes, S.D.; Hunter, T. *Nature* **1996**, *380*, 544-547.
[303] Ranganathan, R.; Lu, K.P.; Hunter, T.; Noel, J.P. *Cell* **1997**, *89*, 875-886.
[304] Behrsin, C.D.; Bailey, M.L.; Bateman, K.,S.; Hamilton, K.S.; Wahl, L.M.; Brandl, C.J.; Shilton, B.H.; Litchfield, D.W. *J. Mol. Biol.* **2007**, *365*, 1143-1162.
[305] Lippens, G.; Landrieu, I.; Smet, C. *FEBS J.* 2007, *274*, 5211-5222.
[306] Lu, K.P.; Finn, G.; Lee, T.H.; Nicholson, L.K. *Nat. Chem. Biol.* **2007**, *3*, 619-629.
[307] Shen, M.; Stukenberg, P.T.; Kirschener, M.W.; Lu, K.P. *Genes Dev.* **1998**, *12*, 706-720.
[308] Okamoto, K.; Sagata, N. *Proc. Natl. Acad. Sci. USA* **2007**, *104*, 3753-3758.
[309] Bernis, C.; Vigneron, S.; Burgess, A.; Labbè, J.C.; Fesguet, D.; Castro, A.; Lorca, T. *EMBO Rep.* **2007**, *1*, 91-98.
[310] Xu, Y.X.; Manley, J.L. *Mol. Cell.* **2007**, *26*, 287-300.
[311] Lu, K.P. *Cancer Cell.* **2003**, *4*, 174-180.
[312] Wulf, G.M.; Ryo, A.; Wulf, G.G.; Lee, S.W.; Niu, T.; Petkowa, V.; Lu, K.P. *EMBO J.* **2001**, *20*, 2459-3472.
[313] Liou, Y.C.; Ryo, A.; Huang, H.K.; Lu, P.J.; Bronson, R.; Fujimori, F.; Uchida, T.; Hunter, T.; Lu, K.P. *Proc. Natl. Acad. Sci. USA* **2002**, *99*, 1335-1340.
[314] Ryo, A.; Nakamura, M.; Wulf, G.; Liou, Y.C.; Lu, K.P. *Nat. Cell. Biol.* **2001**, *3*, 793-801.
[315] Ryo, A.; Suizu, F.; Yoshida, Y.; Perrem, K.; Liou, Y.C.; Wulf, G.; Rottapel, R.; Yamaoka, S.; Lu, K.P. *Mol. Cell.* **2003**, *12*, 1413-1426.
[316] Suizu, F.; Ryo, A.; Wulf, G.; Lim, J.; Lu, K.P. *Mol. Cell. Biol.* **2006**, *26*, 1463-1479.
[317] Zacchi, P.; Gostissa, M.; Uchida, T.; Salvagno, C.; Avolio, F., Volinia, S.; Ronai, Z.; Blandino, G.; Schneider, C.; Del Sal, G. *Nature* **2002**, *419*, 853-857.
[318] Zheng, H.; You, H.; Zhou, X.Z.; Murray, S.A.; Uchida, T.; Wulf, G.; Gu, L.; Tang, X.; Lu, K.P.; Xiao, Z.X. *Nature 2002*, **419**, 849-853.
[319] Mantovani, F.; Tocco, F.; Girardini, J.; Smith, P.; Gasco, M., Lu, X.; Crook, T.; Del Sal, G. *Nat. Struct. Mol. Biol.* **2007**, *14*, 912-920.
[320] De Nicola, F.; Bruno, T.; Iezzi, S.; Di Padova, M.; Floridi, A.; Passananti, C.; Del Sal, G.; Fanciulli, M. *J. Biol. Chem.* **2007**, *282*, 19685-19691.
[321] Brondani, V.; Schefer, Q.; Hamy, F.; Klimkait, T. *Biochem. Biophys. Res. Commun.* **2005**, *328*, 6-13.
[322] Lu, K.P.; Zhou, X.Z. *Nat. Rev. Mol. Cell. Biol.* **2007**, *8*, 904-916.
[323] Butterfield, D.A.; Abdul, H.M.; Opii, W.; Newman, S.F.; Joshi, G.; Ansari, M.A.; Sultana, R.J. *Neurochem.* **2006**, *98*, 1697-1706.
[324] Balastik, M.; Lim, J.; Pastorino, L.; Lu, K.P. *Biochim. Biophys. Acta*. **2007**, *1772*, 422-429.
[325] Lu, P.J.; Wulf, G.; Zhou, X.Z.; Davies, P.; Lu, K.P. *Nature* **1999**, *399*, 784-788.
[326] Tang, B.L.; Liou, Y.C. *J. Neurochem.* **2007**, *100*, 314-323.
[327] Akiyama, H.; Shin, R.W.; Uchida, C.; Kitamoto, T.; Uchida, T. *Biochem. Biophys. Res. Commun.* **2005**, *336*, 521-529.

[328] Pastorino, L.; Sun, A.; Lu, P.J.; Zhou, X.Z.; Balastik, M.; Finn, G.; Wulf, G.; Lim, J.; Li, S.H.; Li, X.; Xia, W.; Nicholson, L.K.; Lu, K.P. *Nature* **2006**, *440*, 528-534.
[329] Butterfield, D.A.; Kanski, J. *Mech. Ageing. Dev.* **2001**, *122*, 945-962.
[330] Butterfield, D.A.; Poon, H.F.; St. Clair, D.; Keller, J.N.; Pierce, W.M.; Klein, J.B.; Markesbery, W.R. *Neurobiol. Dis.* **2006**, *22*, 223-232.
[331] Sultana, R.; Boyd-Kimball, D.; Poon, H.F.; Cai, J.; Pierce, W.M.; Klein, J.B.; Markesbery, W.R.; Zhou, X.Z.; Lu, K.P.; Butterfield, D.A. *Neurobiol. Aging.* **2006**, *27*, 918-925.
[332] Lu, K.P. *Cancer Cell.* **2003**, *4*, 175-180.
[333] Rippmann, J.F.; Hobbie, S.; Daiber, C.; Guilliard, B.; Bauer, M.; Birk, J.; Nar, H.; Garin-Chesa, P.; Rettig, W.J.; Schnapp, A. *Cell. Growth. Differ.* **2000**, *11*, 409-416.
[334] Ryo, A.; Liou, Y,C,; Wulf, G.; Nakamura, M.; Lee, S.W.; Lu, K.P. *Mol. Cell. Biol.* **2002**, *22*, 5281-5295.
[335] Lu, P.J.; Zhou, X.Z.; Liou, Y.C.; Noel, J.P.; Lu, K.P. *J. Biol. Chem.* **2002**, *277*, 2381-2384.
[336] Ryo, A.; Uemura, H.M.; Ishiguro, H.; Saitoh, T.; Yamaguchi, A.; Perrem, K.; Kubota, Y.; Lu, K.P.; Aoki, I. *Clin Cancer Res.* **2005**, *11*, 7523-7531.
[337] Hennig, L.; Christner, C.; Kipping, M.; Schelbert, B.; Rücknagel, K.P.; Grabley, S.;, Küllertz, G.; Fischer, G. *Biochemistry* **1998**, *37*, 5953-60.
[338] Stockwell, B.R.; Haggarty, S.J.; Schreiber, S.L. *Chem. Biol.* **1999**, *6*, 71-83.
[339] Chao, S.H.; Greenleaf, A.L.; Price, D.H. *Nucleic Acids Res.* **2001**, *29*, 767-73.
[340] Uchida, T.; Takamiya, M.; Takahashi, M.; Miyashita, H.; Ikeda, H.; Terada, T.; Matsuo, Y.; Shirouzu, M.; Yokoyama, S.; Fujimori, F.; Hunter, T. *Chemistry and Biology* **2003**, *10*, 15-24.
[341] Bayer, E.; Thutewohl, M.; Christner, C.; Tradler, T.; Osterkamp, F.; Waldmann, H.; Bayer, P. *Chem. Comm.* 2005, *4*, 516-518.
[342] Hart, S.A.; Etzkorn, F.A. *J. Org. Chem.* **1999**, *64*, 2998-2999.
[343] Andres, C.J.; Macdonald, T.L.; Ocain, T.D.; Longhi D. *J. Org. Chem.* **1993**, *58*, 6609–6613.
[344] Wang, X.J.; Xu, B.; Mullins, A.B.; Neiler, F.K.; Etzkorn, F.A. *J. Am. Chem. Soc.* 2004, *126*, 15533-15542.
[345] Daum, S., Erdmann, F.; Fischer, G.; Féaux de Lacroix, B.; Hessamian-Alinejad, A.; Houben, S.; Frank, W.; Braun, M. *Angew. Chem. Int. Ed. Engl.* 2006, 45, 7454-7458.
[346] Zhao, S.; Etzkorn, F.A. *Bioorg. Med. Chem. Lett.* **2007**, *17*, 6615-6618.
[347] Avendano, C.; Menedez, C.J. Medicinal Chemistry of Anticancer Drugs, Elsevier Science.
[348] Martinez, R.; Chacon-Garcia, L. *Curr. Med. Chem.* **2005**, *12*, 127-151.
[349] Palchaudhuri, R.; Hergenrother, P. *Curr. Opin. Biotechnol.* **2007**, *18*, 497-503.
[350] Braña, M. F.; Cacho, M.; Gradillas, A.; Ramos, A. *Curr. Pharm. Des.* **2001**, *7*, 1745-1780.
[351] Braña, M.F.; Beralanga, J.M.C.; Roldan, C.M. DE PATENT 2, 318,136, 1973.
[352] Braña, M.F.; Castellano, J.M.; Roldán, C.M.; Santos, A.; Vázquez, D.; Jiménez, A. *Cancer Chemother. Pharmacol.* **1980**, *4*, 61-66.
[353] Braña, M.F.; Sanz, A.M.; Castellano, J.M.; Roldan, C.M.; Roldan, C. *Eur. J. Med. Chem. Chim. Ther.* **1981**, *16*, 207.
[354] Rosell, R.; Carles, J.; Abad, A.; Ribelles, N.; Barnadas, A.; Benavides, A.; Martin, M. *Invest. New Drugs* **1992**, *10*, 171-175.
[355] Malviya, V.K.; Liu, P.Y.; Alberts, D.S.; Surwit, E.A.; Craig, J.B.; Hannigan, E.V. *Am. J. Clin. Oncol.* **1992**, *15*, 41-44.
[356] Waring, M.J.; González, A.; Jiménez, A.; Vázquez, D. *Nucleic Acids Res.* **1979**, *7*, 217-230.
[357] Hsiang, Y.H.; Jiang, J.B.; Liu, L.F. *Mol. Pharmacol.* **1989**, *36*, 371-376.
[358] Innocenti, F.; Iyer, L.; Ratain, M.J. *Drug Metab. Dispos.* **2001**, 29, 596-600.
[359] Braña, M.F.; Castellano, J.M.; Morán, M.; Emling, F.; Kluge, M.; Schlick, E.; Klebe, G.; Walker, N. *Arzneim. Forsch.* **1995**, *45*, 1311-1318.
[360] Sami, S.M.; Dorr, R.T.; Alberts, D.S.; Remers, W.A. *J. Med. Chem.* **1993**, *36*, 765-770.
[361] Sami, S.M.; Dorr, R.T.; Alberts, D.S.; Soloym, A.M.;Remers, W.A. *J. Med. Chem.* **2000**, *43*, 3067-3073.
[362]
[363] Braña, M.F.; Cacho, M.; Garca, M..A.; Pascual-Teresa, B.; Ramos, A.; Dominguez, M.T.; Pozuelo, J.M.; Abradelo, C.; Rey-Stolle, M.F.; Yuste, M.; Bez-Coronel, M.; Lacal, J.C. *J. Med. Chem.* **2004**, 47, 1391-1399.
[364] Li, Z.; Yang, Q.; Qian, X. *Bioorg. Med. Chem.* **2005**, *13*, 4864-4870.
[365] Braña, M.F.; Castellano, J.M.; Moran, M.; Perez de Vega, M.J.; Romerdahl, C.A.; Qian, X.D.; Bousquet, P.F.; Enling, F.; Schlick, E.; Keilhauer, G. *Anticancer Drug Des.* **1993**, 8, 257-268.
[366] Braña, M.F.; Castellano, J.M.; Moran, M.; Perez de Vega, M.J.; Perron, D.; Conlon, D.; Bousquet, P.F.; Romerdahl, C.A.; Robinson, S.P. *Anticancer Drug Des.* **1996**, *11*, 297-309.
[367] Braña, M.F.; Cacho, M., Gradillas, A., de Pascual-Teresa, B.; Ramos, A. *Curr. Pharmacy Design* 2001, *7*, 1745-1780.
[368] Gallengo, G., Reid, B.R. *Biochemistry* **1999**, *38*, 15104-15115.
[369] Patten, D.A.; Sun, J.H., Ardecky, R U.S. Patent 5, 086,059, 1992.

[370] Braña M.F.; Castellano, J.M; Moran, M.; Perez de Vega, M.J.; Qian, X.D. Romerdahl, C.A.; Keilhauer, G. *Eur. J. Med. Chem.* **1995**, *30*, 235-239.
[371] Nitiss, J. L.; Zhou, J.; Rose, A.; Hsiung, Y.; Gale, K. C.; Osheroff, N. *Biochemistry* **1998**, *37*, 3078-3085.
[372] Liu, Z.; Hecker, K.; Rill, R.L. *J. Biomol. Struct. Dyn.* **1996**, *14*, 331-339.
[373] Montero, A.; Goya, P.; Jagerovic, N.; Callado, L.F., Meana, J.; Girón, R.; Goicoechea, C.; Martín, I. *Bioorg. Med. Chem.* **2002**, *10*, 1009-1018.
[374] Licchelli, M.; Linati, L.; Biroli, A.; Perani, E., Poggi, A.; Sacchi, D. *Chemistry- A European Journal* **2002**, *22*, 5161-5169.
[375] Braña, M.F.; Domínguez, G.; Sáez, B.; Romerdahl, C.; Robinson, S.; Barlozzari, T. *Eur. J. Med. Chem.* **2002**, *37*, 541-551.
[376] Morgan, A.R.; Lee, J.S.; Pulleyblank, D.E.; Murray, N.L.; Evans, D.H. *Nucleic Acids Res.* **1979**, *7*, 547-569.
[377] McConnaughie, A.W.; Jenkins, T.C. *J. Med. Chem.* **1995**, 38**,** 3488-3501.